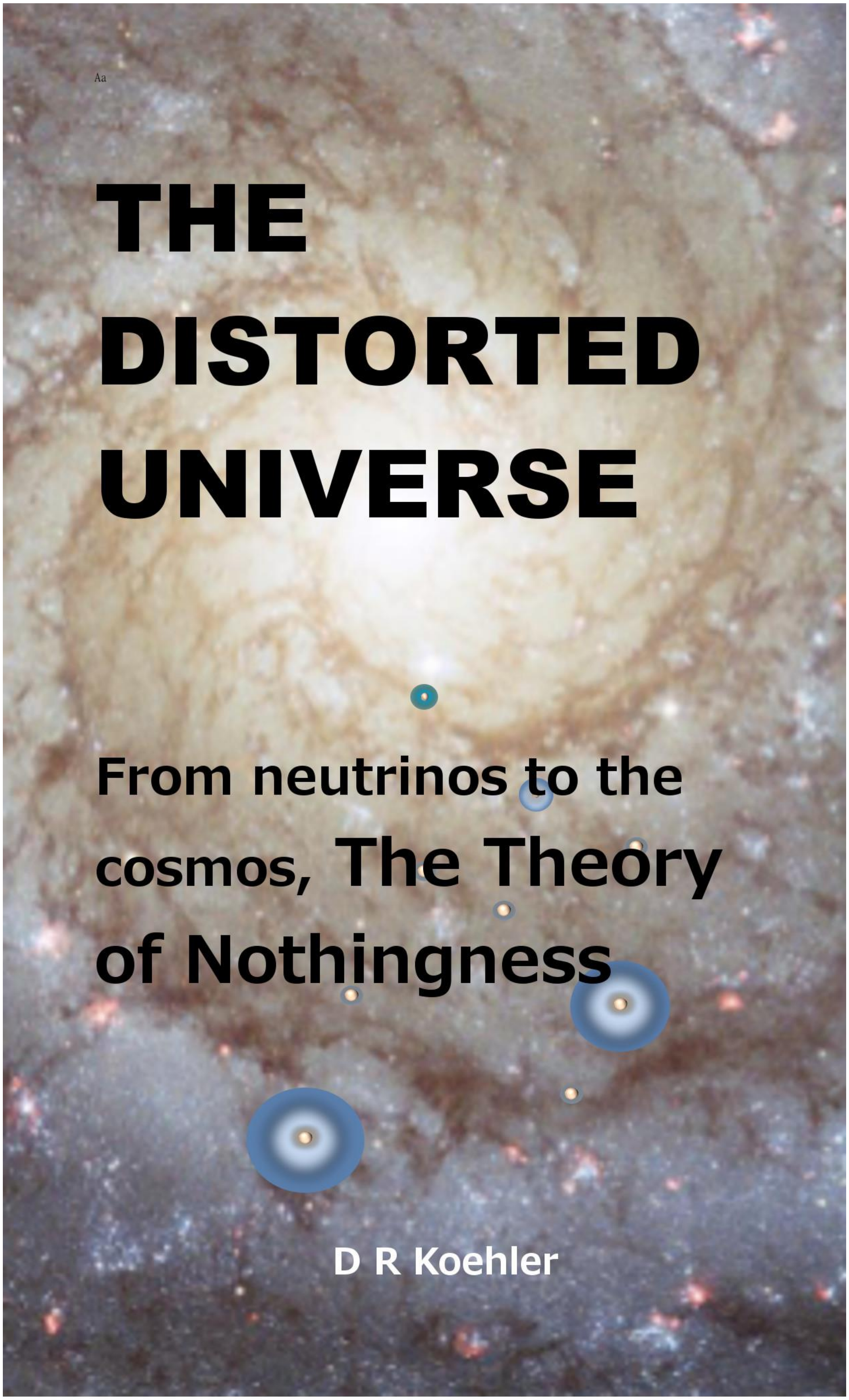
Aa
THE
DISTORTED
UNIVERSE
From neutrinos to the cosmos, The Theory of Nothingness
D R Koehler

THE DISTORTED UNIVERSE

From neutrinos to the cosmos, The Theory of Nothingness

By

D R Koehler

Keywords

Classical Field Theory, General Relativity, Geometry, Classical Mechanics, Structural stability, Beta decay, Electron, Muon, Tauon, W^- boson, Neutrino, Proton, Neutron, Fermi constant, Cosmology

PACS: 04.40.Nr, 04.20.Jb, 12.10.Dm

DISTORTED GEOMETRY
AND
PHYSICAL STRUCTURE

STRUCTURAL MODELING

VIBRATIONAL EIGENFREQUENCIES

STABILITY AND DECAY

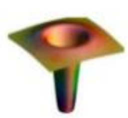

COMPOUND STRUCTURES

PREFACE

WHAT'S IT ALL ABOUT…..OR…

....what images come to mind when you think about A Theory of Nothingness?

START WITH…

DICTIONARY DEFINITIONS (the use of synonyms and other "words" to help form cerebral "understanding"(mental pictures))

NOTHING; no thing, nonentity

NOTHINGNESS; oblivion, nothing, emptiness, void, vacuum,

ENERGY (physics) (from Academic Press, Dictionary of Science and Technology); A QUANTITY THAT DESCRIBES THE CAPACITY TO DO WORK. Commonly divided into three major classifications; kinetic (dynamic) energy, potential (static) energy and radiant (electromagnetic) energy.

DISTORTED (INDISTINCT); twisted, warped, vague, fuzzy, imprecise, "geometrically NOT FLAT"

UNIVERSE; cosmos, space, creation

"THE"; *Definite* **grammatical article that implies necessarily that an entity it articulates is** *presupposed*

"A"; "indefinite article"

I prefer (subjective) to "mentally model", in this “physics realm”, in terms of ENERGY; mental modeling is all about visual image production within the grey matter. Subsequent transmission or communication of that “grey matter visual image” is called language. FORCES and FIELDS are other physics-created "labels" used to communicate physical processes and phenomena; both are derivable from an ENERGY model.

Another DEFINITION; **the absence of ENERGY is NOTHINGNESS**. Given (an assumed hypothesis, or definition in mathematics or logic) these starting concepts, one can then "mentally model" space-time as “NOTHINGNESS and ENERGY”(?). But having said that, can you please "draw a picture" i.e. show me the mental model? Hard, huh?

Now, if I say that the UNIVERSE consists of some NOTHINGNESS and some SOMETHING, what does the SOMETHING look like and what does the NOTHINGNESS look like? A "black void" is usually the "nothingness picture" and the "something picture" takes on various forms, stars, galaxies, elephants, politicians and electrons, the “MATTER model” of SOMETHING.

At the "most fundamental level", we try to "picture" the substance of MATTER, leaving the NOTHINGNESS modeling to the "black void" matter-emptiness "picture". But the MATTER models at this fundamental level are "attribute-like" descriptions; it "quacks" (like a duck), it "walks" (like a duck), it "smells" (like a duck) but actually, NO internal "structural" descriptor is forthcoming. In fact the external structural descriptor (a geometric description of the forces (gravity, electromagnetism..) or energy-distributions surrounding the "fundamental mathematically abstracted" ingredient) is UNSATISFACTORY in that it leads to geometric-infinities (nothing in the physical universe is "infinite"); “mathematical renormalization” techniques to handle

singularities (infinities) notwithstanding. Even for the modern-mathematically-abstracted Quantum mechanics modeling, one should understand Feynman's (the Nobel Laureate) quote about it, "*I think I can safely say that nobody understands Quantum mechanics*".

Now, let's consider the "effect" of the "something" on the "nothingness". If the "nothingness" is really "nothing", then there is NO effect, but if the 4-dimensional "nothingness" is "something" then the "matter something" will displace the "space nothingness" and cause a "space curvature (a geometric descriptor)" in the region of the matter. This curvature or distension of space, caused by the star-matter, has actually been physically (astronomically) measured. So the "black void" mental picture of "space nothingness" is not quite right and although the ENERGY content of the space can be zero (also called a FLAT-SPACE), it can also be non-zero (according to the concept of DISTORTED SPACE); **all regions of space, distorted or not, are mathematically describable by Riemann's geometric equations (general relativity).** When one "distorts" something, it requires ENERGY and that ENERGY is put into that something. Therefore, **any distorted region** of the space-time manifold**, matter-caused or NOT**, becomes SOMETHING, a DISTORTED SPACE with ENERGY, and is presently described by "THE DISTORTED UNIVERSE" or the THEORY OF NOTHINGNESS model, (as opposed to The **Theory** of **Everything** [a]); the "distorted geometry model" can be understood as the "source" of MATTER.

For the "currently described distortions", there is actually exhibited another concept difficult to "mentally and otherwise" grasp, a NEGATIVE ENERGY DENSITY in the "core" region. The illustrations in Figures 1.9a and 1.9b of Chapter 1 of this manuscript display the ENERGY DENSITY attribute of the "geometric distortion" in a 2-dimensional (rotated-radius) presentation.

ENERGY DENSITY however is also really "pressure" (a physics term) (Joules per meter^3 = Newtons per meter^2) and perhaps is a more intuitively resonant language (word) for mental modeling; consider therefore this language-translation possibility in the following manuscript. Furthermore, with structure, a "distortion morphing" between shapes can be created (video in Chapter 1).

A solution to the "model's" resultant nonlinear coupled differential equations must be forthcoming; such a solution has been found. Furthermore this solution, where physical parameters arise from geometric parameters, exhibits strong physically-positive features:

1. **IT PRODUCES MASS-ENERGY.**
2. **IT PRODUCES A CORE AND ENVELOPE ENERGY-DENSITY DISTRIBUTION (PHYSICAL FIELDS) AS A FINITE SUM OF r^{-N} COMPONENTS, THE CORE FUNCTION BEING 0 AT $r = 0$, (NO MATH SINGULARITY) (SEE FIGURES 1.9A AND 1.9B).**
3. **IT PRODUCES A GEOMETRY-BASED FERMI CONSTANT.**
4. **AND IT PRODUCES, WITH COMPOSITE COUPLING, BOTH EM AND GRAVITATIONAL FIELDS AND MASSES (HOLES, DARK STRUCTURES ETC.)**

Allowing for a space-time manifold itself with substantive character also suggests the possibility of an "absorptive-universe", a feature which has been explored earlier [6] and reproduced here in chapter 5. Analysis of such a manifold-attribute results in an alternative explanation for the classical "Hubble-data interpreted as universe expansion" model.

The "philosophical" question arises, not in the environment of "distortion producing" energy sources already in place such as stellar and galactic interiors and high-energy accelerators, but "in the FIRST environment of creation (an anthropomorphic concept)", as to what was (is) the source of the CREATION ENERGY? ....is this question answerable by the human mind? Additionally, is the question, "what was (is) the source of the CREATED GEOMETRIC MANIFOLD?" answerable?

[a] Ellis, John (1986). "The Superstring: Theory of Everything, or of Nothing?" *Nature* **323** (6089): 595-598.

TABLE OF CONTENTS

Spiral Galaxy M101 @ Hubblesite.org

CHAPTER 1

Structural Modeling

Chapter Summary: The classical Riemannian four-dimensional curvature equations have been applied to describe localized geometrical distortions and associated energy distributions at both quantum- and galactic-level magnitudes and distances. By requiring that the geometric distortions mimic the physical characteristics of the elementary particles, a coupling constant between energy and geometry is produced. The theoretical modeling and calculational procedure is limited to those geometric-distortional families satisfying an equation-of-state, which also expresses static, spherically-symmetric Maxwellian tensor behavior. Functional solutions to the differential equations describing the "distorted" space are of such a character that, over portions of the radial extensions of the distortion, the geometrical tensor elements exhibit negative, as well as positive, curvature-magnitudes and energy-densities. The field-observable in the negative energy-density (negative pressure) spatial region (the core region) is non-Coulombic and non-infinite at the radial origin. Mass, electric charge and magnetic moments have been simulated for the down-quark, up-quark, electron, tauon, muon and neutrino as well as for a hypothetical beta-decay transition-mediating distortion-particle; this process also generates a geometric expression for the Fermi constant and conversely predicts a mass-value for the W-boson calculated to the precision of the electron g-factor (gyromagnetic ratio). Finally, by incorporating gravitational-field structures into the geometric modeling and simulation process, a refined coupling-constant is engendered. This process recovers the gravitational coupling-constant of general relativity and leads to a structural description of gravitational-like geometric-distortions.

1.1 INTRODUCTION

We are, in the present undertakings, attempting to advance the notion, or spatial model, of matter expressed by *William Kingdon Clifford* in his communication to the Cambridge philosophical society in 1876 (*On the Space-Theory of Matter*) http://archive.org/details/proceedingscamb06socigoog We excerpt from Clifford's manuscript to illustrate his proposition.

"RIEMANN has shewn that as there are different kinds of lines and surfaces, so there are different kinds of space of three dimensions; and that we can only find out by experience to which of these kinds the space in which we live belongs. In particular, the axioms of plane geometry are true within the limits of experiment on the surface of a sheet of paper, and yet we know that the sheet is really covered with a number of small ridges and furrows, upon which (the total curvature not being zero) these axioms are not true. Similarly, he says, although the axioms of solid geometry are true within the limits of experiment for finite portions of our space, yet we have no reason to conclude that they are true for very small portions; and if any help can be got thereby for the explanation of physical phenomena, we may have reason to conclude that they are not true for very small portions of space.

I wish here to indicate a manner in which these speculations may be applied to the investigation of physical phenomena. I hold in fact

(1) That small portions of space are in fact of a nature analogous to little hills on a surface which is on the average flat; namely, that the ordinary laws of geometry are not valid in them.

(2) That this property of being curved or distorted is continually being passed on from one portion of space to another after the manner of a wave.

(3) That this variation of the curvature of space is what really happens in that phenomenon which we call the motion of matter, whether ponderable or etherial.

(4) That in the physical world nothing else takes place but this variation, subject (possibly) to the law of continuity.

A quote from Wheeler's work [1] published in 1955 reads; "In the 1950's, one of us [2] found an interesting way to treat the concept of body in general relativity. An object can in principle be constructed out of gravitational radiation or electromagnetic radiation, or a mixture of the two, and may hold itself together by its own gravitational attraction…A collection of radiation held together in this way is called a geon (a gravitational electromagnetic entity) and is a purely classical object….In brief, a geon is a collection of gravitational or electromagnetic energy, or a mixture of the two, held together by its own gravitational attraction, that describes *mass without mass*."

Subsequently at *The International Congress for Logic, Methodology, and Philosophy of Science* in 1960, he [3] began by quoting William Kingdon Clifford's [4] "Space-Theory of Matter" of 1870 and stated "The vision of Clifford and Einstein can be summarized in a single phrase, 'a geometrodynamical universe': a world whose properties are described by geometry, and a geometry whose curvature changes with time – a dynamical geometry."

We maintain the geometrical perspectives inherent in this "Curved empty space as the building material of the physical world" [3] supposition. We posit therefore that the classical

Riemannian four-dimensional geometrical curvature equations can be applied to describe distortional-energy-distributions at elementary-particle-level magnitudes and distances by utilizing a localized geometric-distortional equation-of-state (which also mimics spherically-symmetric Maxwellian tensor behavior) and a non-gravitational model-derived coupling-constant between geometry and physical energy. The treatment supposes the fundamental notion that local spatial distensions within the four-dimensional space-time manifold, which are describable by the geometrical curvature relationships, are localized stable energy configurations which can mimic the physical characteristics of the elementary particles (**a geometric mimic of matter).** In this perspective, the geometrostatic equations, flowing from geometric equation-of-state constraints, provide the distortion's structural details from which the modeling of the elementary particles ensues. Subsequently, a particular form of the particle-level metric is yielded. The phenomenological modeling also fundamentally constrains the character of the associated coupling constant and is further used to determine the required values to fit the geometric-distortion descriptors to the physical characteristics of the modeled particles.

To proceed, a solution to the resultant nonlinear coupled differential equations must be forthcoming; such a solution has been found (see eqn.11). Furthermore the solution to the nonlinear geometric equations, where physical parameters arise from geometric parameters, exhibits physically attractive features:

- **IT PRODUCES MASS-ENERGY.**

- **IT PRODUCES A CORE AND ENVELOPE ENERGY-DENSITY DISTRIBUTION (FIELDS) AS A FINITE SUM OF R^{-N} COMPONENTS, THE CORE FUNCTION BEING 0 AT R=0, (NO MATH SINGULARITY)(SEE FIGURES 1.9A AND 1.9B).**
- **IT PRODUCES A GEOMETRY-BASED FERMI CONSTANT.**
- **AND IT PRODUCES, WITH COMPOSITE COUPLING, BOTH EM AND GRAVITATIONAL FIELDS AND MASSES (HOLES, DARK STRUCTURES ETC.)**

Allowing for a space-time manifold itself with absorptive character also suggests the possibility of an "absorptive-universe", a feature which has been explored earlier [6] and reproduced in chapter 5. Analysis of such a manifold-attribute results in an alternative explanation for the classical "Hubble-data interpreted as universe expansion" model.

The functional solutions to the differential equations describing the "distorted" space are of such a character that, over portions of the radial extension of the distortion, the geometrical tensor elements (also formed from the same functional solutions) exhibit negative (in the core-regions), as well as positive, curvature-magnitudes. These are "energy-density" quantities (converted via the coupling constant κ (m/J)) and both the "mass energy-density" and the "field-

tensor energy-density sums" for an "electric-field" and for a "magnetic-field" therefore exhibit spatial regions of negative "energy-density". For the "mass-energy", however, a spatial integral, the result for the total summation (r = 0 to infinity) is a "positive" quantity, a "positive mass-energy". Although the mass energy-density spatial distribution may not be physically measurable, the "field-observable” in the "negative energy-density" spatial region (the core region) is non-Coulombic and is manifested at magnitudes significantly different than the core-region Coulomb values.

We also consider a distortional-, or particle-, transformation process wherein the process is described in terms of a nonlinearly-quantized.geometrical mediating particle with characteristics mimicking the Fermi beta-decay transition; additionally, sub-structures of the neutron and proton have been investigated. Gravitationally-configured distortional-realizations existing throughout our geometric universe would seriously affect cosmological modeling.

A comprehensive and general treatment of the historical, geometric and physical foundations of modern geometrodynamics is found in the already cited publications of Wheeler [1-3]. Additional work in this field continues, some of which is cited in references [5-10]. The present treatment departs from these cited “geon constructional methods” in that we do not constrain the distortional descriptions to only gravitational coupling-constant produced structures.

In Sections 1.2-1.4 of this manuscript, we develop a geometrostatic distortion model to mimic the characteristics of the elementary particles. In Section 1.3 we posit transition processes in terms of the Section 1.2 distortion-particle-structures thereby producing a geometric-mimic for the W^-boson. Section 1.4 illustrates how one incorporates gravitational field-energy-densities into the model via coupling-constant refinements.

1.2 STRUCTURAL EQUATIONS AND PHYSICAL MODELING

The geometrical model begins with the classical curvature representation of a spatial energy distribution defining the particle. Einstein's gravitational equations (see Einstein [11]) are qualified on a microscopic scale to an isotropic space and are modified to unspecify the geometrically-defined coupling-constant, κ, between geometry and physical energy:

(1) $$G_{ab}(g_{ab}) = R_{ab} - g_{ab}\frac{R}{2} = 8\pi\kappa\, T_{ab}.$$

G_{ab} is the Einstein Curvature tensor, a function of the metric g_{ab} and its first two derivatives; R_{ab} is the Ricci tensor and R, the Ricci scalar. T_{ab}, which classically is the stress-energy-tensor describing the material contents of the particle energy distribution, is here viewed as the distortionally-generated geometric-tensor, with its associated energy content resulting from the creation process which produced the distorted feature in the manifold; the energy is fundamentally manifested in the distorted metric itself. The "curved empty space" [3] referred to above is a "curved space" devoid of an "external or foreign" causative matter-entity. The functional form of the spherically-symmetric distorted-metric elements g_{11} and g_{44} appearing in the line element describing the distorted geometric-region, or equation (2), is to be determined.

(2) $$ds^2 = g_{11}[dr^2 + r^2 d\Omega] + g_{44}dt^2 = -e^{\mu}[dr^2 + r^2 d\Omega] + e^{\nu}dt^2.$$

with $\mu = \mu(r,t)$ and $\nu = \nu(r,t)$. Although this initial development is spatial in character, Chapter 6 is an extension to a time dependent regime. We have constructed the geometrically based mathematical development of the distortional structure in (Eq. 3-22) STRUCTURAL EQUATIONS

.

Because we have mimicked the electrostatic and magnetostatic fields, the geometrostatic coupling-constant is essentially Maxwellian, however, the coupling constant can be refined and understood as a composite of the gravitational and Maxwellian entities and, in the case of zero electromagnetic distortional energies, utilized to describe purely gravitational distortions (discussed further in Section 1.4).

The greater distortional energy-densities present at the particle-level radii are achieved through the greater model-produced coupling-constants; the greater the coupling constant the smaller the energy density required to produce the given distortional feature. The distortional model-2 particle (electron) from this perspective requires the smallest energy density to produce the associated geometric distortion.

To graphically illustrate the character of the two-region metric approximation, we produce in Figure 1.1, for the modeled particle-2, the two quantities μ' and μ'(approx.).

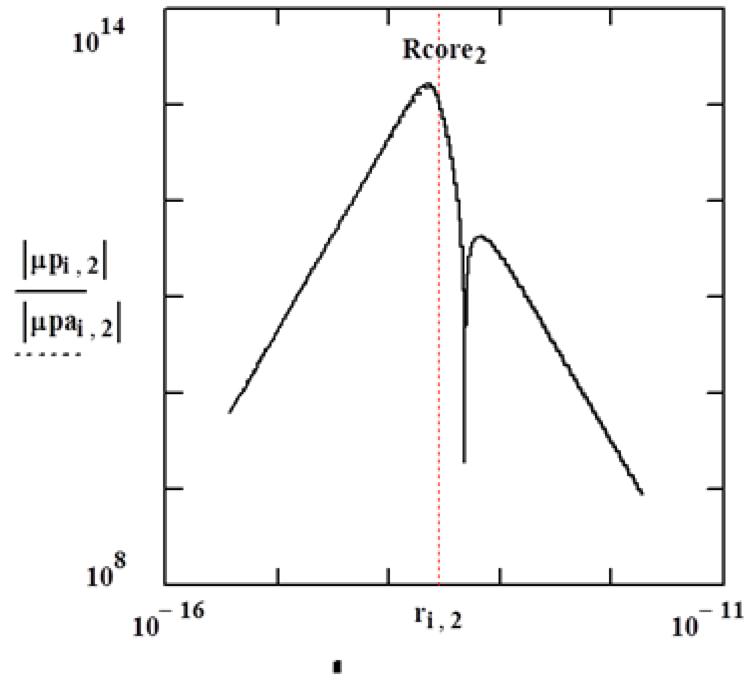

Fig. 1.1 Metric-derivative ($\mu p = \mu'$ and $\mu pa = \mu'$-approximate) functions for a distortion-2(electron) structure; logarithmic ordinate display in metric units (m^{-1}) and abscissa in meters.

In conjunction with, or as a function of, minimization of the error function expressed in equation (13), the core radius, *Rcore*, is determined. This process produces across the two radial regions the approximation errors displayed in Table 1.1.

Table 1.1 Approximation-Function ($\mu a'$) Fitting-errors (%) (Equation (13)) over the radial range for "Core" (0 to Rcore) and for "E-core" (Rcore to 2 Rcore)

Distortion	*Rcore/R0*	*Core Error*	*E-core Error*
Down-Quark	**0.488**	**0.192**	**0.025**
Up-Quark	**0.557**	**0.184**	**0.018**
Electron	**0.599**	**0.180**	**0.017**
Muon	**0.599**	**0.180**	**0.017**
Tauon	**0.562**	**0.186**	**0.075**

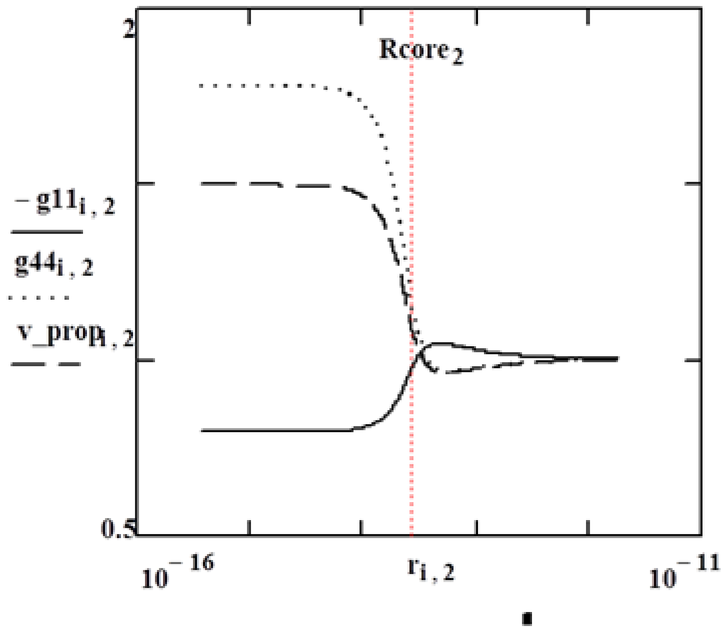

Fig. 1.2 Metrics and propagation-velocity factor for distortion-2 (electron) structure; abscissa in meters.

We calculate the elemental metric quantities μ and ν and the associated metrics g_{11} and g_{44} with the results displayed in Figure 1.2 for the modeled particle 2. Another significant feature of the distortion is the propagation velocity, defined in terms of the null geodesic as $[(-g_{11})^{-1} g_{44}]^{0.5}$, which exhibits a step-like behavior across the boundary region and is of an increased magnitude relative to the external "flat-space region"; this behavior is also graphed in Figure 1.2 (although see APPENDIX) . A characteristic propagation-velocity feature relates to the concepts of "observational physical structure" and "information propagation" internal to or within such geometrostatic distortional entities or in general as to how "physical structure" is achieved. Within the "core regions" of the distortion, the propagation velocity exceeds the velocity of light

(equivalent to an *n* < 1 refractive index). Similar distortions throughout our geometric manifold would seriously impact cosmological calculations.

To illustrate the effects of the distorted metric on the sphere's geometric volume, we show in Figure 1.3 a composite representation for three of the modeled particles of the quantity $[(-g_{11})^3 g_{44}]^{0.5}$. The choice of modeled particles exhibits both a charge and a mass variation from electron characteristics. The distorted volume element is fundamentally important in the geometrostatic-sphere's mass- and field-energy distribution; it also exhibits a step-like functional behavior across the radius Rcore, a fraction of the "characteristic" radius R0.

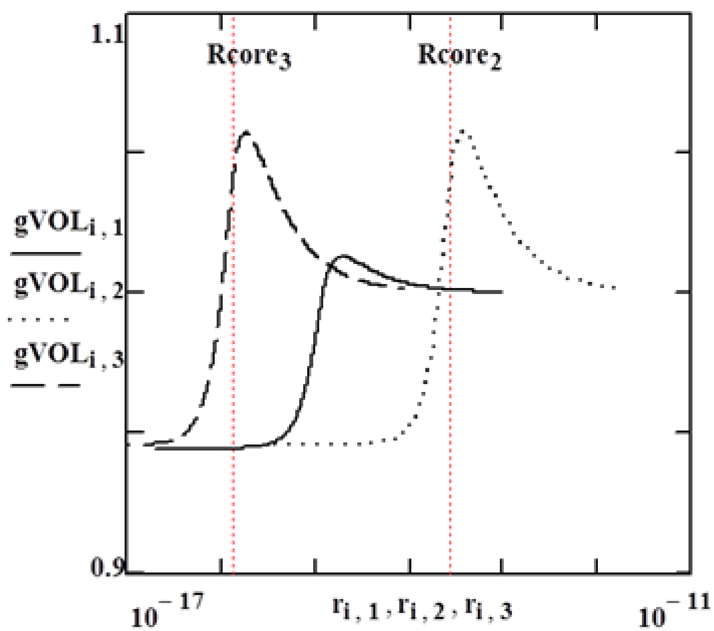

Fig. 1.3 Distortion-volume factors $gVOL = [(-g_{11})^3\ g_{44}]^{0.5}$ for distortions -1,-2 and -3; abscissa in meters.

The mass integrand ($\rho M = \rho\mathrm{Mass}$ from equation (21)) for an electronic-mass, electronic-charge geometric feature is illustrated in Figure 1.4 on a linear scale, with a composite overlay of the metric-derivative and distorted-metric-volume factor $\mathrm{gVOL} = [(-g_{11})^3\, g_{44}]^{0.5}$, to better illustrate the mass-energy distribution's sensitivity to geometric curvature. Both positive and negative energy-density regions [15] are produced by this "shell-like" distortion.

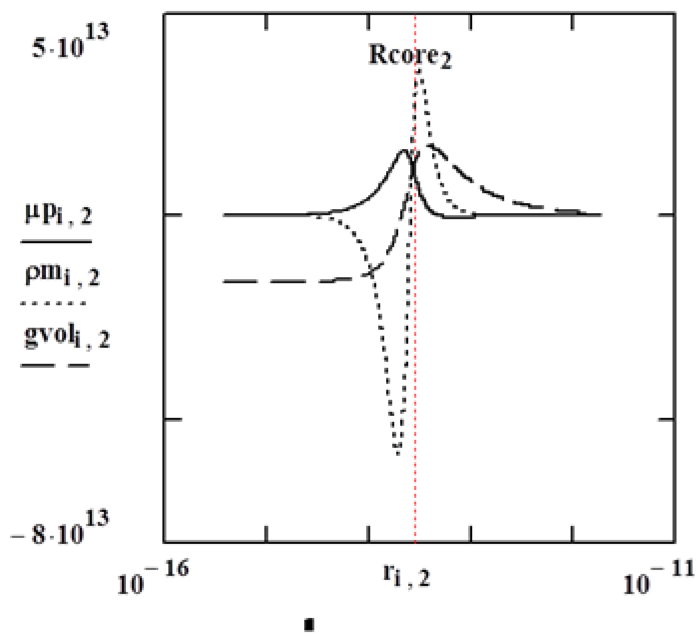

Fig. 1.4 Mass-energy-density distribution function for distortion-model 2 (electron) with metric-volume and metric-derivative overlays. For display purposes, the metric volume function is shown as $\mathrm{gvol} = (\mathrm{gVOL} - 1)\cdot 3(10)^{14}$. Metric-derivative ($\mu p = \mu'$) is in m^{-1} units. The ρm function is the $\rho\mathrm{Mass}$ function multiplied by factor $5(10)^{-15}$ for display purposes; the ordinate is in J/m units and abscissa is in meters. The distorted volume factor is included in the distribution function.

Since Maxwellian-like field characterizations, $(\mathrm{Fd}_{14})^2 = \mathrm{Td}_4{}^4 + \alpha 1\ \mathrm{Td}_1{}^1$ and $(\mathrm{Fd}_{12})^2 = \mathrm{Td}_4{}^4 + \alpha 2\ \mathrm{Td}_1{}^1$, have inherently been used to constrain the geometric descriptors, therefore these "geometric fields" have been implicitly defined. The "pseudo-magnetic spin" quantity was used to quantify the tensor construct $\mathrm{Td}_4{}^4$ - $\mathrm{Td}_1{}^1$ ($\alpha 2$ =-1) and an "electric charge" quantity was used to quantify the tensor construct $\mathrm{Td}_4{}^4 + \mathrm{Td}_1{}^1$ ($\alpha 1$ =1). We illustrate in Figure 1.5 these field results calculated according to equations (6) and (19) with the geometric distortion tensors replacing the Maxwellian tensors. The solution in the core region produces a field variable, an energy density distribution, significant in the fact that it does not exhibit a singularity at the radial origin. One must interpret both positive energy-density and negative energy-density departure from flat curvature as giving rise to "real" as opposed to "imaginary" geometrostatic fields and forces. For comparison purposes, we have also shown the classical Maxwellian electrostatic field quantity $\mathrm{E_{Max}} = \mathrm{q}/4\pi\ \varepsilon\mathrm{o}\ \mathrm{r}^2$, in energy-density form, $\mathrm{u_E} = (\mathrm{E_{Max}})^2 \varepsilon\mathrm{o}/2$. In the core region the geometric fields also differ significantly from the Maxwellian fields in that they exhibit a change of sign relative to the extra-core region and are therefore strongly non-Coulombic; see Figure 1.6 where this feature is illustrated on a linear scale for the model-2 distortion.

The classical Maxwellian field-constructs have been here geometrically generalized to permit the negative energy-density stress-tensor-based functions to still constitute the sources of the fields; we have posited and used therefore, for example, that

(23) $$\varepsilon\mathrm{o}\ \mathrm{E}^2/2 = \alpha\ \mathrm{u} = \pm \mathrm{u} \quad \text{or} \quad \text{with } \mathrm{Fd}^2 = \mathrm{u}\ ,$$

$$\mathrm{E(u{>}0)} = \pm(2\ \mathrm{Fd}^2/\varepsilon\mathrm{o})^{\frac{1}{2}} \quad \text{and} \quad \mathrm{E}(\mathrm{u} < 0) = \pm(-2\ \mathrm{Fd}^2/\varepsilon\mathrm{o})^{\frac{1}{2}}$$

where $(Fd)^2$ is the geometric-field construct $(Fd_{14})^2$, $(Fd_{12})^2$ or $(Fd_{13})^2$ according to equations (5-6). The positive "field-sign" for $E(u>0)$ is associated with a positive "electric-charge" and the negative "field-sign" for $E(u<0)$ is associated with a positive "electric-charge".

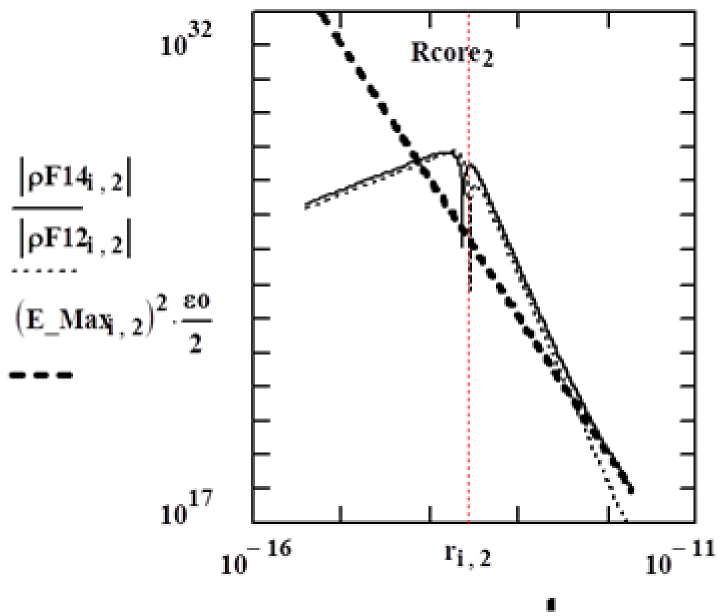

Fig. 1.5 Field-energy-density distribution functions (electric and magnetic) for distortion-model 2 (electron) where $\rho F14 = Fd_{14}{}^2$ and $\rho F12 = Fd_{mag}{}^2$; logarithmic ordinate in J/m^3 units and abscissa in meters.

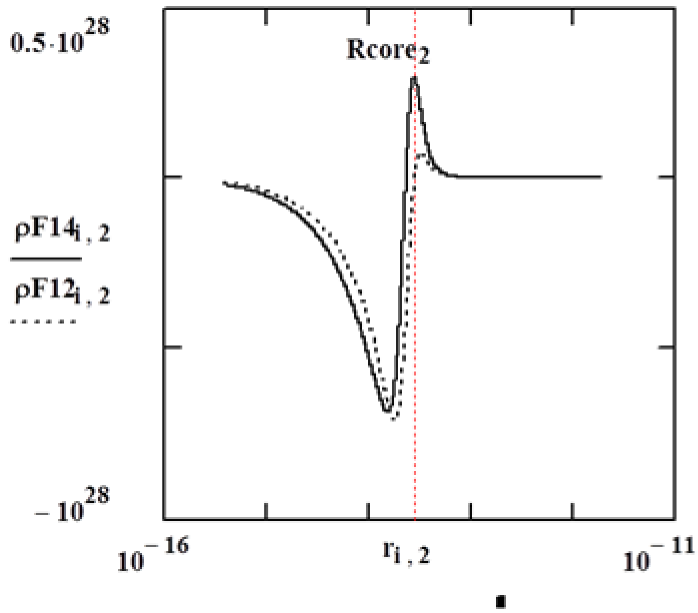

Fig. 1.6 Field.-energy-density distribution functions (electric and magnetic) for distortion-model 2 (electron) where $\rho\mathrm{F14} = \mathrm{Fd}_{14}{}^2$ and $\rho\mathrm{F12} = \mathrm{Fd}_{\mathrm{mag}}{}^2$; linear ordinate in J/m^3 units and abscissa in meters.

Finally, we have created, for relative comparison purposes, Figures 1.7 and 1.8. Displayed in these figures are the "mass" and "electric-field" energy-densities for the distortions simulating the particle characteristics of a model-1 distortion (the down-quark with m_1 = 9.296 and Q_1 = –1/3), a model-2 distortion (the electron with m_2 = 1.0 and Q_2 = –1) and a model-3 distortion (the muon with m_3 = 206.768 and Q_3 = –1) (masses expressed in electron-mass units and charges in electron-charge units).

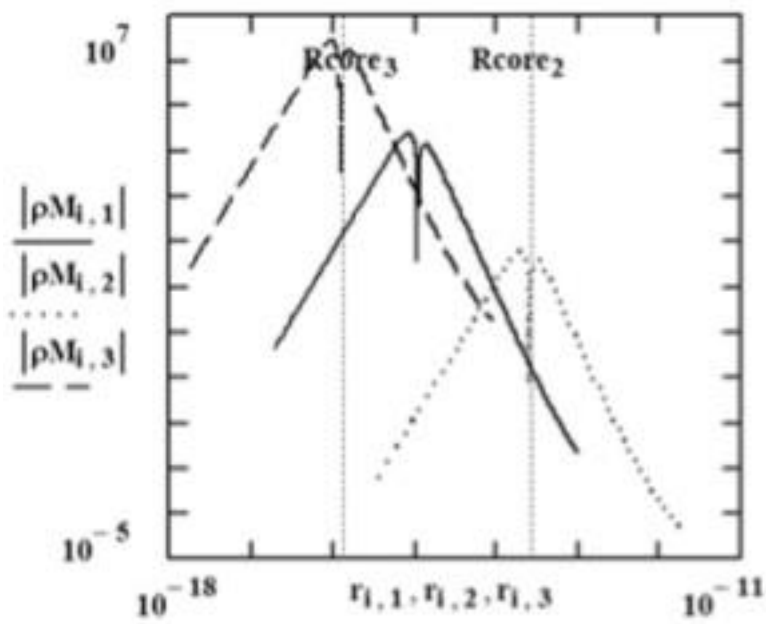

Fig. 1.7 Mass-energy-density distribution functions for distortions -1,-2 and -3; logarithmic ordinate in J/m units and abscissa in meters. The distorted volume factor is included in the distribution functions.

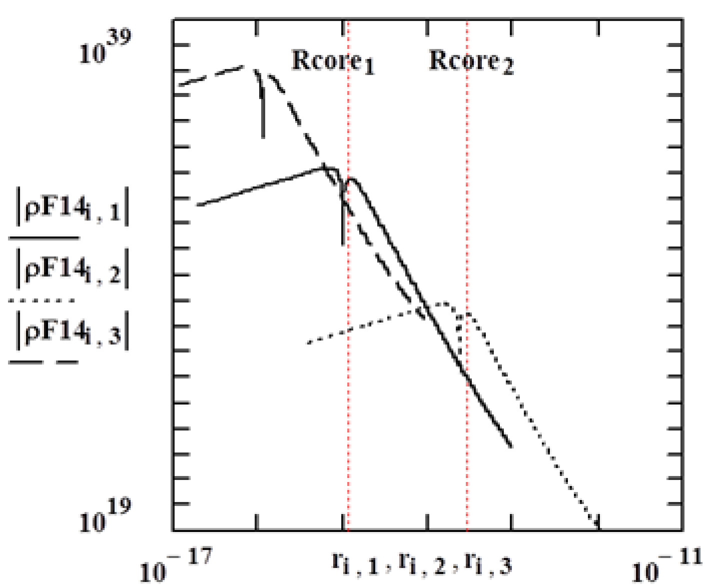

Fig. 1.8 Electric-Field energy-density distribution function for distortions -1,-2 and -3 where $\rho F14 = Fd_{14}{}^{2}$; logarithmic ordinate in J/m^3 units and abscissa in meters.

Table 1.2 summarizes the relevant features of the geometrostatic distortions and the simulated particles where the particle masses are taken from reference [18]. As mentioned above, the model requires that the geometrostatic "mass-energy" be calculable from the "sphere mass-energy" equation (4). The results for that calculation are also indicated in Table 1.2 where $U = U(\mathrm{sphere})$. We suggest that the slight departure from unity for the tabular mass values is due to the use of the imperfect metric-derivative approximations constructed herein.

Table 1.2 Distortional-particle descriptors, charge-states and masses

Distortion	*R0*	*κ*	*U/M*	*Spin*	*Q*	*M*
	Fm	*10⁻⁶m/J*		*μ_B*	*E*	*$m_e c^2$*
Down-Quark	2.44	22.1	1.006	0.0359	-1/3	9.29
Up-Quark	6.66	262	1.009	0.123	2/3	5.405
Electron	47.2	$1.72*10^{4}$	1.012	1.00	-3/3	1.00
Muon	0.228	0.403	1.012	$4.84*10^{-3}$	-3/3	206.77
Tauon	0.0136	$1.42*10^{-3}$	0.9938	$2.88*10^{-4}$	-3/3	3477

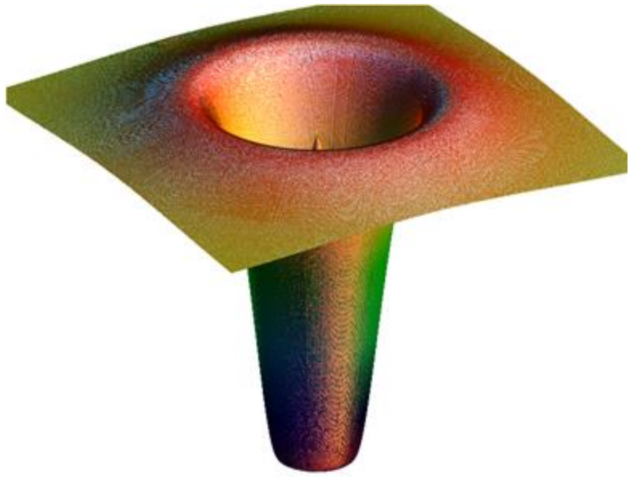

ρMass_n

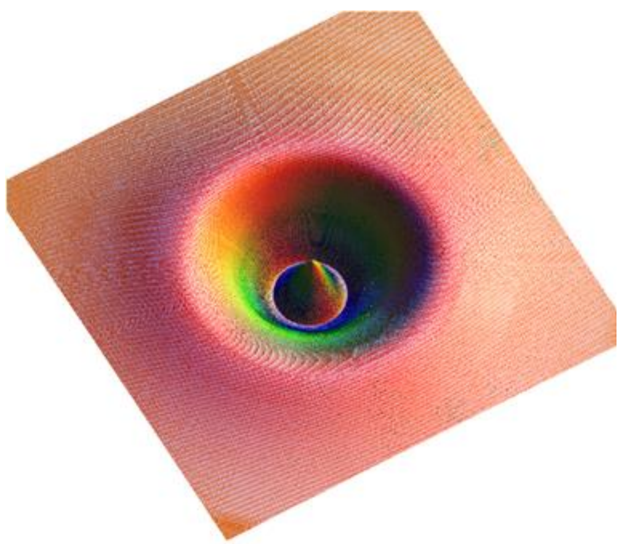

ρMass_n

Fig. 1.9a and 1.9b Mass-Energy-Density distribution-function surface-plots (two views) for the particle-2 distortion, $\rho Mass\_n$, and, $-\rho Mass\_n$, the geometric electron distortion (also see Figures 1.4 and 1.10).

1.3 DISTORTIONAL TRANSITION PROCESSES

Although we have characterized these modeled distortions as stable configurations, we also now consider the possibility of configurational, or distortional, upset followed by a structural rearrangement or transition between distortional-states. Since we will be comparing energy-density-distributions in the spatial domain, such a geometrical restructuring process is considered as more probable, or more energetically realizable, the more geometrically similar [19] the structures or transitional states, a conventional representation of the concept of state-to-state transition probabilities.

A current [20] physical rendition of the process of beta-decay (a state-restructuring or transition process) envisions an intermediate mediating state which “facilitates” the overall reconfiguration process. If “geometric vacuum-fluctuations” are dynamically and structurally allowed, then the description of such a mediating state in the geometric domain requires a distortional entity satisfying at least the “electric-charge” conservation requirement. However, a “structural, or spatial-tensor, similarity” would intuitively and energetically seem an additional facilitating geometric attribute. The latter consideration is of course satisfied if all of the distortional structures are of the same family and, in the present analysis, by the “particle-distortions” discussed in Section 1.2. We quantitatively define “shape- or structural-similarity” in

terms of the magnitude of a modified “Pearson [21, 22] product-moment correlation coefficient” discussed below. For geometric-shape evaluation, we utilize the radial distributions of the mass-energy-density functions as described in the previously defined distribution functions from equations 8-22 STRUCTURAL EQUATIONS .

Fig. 1.10 displays these mass-energy-density distribution functions for the mediating transition-distortion and the associated mimicked beta-decay participants.

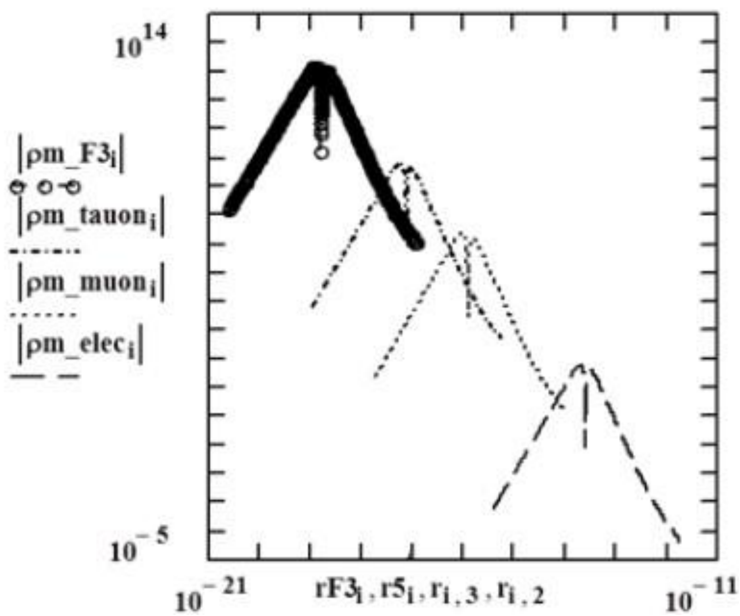

Fig. 1.10 Mass-Energy-Density distribution functions for (a), $\rho\mathrm{mF3} = \mathrm{FermiMass}$ (Q = -3) distortion, (b), $\rho\mathrm{mtauon} = \rho\mathrm{Mp}$ model-5 distortion, (c), $\rho\mathrm{mmuon} = \rho\mathrm{Mp}$ model-3 distortion and (d), $\rho\mathrm{melec} = \rho\mathrm{Mp}$ model-2 distortion, mimicking an (a), Fermi_Mass (Q = -3) particle-distortion, (b), tau-particle, (c), muon and (d), electron; logarithmic ordinate in Joules/m and abscissa in meters (the radial quantity $\mathrm{rN_i}$ is a relabeled $\mathrm{rn_i}$ radius). The distorted volume factor is included in the distribution functions.

Some overlap (a geometric, or isomorphic, measure of the transition probabilities) of the distribution functions is evident between the Fermi-Mass (subsequently defined and characterized below) and the initial-particle-state and similar structural overlap between the other participating distortions.

In equations (24)-(26) (FERMI CONSTANT) we develop the "geometric-distortional" representation of the Fermi constant deriving from a "geometric maximum curvature" origin.

At the minimum end of the distortional geometric-curvature range, we posit, in the absence of a physical constraining criterion, an electron-curvature (from the 1^{st} mass-moment Eq. 20),

(26a) $$\frac{1}{R0e} = 2\pi \left(\frac{me\ c^2}{\beta hc}\right).$$

In summary, although these distortional transition-structures have been characterized at the outset as stable distortions, the subsequent exploitation of the distortional form as the mediating entity in distortional transition processes, suggests that the structural stability can be of a transient nature. As a supplementary visualizing addition to the geometric modeling we include an animated video file (muon to electron beta-decay) produced as a spherically symmetric representation with the following details:

frames 0-15; geometric-distortion mass-energy-density function for muon,

@ frame 15, "muon" transitions (morphs) to "Fermi-mass + neutrino", and

@ frame 30-45, "Fermi-mass" transitions (morphs) to "electron + neutrino".

SEE FIGURE 1.10 FOR “RADII” AND “MASS-DENSITY” FUNCTIONS. THE BETA-DECAY ANIMATION IS CONSTRUCTED WITH LINEAR RADII BUT WITH LOGARITHMIC AMPLITUDES AND LOGARITHMIC NORMALIZING RADII R0 AND IS FURTHER NORMALIZED TO A “NEUTRINO” AMPLITUDE AND AN “ELECTRON” RADIUS.

THIS HOLE SECTION IS INCORPORATED HERE AS A TEMPLATE FOR SEPARATE PUBLICATION

1.3A FERMI CONSTANT AND GEOMETRIC VIRTUAL MEDIATOR STRUCTURES

***Abstract*—** A Riemannian-geometry-based "maximum-energy-density" structure, a "virtual-mediator" feature, was heretofore successfully exploited to geometrically explain and quantify the Fermi constant [5]). Building on this earlier work [5, 6], we presently extend the geometric "virtual-mediator-structure" concept to characterize another mass-energy aggregation or distortional-geometric entity, a "geometric-mass-energy" mimic of the Higgs-boson.

Index Terms*— *Classical Field Theory, General Relativity, Geometry, Classical Mechanics, Structural stability, Beta Decay, Fermi Constant

1.3A-1 INTRODUCTION

WE have previously modeled localized distorted Riemannian-geometry-based regions of space to maintain and expand the geometrical perspectives inherent in a "Curved empty space as the building material of the physical world" supposition [1-6]. The four-dimensional geometrical curvature equations, with solution, were applied to describe localized distortional-energy-distributions, with a modified-gravitational model-derived coupling-constant between geometry and physical energy [5,6].

In the perspective of [5], the distorted-geometry model is a departure from the classical

geometry model where the Einstein Curvature tensor is the stress-energy-tensor describing the "material contents" of the energy distribution. The distorted-geometry model is rather viewed with the energy-content residing in the warping of the manifold and therefore in its geometric-tensors, with the associated energy content resulting from the creation process which produced the distorted feature in the manifold; the energy is fundamentally manifested in the distorted manifold itself and the "curved empty space" [4] referred to above is a "curved space" devoid of an "external or foreign" causative matter-entity.

A "geometric maximum-energy-density" feature, a "virtual-mediator structure", was successfully exploited to geometrically explain and quantify the Fermi constant [5]). Building on this earlier work [5, 6], we presently extend the geometric "virtual-mediator-structure" concept to characterize another mass-energy aggregation or distortional-geometric entity, a "geometric-mass-energy" mimic of the Higgs-boson.

1.3A-2 DISTORTIONAL MEDIATOR STRUCTURE

The geometric-Fermi-constant and its derivation (eq. 11a) in [5] is again presented, with the various symbols noted in the reference [1], illustrated here as equations (1), (2) and (3); the distortional magnetic force function $\mathrm{Fd}_{\mathrm{mag}}$ is related to the Schwarzschild radius Rs, the distortional coupling constant k and a normalization radius R0,

$$\left(\mathrm{Fd}_{\mathrm{mag}}\right)^2(\mathrm{r}\rightarrow\infty)\cong\ 3\,\frac{\mathrm{Rs}\;\mathrm{R0}^3}{8\pi\kappa}\frac{1}{\mathrm{r}^6}\quad ; \qquad (1.3A\text{-}2\text{-}1)$$

$$3\ \frac{2\ \mathrm{Mc}^2\ \mathrm{R0}^3}{8\pi}\frac{1}{\mathrm{r}^6} = \frac{\mu\mathrm{o}}{2}\left(\frac{\mu\_\mathrm{spin}}{2\pi}\right)^2\frac{1}{\mathrm{r}^6} \qquad \text{or}$$

defining the “geometric Fermi constant” as a descriptor of the “virtual-mediator” structure where FM is its mass-energy, then

$$\mathrm{gF_{geo}} \stackrel{\mathrm{def}}{=} \left[\mathrm{fe}\ \frac{4\pi}{3}\mathrm{R0}^3\right]\mathrm{FM} = \frac{4\pi}{3}(\hbar c)^3\left(\frac{\mathrm{G_{geo}}}{\mathrm{m_F\ me\ c^2}}\right)^2$$

$$\text{where} \qquad \mathrm{fe} = \frac{3}{2}\left(\frac{\pi}{2}\right)^2 \quad \text{and} \quad \mathrm{G_{geo}} = \left(\frac{\alpha}{4}\right)^{1/2}\pi\ \mathrm{g_e}\frac{\mathrm{S}}{2}\frac{\mathrm{Q}}{3}\ ;$$

α, g_e, S and Q are respectively the fine-structure-constant, the gyromagnetic ratio, the spin quantity and the charge quantity.

With $\mathrm{m_F} \stackrel{\mathrm{def}}{=} \frac{\mathrm{Q}}{3}\mathrm{m_{F0}}$ to satisfy charge universality, then if

$\mathrm{m_{F0}} = \frac{\mathrm{m_{W\text{-}boson}}}{\mathrm{me}}$, we produce

$$\mathrm{GF_{geo}} \stackrel{\mathrm{def}}{=} \frac{4\pi}{3}(\hbar c)^3\frac{1}{\left(\mathrm{m_{W\text{-}boson}}\ \mathrm{c}^2\right)^2}\left[\left(\pi\frac{\mathrm{S}}{2}\mathrm{g_e}\right)^2\frac{\alpha}{4}\right]_{\mathrm{S}=1} = \mathrm{GF}\,. \qquad (1.3\mathrm{A}\text{-}2\text{-}2)$$

After having related the geometric descriptors to the pertinent physical parameters, the geometry-based Fermi constant, $\mathrm{GF_{geo}}$, is expressed explicitly in (2). The geometric factor fe was introduced as a “volume adjustment” factor to produce perfect agreement with GF, the Fermi constant.

With further symbol abbreviation we use

$$\mathrm{GF_{geo}} \stackrel{\mathrm{def}}{=} \frac{(\mathrm{a_W})^2\ \mathrm{fe}}{\left(\mathrm{m_{W\text{-}boson}}\ \mathrm{c}^2\right)^2}\,.$$

From experimental particle-decay data, a "Higgs-boson-mimic" structure appears to be a "geometric-couple ($w_{\text{ boson}}$)" in form, that is the two W-boson charge-versions (Q = 0, S = 0, a superposition principle?). Assuming therefore a "geometric maximum-energy-density" structure, in the manner of equation (2), for both beta-decay "and" higher-order (greater mass-energy) structures, we write

$$\mathrm{GF_{geo}} = \frac{(\mathrm{a_W})^2\ \mathrm{fe}}{\left(\mathrm{m_{W\text{-}boson}}\ \mathrm{c}^2\right)^2} = \frac{(\mathrm{a_W})^2\ \mathrm{feH}}{\left(\mathrm{m_{H\text{-}boson}}\ \mathrm{c}^2\right)^2}\ , \tag{1.3A-2-3}$$

where the mediator structural characteristics are incorporated into a_x. Introducing the geometric scale factor, in the manner of fe,

$$\mathrm{feH1} = \left[\frac{3}{2}\left(\frac{\pi}{2}\right)^{\frac{1}{12}}\right]^2 \mathrm{fe} \quad \text{or} \quad \mathrm{feH2} = \left[\frac{3}{2}\left(\frac{\pi}{3}\right)^{\frac{13}{16}}\right]^2 \mathrm{fe}\ ,$$

then equation (3) yields, for the geometric-mass-energy mimic of the Higgs-boson mass-energy (using feH1, e.g.).

$$\mathrm{m_{H\text{-}boson}}\ \mathrm{c}^2 = \left[\mathrm{a}_W\ \mathrm{GF}^{-1/2}\right]\sqrt{\mathrm{feH1}} =$$

$$= \left[\frac{3}{2}\left(\frac{\pi}{2}\right)^{\frac{1}{12}}\right] \mathrm{m_{W\text{-}boson}}\ \mathrm{c}^2 = 125.19217\ \mathrm{GeV}. \tag{1.3A-2-4}$$

Compare with the experimentally accepted [7,8] value of $125.18 \pm 0.16\ \mathrm{GeV}$.

To reiterate, equations (3) and (4) incorporate the assumption that, in addition to the fundamental W-boson mediator structure involved in beta–decay, (2), with the associated Fermi constant GF, there exist additional “geometric maximum-energy-density structures” which function as other ‘virtual-mediator-structures”. Such structures are being described according to their gyromagnetic or geometric-curvature characteristics as per (1).

ACKNOWLEDGMENT

Since this work is a continuation of the fundamental endeavor expressed in [5], we again acknowledge the creative critique offered by, Dr. J T Grissom for his valuable suggestions for technical clarification and material emphasis and, the helpful corrective conceptual commentary of Dr. J D Weiss, relative to that work.

REFERENCES

[1] Ciufolini, I. and Wheeler, J. A., Gravitation and Inertia, USA, Princeton University Press, 1996.
[2] Wheeler J. A., Phys. Rev., vol. 97, p.511, 1955.
[3] Wheeler J. A., “Logic, Methodology, and Philosophy of Science”, Proc. 1960 International Congress, USA, Stanford University Press, p.361, 1962.
[4] Clifford, W. K., Proc. Cambridge philosophical society vol.2, p.157, 1876.
[5] Koehler, D. R., Indian Journal of Physics, vol. 87, p.1029, 2013.
[6] Koehler, D. R., The Distorted Universe: From Neutrinos to the Cosmos, The Theory of Nothingness, Kindle: ASIN B00TG26Q7Y, 2015.
[7] https://en.wikipedia.org/wiki/Higgs_boson#cite_note-PDG2018-3]
[8] *M. Tanabashi et al. (Particle Data Group) (2018).* "Review of Particle Physics"*. Physical Review D.* ***98*** *(3).*

1.4 GEOMETROSTATIC GRAVITATIONAL DISTORTIONS

As suggested earlier (Section 1.2), a more inclusive treatment of the total mass energy-density would include in addition to the electromagnetic component, and however small, a gravitational contribution. This notion was partially addressed by requiring that the metric for the Section-1.2 solution mimic the Schwarzschild [25] metric solution. But a more comprehensive inclusion of gravitation in the present undertaking has to include the gravitational field energy in constructing the total field energy equation and subsequently the total, or more appropriate, geometric coupling constant. That is, according to equation (22), the geometrical mimicking process has now produced an expanded composite coupling-constant, $\kappa_{\text{geo}} = \kappa o + \kappa_G/2$ or $\text{Rs}_{\text{geo}} = 2\ \text{Mc}^2(\kappa o + \kappa_G/2)$. This procedure recovers the gravitational coupling-constant of general relativity and consequently both Maxwellian and gravitational physical-structures are geometrically mimicked with a single compound coupling-constant.

Again, after equating the distortional-geometric metric-form to a Schwarzschild metric-form, we also produce the result that $-2/\text{C1} = \text{Rs}_{\text{geo}} = \text{Rs}_{\text{grav}} + \text{Rs}_{\text{geo\_E}}$. In addition, R0 and γ, expressed as ‘weighted means”, which allows for distortional structures with coupling, are

(27) $$\text{R0}_{\text{geo}} = \text{R0}_{\text{E}} + \text{R0}_{\text{G}} \qquad \text{and} \qquad \gamma_{\text{geo}} = 2\,\frac{\text{R0}_{\text{geo}}}{\text{Rs}_{\text{geo}}}.$$

The impact of this more comprehensive field-energy treatment is negligible for a “charged” particle mimic but the expanded coupling-constant characterization transitions to a classical gravitational form as the mass-energy increases or as the coulomb-charge decreases. In this way, the single geometric-distortional solution (equations (11) and (14-18)), with the compound-

coupling-constant, mimics both Maxwellian charged-particle structures and gravitational structures. A “gravitational geometric-distortion” is manifest when the geometric r^{-6} feature, $g_{11}g_{11}((Td_{44} - Td_{11})/2) = (Fd_{mag})^2$, of this distortion is diminished.

It is posited that the radial zero, $\gamma = 2u(ro) = 3.27512 \text{ if } ro = Rs_{geo} = R0_{geo}/u(ro)$ (see equation (19) for the geometric mimic of the Maxwellian tensors), is the geometric manifestation of the Schwarzschild “metric-radial-zero” (the radial singularity classically interpreted as a “black-hole” radius). The radial zeroes, from the tensor field-functions expressed in equation (12), are

(28) $$(1-3u^3)(1-u^3)^2 - 4u^2(Iu-\gamma) = 0 \;\; for \;\; Td_2^2 \,,$$

$$(1-3u^3)(1-u^3)(1-2u^3) - 6u^2(Iu-\gamma) = 0 \;\; for \;\; Td_4^4 \;\; and$$

$$(1-3u^3)(1-u^3)u^3 + 2u^2(Iu-\gamma) = 0 \;\; for \;\; Td_1^1 + Td_2^2 \,.$$

These are the distortional radii at which the geometric-field energy-density-distributions transition from a positive-energy-density configuration to a negative-energy-density configuration; for example, the mass-energy-density-distribution tensor $Td_4{}^4$ transitions at $uo = 1.453 \text{ if } ro = Rs_{geo} = R0_{geo}/uo$. The radial-zero-solution, uo, for the “electric-charge-distortion mimic” is a function only of “electric-charge” Q, by 40 orders of magnitude and is quantized accordingly or, conversely, a quantized negative-energy-density core, described by a geometric radial-zero (uo and ro) produces a quantized “electric-charge”.

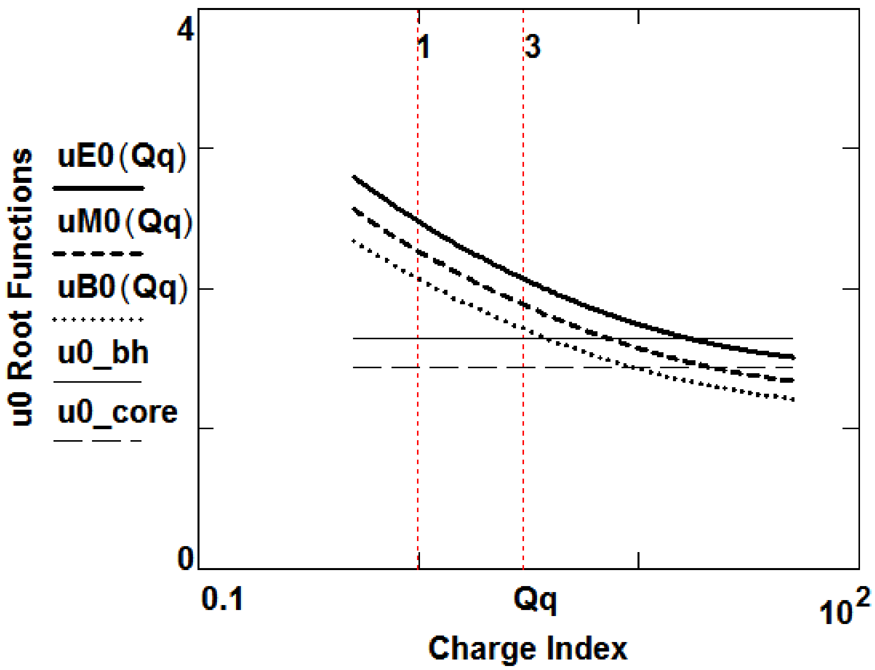

Fig. 1.11 Radial-zero functions u_0 relative to electric-charge values; uE0 for the electrical Td_2^2 function, uM0 for the mass-energy-density Td_4^4 function and uB0 for the magnetic-energy-density $Td_1^1 + Td_2^2$ function.. Abscissa charge-values are displayed as a function of the index Qq. $\mathrm{uo(Qq)}$ is graphically used for the zero-radial-function uo. Also indicated is the E_field quantity, $\mathrm{u0\_core} = \mathrm{uE0(Qq = 0)}$, and a gravitational "black-hole u0_bh" value.

In Fig. 1.11 Qq is the $\mathrm{uo\text{-}quantum\text{-}number}$ = 1, 2, 3 resulting from equation (28) with the solution-defining metric-derivative integration-constant. There is therefore illustrated an overall incremental increase (see equations (11) and (20)) in the radial extent of the electric-charge-mimicked negative-energy-density region caused by the "geometric (γ, $\mathrm{R0}$ and Rs) mimics" of the "electric-charge" physical features.

We see that the negative-energy-density radial region of the distortional-field construct is present even in the absence of the “electric-charge-based” component and is interpreted as, and constitutes, a “gravitational” core-element.

Both Maxwellian and gravitational structures are thereby manifested in the single geometric distortion wherein the gravitational structure is the ground-state interpretation, or the zeroth-order state, of the “geometric-distortional-charge”; the “Q quantum number” is thereby extended to the integer-range 0, 1, 2, 3.

The physical gravitationally-manifested version of the basic geometric structure is exhibited with a significantly smaller coupling constant and, as per the Schwarzschild representation, with a radius dependent on both coupling-constant and physical mass (as compared to the electromagnetically mimicked particle-structures). Without further mimicking constraints, and since the mass-energy equation is an identity, the geometric descriptors $\mathrm{C1_{geo}}$ and $\mathrm{R0_{geo}}$ of this geometrically-modeled gravitational-solution, remain functions only of a mimicked mass-quantity M.

We can also posit and construct a “geometric-mimic” of the “vacuum-fluctuation-radius”. The quantity $\mathrm{Lf} = (\mathrm{hc}\kappa/2\pi)^{1/2}$, in conjunction with a gravitational coupling constant, (i.e. $\kappa = \kappa_{\mathrm{G}} = \mathrm{G}/\mathrm{c}^4$) has heretofore been posited as a vacuum-fluctuation radius [16], or Planck length. Examination and calculation of the negative-energy-core radius, using $\mathrm{ro} = \mathrm{R0}/\mathrm{uo} = \mathrm{Lf}(\mathrm{Lf}/\mathrm{Rs})^{3/2}(\mathrm{Sg_e})^{2/3}/\mathrm{uo}$, reveals that this geometric feature is within 10% of such a “quantum vacuum fluctuation” radius. It is therefore also posited that, in this geometric modeling, the distortional negative-energy region is the analog of the “quantum vacuum fluctuation” region. The

energy-density of the vacuum fluctuation region contributes proportionally to the overall energy-density of the distortional structure since, in particular, the total mass-energy expressed in equations (4 and 21) is a summation from *0 to* infinity. Additionally, in the discussion of "the uncertainty principle of quantum theory and the gravitational effects described by general relativity", where the Planckian fluctuation length (and Planckian mass) is forthcoming, a "modified coupling-constant per the geometric-distortional form for microscopic fundamental particle distortions" produces a statement about "charge and mass". That is, "$\text{planck length} = (hG/2\pi c^3)^{1/2} = (hc\kappa_{geo}/2\pi)^{1/2} = Lf$ ", where Lf is the fluctuation length and $\kappa_{geo} = b(Q/M)^2 + G/2c^4$ is the distortional-coupling constant (see equations (20) and (22)). Such a fluctuation length in the geometric model is not a constant but depends on the mass and charge which produce the geometric distortion, a significantly different result.

However in considering this distortion as a mimic of a gravitational entity ($Q = 0$), a minimum distortional gravitational-mass condition exists. This situation occurs by virtue of the association of the negative-energy core radius with the Schwarzschild radius and by virtue of the geometric maximum-curvature interpretation expressed in the Fermi constant derivation (in Section 1.3). One can, therefore, construct a maximum curvature equation with a resultant gravitationally-minimum mass-energy-representation $(Mc^2)_{grav\_min}$ for a "hole-like" structure (equations 29-30, HOLES). In discusssions of the negative energy-density (pressure) core-regions of this universal (EM as well as gravitational) distorted-geometry structure, it should be emphasized that a negative energy-density gravitational feature (a repulsive gravitational force) is non-Newtonian.

Finally, it is of interest to examine the ratio of the $1/r^6$ tensor-component to the $1/r^4$ tensor-component in the construction of the geometric fields. The "distorted-geometry" field-ratio of the classical energy-density ratio is (@ r = 4 Rs for example)

(31) $\frac{Fd_{mag}^2}{Fd_{14}^2}(r \to 4\ Rs) = 2\ Rs(R0)^3/r^6][[Rs^2/2]/r^4]^{-1} = \gamma^3\ (Rs^2/2)\ (4\ Rs)^{-2} = 782$ with

$\gamma \stackrel{\text{def}}{=} \frac{2\ R0}{Rs}\ ;\ \gamma = \frac{2\ \beta}{\alpha}\ \ for\ EM(\beta elec = 0.1068) structures\ \ and\ \gamma =$

$3.27512\ \ for\ grav. structures.\ \ \frac{Fd_{mag}^2}{Fd_{14}^2}(r \to 4\ Rs) = 1.0978\ \ for\ grav. structures.$.

Actually, the Fd_{14}^2 fields contain r^{-6} elements (see Eq. 8H) of a magnitude comparable to the magnetic-field strengths Fd_{mag}^2, which therefore makes the field-strength ratios comparable in magnitude. Nevertheless, the field strengths (8H and 9H) depart markedly (orders of magnitude) from the classical Newtonian r^{-4} behavior and exhibit potential-well behavior as they radially transition to repulsion at the hole-core.

REFERENCES

[1] Ciufolini, I.; Wheeler, J. A. Gravitation and Inertia; Princeton University Press: Princeton, NJ, 1996

[2] Wheeler, J. A. Phys. Rev. 1955, 97 511-36

[3] Wheeler, J. A. In Logic, Methodology, and Philosophy of Science. Proc.of the 1960 International Congress; Nagel, E.; Stanford University Press, 1962

[4] Clifford, W. K. Proc. of the Cambridge philosophical society 1876, 2 157-58

[5] Anderson, P.R.; Brill, D.R. Phys.Rev. 1997, D56 4824-33

[6] Perry, G.P.; Cooperstock, F.I. Class.Quant.Grav. 1999, 16 1889

[7] Sones, R.A. Quantum Geons, (2018) arXiv:gr-qc/0506011

[8] Stevens, K.A.; Schleich, K.; Witt, D.M. Class.Quant.Grav. 2009, 26:075012

[9] Vollick, D.N. *Class.Quant.Grav*. 2010, 27:169701

[10] Louko, J. J. Phys.: Conf. Ser. 2010, 222:012038

[11] Einstein, A. The Meaning of Relativity; Princeton: Princeton, NJ, 1955

[12] Tolman, R. Relativity, Thermodynamics and Cosmology; Dover: Mineola, NY, 1987; p245

[13] Tolman, R. Phys. Rev. 1930, 35 875

[14] Visser, M. Lorentzian Wormholes: from Einstein to Hawking; AIP Press: Woodbury, NY, 1995

[15] Linder, E. V. First Principles of Cosmology; Addison Wesley: Essex, England, 1997; p23

[16] Reissner, H. Ann. Phys. 1916, 59 106

[17] Nordström, G. Proc. Kon. Ned. Akad. Wet. 1918, 20 1238

[18] C. Amsler *et al.* (Particle Data Group) Physics Letters 2010, B667 1

[19] Mandelbrot, B. Science New Series 1967, 156 No. 3775 636-38

[20] Bromley, D. A. Gauge Theory of Weak Interactions; Springer, 2000

[21] Pearson, K. Philosophical Magazine Series 1900, 50 157-175

[22] Soper, H. E.; Young, A. W.; Cave, B. M.; Lee, A.; Pearson, K. Biometrika 1917, 11 328-413

[23] Fermi, E. Z. Physik 1934, 88 161

[24] Halzen, F.; Martin, A. D. Quarks and Leptons; John Wiley and Sons, 1984; p257

[25] Schwarzschild Berl. Ber. 1916, 424

[26] Antonucci, R., Ann Rev in Astronomy and Astrophysics 1993 31 (1), 473–521

[27] Urry, C.; Padovani, P. Publications of the Astronomical Society of the Pacific 1995 107, 803–845

[28] Koehler, D. R., Indian J. Phys. 87 1029 (2013) DOI 10.1007/s12648-013-0321-5 .

[29] Koehler, D. R., The Distorted Universe: From Neutrinos to the Cosmos, The Theory of Nothingness, Kindle: ASIN B00TG26Q7Y, 2015 .Distorted-Universe-neutrinos-cosmos-Nothingness-ebook

[30] https://en.wikipedia.org/wiki/Sagittarius_A*

Appendix

Approximating the metric

Approximating the metric-derivative function is accomplished by expanding the core-region μ' function around the term u^7 and the flat-region (e-core) μ' function around γ . A mod-function is introduced to help produce derivative-magnitude (μ') equality and derivative-slope (μ'') equality at the transition-radius. The two-region approximation approach is further constrained wherein the core and e-core integrable approximate μa' quantities and the resultant approximate metric, μa, quantities are equated in a continuity fashion at the common radial boundary, labeled Rcore, of the transition region. An "approximation fitting-error" is constructed according to equation (13) and the fitting error is minimized to determine Rcore;

(13) $$\mathrm{rms_{error}} = \sqrt{\frac{1}{\mathrm{N}}\sum\left(\frac{\mu' - \mu'(approx)}{\mu'}\right)^2}.$$

The core and exterior-core (e-core) approximate, μa', solutions are functionally correct at their respective asymptotic values, $\mu'_{\_ecore}$ at $r = \infty$ and $\mu'_{\_core}$ at $r = 0$. Having used the earlier-referenced equation for the temporal metric, $\nu' = (-2 + \mathrm{f(r)})\mu'$, the resulting two-region approximate integrable spatial-metric equations are given by

$$\mathrm{Iu(u)} = \mathrm{u}\left(-1 + \frac{3}{4}\mathrm{u}^3 - \frac{3}{7}\mathrm{u}^6\right),$$

$$\mu'\mathrm{ecore}_{\mathrm{Rcore}}^{\infty} = 2\,\frac{1-\mathrm{u}^3}{\mathrm{Iu(u)} - \gamma}\,\frac{\mathrm{u}^2}{\mathrm{R0}}$$

$$\cong -2(1-\mathrm{u}^3)\,\frac{\mathrm{u}^2}{\mathrm{R0}\,\gamma}\left[1 + \sum_{\mathrm{n}=1}^{2}(-\Delta_{\mathrm{ec}})^{\mathrm{n}}\right] \quad \text{with}$$

$$\Delta_{ec} \stackrel{\text{def}}{=} \frac{-\mathrm{Iu(u)}}{\gamma} \quad \text{and} \quad \gamma = -\mathrm{C1\ R0} \quad \text{and}$$

$$\mu'\mathrm{core}_0^{\mathrm{Rcore}} = -2(1-\mathrm{u}^3)\frac{7}{3}\frac{1}{\mathrm{R0\ u}^5}(1+\Delta_c)\,\mathrm{mod(u)} \quad \text{with}$$

(14) $$\Delta_c \stackrel{\text{def}}{=} \left(-\tfrac{7}{3}\mathrm{u}^{-6} + \tfrac{7}{4}\mathrm{u}^{-3}\right) \quad \text{and} \quad \mathrm{mod(u)} = 1 - \mathrm{B1\ u}^{-3} - \mathrm{B2\ u}^{-6}\,.$$

In the e-core region, the summation function is sufficiently accurate at two terms while one summation term with the *mod* function is used in the core region; see the fitting error calculated below and entered in table 1. Also

(15) $$\nu'_{\mathrm{core}} = \left(-2 + \tfrac{1}{1-\mathrm{u}^3}\right)\mu'_{\mathrm{core}} \quad \text{and} \quad \nu'_{\mathrm{ecore}} = \left(-2 + \tfrac{1}{1-\mathrm{u}^3}\right)\mu'_{\mathrm{ecore}}\,.$$

Therefore,

$$\mu_{\mathrm{ecore}} = \frac{2}{\gamma}\int (1-\mathrm{u}^3)\left[1 + \sum_{\mathrm{n}=1}^{2}(-\Delta_{\mathrm{ec}})^{\mathrm{n}}\right]\mathrm{du}\,; \quad \mathrm{g(ecore)}_{11} = -\exp(\mu_{\mathrm{ecore}})$$

and $$\mu(\mathrm{r}\to\infty) \cong \tfrac{2}{\gamma}\mathrm{u} = -\tfrac{2}{\mathrm{r\ C1}} \quad \text{to yield}$$

$$\mathrm{e}^{\mu} \cong 1 + \mu + \frac{\mu^2}{2} + \cdots \cong 1 - \frac{2}{\mathrm{r\ C1}} + \frac{2}{(\mathrm{r\ C1})^2} - \cdots \stackrel{\text{def}}{=} 1 + \frac{\mathrm{R}s}{\mathrm{r}} + \alpha\mathrm{e}\frac{\mathrm{re}^2}{\mathrm{r}^2}\ldots,.$$

(16) $$\nu_{\mathrm{ecore}} = -2\,\mu_{\mathrm{ecore}} + \tfrac{2}{\gamma}\int[1 + \textstyle\sum_{n=1}^{2}(-\Delta_{\mathrm{ec}})^{\mathrm{n}}]\mathrm{du} \quad \text{and} \quad \mathrm{g(ecore)}_{44} = \exp(\nu_{\mathrm{ecore}}).$$

For the core region,

$$\mu 0_{\text{core}} = \frac{14}{3\ \text{R0}} \int (1 - u^3) u^{-7} (1 + \Delta_c)\, mod(u) du \quad \text{and} \quad \mu_{\text{core}} = \mu 0_{\text{core}} + C_{\mu c} \quad \text{where}$$

(17) $C_{\mu c} = \mu_{\text{ecore}}(@\ r = \text{Rcore}) - \mu 0_{\text{core}}(@r = \text{Rcore})\ \ and\ \ g(\text{core})_{11} = -\exp(\mu_{\text{core}})$.

For the temporal core-metric,

$$\nu 0_{\text{core}} = -2\ \mu 0_{\text{core}} + \frac{14}{3\ \text{R0}} \int \text{u}^{-7} (1 + \Delta_c)\, \text{mod}(\text{u})\text{du} \quad \text{and} \quad \nu_{\text{core}} = \nu 0_{\text{core}} + C_{\nu c} \quad \text{where}$$

(18) $C_{\nu c} = \nu_{\text{ecore}}(@\ r = \text{Rcore}) - \nu 0_{\text{core}}(@r = \text{Rcore})$ and $g(\text{core})_{44} = -\exp(\nu_{\text{core}})$.

AN INTEGRABLE FORMULATION OF THE METRIC DERIVATIVES

9/2015

If the metric derivative μ' is partitioned around u according to Eqs (11) and (A1), then a resultant integrable form becomes

(A1) $$\mu(\mathrm{r}) = \int \frac{2(1-\mathrm{u(r)}^3)}{\mathrm{Iu(u(r))}-\gamma}\frac{\mathrm{u(r)}^2}{\mathrm{R0}}\mathrm{dr} = \int \mu'\,\mathrm{dr} = \int_0^{\mathrm{roo}} \mu\mathrm{C}'\mathrm{dr} + \int_{\mathrm{roo}}^{\infty} \mu\mathrm{EC}'\mathrm{dr} \stackrel{\text{def}}{=}$$

$$\stackrel{\text{def}}{=} \int \left| \frac{2(1-\mathrm{u(r)}^3)}{\mathrm{u(r)}\left[-\mathrm{b}+\frac{3}{4}\mathrm{u(r)}^3-\frac{3}{7}\mathrm{u(r)}^6\right]}\frac{\mathrm{u(r)}^2}{\mathrm{R0}}\mathrm{dr}\right|_0^{\mathrm{roo}} + \int \left|\frac{2(1-\mathrm{u(r)}^3)}{\mathrm{u(r)}[-\mathrm{h}]-\gamma}\frac{\mathrm{u(r)}^2}{\mathrm{R0}}\mathrm{dr}\right|_{\mathrm{roo}}^{\infty}$$
$$+$$
$$\equiv \mathrm{if}(\mathrm{r} < \mathrm{roo}, \mu\mathrm{C}, \mu\mathrm{EC})\,.$$

A first boundary condition, $\mu\mathrm{C(rM0)}' = \mu\mathrm{(rM0)}'$, determines the quantity *b*; $b = 1 + \frac{\gamma}{uM0}$ thus making the core-metric component γ-dependent. $\mathrm{rM0}$ is fixed at the mass-root $\mathrm{uM0}$ with Q = 0 for a “gravitational” distortion or Q = 3 for a distortional electron-mimic. The radial core descriptor *roo* is then determined from the second derivative-matching boundary condition $\mu\mathrm{C(roo)}' = \mu\mathrm{EC(roo)}'$. From this boundary condition on the metric-derivatives at *roo*, we get

(A2) $$\mathrm{uoo} = \mathrm{root}\left(\mathrm{u}\left(-\mathrm{b}+\frac{3}{4}\mathrm{u}^3-\frac{3}{7}\mathrm{u}^6\right)+\mathrm{h\,u}+\gamma,\mathrm{u}\right).$$

A minimization of the fitting-error between $\mu\mathrm{C(r)}' + \mu\mathrm{EC(r)}'$ and $\mu\mathrm{(r)}'$ fixes h at $\mathrm{h} = 0.842(\mathrm{grav})$ or $\mathrm{h} = 1.0(\mathrm{elec})$ and produces, for example, with $\gamma = 2\,\mathrm{uM0}$ (the description of a chargeless mass or

gravitational distortion), $uM0 = 1.45302$ and $uoo = 1.27394$; for the electron-mimic $uM0 = 1.87771$ and $uoo = 1.56937$.

The spatial (μ) metric-derivative functions are illustrated in Fig.A1.

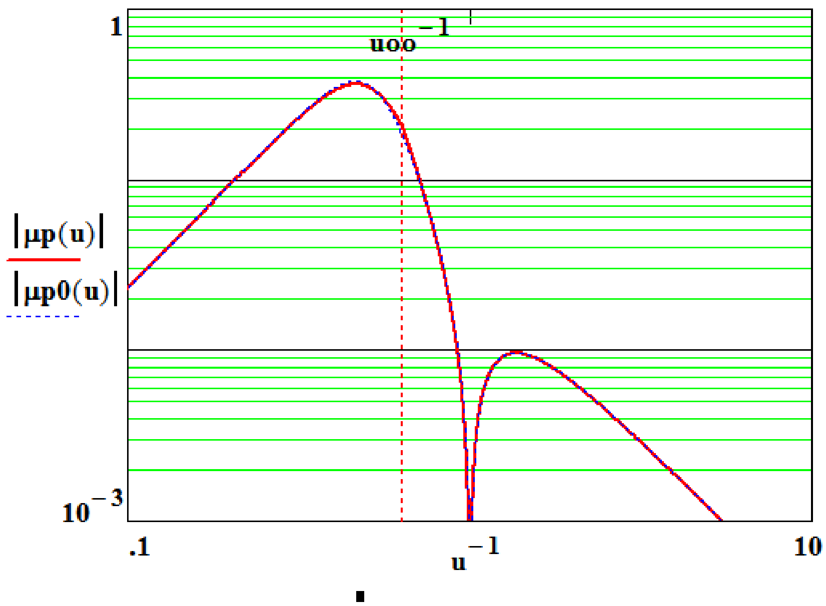

Figure A1. A comparison of the metric-derivative functions $\mu p = \mu C' + \mu EC'$ and $\mu p0 = \mu'$ for a distortional electron-mimic, as a function of the normalized radius u^{-1} .

The analytic forms for $\mu C(r)$, $\mu EC(r)$ and $\mu(r)$ are

(A3) $$\mu C(r) = \frac{1}{3b} \ln\left[\frac{u^6}{28b - 21\,u^3 + 12\,u^6}\right] + \frac{\frac{14}{b} - \frac{112}{3}}{\sqrt{1344\,b - 441}} \operatorname{atan}\left(\frac{-21 + 24\,u^3}{\sqrt{1344\,b - 441}}\right) + Co \quad \text{and}$$

$$\mu EC(r)=\frac{2}{h}\left[-\left(\frac{1}{3}u^2-u\ \frac{\gamma}{2h}+\ \gamma^2\right)u+\left(\left(\frac{\gamma}{h}\right)^3+1\right)\ln\left(\frac{u\,h+\gamma}{\gamma}\right)\right]+Do;$$

$$u=R0/r\,.$$

$$\mu(r)=\text{if}(r<roo,\mu C(r),\mu EC(r)).$$

$Do=0$ is set by the boundary condition for a flat-space metric at $r=\text{infinity}$. A function restricting requirement ($\mu C(roo)=\mu EC(roo)$) for the magnitudes μC *and* μEC at roo determines Co.

Similarly for the temporal metric,

(A4)

$$\nu(r)=\int\frac{-2\left(2\,u(r)^3-1\right)}{Iu\left(u(r)\right)-\gamma}\frac{u(r)^2}{R0}dr=\int\nu'\,dr=\int_0^{roo}\nu C'dr+\int_{roo}^{\infty}\nu EC'dr\stackrel{\text{def}}{=}$$

$$\int\left|\frac{-2\left(2\,u(r)^3-1\right)}{u(r)\left[-b+\frac{3}{4}u(r)^3-\frac{3}{7}u(r)^6\right]}\frac{u(r)^2}{R0}dr\right|_0^{roo}+\int\left|\frac{-2\left(2\,u(r)^3-1\right)}{u(r)[-h]-\gamma}\frac{u(r)^2}{R0}dr\right|_{roo}^{\infty}=\text{if}(r<roo,\nu C,\nu EC).$$

(A5) $$\nu C(r)=\frac{-1}{3\,b}\ln\left[\frac{u^6}{28b-21\,u^3+12\,u^6}\right]-\frac{\frac{14}{b}-\frac{224}{3}}{\sqrt{1344\,b-441}}\text{atan}\left(\frac{-21+24\,u^3}{\sqrt{1344\,b-441}}\right)+Eo\quad\text{and}$$

$$\nu EC(r)=\frac{2}{h}\left[\left(\frac{2}{3}u^2-u\ \frac{\gamma}{h}+2\ \left(\frac{\gamma}{h}\right)^2\right)u-\left(2\left(\frac{\gamma}{h}\right)^3+1\right)\ln\left(\frac{u\,h+\gamma}{\gamma}\right)\right]+Fo\,.$$

$$\nu(r)=\text{if}(r<roo,\nu C(r),\nu EC(r)).$$

The same boundary conditions, as were applied to the spatial μ-metrics, are applied to the $\nu(r)$ functions to define Eo and Fo; Fo is set by the boundary condition for a flat-space metric at $r = \text{infinity}$ and a function restricting requirement for the magnitudes νC *and* νEC at roo *(now*

determined from Eq. A2) sets Eo. The spatial (ν) metric-derivative functions are illustrated in Fig.A2.

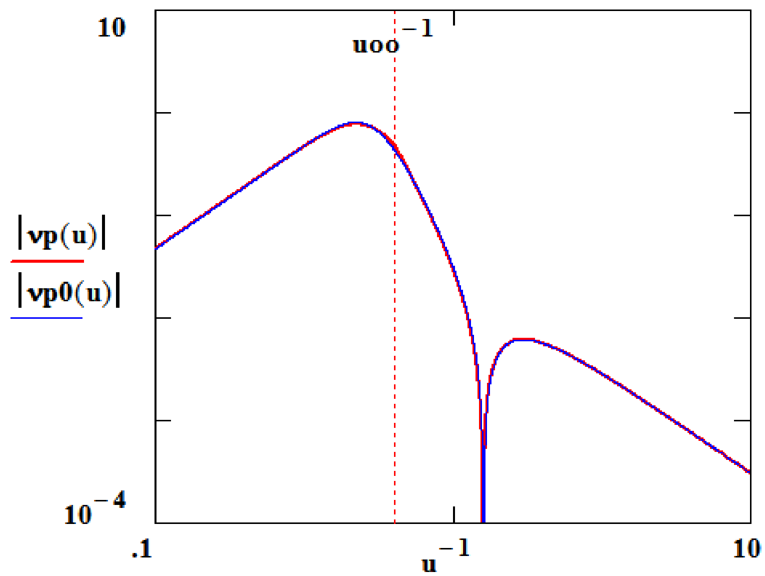

Figure A2. A comparison of the metric-derivative functions $\nu p = \nu C' + \nu EC'$ and $\nu p0 = \nu'$ for a distortional electron-mimic, as a function of the normalized radius u^{-1} .

At the core origin both metric functions are dependent on γ thus producing an "energy-dependent distortion-distinctive" characteristic. All mimics (electromagnetic (electron, muon, tauon, W^{-}boson) and gravitational (holes...) constructed herein therefore exhibit this energy-dependent-metric distortional-core feature.

The null-geodesic core-propagation velocity at $r = 0$ for the electron-mimic is

(A6) $$\mathrm{vel}(0) = \sqrt{\frac{g_{44}}{-g_{11}}} \stackrel{\mathrm{def}}{=} \sqrt{\nu\mu} \quad \text{where} \quad \nu\mu =$$

$$= \exp\left(\frac{1}{3\,b}\ln(144) + \frac{112 - \frac{28}{b}}{\sqrt{1344\,b - 441}}\,\frac{\pi}{2} + Eo - Co \right);\;\; vel(0) = 1.519c.$$

These metric functions and the propagation velocity function are illustrated in Fig. A3.

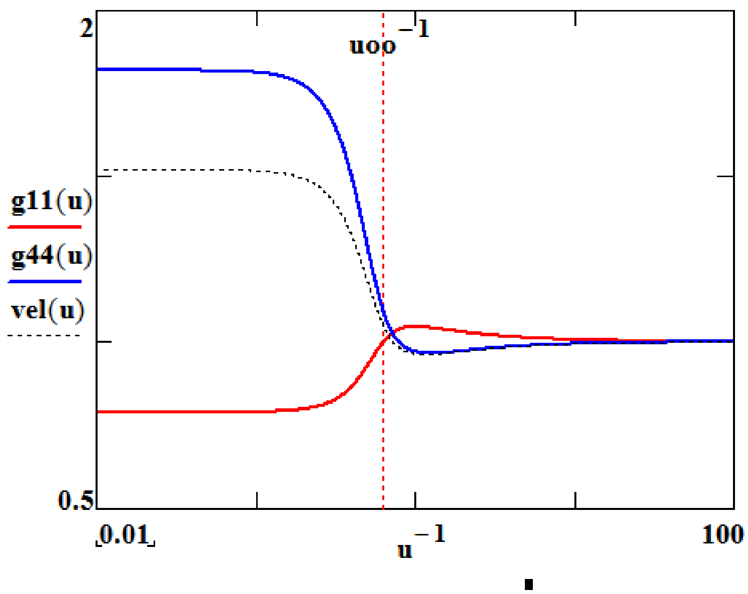

Figure A3. Metric and propagation-velocity functions for a distortional electron-mimic as a function of the normalized radius u^{-1}.

Figures A4 through A6 display the metric functions for a gravitational distortion.

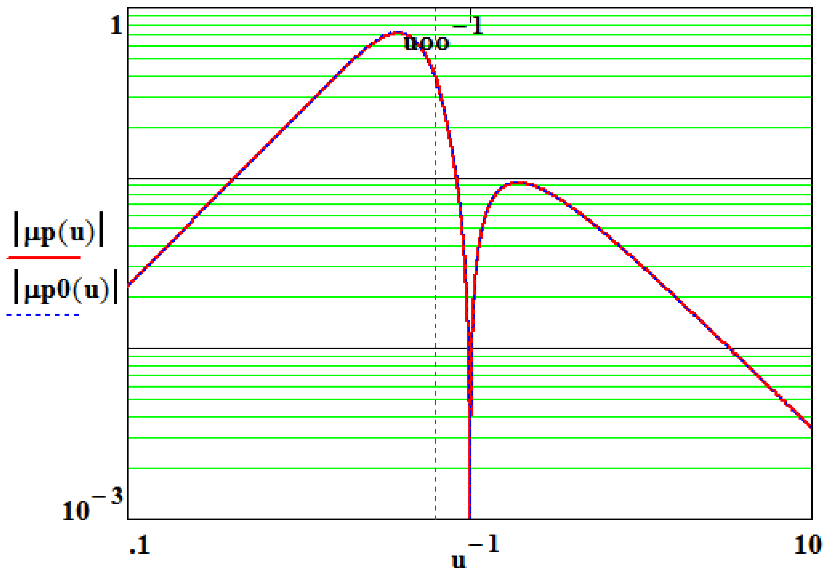

Figure A4. A comparison of the metric-derivative functions $\mu p = \mu C' + \mu EC'$ and $\mu p0 = \mu'$ for a gravitational distortion, as a function of the normalized radius u^{-1} .

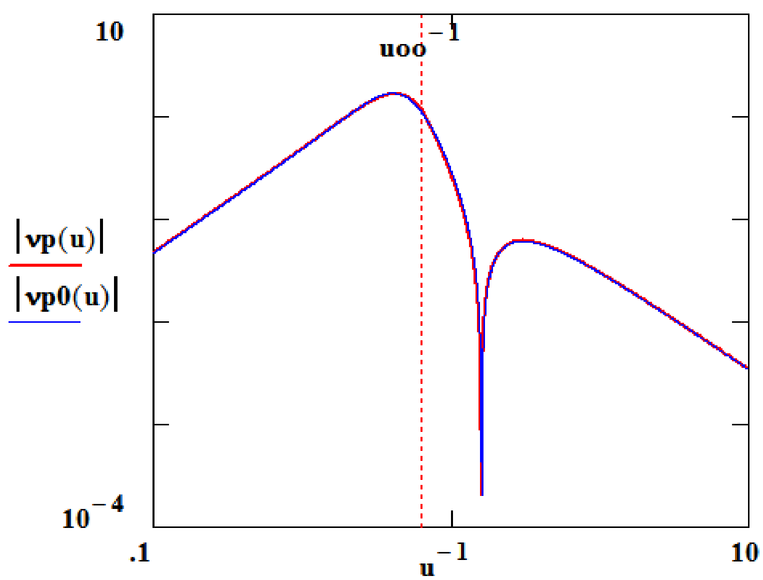

Figure A5. A comparison of the metric-derivative functions $\nu p = \nu C' + \nu EC'$ and $\nu p0 = \nu'$ for a gravitational distortion, as a function of the normalized radius u^{-1} .

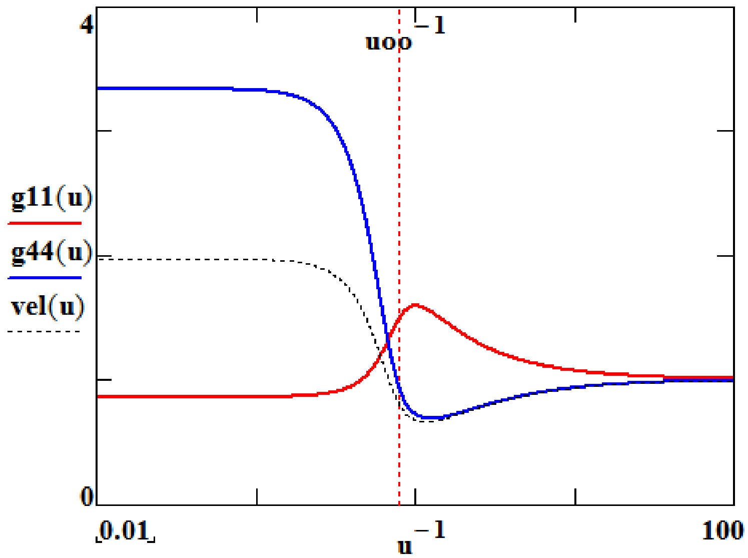

Figure A6. Metric and propagation-velocity functions for a gravitational distortion as a function of the normalized radius u^{-1}.

An increase in the propagation velocity in the core region ($\mathrm{vel}(0) = 1.971c$) for a gravitational distortion (as compared to the electron-mimic distortion) is evident in Fig. A6.

STRUCTURAL EQUATIONS

The calculational treatment employs the isotropic coordinate description of equation (2) and utilized by Tolman [12], where the system of equations represented by equation (1), is shown more explicitly in equation (3) in mixed tensor form;

(3) $$8\pi\kappa T_1^1 = -e^{-\mu}\left[\frac{\mu'^2}{4} + \frac{\mu'\nu'}{2} + \frac{\mu' + \nu'}{r}\right] + e^{-\nu}\left[\ddot{\mu} + \frac{3}{4}\dot{\mu}^2 - \frac{\dot{\mu}\dot{\nu}}{2}\right],$$

$$8\pi\kappa T_2^2 = -e^{-\mu}\left[\frac{\mu''}{2} + \frac{\nu''}{2} + \frac{\nu'^2}{4} + \frac{\mu' + \nu'}{2r}\right] + e^{-\nu}\left[\ddot{\mu} + \frac{3}{4}\dot{\mu}^2 - \frac{\dot{\mu}\dot{\nu}}{2}\right] = 8\pi\kappa T_3^3,$$

$$8\pi\kappa T_4^4 = -e^{-\mu}\left[\mu'' + \frac{\mu'^2}{4} + \frac{2\mu'}{r}\right] + e^{-\nu}\left[\frac{3}{4}\dot{\mu}^2\right],$$

$$8\pi\kappa T_4^1 = + e^{-\mu}\left[\dot{\mu}' - \frac{\dot{\mu}\nu'}{2}\right],$$

$$8\pi\kappa T_1^4 = -e^{-\nu}\left[\dot{\mu}' - \frac{\dot{\mu}\nu'}{2}\right].$$

Metric coupling, that is terms such as $\mu'\nu'$, are apparent in the fundamental curvature equations. The usual notation, where primes denote differentiation with respect to the radial coordinate r and dots denote differentiation with respect to the time coordinate t, is employed. We are considering the static case (where total differentiation replaces partial differentiation) as was also used for Schwarzschild's (gravitational) interior and exterior solutions for the model of an incompressible perfect-fluid sphere of constant density surrounded by empty space [12]. In that work a zero-pressure surface-condition and matching and normalization of the interior and exterior metrics at the sphere radius were used as boundary conditions.

Tolman [13] has shown that the energy of a “quasi-static isolated system” can be expressed as “an integral extending only over the occupied space”, which we will allow to extend to infinity, and where the total energy of such a sphere is therefore expressed as

$$\text{(4)} \qquad \mathrm{U(sphere\ total)} = \int_0^\infty \left(T_4^4 - T_1^1 - T_2^2 - T_3^3\right)\sqrt{\left(-g_{11}\right)^3 g_{44}}\, 4\pi\, r^2\, dr = M_{\mathrm{sphere}}\, c^2 \ .$$

This mass-energy representation will be used throughout in calculating the distortional mass-energies. The distortional-tensor energy-density amplitudes manifested in these presently calculated geometric representations are both negative and positive, that is, there are both negative energy-density [14] and positive energy-density regions internal to the distortions. However, the modeled distortions for the mimicked elementary particles all exhibit positive mass-energies. Since geometric distortional fields arise from the same energy-density tensors, the negative energy-density geometric regions are also sources of negative energy-density field quantities.

We constrain the modeling by requiring that the descriptive stress-energy tensors satisfy a “constitutive relation” or an “equation-of-state” between the temporal and spatial tensor-curvature elements, namely

$$Td_4^4 = -\left(Td_1^1 + Td_2^2 + Td_3^3\right).$$

We have introduced the explicit distortional-tensor symbolism Td for the geometric quantities. Contrast this perspective with cosmological renditions of geometric curvature structure resulting from “matter” causation, wherein several “equations of state” relating to the “matter”

variables ρ (density) and p (pressure) have been forthcoming [15] where $p = \sigma\, \rho$ and where σ varies from -1 to +1.

Inherent in the geometric "equation-of-state" constraint is the requirement that the descriptive stress-energy tensor, Td, be Maxwellian in nature; the mimicking process is therefore limited to asymptotically flat-space regions of the manifold since $1/r^2$ field behavior does not adequately describe elementary-particle structural-detail. For the presently described spherically symmetric Maxwellian case, ϕ, the electrostatic potential, is a function of r alone, and the Maxwellian electromagnetic tensor and the associated field tensor $F_{1\mu}$ can be constructed according to equation (5), where the only surviving field tensor components are

$$F_{21} = - F_{12}\,,\, F_{13} = - F_{31} \quad \text{and} \quad F_{14} = - F_{41}\,, \quad \text{i.e.}$$

(5) $$T^{\mu\nu} = - g^{\nu\beta}F^{\mu\alpha}F_{\beta\alpha} + \frac{1}{4}g^{\mu\nu}F^{\alpha\beta}F_{\alpha\beta} \quad \text{or} \quad T^{\mu\mu} = - g^{\mu\mu}F^{\mu\alpha}F_{\mu\alpha} + \frac{1}{4}g^{\mu\mu}F^{\alpha\beta}F_{\alpha\beta}\,,$$ then

$$T_4^4 = \frac{(F_{12}F^{12} + F_{13}F^{13} - F_{14}F^{14})}{2}, \quad T_1^1 = \frac{(- F_{12}F^{12} - F_{13}F^{13} - F_{14}F^{14})}{2},$$

$$T_2^2 = \frac{(- F_{12}F^{12} + F_{13}F^{13} + F_{14}F^{14})}{2} \quad \text{and} \quad T_3^3 = \frac{(F_{12}F^{12} - F_{13}F^{13} + F_{14}F^{14})}{2}\,.$$

The resultant field quantities are

(6) $$(F_{14})^2 = - \left(T_4^4 + T_1^1\right)g_{11}\, g_{44} = \left(T_2^2 + T_3^3\right)g_{11}\, g_{44}\,,$$

$$(F_{12})^2 = - \left(T_2^2 + T_1^1\right)g_{11}\, g_{11} \quad \text{and} \quad (F_{13})^2 = - \left(T_3^3 + T_1^1\right)g_{11}\, g_{11}\,.$$

Therefore, we see that the static-spherically-symmetric Maxwellian tensors exhibit the same stress and energy relationship as the geometric tensors,

(7) $$T_4^4 = -\left(T_1^1 + T_2^2 + T_3^3\right).$$

The present geometric-modeling endeavor, with its Maxwellian-tensor-form mimicking-component, has produced the fundamental and limiting agent for the currently-studied distorted geometry, namely a particular constraining functional relationship between the geometry-defining tensors (for an empty-space geometry, all of the components of the energy-momentum tensor are zero). In using this simple equation-of-state, equation (7), as a restricting distortional-model tensor relationship, we thereby elicit the metric-defining differential equations for such a family of geometric distortions.

In the current procedural characterization, one has sufficient information to move to a solution of the differential equations without explicitly stating any “material” energy densities, thereby maintaining the spatial-distortion causative-perspective. The metric μ and ν solutions can consequently determine the resultant energy tensors. The consequent equation however still involves both temporal, ν, and spatial, μ, variables and accordingly requires one further qualifying distortional relationship to afford solution. In generalized format we write such a relationship as

$$\nu' = \left[-2 + f(r)\right]\mu' \text{ (conveniently simple)}$$

with $f(r)$ further defined in order to mimic Maxwellian behavior. Examination of the Maxwellian field quantities F_{12} and F_{14} helps in regard to defining $f(r)$ and for the present modeling work, we use the fundamental distortion-defining form

(8) $$f(r) \stackrel{\text{def}}{=} \left(1 - u(r)^n + \beta\, u(r)^{2n}\right)^{-1} \text{ with } u(r) \stackrel{\text{def}}{=} \left(R0/r\right).$$

$R0$ is a distortional-characteristic, or normalizing, radius and β is a measure of the second-order radial-function present in the distortion. In the following development we utilize n = 3 for the modeled particles; down-quark (particle 1), electron (particle 2), muon (particle 3), up-quark (particle 4) and tauon (particle-5). The present functional construction can be compared with the Schwarzschild solution [12] in isotropic coordinates where

(9) $$g_{11} \stackrel{\text{def}}{=} -\exp(\mu) = -(1+u(r))^4 \quad \text{and} \quad g_{44} \stackrel{\text{def}}{=} \exp(\nu) = \left[\frac{1-u(r)}{1+u(r)}\right]^2 \quad \text{or}$$

$$\nu' = -\left(1-u(r)\right)^{-1}\mu' \text{ with } u(r) \stackrel{\text{def}}{=} \frac{Rs}{4r}; \quad Rs \stackrel{\text{def}}{=} \text{Schwarzschild radius}.$$

It will be found in the following development that the simpler $(\beta = 0)$ distortional form is adequate to mimic the physical characteristics of the modeled particles.

Imposing equation-of-state relationship (7), the metric differential equation is

(10) $$\mu'' + \frac{f'}{f}\mu' + \frac{1}{2f}\left[\left(f-3\right)\left(f-1\right)+f\right]\mu'^2 + \frac{2\mu'}{r} = 0.$$

A solution to this equation is found to be

(11) $$\mu' = \frac{2}{r^2 f}H(r) \text{ with } H(r)^{-1} = \int \frac{(f-3)(f-1)+f}{(r\,f)^2}\,dr + C1 \stackrel{\text{def}}{=} \frac{Iu}{R0} + C1 \quad \text{or}$$

$$\mu' = \frac{2(1-u^3+\beta u^6)}{(Iu + R0\,C1)}\frac{u^2}{R0} = \frac{2(1-u^3)}{(Iu-\gamma)}\frac{u^2}{R0} \quad \left(\begin{matrix}\text{for } \beta = 0) \\ \text{and } \gamma \stackrel{\text{def}}{=} -C1\,R0\end{matrix}\right)$$

where

$$Iu(u) = u\left[-1 + \frac{3}{4}u^3 - \frac{3}{7}(\beta+1)u^6 + \frac{3}{5}\beta\,u^9 - \frac{3}{13}\beta^2 u^{12}\right] =$$

$$= \mathrm{u}\left[-1 + \frac{3}{4}\mathrm{u}^3 - \frac{3}{7}\mathrm{u}^6\right] \text{ (for } \beta = 0) .$$

Equation set (3) can now be rewritten for a static system and, while maintaining the use of relationship (8), the result is,

(12) $$8\pi\kappa\, \mathrm{Td}_1^1 = -\mathrm{e}^{-\mu}\mu' \left[\frac{\mu'}{4}\left(2\,\mathrm{f} - 3\right) + \frac{\mathrm{f} - 1}{\mathrm{r}}\right], \quad \text{or}$$

$$8\pi\kappa\, \mathbf{Td_1^1} = -\mathrm{e}^{-\mu}\frac{1}{(\mathrm{Iu} - \gamma)}\left(\frac{\mathrm{u}^2}{\mathrm{R0}}\right)^2 \left[\frac{1 - \mathrm{u}^3}{(\mathrm{Iu} - \gamma)}\ (3\, u^3 - 1\,) + 2u^2\right]$$

$$8\pi\kappa\, \mathrm{Td}_2^2 = \mathrm{e}^{-\mu}\, \mu' \ \left[\frac{-1}{2\,\mathrm{f}}\mathrm{f}\,' + \frac{1}{4\,\mathrm{f}}\left(2\mathrm{f} - 3\right)\mu\,' + \frac{1}{2\,\mathrm{r}}\left(\mathrm{f} - 1\right)\right] = 8\pi\kappa\, \mathrm{Td}_3^3\,, \quad \text{or}$$

$$8\pi\kappa\, \mathbf{Td_2^2} = \mathrm{e}^{-\mu}\frac{1}{(\mathrm{Iu} - \gamma)}\left(\frac{\mathrm{u}^2}{\mathrm{R0}}\right)^2 \quad \left[4\, u^2 + (3u^3\ - 1\,)\,\frac{(1 - u^3)^2}{(\mathrm{Iu} - \gamma)}\right] = \ 8\pi\kappa\, \mathrm{Td}_3^3$$

$$(\mathbf{Fd_{14}})^{\mathbf{2}}(r \to \infty) = -\mathrm{g}_{11}\mathrm{g}_{44}\left(-2\ \mathrm{Td}_2^2\,\right) \ = \ \frac{-2}{8\pi\kappa}\frac{1}{(\,-\gamma)}\left(\frac{\mathrm{u}^2}{\mathrm{R0}}\right)^2 \quad \left[4\, u^2 + \frac{1}{(\,\gamma)}\right]$$

$$\left(\mathbf{Td_2^2} + \mathbf{Td_1^1}\right) = \frac{1}{8\pi\kappa}\ \mathrm{e}^{-\mu}\frac{1}{(\mathrm{Iu} - \gamma)}\left(\frac{\mathrm{u}^2}{\mathrm{R0}}\right)^2 \ \left[2\, u^2 - \frac{1 - \mathrm{u}^3}{(\mathrm{Iu} - \gamma)}\ (3\, u^3 - 1\,)\, u^3\right]$$

$$((\mathbf{Fd_{12}})^{\mathbf{2}} + \ (\mathbf{Fd_{13}})^{\mathbf{2}})(r \to \infty) = -2\mathrm{g}_{11}\mathrm{g}_{11}\left(\mathbf{Td_2^2} + \mathbf{Td_1^1}\,\right) \stackrel{\text{def}}{=} \mathbf{Fd_{mag}}^2 \ =$$

$$= \frac{-2}{8\pi\kappa}\ \frac{1}{(\,-\gamma)}\left(\frac{\mathrm{u}^2}{\mathrm{R0}}\right)^2 \ [2\, u^2]$$

$$8\pi\kappa\, \mathrm{Td}_4^4 = \mathrm{e}^{-\mu}\mu'\left[\frac{1}{\mathrm{f}}\mathrm{f}\,' + \frac{\mu'}{4\mathrm{f}}(2\mathrm{f} - 3)(\mathrm{f} - 2)\right] .$$

Both mass and field equations are dominated by the μ' function, but the radial region near the geometric origin requires a precise functional description of the metric quantities g_{44} and g_{11} to accurately characterize the fundamental physical quantities. In fact, as will be shown, the mass-energy quantity is almost exclusively generated by the transition region from "flat-space" to "distorted-space". Although integration of the μ' form of the non-integrable equation (11) for the "total" region has not been forthcoming, we have constructed approximate metric-derivative, μ', solutions in both the asymptotically flat region and the core region; for equations (13-18), see APPENDIX "approximating the metric".

The metric quantities g_{44} and g_{11} behave consistently with the classical notion of a "Lorentzian-Riemannian smooth manifold with a continuous two-index metric tensor field, non-degenerate at each point of the manifold, which is a basic ingredient of general relativity and other metric theories of gravity" [1].

After solving for μ and subsequently forming the asymptotic metric form, that is, the expanded large-radius metric, we have equated the distortional-geometric form to a Schwarzschild form with the result that $2/C1 = \text{-}Rs$. See for comparison the Reissner [16] and Nordstrom [17] metric form constructed in the standard coordinate system for an object with mass *m* and charge *e*. Having constrained the first order large-r (or $r\rightarrow\infty$) metric behavior to the Schwarzschild value $Rs/r \stackrel{\text{def}}{=} 2\kappa\frac{Mc^2}{r} = \text{-}\,2/(C1\,r)$, we have ascribed to the model the geometrically-generated characteristic of "mass-energy" via an undetermined "microscopic geometrostatic coupling-factor", κ. In this characterization, $C1$ must also be negative to satisfy the "pseudo-magnetostatic" field constraint elaborated below. Incorporation of the $Fd_{14}{}^2 \stackrel{\text{def}}{=} \left(\frac{q}{4\pi\varepsilon o\, r^2}\right)^2\frac{\varepsilon o}{2}$ term (q

is the charge quantity and εo is the permittivity constant) implies an inclusion of the geometrically-generated characteristic of "electrostatic charge-energy" in the model (also see Tolman [12]).

We now examine the geometrostatic field quantities mimicking the Maxwellian field quantities ${F_{14}}^2$ and ${F_{12}}^2$. We do so by comparing at "classical large-radii regions" with the geometrostatic field quantities of equation (19).

(19) $\quad (\mathbf{Fd_{14}})^2 = \text{-}g_{11}g_{44}\left(\mathbf{Td_4^4} + \alpha 1\ \mathbf{Td_1^1}\right)$ and

$$(\mathbf{Fd_{14}})^2(r\rightarrow\infty) \stackrel{\text{def}}{=} \left(\frac{1}{C1}\right)^2 \frac{2}{8\pi\kappa}\ \frac{1}{r^4} = \frac{Rs^2}{2}\frac{1}{8\pi\kappa}\ \frac{1}{r^4} \stackrel{\text{def}}{=} \left(\frac{q}{4\pi\varepsilon o\ r^2}\right)^2 \frac{\varepsilon o}{2}\ .$$

$$({\mathbf{Fd_{12}})^2}^2 + ({\mathbf{Fd_{13}})^2}^2 = 2g_{11}g_{11}\left(\frac{\mathbf{Td_4^4}\text{ - }\mathbf{Td_1^1}}{2}\right) \stackrel{\text{def}}{=} {\mathbf{Fd_{mag}}}^2 \quad \text{and}$$

$$ {\mathbf{Fd_{mag}}}^2(r\rightarrow\infty) = 2\ Rs\ R0^3\,\frac{1}{8\pi\kappa}\ \frac{1}{r^6} \stackrel{\text{def}}{=} \frac{\mu o}{2}\left(\frac{\mu_{spin}}{2\pi}\right)^2 \frac{1}{r^6}$$

where

$$\mu\_spin \stackrel{\text{def}}{=} \left(\frac{g_e}{2}\frac{Qe}{3M}\right)S\hbar \quad \text{and} \quad g_e{=}2.0023193043\ 6\ .$$

For forming the "geometric-field tensors", the tensors Td_4^4 and Td_1^1 are considered and defined as the basis elements of the geometric function space, that is, ${Fd_{14}}^2 = \alpha 0\ Td_4^4 + \alpha 1\ Td_1^1$ and ${Fd_{12}}^2 = \alpha 3\ Td_4^4 + \alpha 2\ Td_1^1$. From a geometric mimicking perspective we use therefore $\alpha 0 = 1$ and $\alpha 1 = 1$ to generate the electrostatic field and $\alpha 3 = 1$ and $\alpha 2 = \text{-}1$ to generate the magnetic field (see equations (6) and (7)). Mathematically, it would appear that the physical-field elements

thus formed are geometric set-elements in that the numbers, the coordinates of the “vector” Fd^2 with respect to the basis set, are integer in character.

Because of the fundamental geometrostatic equation-of-state relationship, the remaining Td_2^2 and Td_3^3 tensor elements are considered constructs of the basis tensors Td_4^4 and Td_1^1, since $\mathrm{Td}_2^2 = \mathrm{Td}_3^3 = -\left(\mathrm{Td}_4^4 + \mathrm{Td}_1^1\right)/2$, and therefore not basis elements themselves. Also for the geometrostatic case, the ${\mathrm{Fd}_{12}}^2$ and ${\mathrm{Fd}_{13}}^2$ field quantities are identical and therefore considered functionally addable, at the tensor expression level, to form the single field quantity ${\mathrm{Fd}_{\mathrm{mag}}}^2$, we have inherently used the Maxwellian values $\alpha 3 = 1$ and $\alpha 2 = -1$ to achieve asymptotic r^{-6} behavior. Although there are no “moving” charges in this static spherically symmetric model, the geometric field tensor entity $\left(\mathrm{Fd}_{\mathrm{mag}}\right)^2$ is non-zero and therefore both “pseudo-electrostatic” and “pseudo-magnetostatic” distortional-fields are produced. Spherical symmetry precludes azimuthal and polar fields and therefore we are mimicking an r-dependent, r-directed field. The “pseudo-magnetostatic” distortional-field source-strength is that of a “magnetic-dipole of magnitude to produce the dipole-axial-field”.

The electrostatic and magnetostatic constraints (where h = Planck’s constant q = particle electric-charge, M = particle mass, μo = permeability constant and c = speed of light ≡ the flat-space propagation-velocity within the geometric manifold), constructed at large radii with r^{-4} and r^{-6} behaviors, have therefore produced (or required for mimicking), in conjunction with the “metric mass-energy” constraint, that the coupling constant be a variable, $\kappa\mathrm{o} \stackrel{\mathrm{def}}{=} \kappa = \mu\mathrm{o}\left(\frac{\mu\mathrm{spin}}{\hbar\,\mathrm{c}\,\mathrm{S}\,g_e}\right)^2 /2\pi$. Having mimicked both mass-energy and electromagnetic-energy behavior, the coupling constant is a function of both source entities, the electric charge and the mass, but in a combined fashion

expressed through the single physical descriptor μ_spin. These constraints have also determined the geometrostatic quantities, R0 (the distortional-characteristic radius), and C1 (the metric-derivative integration constant). The results are summarized in equation (20); κ, C1 and R0 have been expressed to show more explicitly the charge q and mass M dependence. The three geometric descriptors have been fixed by the two physical descriptors since C1=C1(κ,M) and R0=R0(κ,M).

(20) $$\kappa o = \frac{\alpha\,\hbar c \left(\frac{Q}{3}\right)^2}{2\left(Mc^2\right)^2} = \frac{\mu o}{2\pi}\left(\frac{\mu\_spin}{\hbar\, c\, S\, g_e}\right)^2 \;,\;\; C1 = -\frac{2}{Rs} = -\frac{1}{\left(\kappa o\, Mc^2\right)}$$

and $$R0^3 = \frac{1}{3}\left(\hbar c\, S\, g_e\right)^2 \frac{\kappa o}{Mc^2} = \frac{1}{3}\frac{\mu o}{2\pi}\frac{\mu\_spin^2}{Mc^2}\;.$$

A structural-constant is manifested in the 1st mass-moment, $R0\, Mc^2$, or

(20a) $$R0\, Mc^2 = \beta\, \hbar c \quad \text{with} \quad \beta = \left[\left(S\frac{ge}{2}\frac{Q}{3}\right)^2 \alpha\, \frac{2}{3}\right]^{1/3}\;.$$

β originally [28-29] erroneously presented as $\beta = \left[\left(S\frac{ge}{2}\frac{Q}{3}\right)^2 \alpha\right]^{1/3}$.

The quantity $Lf \stackrel{\text{def}}{=} \sqrt{hc\,\kappa o}$ in conjunction with a geometrically-defined gravitational coupling constant, (i.e. $\kappa o \equiv \kappa_G \equiv G/c^4$) has heretofore been posited as a vacuum-fluctuation radius [2]. Q (quantized) = ± 1, ± 2, or ± 3, e ≡ electron charge, α ≡ αfs ≡ fine structure constant, g ≡ particle g-factor and S ≡ particle spin-factor. Although a classical presentation would not require a "quantization" restriction, we have included this feature to reflect experimental reality.

Finally, the geometrostatic sphere "mass-energy" equation must be satisfied for internal integrity and modeling success. If the second-order distortion-component were present, the remaining geometric descriptor, β, would be constrained through the "sphere-mass-energy" equation (4). By using the "equation-of-state" relationship for the geometric tensors, the mass equation integrand becomes $2\,\mathrm{Td}_4^4 \sqrt{\left(\text{-}g_{11}\right)^3 g_{44}}\, 4\pi r^2$, a function of the single geometric tensor element Td_4^4. Writing the tensor component explicitly, we have for the "sphere mass energy", a product of tensor energy-density and the distortional differential volume element.

(21) $\quad \mathrm{U(sphere)} = \int_0^\infty 2\,\mathrm{Td}_4^4 \sqrt{\left(\text{-}g_{11}\right)^3 g_{44}}\, 4\pi\, r^2\, dr \stackrel{\text{def}}{=} M_{\text{sphere}}\, c^2$

or $\quad \mathrm{U(sphere)} = \int_0^\infty \rho\mathrm{Mass}\, dr \quad$ where

$$\rho\mathrm{Mass}\ (\text{for } \beta = 0) = \frac{1}{\mathrm{Iu} - \gamma}\left[\frac{f^{-1}}{\mathrm{Iu} - \gamma}\left(2 - \frac{3}{f}\right)\left(1 - \frac{2}{f}\right) - 6u^2\right]\frac{u^2}{\kappa}\left(|g_{11}|g_{44}\right)^{0.5} \quad \text{and}$$

$$\gamma \stackrel{\text{def}}{=} \text{-C1 R0} = \frac{2\ \mathrm{R0}}{\mathrm{Rs}} = \left(\frac{1}{3}\left(\frac{2\ \mathrm{ge\ S}}{\alpha}\right)^2 \left(\frac{Q}{3}\right)^{-4}\right)^{1/3}.$$

One can express the mass-energy integral in "normalized coordinates";

(21a) $\quad \mathrm{U(sphere)} = Mc^2 \int_0^\infty \rho\mathrm{Mass1}\, du \stackrel{\text{def}}{=} M_{\text{sphere}} c^2 \quad$ with

$$\rho\mathrm{Mass1} = \frac{\gamma}{\mathrm{Iu} - \gamma}\left[\frac{f^{-1}}{\mathrm{Iu} - \gamma}\left(2 - \frac{3}{f}\right)\left(1 - \frac{2}{f}\right) - 6u^2\right]\left(|g_{11}|\, g_{44}\right)^{0.5}.$$

Then it is seen that the integral must evaluate to unity for equality. Expressing the mass energy-density in this fashion incorporates the effect of the distorted volume on the mass-energy's radial

dependence. The sphere-distortion energy is thus seen to be a function of the geometric descriptor β (if non-zero), to “charge energy” through the integration constant γ and to “spin-energy” through the coupling constant κ.

One comprehensively describes such a geometric distortion family therefore by mimicking a physical “mass” quantity and a “spin” quantity, the “charge” quantity being subsumed in the former “spin” quantity. This should arise from the “two-basis-tensor” geometric foundation. The “mass-energy” quantity is further satisfied internal to the model in the geometrostatic tensor construct of equation (4). In summary, equations (8, 10-12 and 14-20) form the equation set for describing the distortional family’s “particle-like” characteristics and its associated Maxwellian-like fields. Classically and geometrically, any mass quantity is allowed and describable.

Since the distortional description itself yields a constrained value for the geometrostatic coupling constant, we see that at the mass and charge levels considered here, considerably larger values than the gravitational coupling constant are involved. It is to be noted that the gravitational coupling constant, G/c^4, is approximately 37−42 orders of magnitude smaller than these geometrostatic Maxwellian-mimicked coupling-constant values (see equation (20) for mass and Q dependence or the following defining-equation (22) for comparison purposes).

(22) $\text{Gravitational Field Energy density(units of Joules/meter}^3,$

$$u_G = \frac{G(Mc^2)^2}{8\pi c^4}\frac{1}{r^4} = \kappa_G \frac{(Mc^2)^2}{8\pi r^4};\ \kappa_G \overset{\text{def}}{=} \frac{G}{c^4}\ .$$

$\text{Electrostatic Field Energy density}$

$$u_E = \frac{\varepsilon o}{2} E^2 = \frac{\varepsilon o}{2} \left(\frac{q}{4\pi\varepsilon o}\right)^2 \frac{1}{r^4} = 2\ \kappa o \frac{(Mc^2)^2}{8\pi r^4}; \quad \kappa o = \frac{1}{8\pi\ \varepsilon o} \frac{(q)^2}{(Mc^2)^2}\ .$$

Magnetostatic Field Energy density,

$$u_B = \frac{1}{2\mu o} B^2 = \frac{\mu o}{2} \left(\frac{\mu\_spin}{2\pi}\right)^2 \frac{1}{r^6} = 2\ \kappa o \frac{1}{8\pi r^6} (\hbar\ c\ S\ g_e)^2\ .$$

Geometrostatic Field Energy density,

$$u_{geo} = \text{-}g_{11} g_{44} \left(Td_4^4 + Td_1^1\right) + 2 g_{11} g_{11} \left(\frac{Td_4^4 \text{ - } Td_1^1}{2}\right) =$$

$$= \text{as } r \to \infty\ = \kappa_{geo} \frac{(Mc^2)^2}{4\pi r^4} \left\{1 + \frac{(\hbar c\ S\ g_e)^2}{(Mc^2)^2 r^2}\right\}, \quad \kappa_{geo} = \kappa o + {}^{\kappa_G}/_2\ ,$$

$$u_{G\_geo}\ = \kappa_{geo} \frac{(Mc^2)^2}{8\pi r^4}\ , u_{E\_geo} = 2\ \kappa_{geo} \frac{(Mc^2)^2}{8\pi r^4}\ \text{ and }\ u_{B\_geo} =\ 2\ \kappa_{geo} \frac{1}{8\pi r^6} (\hbar\ c\ S\ g_e)^2\ .$$

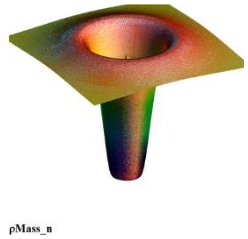

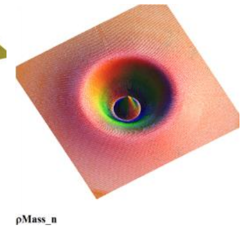

FERMI CONSTANT

To further illustrate quantitatively the relative shape-similarity of the distortional structures manifested in a structural rearrangement process, we form a geometric-similarity measure taken from Pearson's "product-moment correlation function" [21,22] and specified in modified form in equation (24), where the subscripts *m* and *n* are those of section 1.2;

$$\text{(24)} \qquad \mathrm{rPear}_{m,n} \stackrel{\text{def}}{=} \frac{\sum_{i=1}^{n} |\rho\mathrm{Mass}_m||\rho\mathrm{Mass}_n|}{\sqrt{\sum_{i=1}^{N} (\rho\mathrm{Mass}_m)^2}\sqrt{\sum_{i=1}^{N} (\rho\mathrm{Mass}_n)^2}} \ .$$

Removal of Pearson's functional averaging element and the use of the absolute-value characterization of the mass-energy-distributions produce equal functional weighing of the negative mass energy-density radial regions of the distortional-state. In Fermi's characterization of the beta decay particle-restructuring process [23], now described as an "electroweak interaction" phenomenon, we see a characterization of the strength of the process quoted as a product-function involving an "energy (field)" factor and an "associated spatial volume factor". For the geometric domain we interpret such a characterization as a constraining structural description of the distortional-feature which mediates the restructuring or decay process. The constraint on the geometrical transitional entity therefore is that it exhibits the physical features characteristic of the Fermi (Universal Fermi Interaction) constant, GF, or, that it possesses a "pseudo-volume" and

“mass-energy-content” product equal to GF. The candidate satisfying such a description most comprehensively is the presently described “elementary particle” distortion discussed in Section 1.2. The constraining criterion is satisfied as represented in the earlier equation (20). We use the designation $\mathrm{FM} \stackrel{\mathrm{def}}{=} \mathrm{Fermi\ Mass} = \mathrm{m_F\ me\ c^2}$ for the transition-distortion mass-energy. Then we set

$$\mathrm{gF_{geo}} \stackrel{\mathrm{def}}{=} \left[\mathrm{fe}\ \frac{4\pi}{3}\mathrm{R0}^3\right]\mathrm{FM} = \frac{4\pi}{3}(\hbar c)^3\left(\frac{\mathrm{G_{geo}}}{\mathrm{m_F\ me\ c^2}}\right)^2 \quad \text{where}$$

$$\mathrm{fe} = \frac{3}{2}\left(\frac{\pi}{2}\right)^2 \quad \text{and} \quad \mathrm{G_{geo}} = \left(\frac{\alpha}{4}\right)^{1/2}\pi\ g_e\frac{S}{2}\frac{Q}{3} \qquad \text{or with}$$

$$m_F \stackrel{def}{=} \frac{Q}{3}m_{F0} \quad \text{to satisfy charge universality, then if}$$

$$m_{F0} = \frac{m_{W\text{-}boson}}{me} \;, \quad \text{we produce}$$

(25) $$\mathrm{GF_{geo}} \stackrel{\mathrm{def}}{=} \frac{4\pi}{3}(\hbar c)^3\frac{1}{\left(\mathrm{m_{W\text{-}boson}}\ c^2\right)^2}\left[\left(\pi\frac{S}{2}g_e\right)^2\frac{\alpha}{4}\right]_{S=1} = \mathrm{GF}\ ;$$

conversely,

$$\mathrm{FM_{Q=\text{-}3}} = \left[\sqrt{\frac{4\pi}{3}(\hbar c)^3\left(\pi\ \frac{S}{2}\ \frac{Q}{3}g_e\right)^2\frac{\alpha}{4\ \mathrm{GF}}}\right]_{Q=\text{-}3} = \mathrm{m_{W\text{-}boson}}c^2\ .$$

$$\mu_{\mathrm{spin}} \stackrel{\mathrm{def}}{=} \left(\frac{g_e}{2}\frac{\mathrm{Qe}}{3\mathrm{M}}\right)S\hbar \quad \text{and} \quad g_e = 2.0023193043\ 6.$$

The quantity $\mathrm{fe} = 3\pi^2/8$ represents an effective radial-, or volume-, factor specified to represent the “shell-like” mass-energy distribution and quantified here to precisely produce numerical agreement with GF (see Figures 1.6 and 1.10, for example, for an illustration of the distorted volume and the transition-state’s geometric shell-mass-energy distribution).

Since the geometric representation of the state-to-state transition for $\mathrm{Q} = -3$ is apparently realized with a “transition, or mediating, mass” equal to the W^{-}boson mass, and because “universality” is required in the physical realm, the geometric realization of this requirement, when positing the “transitional state” as a “Section 1.2 particle structure”, is a non-classical “quantization” of the “Fermi Mass” according to the specification $\mathrm{m_F} = (\mathrm{Q}/3)\mathrm{m_{F0}}$. If GF is considered a fundamental physical constant, then equation (25) can be interpreted as the determining expression for the mediating mass-energy in beta-decay.

The relationship for the distortional-geometric-Fermi-constant is satisfied with a Fermi-mass (boson)-energy of 80.39664543913 GeV (calculated to the precision of the electron magnetic moment [18]); the associated structural radius is $\mathrm{R0} = 4.7643747163326(10)^{-19}\ \mathrm{m}$. For experimental comparison, the boson-mass-energy is cited as “$\mathrm{Mass} = 80{:}398 \pm 0{:}023\ \mathrm{GeV}$” [18]. We have interpreted the geometric manifestation of the “Fermi-energy-volume product (GF)” as the condition of distortionally-produced “maximum curvature” of $\mathrm{Q} = 3$ structures in the geometric manifold; the “maximum curvature” producing element is the energy-density sum-quantity $\mathrm{Td}_2^2 + \mathrm{Td}_1^1$ (see equation (19)) constrained by the equation-of-state geometric-tensor energy-density relationship $\mathrm{Td}_4^4 = -\mathrm{Td}_1^1 - \mathrm{Td}_2^2 - \mathrm{Td}_3^3$. The Fermi-constant interpretation derives from a product of the magnetostatic energy-density cofactor, the “boson (maximum particle mass) magnetic moment”, and the associated “geometric volume factor”.

When expressing the geometric Fermi-mass-energy as the W^{-}boson mass-energy, we do indeed produce the Fermi constant for muon beta-decay, however the family of Fermi-Mass transition states allows for W^{Q}boson mass-states, with $Q = \pm 1, \pm 2 \text{ and } \pm 3$, and would allow for state-participation in other decay processes; e.g. $dq^{-\frac{1}{3}} \Longrightarrow \nu_{dq} + W^{-\frac{1}{3}}$; $W^{-\frac{1}{3}} \Longrightarrow uq^{\frac{2}{3}} + e^{-1}$.

The resulting coupling constant value is $\kappa = \frac{1}{2}(\hbar c\, \alpha)\left(m_{\text{W-boson}} c^2\right)^{-2} = \frac{\mu o\left(\mu_{spin}/\hbar c\right)^2}{2\pi} = 6.95(10)^{-13} m/J$ for the transition-distortions ($Q = -1 \text{ and } Q = -3$); compare with the distortion-model-1 (quark) value of $\kappa o = 2.21(10)^{-5} m/J$ and the distortion-model-3 (muon) value of $\kappa o = 4.03(10)^{-7} m/J$. It is seen that the transition-distortions are expressed with coupling constants lesser than the source-, or initial state-, distortions thereby suggesting a more energetically-difficult structural-state to render. The characteristic radii are $R0 = 4.76(10)^{-4}$ fm for the $Q = -3$ transition-distortion and $R0 = 6.87(10)^{-4}$ fm for the $Q = -1$ transition-distortion.

Equation (26), for comparison purposes, is a contrast of the “geometric-Fermi-constant formulation” with the “electroweak representation [24] involving the W^{-}boson”;

(26) $$GF_{geo} = \frac{4\pi}{3}(\hbar c)^3 \frac{g_{geo}{}^2}{\left(FM_{Q=-3}\right)^2} \quad \text{and}$$

$$g_{geo} \stackrel{\text{def}}{=} \left|G_{geo}\right|_{Q=-3} = \frac{\pi}{2} g_e \sqrt{\alpha/4}$$

compared with

$$\mathrm{GF} = \frac{\sqrt{2}}{8}(\hbar \mathrm{c})^3 \frac{\mathrm{g_{electroweak}}^2}{(\mathrm{m_{W\text{-}boson}} \mathrm{c}^2)^2} \quad .$$

MATTER AS DISTORTED SPACE

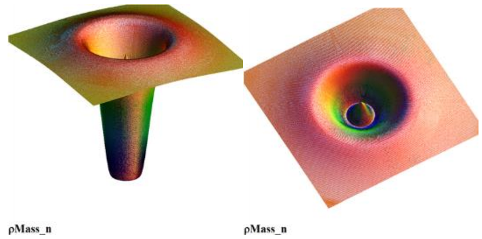

This Hole Section is incorporated here as a template for separate publication.

https://archive.org/details/gravitational-distortional-extrema-scir_202110

DISTORTIONAL EXTREMA AND HOLES IN THE GEOMETRIC MANIFOLD

Dale. R. Koehler

Sandia National Laboratory (retired), Albuquerque, NM 87123

Corresponding author. Dale. R. Koehler, *82 Kiva Place, Sandia Park, NM 87047*

Phone #: (505) 273-3570, Email: *drkoehler.koehler@gmail.com*

Keywords: Astrophysics; Black Holes; Cosmology; General Relativity; Geometry

Summary

The work is a non-conventional mathematically-geometric approach to describing “black-hole” structures. We have produced a description of the “black hole” as a geometric-mimic, a “distorted geometry” structure, formulated from a solution of Riemann’s geometric equations. The model is essentially the “Curved empty space as the building material of the physical world” supposition of Clifford [1] in 1876 and is the conceptual basis for this “distorted-geometry” modeling. The resulting geometric description of matter (mass-energy) mimics the classical-physics electromagnetic and gravitational-field models at large radii but departs significantly at small radii to produce a magnetic-field (spin) mimic as well as a weak-field mimic (beta decay and the Fermi constant) and a strong-field mimic without an infinity at the origin (no singularity) [2]. The structure is constituted by a core-region within which the propagation-velocity, by virtue of the distorted metrics, is greater than c and exhibits a “partial light trapping phenomenon”, a “black hole”. Distorting the geometry in our spatial-manifold requires energy but with limits as to the degree of distortion thereby predicting and describing fundamental-electromagnetic-particle structures as well as gravitational (dark-matter, black-hole) structures. Such a geometric description of localized warping or distorting of the spacetime manifold would seem (?) to constitute a “first-principle” model of the universe.

Abstract

It is shown in the present work that the distorted-space model of matter as extended to extreme curvature limits results in characteristics mimicking those of galactic-holes. The distorted-geometry structures exhibit non-Newtonian features wherein the hole or core-region fields of the structure are energetically-repulsive (negative pressure), do not behave functionally in an r^{-4} manner and terminate at zero at the radial origin

(no singularity). Of particular interest is that of r^{-6} energy-density behavior at structural radial distances near the core of the distortion, a region also displaying potential-well behavior.

Introduction

A "Curved empty space as the building material of the physical world" supposition of Clifford [1] in 1876 is the conceptual basis for this "distorted-geometry modeling" [2.3]. We maintain and expand the geometrical perspectives inherent in the earlier work [2] and building on that work, we apply the geometric concepts to produce a distortional-geometric extremum, a "*stability-based* *minimum*-*energy-density*" condition or "*maximum geometrically-distorted gravitational radius*" condition. Additionally, we showed in [2,3] that the propagation velocity in the core region of these distorted-geometry structures was approximately 1.5 times that external to the core (see Fig.1). This feature, which is present for all such structures, is equivalent to a "partial light trapping" phenomenon (a black hole core?).

A "*geometric maximum-energy-density*" feature, in the EM (electromagnetic) energy-density realm, was successfully exploited to geometrically explain and quantify the Fermi constant [2] and in addition a "*stability-based* *minimum*-*energy-density*" condition was fundamental to describing the structure of the *"stable distortional-geometry electron"* feature.

In this perspective, the distorted-geometry model is a departure from the classical geometry model where the Einstein Curvature tensor is the stress-energy-tensor describing the “material contents” of the energy distribution. This distorted-geometry model is rather viewed with the energy-content residing in the warping or distorting of the manifold and therefore in its geometric-tensors, and the “curved empty space” [2,3] referred to above is a “localized curved or distorted space” devoid of an “external or foreign” causative matter-entity. The “distorted metrics” and the core propagation velocity are displayed for example, for the distorted-geometry electron-mimic in Fig. 1.

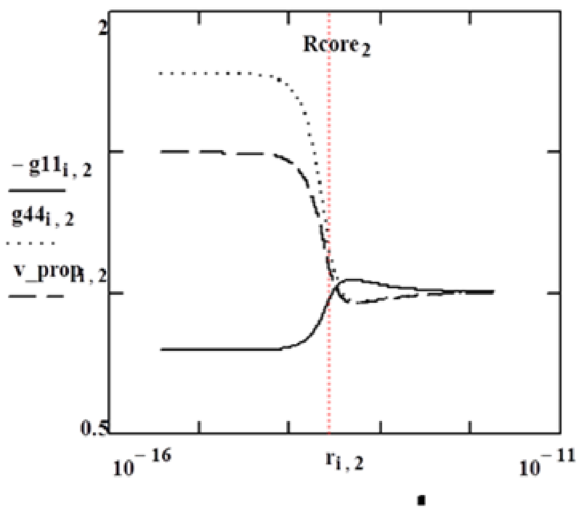

Fig.1 Metrics and propagation-velocity factor for the distortional electron structure; abscissa in meters.

Theoretical Modeling for Distortional Extrema and Holes

Both gravitational and electromagnetic energy-densities are capable of distorting the geometric manifold. This feature of these *distorted-space structures* is a manifestation of a composite coupling-constant between energy and geometry,

$$\kappa = \kappa_G + \kappa_{EM} = \frac{G}{c^4} + \frac{\mu o\left(\frac{\mu_{spin}}{\hbar c\, S\, g_e}\right)^2}{2\pi} = \frac{G}{c^4} + \frac{\alpha\, \hbar c}{2}\left(\frac{Q}{3\, Mc^2}\right)^2 ;\ Q = 3 \text{ for the electron.} \qquad (1)$$

We have used a modified coupling–constant definition by omitting the factor 8π and retaining the factor in the energy-density equations; conventionally, the coupling-constant definition would be 8πκ.

The following mathematical development is taken from [2] and is reproduced here to render the manuscript more readable without constant attribution to the earlier manuscript.

Allowing the distorted space itself to be material in nature, we constrain the modeling by requiring that the descriptive stress-energy tensors satisfy a "constitutive relation" or an "equation-of-state" between the temporal and spatial tensor-curvature elements, namely

$$\mathbf{Td}_4^4 = -\left(\mathbf{Td}_1^1 + \mathbf{Td}_2^2 + \mathbf{Td}_3^3\right). \tag{2}$$

We have introduced the explicit distortional-tensor symbolism **Td** for the geometric quantities. Contrast this perspective with cosmological renditions of geometric curvature structure resulting from "matter" causation, wherein several "equations of state" relating to the "matter" variables ρ (density) and p (pressure) have been forthcoming [4] where $p = \sigma\,\rho$ and where σ varies from -1 to +1.

Inherent in the geometric "equation-of-state" constraint is the requirement that the descriptive stress-energy tensor, **Td**, be Maxwellian in nature; the mimicking process is therefore limited to asymptotically flat-space regions of the manifold since $1/r^2$ field behavior does not adequately describe elementary-particle structural-detail [5]. The field equations, in both the EM realm and the gravitational realm (Q = 0), exhibit r^{-6} geometric behavior which we have interpreted as constituting a "magnetic monopole" mimic (what is a "magnetic monopole" ?).

This description, Eq.(2), of the *distorted-space volume*, has led to the *universal structural solution*, Eq.(9), (see Eqs. (6)-(8) in the SI for variable definitions) for the fundamental Riemann geometric-equation-set (Eqs. (3-4) leading to Eqs. (6-8));

$$\mu' = \frac{2(1-u^3)u^2}{(\mathrm{Iu} - \gamma)\mathrm{R0}}, \tag{9}$$

where the metric quantity $g_{11} \equiv - e^{\mu}$ and $g_{44} \equiv e^{\nu}$; $\nu' = \left[-2 + \frac{1}{1-u^3}\right]\mu'$ and the transformed radial variable $u \equiv \frac{R0}{r}$. Riemann's geometric equations are expressed in the metric-variables μ' and ν' and the manifestation of the composite coupling-constant appears in the geometric quantities γ (Eq.14) and the geometric "transformation radius" R0 (Eq.14) both determined from the "distorted spatial volume" with electromagnetic and/or gravitational energy-density components.

A radial zero in the field quantity $(\mathbf{Fd_{14}})^2$, namely r0 ≡ Rs_{geo} = $R0_{geo}$/u(r0), with u(r0) = γ(grav)/2 = 3.27512/2, is the geometric manifestation of the Schwarzschild "metric-radial-zero", the radial singularity classically interpreted as a "black-hole" radius. The core-radius is a fundamental feature of the "distorted-space" structures; it is the radial point at which the energy-density-distortion transitions from a positive shell-like value to a negative core-like value. The structures inherently illustrate r^{-4}, r^{-6} and repulsive-radial energy-density behavior (relative to the shell energy-density behavior), thereby accounting for Newtonian, weak and strong field-attributes.

In discussions of the negative energy-density core-regions of this universal (EM as well as gravitational) distorted-geometry structure, it should be emphasized that a negative energy-density gravitational feature (a repulsive gravitational force or negative pressure) is non-Newtonian. The hole or core region-fields of the structures are repulsive (relative to the extra-core, or shell, region), do not behave functionally in an r^{-4} manner and terminate at zero at the radial origin (no singularity). See Fig. 2 where the magnetic and radial field energy-densities are graphed for quantitative and qualitative purposes and Fig, 3 where the same quantities are shown in absolute values to more clearly identify the relative strengths of these energy densities in the shell to core transition regions. Fig. 4 is constructed to complement the theoretical results exhibited in Figures 2 and 3.

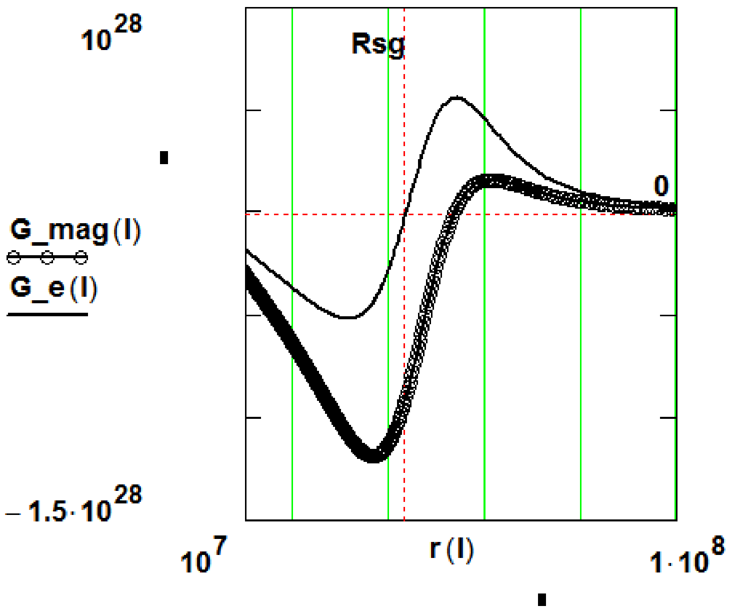

Fig.2 Field-Energy-Density distribution functions (at creation) for mimicking the Sagittarius A* galactic-hole; **G_mag** is the r^{-6} magnetic-field-mimic, $\mathbf{Fd_{mag}}^{2}$, and **G_e** is the radial-field-mimic $\mathbf{Fd_{14}}^{2}$. The ordinate is linear in Joules/m^3 and the abscissa is logarithmic in meters. Rsg is the Schwarzschild radius 2 G c^{-4}Mc^2.

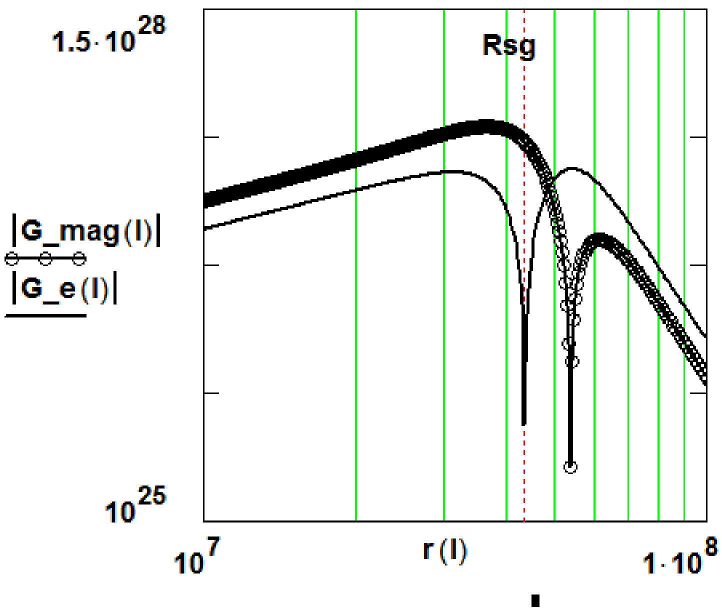

Fig.3 Field-Energy-Density distribution functions (at creation) for mimicking the Sagittarius A* galactic-hole; **G_mag** is the r^{-6} magnetic-field-mimic, $\mathbf{Fd_{mag}}^{\mathbf{2}}$**,** and **G_e** is the radial-field-mimic $\mathbf{Fd_{14}}^{2}$. The ordinate is logarithmic in Joules/m^3 and the abscissa is logarithmic in meters. An absolute value ordinate is used to display the "negative pressure or negative energy density" core behavior. Rsg is the Schwarzschild radius 2 G c^{-4}Mc^2.

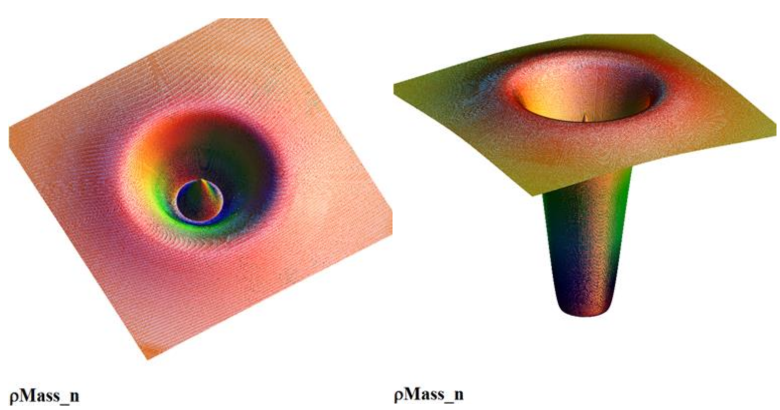

Fig.4 Mass-Energy-Density distribution-function surface-plots (two views) (linear radii and logarithmic amplitudes) for the geometric hole distortion.

Results

We are considering, in the present undertaking, the gravitational energy realm. Incorporating the symbolism utilized in [2], we write Eq.(10) for the "*geometric-maximum-energy-density*" feature, the *maximum curvature extremum* or minimum-radius-extremum, of a "geometric" gravitational-distortion. In the EM realm, the "*geometric-maximum-energy-density*" structure is represented by the W-boson which is understood to be the transition-mediator-particle in beta-decay, a high-energy short-lifetime fundamental-particle satisfying the Heisenberg uncertainty principle ΔE Δt = ħ/2.

$$\left(8\pi\, \kappa_{\mathrm{grav}} (\mathrm{R0}_{\mathrm{Schwarzschild}})^2 \right)^{-1} \equiv \left(8\pi\, \kappa_{\mathrm{boson}} (\mathrm{R0}_{\mathrm{boson}})^2 \right)^{-1} \tag{10}$$

with $\kappa_{\mathrm{boson}} = \frac{\alpha\, \hbar c}{2} \left(\frac{1}{m_{boson}\, c^2} \right)^2$, $R0_{boson} = \beta_{boson} \frac{\hbar \mathrm{c}}{m_{boson}\, c^2}$, $\kappa_{\mathrm{grav}} = \mathrm{G}\, \mathrm{c}^{-4}$, $\beta_{boson} = \left(\alpha \left(\frac{ge}{2} \right)^2 \frac{2}{3} \right)^{1/3}$

and $R0_{Schwarzschild} = 2\ \kappa_{\mathrm{grav}}\, M_{grav} c^2$. This equivalence relationship produces the mass-energy equation for the extremum gravitational structure,

$$(\mathrm{Mc}^2)_{\mathrm{grav\_min}} = \sqrt[2]{\left(\frac{\kappa_{\mathrm{boson}}}{\kappa_{\mathrm{grav}}} \frac{1}{1.6375} \right)} \frac{\mathrm{R0}_{\mathrm{boson}}}{2\, \kappa_{\mathrm{grav}}} = 1.80\ 10^{41}\, Joules \tag{11}$$

at a radius

$$r0_{grav}(\min) = 2.98\ 10^{-3}\ \text{ meters}\,. \qquad (12)$$

By the same modeling as for the boson, the Heisenberg lifetime would be approximately 10^{-75} seconds. The Heisenberg lifetime for the W-boson is approximately 10^{-26} seconds.

Inherent in the "structural-geometric" equations for the boson are their relations to the Fermi constant GF, a measure of the "strength of interaction" in beta decay, which can be written as [2],

$$GF = \frac{\pi^3}{2}\ m_{boson}c^2\ R0_{boson}{}^3 \quad = \frac{1}{3\ \kappa_{boson}} R0_{boson}{}^4 = 1.4359\ 10^{-62}\ \text{Joule m}^3\ , \qquad (13)$$

the latter form of which emphasizes the "geometric-curvature" facet of the "interaction strength" quantity GF.

R0 is the *geometric* normalization radius (R0e is calculated from the fundamental-particle magnetic-field component and R0g is determined from the γ radius-ratio equation for the distorted-geometry structures).

$$R0 \equiv R0e + R0g\ ,\ \ R0e = \frac{\beta\ \hbar c}{m_{boson}c^2}\ ,\ \ R0g = 2\ \kappa_{boson}\ m_{boson}c^2\ ,$$

$$Rs \equiv Rse + Rsg = 2\ \left(\kappa_{boson} +\ \kappa_{grav}\right) m_{boson}c^2\ \text{ and }\ \gamma \equiv \frac{2\ R0}{Rs}\ . \qquad (14)$$

Then,

$$\gamma \equiv \frac{2\ (R0e+R0g)}{Rse+Rsg} = \frac{2\ (0+R0g)}{0+Rsg} = 2\ u(r0)\ \text{ and }\ u(r0) = \frac{3.27512}{2}\ (\text{if }\ r0 = Rsg = \frac{R0_{geo}}{u(r0)}).$$

For a gravitational distortion, R0e and Rse are zero.

If, in the absence of a physical structural constraint, one posits a "***minimum***" curvature, or a "*minimum*" EM-energy-density condition (which was posited [2] for the "*electron-mimic*" and

which is equivalent to a "*maximum*" geometric EM core-radius) as the *"stability" criterion to produce the maximum-core-radius-extremum, distorted-geometry, gravitational-entity,* one can write for the *electron-mimic*,

$$r0_{geo\_max} = \mathrm{r0(electron)} = \frac{\beta(1/2,3)}{\mathrm{uB0}(1/2,3)} \frac{\hbar c}{\mathrm{me}\, c^2} ,$$

with $\beta(S,Q) = \left[\frac{2}{3}\alpha \left(\frac{g_e}{2} S \frac{Q}{3}\right)^2\right]^{\frac{1}{3}}$, α = fine structure constant, S is the spin quantity and g_e is the gyromagnetic ratio factor. Then,

$$\mathrm{r0}_{\mathrm{geo\_max}} = 3.329(10)^{-14} \text{ meters.} \tag{15}$$

By using the associated EM "*geometric-energy-density minimum*" as the equivalent gravitational constraint for determining a "*maximum gravitational core-radius*", and using Eq. (10) with electron characteristics substituted for boson characteristics, we produce the more classical "*HOLE-like*" structure; the *"distorted-geometry"* gravitational Schwarzschild radius is the *"hole radius"* (see the earlier development in [2] for the Fermi-constant GF where $\mathrm{GF}_{geo} \stackrel{def}{=} \left[\ \mathrm{fe}\ \frac{4\pi}{3} R0_{boson}{}^3\right] m_{boson} c^2$; also see YouTube educational video with included citations Largest Black Holes in the Universe or Wikipedia entry, Black hole).

We construct the energy-density relationship (Eqs.6 in the SI for $\mathbf{Td_4^4}$), calculate the energy-density maximum for the electron and set $\mathbf{Td_4^4}$ max (from the stable electron structure) = $\mathbf{Td_4^4}$ max (for a stable gravitational hole structure). Then, using the "transformation radii R0",

$$[8\pi\ \kappa\mathrm{o(elec)R0(elec)}^2]^{-1}[\gamma(\mathrm{elec})\frac{2}{3\pi}] = [8\pi\ \kappa\mathrm{G(hole)R0(hole)}^2]^{-1}[\gamma(\mathrm{elec})\frac{2.85}{3\pi}] \tag{16}$$

$$\text{where} \qquad \kappa o(\text{elec}) = \frac{\alpha\, \hbar c}{2}\left(\frac{Q/3}{me\; c^2}\right)^2 \text{ and } \kappa G(\text{hole}) = G\, c^{-4};$$

$$R0(\text{elec}) = \frac{\beta(\text{elec})\, \hbar c}{\text{me } c^2}\ ,\ R0(\text{hole}) = \frac{3.275}{2}\, 2\, \kappa G(\text{hole})\, M(\text{hole}) c^2\ ,$$

$$\text{and} \quad \gamma(\text{elec}) = \frac{2\, R0(\text{elec})}{Rs(\text{elec})} = 29.255.$$

The cofactors $\gamma(\text{elec})2/3\pi$ and $\gamma(\text{elec})2.85/3\pi$ have been introduced to account for the slight dependence of the energy-density functions $\mathbf{Td_4^4}$ max (in Eqs. (10) and (16)) on γ: $\mathbf{Td_4^4}$ is displayed explicitly in Eqs. (6) in the SI.

The resultant $Mc^2(\text{hole}) = \frac{\beta(\text{elec})}{\gamma(\text{grav})}\left(\frac{1}{\text{me } c^2}\right)^2 \left(\frac{\hbar c}{G\, c^{-4}}\right)^{3/2} \frac{1}{3}\sqrt{\left(2\pi\left(\frac{\pi}{3}\right)^{0.5}\alpha\right)}$, where α is the fine-structure constant and

$$(Mc^2)_{\text{grav max}} \equiv Mc^2(\text{hole}) = 1.461\ (10)^4 \ \text{ solar masses} \tag{17}$$

at a core radius

$$(\text{Schwarzschild\_radius for } \mathbf{Td_4^4}) = 2\, G\, c^{-4}\, Mc^2(\text{hole}) = 4.34\ 10^7 \text{ meters.} \tag{18}$$

Such a primordial distortional-hole, after $13.8(10)^9$ years of mass accretion at a rate of $3.01(10)^{-4}$ solar-masses/year, would exhibit the present mass of the "Milky Way galactic black-hole (Sagittarius A*)" at $4.154(10)^6$ solar masses [6,7,8] and a core (Schwarzschild)-radius of Rsg = $1.23(10)^{10}$ meters; its distortional energy-density distribution functions are shown in Fig. 5. The distortional peak energy-densities are reduced over this time period from the 10^{27} range to a 10^{23} range (see Figs. 3 and 5). These extremely high energy-densities (both positive and negative $\mathbf{Td_4^4}$) integrate to a composite total energy which is the mass-energy of the structure

[5]. Also illustrated in Fig. 5 is the Newtonian $1/r^4$ field energy-density (grav_r) function wherein the “distorted-geometry” function is an order of magnitude greater than the Newtonian function near the core. Functionally the “distorted-geometry-field” transitions to a repulsive core-function at Rsg the Schwarzschild radius. Accreted-mass and the “black hole” constitute a “field-modified energy-altered structure” as, analogously, for example, the neutron, which is unstable when free, but becomes a stable structure when in the nucleus-field-environment.

Therefore this “distortional-geometry hole-structure”, created at the “birth of the universe” (also see reference [13]), registers as a viable candidate for the structure of “black holes”.

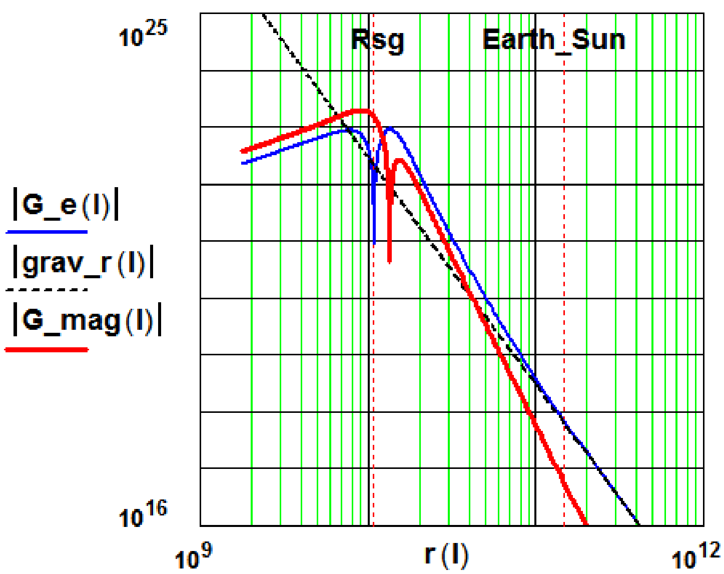

Fig.5 Field-Energy-Density distribution functions (after $13.8(10)^9$ years of accretion) for mimicking the Sagittarius A* galactic-hole; **G_mag** is the r^{-6} magnetic-field-mimic, $\mathbf{Fd_{mag}}^{2}$, and **G_e** is the radial-field-mimic $\mathbf{Fd_{14}}^{2}$. The ordinate is logarithmic in Joules/m^3 and the abscissa is logarithmic in meters. An absolute value ordinate is used to display the “negative pressure or negative energy density” core behavior. Rsg is the Schwarzschild radius 2 G $c^{-4}Mc^2$ and “Earth-Sun” designates the earth to sun distance. Also illustrated for comparison is the classical Newtonian field energy-density function “grav_r”.

Mass-energy "black-hole" growth rates [9-13] however range from "~1 solar mass/3000 years (for the Milky Way Galaxy)" up to "~1 solar mass/20 years (for NGC 4594)", therefore the "Milky Way Black-Hole mass-accretion rate" allows for even a "zero-mass black-hole" at creation-time. Accretion rates are in part based on distance, times and the universe-expansion model (see reference [14]) and would be subject to revision according to the model selected. The average accreted-hole mass-energy, as calculated from the present-day Universe model is approximately $6.2(10)^{55}$ Joules (1/2* mass-energy of NGC 4594). This calculation puts the "galaxy black holes" at 0.17% of the Universe mass-energy if there are 10^{11} to 10^{12} galaxies. If the "TON 618 hole" mass-energy ($1.19(10)^{70}$ Joules) is used to calculate the total "hole mass-energy", (average ≡ ½ TON 618 mass-energy), at 10^{12} galaxies, the holes constitute 11 % of the total Universe mass-energy. Therefore, "dark gravitational hole entities" might be responsible for most of the posited dark-mass-energy.

This "<u>DG</u> Black hole", <u>distorted-geometry</u> primordial gravitational-structure, a "<u>*geometric-energy-density minimum*</u>" structure (DG_Hole ≡ $2.63(10)^{51}$ Joules), along with the "<u>*geometric maximum-energy-density*</u>" structure, constitute the extrema, the mass-energy bounds of the gravitational-structure particle-spectrum, a range from $1.80(10)^{41}$ Joules to $2.63(10)^{51}$ Joules. The extrema for electromagnetic structures range from $8.19(10)^{-14}$ Joules for the electron to $1.29(10)^{-8}$ Joules for the W^-boson. The distorted-geometry model, and its "gravitational-mass-energy spectrum" at the maximum energy-density extremum, incorporates the transitory short-lived character (not stable) of a "mediator structure", a gravitational mimic of the electromagnetic W-boson structure.

Production numbers at creation depend on the “Universe-Creation-Model” utilized (see [14]), and the mass-energy distribution function. Here we tailor the Planckian “thermodynamically-constructed” black-body radiation-emission function to produce a mass-energy-creation, emission and energy-distribution function. We incorporate this “Mass-energy Black-Body” function to describe the “Universe-mass-energy” structure and its mass-energy emission (at creation) distribution.

The “Universe-mass-energy” ≡ U0 ≡ $5.38(10)^{70}$ Joules and the “mass-energy ratio” for “Milky-Way gravitational-hole” production is ≡ Bu(x = DG_Hole/U0) / DG_Hole = $2.25(10)^{11}$, posited as “the number of hole-seeded galaxies”, generated with the Planckian-like mass-energy distribution-function Bu(x);

$$\mathrm{Bu}(x) \equiv \frac{1}{\mathrm{C0}}\, \mathrm{U0}\, [\, \mathrm{x}^{\mathrm{N}} (\mathrm{e}^{\mathrm{x}} - 1)^{-1}]\, \mathrm{fBB(x)} \;\; with\ x \equiv \frac{mass\ energy}{U0} \;\; , \;\; N = 1.4$$

$$\text{and} \qquad \mathrm{C0} \;=\; \int_0^{\infty} [\, \mathrm{x}^{\mathrm{N}} (\mathrm{e}^{\mathrm{x}} - 1)^{-1}]\, \mathrm{fBB(x)\, dx} = 1.72 \;\; \text{with fBB(x)} = 1. \qquad (19)$$

$$\mathrm{Bu2}(x) \equiv \frac{15}{\pi^4}\, U0\, [\, x^3 (e^x - 1)^{-1}] \;\; with\ x \equiv \frac{mass\ energy}{U0} \;\; , \;\; N = 3 \ldots\ldots Planck's\ Law\ .$$

For N = 1.35 and C0 = 1.69, Bu(x = DG_Hole / U0) / DG_Hole = $2.11(10)^{12}$ galaxies. The black body mass-limitation function fBB = 1 in this calculation. The “thermodynamic” Planckian functions Bu(x) and Bu2(x) exhibit no energy-emission limit.

The Distorted-Geometry Black-Body Planckian distribution-function, Bu(x) with N = 1.4, and the classical black-body Planckian radiation-emission distribution-function, Bu2(x) are displayed in Fig.6. Because the Universe, primordially modeled as a black-body, is at an extreme temperature, the galaxy DG-Hole-energy appears in the “u^{N-1} mass-energy range” and is off-scale in the Figure.

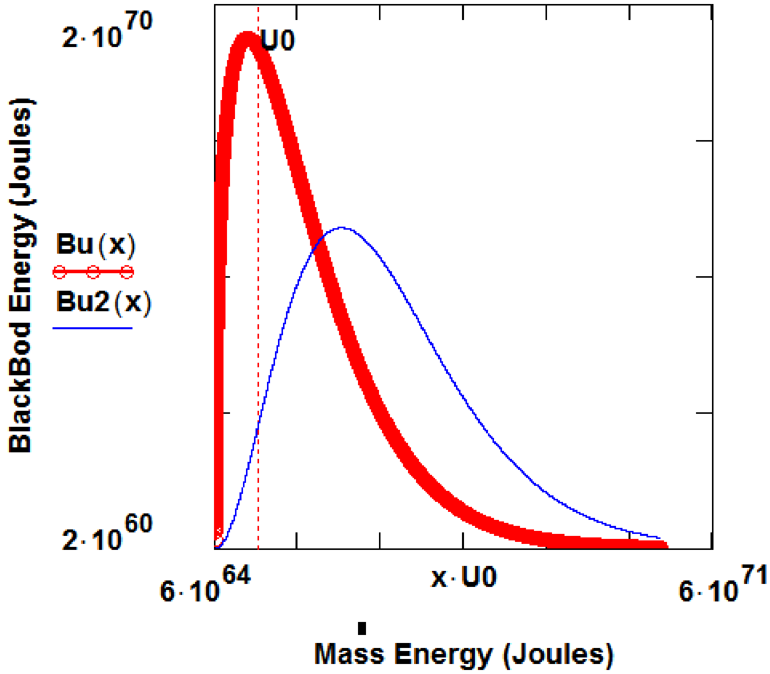

Fig.6 Black-Body energy distribution functions; DG-Bu(mass-energy) and Planckian-Bu2(radiation energy), are expressed in Joules on the logarithmic ordinate scale as a function of mass-energy (Joules) on the logarithmic abscissa. For the classical Planck-distribution, N = 3 and for the posited Universe-energy distribution (2.25 $(10)^{11}$ hole-seeded galaxies), N = 1.4. The integral function C0 is 1.72 for the Universe-energy distribution and the classical black-body Planckian radiation-energy distribution integral is $\pi^4/15$. U0 is the "Universe mass-energy".

The mass-energy ratio, "Bu(DG_Hole)) mass-energy-to-hole mass-energy ", is postulated to be the number of "hole-seeded-galaxies" and equal to 10^{11} to 10^{12} [15,16], The density of "dark-matter" in the universe, posited as necessary in the presently accepted Universe-model, is not accounted for in this purely "gravitational-mass-energy spectrum" although a "black body" is considered "dark".

However these distribution functions do not describe the "Universe as a Black-Body" entity in that the mass-energies exceed the "Universe-Energy" itself; it is a "continuous-energy

distribution function" as opposed to a "discrete-energy distribution function". In the absence of a known experimental mass-energy distribution function, we have posited a modified Planckian distribution function by incorporating the classical 3-dimensional "density of states" function, fBB(x) = $(x - 1)^2$, thereby terminating the Distorted-Geometry Black-Body Planckian distribution function at the "Universe-Energy" U0;

$$\mathrm{Bu}(x) \equiv \frac{1}{C0}\, U0\, [\, x^N (e^x - 1)^{-1}\, \mathrm{fBB(x)}]\ \ with\ x \equiv \frac{mass\ energy}{U0}\ \ ,\ \ N = 1.46\ ,$$

$$\mathrm{fBB(x)} = (x-1)^2\quad and\quad C0 = \int_0^1 [\, x^N (e^x - 1)^{-1}]\, \mathrm{fBB(x)}\, dx = 0.137\ . \qquad (20)$$

$$\mathrm{Bu2(x)} \equiv \frac{15}{\pi^4}\, \mathrm{U0}\, [\, \mathrm{x}^3 (\mathrm{e}^{\mathrm{x}} - 1)^{-1} \mathrm{fBB(x)}]\ \ \mathrm{with\ x} \equiv \frac{\mathrm{mass\ energy}}{\mathrm{U0}}\ ,$$

$$\mathrm{N} = 3\qquad \mathrm{Geo\_Planck's\ Law}\ .$$

This distribution function, Eq. (20), (see Fig.7) produces 1.96 $(10)^{11}$ as the number of hole-seeded galaxies, that is Bu(x = DG_Hole / U0) / DG_Hole = 1.96$(10)^{11}$.

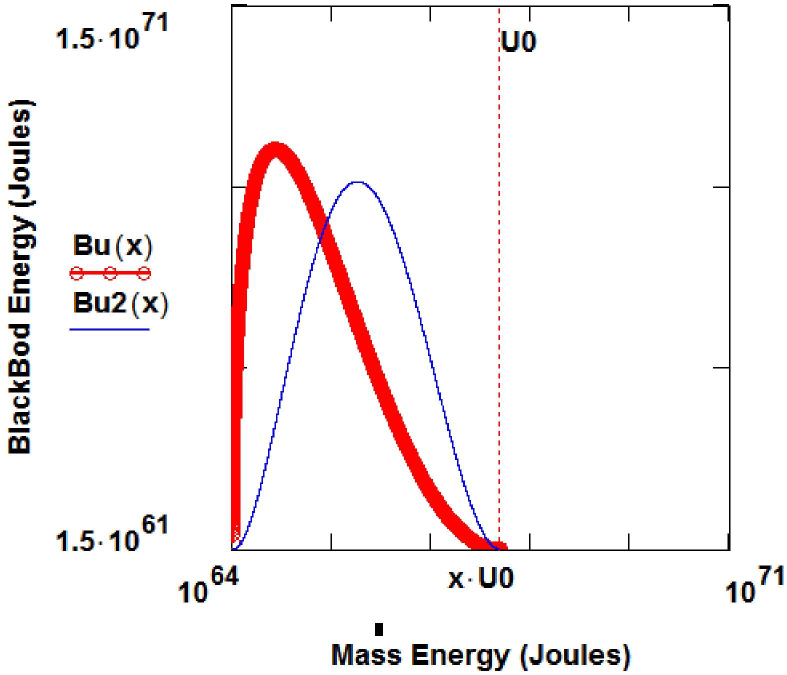

Fig.7 Modified Black-Body energy distribution functions; Universe-Bu(mass-energy) and Planckian-Bu2(radiation energy), are expressed in Joules on the logarithmic ordinate scale as a function of mass-energy (Joules) on the logarithmic abscissa. For the classical Planck-distribution, N = 3 and for the posited Universe-energy distribution ($1.96(10)^{11}$ hole-seeded galaxies), N = 1.46. The integral function C0 is 0.137 for the Universe-energy distribution and the classical black-body Planckian radiation-energy distribution integral is 0.0258. U0 is the "Universe mass-energy".

Finally, for hole-like-structure elucidation, it is of interest to examine the ratio of the $1/r^6$ tensor-component to the $1/r^4$ tensor-component in the construction of the geometric fields. To further illustrate the structural character of the "distortional-geometry mimics", we compare at "near-core radial regions" the geometrostatic field quantities $\mathbf{Fd_{14}}^2$ and $\mathbf{Fd_{mag}}^2$. For both gravitational and electromagnetic distortions, the magnetic field component, $\mathbf{Fd_{mag}}^2$, is non-zero at the "radial field zero", $\mathbf{Fd_{14}}^2 = 0$, or "core radius". This field feature would seem responsible

for accretion-disk and galaxy-matter rotational-distribution behavior. Actually, the $\mathbf{Fd_{14}}^{\mathbf{2}}$ fields contain r^{-6} elements of a magnitude comparable to the magnetic-field strengths $\mathbf{Fd_{mag}}^{\mathbf{2}}$ (see Eqs. (6-8) in SI), resulting in a significant departure from the classical Newtonian r^{-4} (or r^{-6}) behavior. The fields exhibit potential-well behavior as they radially transition to repulsion at the hole-core radius.

Discussion

It has been shown in the present work that the distorted-space model of matter, as extended to extreme curvature-limits, results in characteristics mimicking those of galactic-black-holes. The distorted-geometry structures exhibit non-Newtonian features wherein the hole or core-region fields of the structures are gravitationally-repulsive, do not behave functionally in an r^{-4} manner and terminate at zero at the radial origin (no singularity) while exhibiting a propagation velocity in the core region approximately 1.5 times that external to the core (light trapping or black hole behavior). Of particular interest is that of r^{-6} energy-density behavior at structural radial distances near the core of the distortion, a region also displaying potential-well behavior.

References

1. Clifford, W. On the Space Theory of Matter. *Proc. of the Cambridge philosophical society*. **2**, 157 (1876).
2. Koehler, D. Geometric-Distortions and Physical Structure Modeling. *Indian J. Phys*. **87**, 1029 (2013).
3. Koehler, D. *The Distorted Universe: From Neutrinos to the Cosmos, The Theory of Nothingness*. USA, Kindle (2015).
4. Linder, E. V. *First Principles of Cosmology*. Addison Wesley, England (1997).
5. Tolman,R. *Relativity, Thermodynamics and Cosmology*. Dover, NY, 248 (1987).
6. Abuter, R. et al., A geometric distance measurement to the Galactic center. *Astronomy & Astrophysics*. L10, **625** (2019).

7. Falcke, H. Viewing the shadow of the black hole at the Galactic center. *Astrophysical Journal Letters*. L13, **528** (2000).
8. Lu, R. Detection of Intrinsic Source Structure at ~3 Schwarzschild Radii with Millimeter-VLBI Observatiions of SAGITTARIUS A*. *Astrophysical Journal*. **60**, 859 (2018).
9. Rees, M.J., Volonteri, M., Karas, V., Matt, G. Massive black holes: formation and evolution. *Proceedings of the International Astronomical Union*. 51-58 **238** (2007). doi:10.1017/S1743921307004681.
10. Vesperini, E., et al. Unified Field Theory and the Hierarchical Universe. *The Astrophysical Journal Letters* **713**(1) L41-L44 (2010). doi: 10.1088/2041-8205/713/
11. Zwart, S., et al. Formation of massive black holes through runaway collisions in dense young star clusters. *Nature*. **428** (6984), 724–726 (2004). doi:10.1038/nature02448
12. O'Leary, R., et al. Binary mergers and growth of black holes in dense star clusters. *The Astrophysical Journal*. **637** (2): 937–951 (2006). doi:10.1086/498446.
13. Kormendy, J., et al. Hubble Space Telescope Spectroscopic Evidence for a 1 X 10 9 M ☉ Black Hole in NGC 4594. *The Astrophysical Journal*. **473** (2): L91–L94 (1996). doi:10.1086/310399.
14. Koehler, D. Radiation-Absorption and Geometric-Distortion and Physical-Structure Modeling. *IEEE Transactions on Plasma Science*. **45**, 3306 (2017).
15. Conselice, C. J., et al, The Evolution of Galaxy Number Density at z < 8 and its Implications. *The Astrophysical Journal*. **830** (2): (2016). doi: 10.3847/0004-637X/830/2/83.
16. Lauer, T.R. New Horizons Observations of the Cosmic Optical Background. *The Astrophysical Journal*. **906** (2) (2021) doi: 103847/1538-4357/abc881.
https://arxiv.org/abs/2011.03052

SI Supplementary Information

Supplementary Equations

DISTORTIONAL EXTREMA AND HOLES IN THE GEOMETRIC MANIFOLD

For the presently described spherically symmetric Maxwellian case, ϕ, the electrostatic potential, is a function of r alone, and the Maxwellian electromagnetic tensor and the associated field tensor $\mathbf{F_{1\mu}}$ can be constructed according to equation (3), where the only surviving field tensor components are (following the symbolism and development of Tolman[17]):

$$ds^2 = g_{11}[\, dr^2 + r^2 d\Omega \,] + g_{44} dt^2 = -e^{\mu}[\, dr^2 + r^2 d\Omega \,] + e^{\nu} dt^2 \,,$$

$$\mathbf{F_{21}} = -\mathbf{F_{12}}\,, \mathbf{F_{13}} = -\mathbf{F_{31}} \text{ and } \mathbf{F_{14}} = -\mathbf{F_{41}}\,, \quad \text{i.e.}$$

$$\mathbf{T^{\mu\nu}} = -\mathbf{g^{\nu\beta}F^{\mu\alpha}F_{\beta\alpha}} + \frac{1}{4}\,\mathbf{g^{\mu\nu}F^{\alpha\beta}F_{\alpha\beta}} \text{ or } \mathbf{T^{\mu\mu}} = -\mathbf{g^{\mu\mu}F^{\mu\alpha}F_{\mu\alpha}} + \frac{1}{4}\,\mathbf{g^{\mu\mu}F^{\alpha\beta}F_{\alpha\beta}}\,, \qquad (3)$$

then

$$\mathbf{T_4^4} = \frac{(\mathbf{F_{12}F^{12} + F_{13}F^{13} - F_{14}F^{14}})}{\mathbf{2}}, \quad \mathbf{T_1^1} = \frac{(-\mathbf{F_{12}F^{12} - F_{13}F^{13} - F_{14}F^{14}})}{\mathbf{2}},$$

$$\mathbf{T_2^2} = \frac{(-\mathbf{F_{12}F^{12} + F_{13}F^{13} + F_{14}F^{14}})}{\mathbf{2}} \quad \text{and} \quad \mathbf{T_3^3} = \frac{(\mathbf{F_{12}F^{12} - F_{13}F^{13} + F_{14}F^{14}})}{\mathbf{2}}.$$

The resultant field quantities are

$$(\mathbf{F_{14}})^2 = -\left(\mathbf{T_4^4} + \mathbf{T_1^1}\right)\mathbf{g_{11}\,g_{44}} = \left(\mathbf{T_2^2} + \mathbf{T_3^3}\right)\mathbf{g_{11}\,g_{44}}\,, \qquad (4)$$

$$(\mathbf{F_{12}})^2 = -\left(\mathbf{T_2^2} + \mathbf{T_1^1}\right)\mathbf{g_{11}\,g_{11}} \quad \text{and} \quad (\mathbf{F_{13}})^2 = -\left(\mathbf{T_3^3} + \mathbf{T_1^1}\right)\mathbf{g_{11}\,g_{11}}\,.$$

Therefore, we see that the static-spherically-symmetric Maxwellian tensors exhibit the same stress and energy relationship as the geometric tensors[17],

$$\mathbf{T_4^4} \;=\; -\left(\mathbf{T_1^1} \;+\; \mathbf{T_2^2} \;+\; \mathbf{T_3^3}\right). \tag{5}$$

The present geometric-modeling endeavor, with its Maxwellian-tensor-form mimicking-component, has produced the fundamental and limiting agent for the currently-studied distorted geometry, namely a particular constraining functional relationship between the geometry-defining tensors (for an empty-space geometry, all of the components of the energy-momentum tensor are zero). In using this simple equation-of-state, equation (5), as a restricting distortional-model tensor relationship, we thereby elicit the metric-defining differential equations for such a family of geometric distortions.

The geometric-energy-density or field equations (2-5), after using solution Eq. (9), are repeated here (from[16]); also see[17];

$$\mathrm{Iu} \;=\; -\mathrm{u}\left[\frac{3}{7}\mathrm{u}^6 - \frac{3}{4}\mathrm{u}^3 + 1\right],$$

$$8\pi\kappa\,\mathbf{Td_1^1} \;=\; -\mathrm{e}^{-\mu}\,\frac{1}{(\mathrm{Iu}-\gamma)}\left(\frac{\mathrm{u}^2}{\mathrm{R0}}\right)^2\left[\,2\,\mathrm{u}^2 + (3\,\mathrm{u}^3 - 1\,)\,\frac{1-\mathrm{u}^3}{(\mathrm{Iu}-\gamma)}\right],$$

$$8\pi\kappa\,\mathbf{Td_2^2} \;=\; e^{-\mu}\,\frac{1}{(Iu-\gamma)}\left(\frac{u^2}{R0}\right)^2\left[\,4\,u^2 + \,(3u^3\,-1\,)\,\frac{\left(1-u^3\right)^2}{(Iu-\gamma)}\right],$$

$$8\pi\kappa\,\mathbf{Td_4^4} \;=\; -\,8\pi\kappa\,(\,\mathbf{Td_1^1} \;+\; \mathbf{2}\,\mathbf{Td_2^2}\,)\;\;\text{since}\quad \mathbf{Td_3^3} = \mathbf{Td_2^2}$$

or

$$\mathbf{Td_4^4} \;=\; \mathrm{e}^{-\mu}\,\frac{1}{8\pi\kappa(\mathrm{Iu}\;-\;\gamma)}\left(\frac{\mathrm{u}^2}{\mathrm{R0}}\right)^2\left[-6\,u^2-(3u^3\;-1\,)\,\frac{(2u^3-1)(u^3-1)}{(Iu\;-\;\gamma)}\right]$$

and

$$8\pi\kappa\;(\,\mathbf{Td_2^2}\;+\;\mathbf{Td_1^1}\,)\;=\;e^{-\mu}\,\frac{1}{(Iu-\gamma)}\left(\frac{u^2}{R0}\right)^2\left[\,2\,u^2-\;(3u^3\;-1\,)\,\frac{(1-u^3)u^3}{(Iu-\gamma)}\right] \qquad (6)$$

leading to

$$(\mathbf{Fd_{14}})^2\;=\;-\,\mathrm{g}_{11}\mathrm{g}_{44}\big(\mathbf{Td_4^4}\;+\;\;\mathbf{Td_1^1}\big)\;=\;\mathrm{g}_{11}\mathrm{g}_{44}\big(2\;\mathbf{Td_2^2}\;\big)\quad \text{and}$$

$$(\mathbf{Fd_{14}})^2(r\to\;\infty\,)\;\stackrel{\text{def}}{=}\;\left(\frac{\mathrm{Rs}}{2}\right)^2\frac{2}{8\pi\kappa}\,\frac{1}{\mathrm{r}^4}=\frac{\mathrm{Rs}^2}{2}\,\frac{1}{8\pi\kappa}\,\frac{1}{\mathrm{r}^4}\;\stackrel{\text{def}}{=}\;\left(\frac{\mathrm{q}}{4\pi\varepsilon o\;\mathrm{r}^2}\right)^2\frac{\varepsilon o}{2}. \qquad (7)$$

$$(\mathbf{Fd_{12}})^2+\;(\mathbf{Fd_{13}})^2\;\;=\;\mathbf{2\;g_{11}g_{11}}\left(\frac{\mathbf{Td_4^4}\;-\;\mathbf{Td_1^1}}{\mathbf{2}}\right)\;\stackrel{\text{def}}{=}\;\mathbf{Fd_{mag}}^{\mathbf{2}}\;=$$

$$=\;-\,2\;\mathbf{g_{11}g_{11}}\big(\mathbf{Td_1^1}\;+\;\mathbf{Td_2^2}\big)\quad \text{and}$$

$$(\mathbf{Fd_{12}})^2+\;(\mathbf{Fd_{13}})^2(\mathbf{r}\to\;\infty\,)=\;\;2\;\mathrm{Rs}\;\mathrm{R0}^3\,\frac{1}{8\pi\kappa}\,\frac{1}{\mathrm{r}^6}\;\stackrel{\text{def}}{=}$$

$$\stackrel{\text{def}}{=}\;\;\frac{\mu o}{2}\,(\frac{\mu_{spin}}{2\pi}\,)^2\,\frac{1}{r^6} \qquad (8)$$

where

$$\mu\_spin\;\;\stackrel{\text{def}}{=}\;\;(\,\frac{g_e}{2}\frac{Qe}{3M}\,)\;S\;\hbar\quad \text{and}\quad g_e\;=\;\;2.0023193043\;6\;(\text{for the electron})\;.$$

The field equations, in both the EM realm and the gravitational realm ($Q = 0$), exhibit r^{-6} geometric behavior which we have interpreted as constituting a "magnetic monopole" mimic (what is a "magnetic monopole" ?).

References

16. D. Koehler, Geometric-Distortions and Physical Structure Modeling. *Indian J. Phys*. **87**, 1029 (2013).
17. R. Tolman, Relativity, Thermodynamics and Cosmology. Dover, NY, 248 (1987).

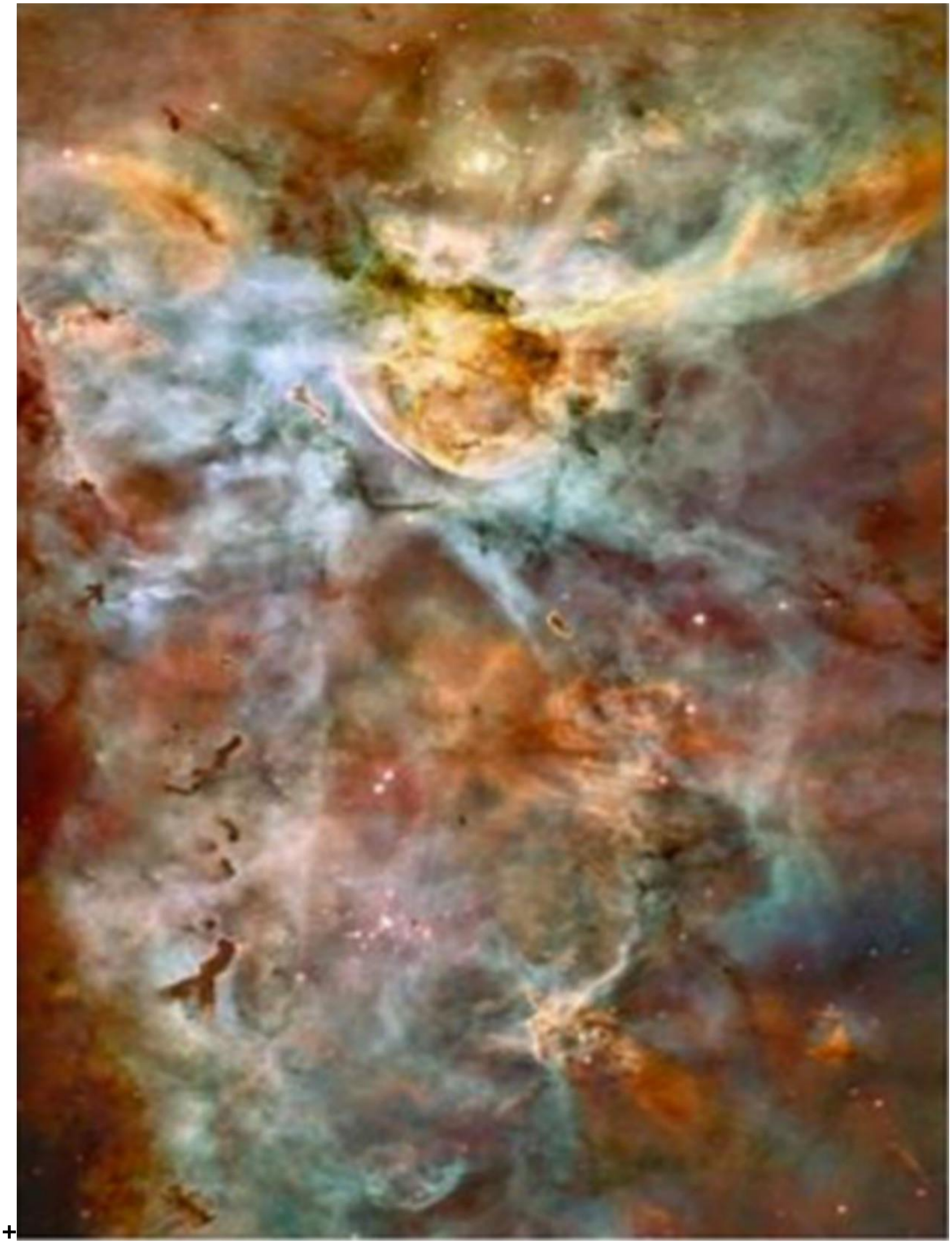

Panorama of the Carina Nebula @ Hubblesite.org

CHAPTER 2

Vibrational Eigen-frequencies

Chapter Summary: Eigen-modes, or the excited unstable vibrational states of the distortion-mimic of the electron, are posited as distortional-mimics of the fundamental fermions while a distortionally mimicked boson family is generated to include the W-boson.

2.1. INTRODUCTION

The work of the present chapter extends the modeling effort [1] and Chapter 1 to examine the apparent quantization or sequencing of the mimicked physical structures; masses and field variables (charge and spin) are the physical entities which influence the geometric structure and are the entities we mimic.

A distortional, or particle, transformation process was previously quantified in terms of a geometrical mediating particle with characteristics mimicking the Fermi β-decay transition [1].

2.2. STRUCTURAL EQUATIONS AND PHYSICAL MODELING

The geometrical model utilizes the classical curvature representation of a spatial energy distribution to define the particle structure and was extensively developed in ref. [1]. The line element describing the distorted geometric-region, here labelled Eq. 1, was determined;

(1) $$ds^2 = g_{11}[dr^2 + r^2 d\Omega] + g_{44} dt^2 = -e^{\mu}[dr^2 + r^2 d\Omega] + e^{\nu} dt^2$$

with $\mu = \mu(r,t)$ and $\nu = \nu(r,t)$. The metric quantity g_{11} , in ref. [1]], was however, incorrectly displayed as $g_{11} = -e^{-\mu}$. (see STRUCTURAL EQUATIONS from chapter 1).

2.3. DISTORTIONAL VIBRATIONAL-SEQUENCES

The composition of the fermion mass-energy family, including the electron, the muon and the tauon, suggests in the geometric domain, that some structural sequence or quantization could be manifest.

We here consider a structural mass-sequence by assuming “spherical vibrations of the distortional electron-structure, with its negative-energy core r_o”, as the fundamental geometric structural sequencing principle, wherein the distortional muon and tauon are then modeled as excited distortional-electrons. The importance of the radial function r_o, or its reciprocal, stems from a consideration of the mimicked energy

densities, inherent in the geometric distortions of the manifold, where electric-charge, spin and mass arise distinctively from this negative-energy-density core.

The radial zeroes, the determiners of the negative energy-density cores, emerge from the energy tensors of Eq. 3, and are stated through the zeroes of Eq. 28 Chapter 1 and the fundamental definitions of Eq. 5. These root functions for electrical-field energy $(\mathrm{Td}_2{}^2)$, mass-energy $(\mathrm{Td}_4{}^4)$, and magnetic-field energy $(\mathrm{Td}_2{}^2 + \mathrm{Td}_1{}^1)$, were illustrated in Fig.1.11, Chapter 1. For the "E/grav"-field case, with $\mathrm{ro} = \mathrm{Rs}$ and $\gamma = 2\ \mathrm{uo}$, $\mathrm{uo(root)} = \mathrm{uE0(Q{=}0\ or\ grav)} = 1.638$; for the mass-energy case, with $\mathrm{ro} = \mathrm{Rs}$ and $\gamma = 2\ \mathrm{uo}$, $\mathrm{uo(root)} = \mathrm{uM0(Q{=}0\ or\ grav)} = 1.453$; for the B-field case, with $\mathrm{Q} = 3$, $\mathrm{uo(root)} = \mathrm{uB0(Q{=}3,S{=}1)} = 1.807$ and for $\mathrm{Q} = 0\mathrm{(grav)}$ with $\mathrm{ro} = \mathrm{Rs}$ and $\gamma = 2\mathrm{uo}$, $\mathrm{uo(root)} = \mathrm{uB0(Q{=}0,S{=}1/2)} = 1.304$.

The classical wave-equation solution for the eigen-mode spectrum of a spherically-symmetric vibrating-sphere with a stress-free surface assumes (1), a constant propagation-velocity throughout the sphere (structural material elastic-properties, namely the Bulk and Shear-moduli, determine the velocity and mass) and (2), a stress-free boundary condition at the sphere's radius. These modeling assumptions lead to an eigen-frequency Bessel-function-solution involving $(\mathrm{a{+}bj{+}cj^2})^{1/2}$ -type polynomials for the integer-sequencing-index. The present geometric spherical model, with a variable core-velocity, created by a non-linear torsional-driving force, a radius-dependent mass density and a mass, or S- and Q-dependent sphere radius, uses an equivalent-form for the wave-propagation velocity (see the classical development of

#Love [3]) and is expressed in distortional energy-density tensor terms (see Eq. 2-8, SEQUENCING)(equation numbering is chapter specific as is Eq. 1).

In Chapter 4 we model baryon structures with muonic-substructures, thereby producing a requirement to mimic muonic-like structures where the distortional Q state mass energies are equivalent. This mimicking can be realized if the "vibrating structure" ground states are expressed as

(9) $$\mathrm{M}(1,1/2,1)\ \mathrm{me}\ \mathrm{c}^2 = 0.1375\ \mathrm{me}\ \mathrm{c}^2 \text{ and}$$

$$\mathrm{M}(1,1/2,2)\ \mathrm{me}\ \mathrm{c}^2 = 0.2851\ \mathrm{me}\ \mathrm{c}^2\ .$$

Distortions with $S = 1/2$, $\mathrm{Q} = \pm 1$ and ± 2, which will produce muon-mimics with charge-values $\pm \mathrm{e}/3$ and $\pm 2\mathrm{e}/3$, are therefore calculated as excited states of

$\mathrm{M}(1,1/2,1)\ \mathrm{me}\ \mathrm{c}^2$ and $\mathrm{M}(1,1/2,2)\ \mathrm{me}\ \mathrm{c}^2$ and illustrated in Fig. 2.1.

Justification for the simple 1-parameter sequencing function, $(\mathrm{j}^{\mathrm{geo}2} - 1)$, is its ability to mimic both the muon and tauon mass-energies as vibrational states of the electron. Fundamental mathematical construction of the sequencing function would require solution of the non-linear, radius(r)-dependent, wave equation.

These vibrational-mass-states are, furthermore, unstable since evanescent-wave-energy propagation, or tunneling [4], or energy equilibration, from the "oscillatory-core with its absorbent-shell" to the "positive-energy-envelope" will ensue. For the boson-structures, the absorbent-shell region is "thinner" than for the fermion structures

therefore producing a shorter boson-decay-time and a more unstable structure; $\Delta r_{absorption} = (1/uB0 - 1/uM0)\ hc\beta/(2\pi Mc^2)$. The same structural character differentiation is evident for the muon-mimic distortions. The radial extent of the absorption layer for the distortional mimic of the $Q = 3$ muon is 0.012 fm while the shell thickness, "imaginary velocity", or "equivalent absorption" layer, is $2.4(10)^{-5}$ fm for the distortional-boson $M(4,1,3)$ state. However, in considering the distortionally calculated "quantum-mechanical vacuum fluctuation" lengths for these geometric structures, at 0.113 fm for the muon and $1.48(10)^{-4}$ fm for the W^-boson, we see that structural details at these shell-thickness dimensions are "smeared" [5,6] to the point of extinction, that is, functional integral representations would render geometric detail undetectable. However a physically beneficial effect of fluctuation, or smearing, would be the diminution of the infinite-velocity-value at $uM0$. Nevertheless, re-establishing the vacuum fluctuation length as a gravitational representation ($\kappa = \kappa_G = G/c^4$) would allow the geometric dimensional detail to be manifest.

The mass of a fermion version ("fermion cousin" = W^-fermion ($S = ½$)) of the W^- fermion ($S = 1$) is manifest at $j = 4$ while the muon mass occurs at $j = 2$ and the tauon mass occurs at $j = 3$ as illustrated in Fig. 2.1. The boson-family-states sequence uses the W^-boson mass-energy for the reference mass-state at $j = 4$ where we have assumed that a distortional W^-boson is also such a vibrational structure.

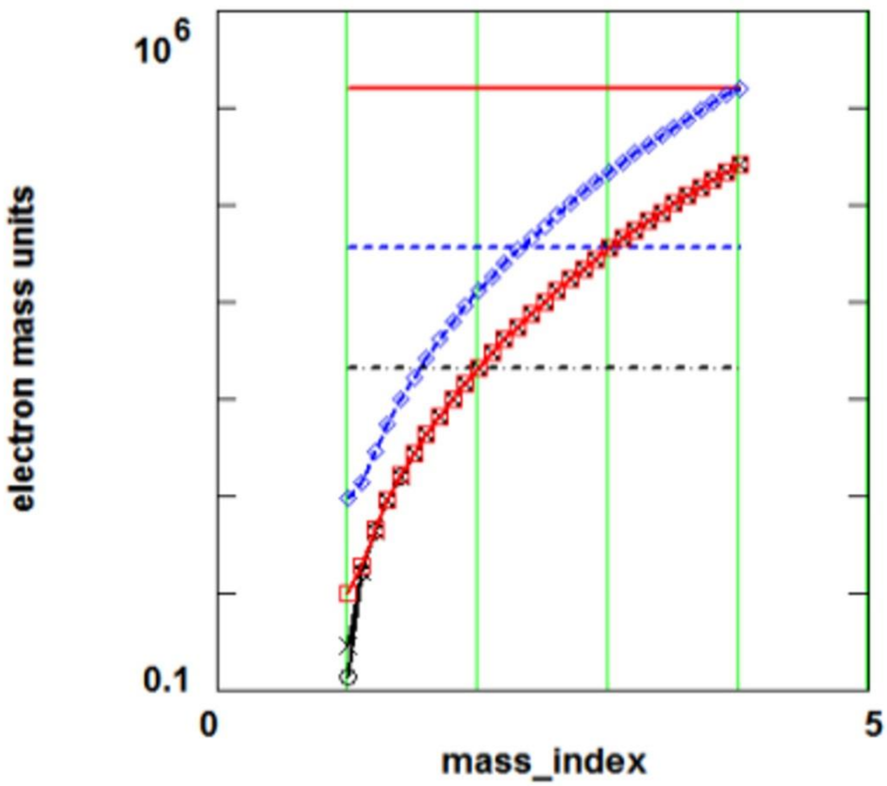

Fig. 2.1 Vibrational-mode mass-function $M(j,1/2,3)$ represented by (⊡), reference mass-energy W^-boson represented by *(——)*, reference tauon mass-energy represented by *(-----)*, reference muon mass-energy represented by (− · − · − ·), vibrational-mode mass-function $M(j,1,3)$ represented by (◊◊◊◊◊); muon- mimic mass-energies $M(j,1/2,2)$ and $M(j,1/2,1)$ are represented by (x) and (o) as a function of a decimal representation of the mass index j.

The theoretical mass values generated from the above mass equations for the muonic structures, Eq.12, and used to construct Fig. 2.1 are

free-muon-mass-3 $(Q = 3e/3) = mp_3 = 206.768$ [theoretical

& experimental] ,

free-muon-mass-2 $(Q = \pm 2e/3) = mp_2 = 206.768$, and

free-muon-mass-1 $(Q = \pm\, e/3) = mp_1 = 206.768$.

Fig. 2.2 displays the geometric velocity-function as a function of r throughout the distortional volume. The premise that the radius of the vibrating sphere, $r_{sphere} \sim R0(j,1,3)\ uB0(1,3)^{-1}$, is evident in the figure.

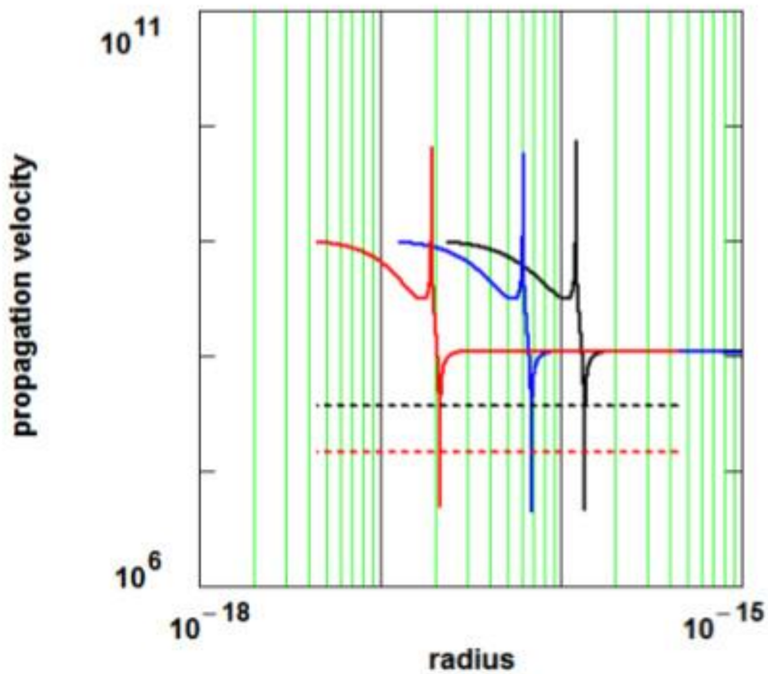

Fig. 2.2 Eigen-mode velocity function, $vel_{geo}(u,1/2,3)$ represented by (**-----**), eigen-mode velocity function, $vel_{geo}(u,1/2,2)$ represented by (**-----**), $vel_{geo}(u,1/2,1)$

represented by (**-----**) and solution ($S{=}1/2$, $Q{=}1$ and 3) propagation-velocities (vel @ $u = uo$) represented by (----- and -----), in meters/second, as a function of the radius in meters.

The absorptive shell-region thicknesses are realized at $1.90(10)^{-3}$ fm, $6.19(10)^{-3}$ fm and $12.3(10)^{-3}$ fm, i.e. there is less evanescent transmission of energy, from core through shell, as Q increases.

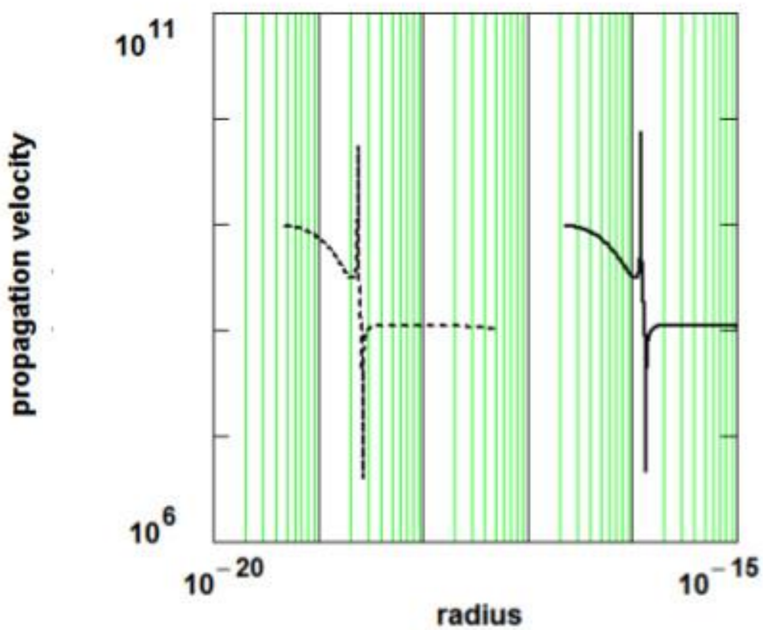

Fig. 2.3 The muon-mimic eigen-mode velocity function, $vel_{geo}(u,1/2,3)$, represented by (**-----**) and the W⁻boson mimic eigen-mode velocity function $vel_{geo}(u,1,3)$, represented by (---), expressed in meters/second, as a function of the radius in meters.

Fig. 2.3 displays the contrast between the distortional muon-mimic and the distortional W^-boson mimic where the boson-shell region has shrunk to $2.40(10)^{-5}$ fm, which is the most unstable structural configuration.

The magnetic-field mimicking tensors, but more explicitly the r^{-6} element of all the distortional tensors, are the source of the coupled field quantities j, S and Q. Furthermore, the inverse Fermi constant, $1/GF$, representing the condition of "maximum" curvature or maximum energy-density, of $Q = 3$ structures, originates in the energy-volume product, $2\ Mc^2R0^3 = \mu\_spin^2\ \mu o/2\pi$, the coefficient of the $1/r^6$ component of all the electric-charge-based distortions.

REFERENCES

[1] D R Koehler Indian J. Phys. 87 1029 (2013) DOI 10.1007/s12648-013-0321-5

[2] E V Linder *First Principles of Cosmology* (Addison Wesley: Essex, England) (1997) p23

[3] A E H Love *A Treatise on the Mathematical Theory of Elasticity* (Dover, New York) (1944)

[4] M Razavy *Quantum Theory of Tunneling* (World Scientific) pp.4, 462 (2003) ISBN 9812564888

[5] J T Grissom, D R Koehler and B G Gibbs *Nucl. Instrum. Methods* 45 190 (1966) DOI: 10.1016/0029-554X(66)90290-4

[6] J T Grissom and D R Koehler *Am. J. Phys.* 35 *753 (1967)* DOI*:* 10.1119/1.1974231

SEQUENCING

(2) $$\mathrm{vel_{geo}} = \sqrt{\frac{\mu}{\rho}}\ , \qquad \omega o = \frac{\mathrm{vel_{geo}}}{R},\ \text{ where } R = \text{sphere radius},\ \text{ and}$$

$$\rho = \text{mass density} \stackrel{\text{def}}{=} -\frac{2}{c^2}\left(\mathrm{Td}_1^1(u,S,Q) + 2\ \mathrm{Td}_2^2(\ u,S,Q)\right)\ ;\ \text{also}$$

$$\sigma(u,S,Q) = \text{Poisson's\_ratio} \stackrel{\text{def}}{=} -\sigma o\ \frac{\mathrm{Td}_2^2(u,S,Q)}{\mathrm{Td}_1^1(u,S,Q)} \quad \text{and}$$

$$\mu = \text{shear modulus} \stackrel{\text{def}}{=} 3\ \mathrm{Td}_1^1(u,S,Q)\left(\frac{1-2\sigma}{2(1+\sigma)}\right) =$$

$$= 3\ \mathrm{Td}_1^1(u,S,Q)\left(\frac{\mathrm{Td}_1^1(u,S,Q)\ + 2\sigma o\ \mathrm{Td}_2^2(u,S,Q)}{2\left(\mathrm{Td}_1^1(u,S,Q)\ - \sigma o\ \mathrm{Td}_2^2(u,S,Q)\ \right)}\right)\ .$$

Because the mass-energies are relativistic, we accommodate the velocity (momentum) term as

(3) $$pc = M\ \gamma\ \mathrm{vel}\ c = Mc\left[\frac{\sqrt{\frac{\mu(u,S,Q)}{\rho(u,S,Q)}}}{\sqrt{1-\frac{\mu(u,S,Q)}{\rho(u,S,Q)}\left(\frac{1}{c'}\right)^2}}\right] \stackrel{\text{def}}{=} Mc\ \mathrm{vel\_r}\ .$$

In order to mimic the distortional mass-families and in particular the fermion mass-family ($S = ½$, $uB0\ (Q = 3)$), we use the negative-energy core-radius $rB0$ (j, $S = ½$, $Q{=}3$) as closely approximating the radius of the vibrating sphere in its jth mode; utilization of the velocity function at this geometric radius satisfies the “vibration-energy ≡ mass-energy” model. Since $rB0(j,S,3) = R0(j,S,3)/uB0(S,3)$, we write, for the sphere’s

frequency spectrum, with a relativistic velocity representation and using the classical development of Love [3],

(4) $$\omega(\text{torsional})_j = \frac{\text{vel\_r}_{\text{geo}}(u,S,3)}{rB0(j,S,3)} = \frac{\text{vel\_r}(uo,S,3)}{rB0(j,S,3)} =$$

$$= \frac{1}{rB0(j,S,3)} \left[\frac{\sqrt{\dfrac{\mu(u,S,3)}{\rho(u,S,3)}}}{\sqrt{1 - \dfrac{\mu(u,S,3)}{\rho(u,S,3)}\left(\dfrac{1}{c'}\right)^2}} \right]_{u=uo} \qquad \text{where}$$

the mode(j)-dependent, spin(S)-dependent, charge(Q)-dependent vibrating sphere radius is

$$\frac{1}{rB0(j,S,3)} = \frac{M(\,j=1,S,3)c^2}{\hbar c} \frac{uB0(S,3)}{\beta(S,3)} f1(j) \text{ and}$$

$$\beta(S,3) = \left(S \frac{g_e}{2} \frac{3}{3} \sqrt{2\,\alpha fs/3}\right)^{\frac{2}{3}} .$$

Therefore, if the vibrational-energy is manifest as mass-energy, and the geometric-distortional-radius rB0 is the source of the integer-sequencing-function for the sphere's eigen-frequency spectrum, that is, if with a non-polynomial sequencing-function,

$$(5) \qquad \hbar\omega = M(1,S,3)c^2 \, \frac{uB0(S,3)}{\beta(S,3)\ c} \left[\frac{\sqrt{\frac{\mu(u,S,3)}{\rho(u,S,3)}}}{\sqrt{1 - \frac{\mu(u,S,3)}{\rho(u,S,3)} \left(\frac{1}{c'}\right)^2}} \right]_{u=uo} \quad f1(j) \stackrel{\text{def}}{=} \Delta(Mc^2) \quad \text{then}$$

$$\left(\frac{M0_{distortion}c^2}{M(1,S,3)c^2}\right)^2 = 1 + \left[\frac{uB0(S,3)}{\beta(S,3)} \ \frac{vel(r{=}0)}{4\pi} \left(\frac{\pi}{3}\right)^{19/8} 1.000085 \left(j^{geo2}\text{-}1\right)\right]^2 .$$

The Poisson's-ratio cofactor, as a result of imposing a positive-velocity → 0 as a boundary condition at infinity, is $\sigma o = 0.5$ with a negative bulk-modulus. To mimic the muon-mass-energy state ($j = 2$), to six-place numerical accuracy, as the first eigen-mode of an "excited vibrating electron", the propagation velocity-value, equivalent to the classical constant-velocity-value for the structure, is manifest at $r = ro(0.9934852\ uB0)$.

The velocity function is expressed as (see Eq. 10 also),

$$(6) \qquad vel(uo) = \frac{\beta(S,3)}{uB0(S,3)} \ \frac{\sqrt{m\mu^2\text{-}1}}{2^{geo2}\text{-}1} = \left(4\pi \left(\frac{3}{\pi}\right)^{\frac{19}{8}} 0.9999146\right)^{-1} \times vel(r{=}0) \ ;$$

$$vel(r = 0) = c\sqrt{\frac{15}{8}} .$$

The modeling leads to a relativistic radially-dependent-velocity (Eqs.5, 6 and 9 for a geometrically-distorted structure) exhibiting an absorptive shell (an imaginary propagation velocity) from $ro(uM0)$ to $ro(uB0)$; the functional zero-velocity at $uB0$

constitutes a natural node. The “absorptive shell, $\mathrm{ro(uB0)}\ \Delta$,” is created or caused (akin to the μspin origin of the Fermi-constant [1]) by the distortional-spherical magnetic-field energy-density distribution $\mathrm{Td}_1^1(\mathrm{u},S,\mathrm{Q}) + 2\,\sigma\mathrm{o}\,\mathrm{Td}_2^2(\mathrm{u},S,\mathrm{Q})$; the mass-energy density crossover from the negative-energy core is physically acceptable as a zero at $\mathrm{ro} = \mathrm{R0/uM0}$.

Additionally the wave-velocity behaves according to the form, $\mathrm{vel_{geo}(uo},S,3)=\sqrt{\frac{\mu(\infty,S,3)}{\rho(\infty,S,3)}}\ \mathrm{f}$, with the ratio factor $\mathrm{f} = \frac{1}{4\pi}\left(\frac{\pi}{3}\right)^{19/8} 1.000085$. For this structural-deformational vibration then, a $\text{propagational velocity} = 0.1215894\ \mathrm{c}$ ensues where $\mathrm{uB0} = 1.705168$. The mass-energy function, Eq. 8 for the electron vibrational structures, becomes

(7) $$\mathrm{M(j},S)\mathrm{c}^2 = \mathrm{M(1,1/2,Q)\ me\ c}^2\sqrt{1+\left(\mathrm{geo1}\left(\mathrm{j^{geo2}}\text{-}1\right)\right)^2}$$

$$\text{with} \quad \mathrm{geo1} = \frac{\sqrt{[\,\mathrm{M(2,1/2,Q)/M(1,1/2,Q\,)}]^2\text{-}1}}{2^{\mathrm{geo2}}\text{-}\ 1} \qquad \text{and}$$

$$\mathrm{geo2} = \mathrm{root}\left(\frac{2^{\mathrm{x}}\ \text{-}\ 1}{3^{\mathrm{x}}\ \text{-}\ 1}\ \text{-}\ \sqrt{\frac{\mathrm{m\mu}^2\ \text{-}\ 1}{\mathrm{m\tau}^2\ \text{-}\ 1}}\ ,\mathrm{x}\right) = 6.941805.$$

The quantities $\mathrm{m\mu}$ and $\mathrm{m\tau}$ denote the mass energies of the muon and tauon in electron-mass-energy units. For the $\mathrm{S{=}1,\ Q{=}3}$ boson states,

(8) $$\mathrm{M(1,1,3)} = 9.1918\ \mathrm{me\ c}^2 \quad \text{and}$$

$$\text{geo1} = \frac{\sqrt{[\,M(4,1,3)/M(1,1,3\,)]^2 - 1}}{4^{\text{geo2}} - 1} \quad \text{where}$$

$$M(4,1,3)\ \text{me}\ c^2 = W^{-}\text{boson mass energy}.$$

Because the present vibrational-energy-model is S-dependent through uB0, vel and β, a "boson ($S=1$)" mass-family is energetically greater than the "fermion ($S=1/2$)" mass-family; there are presently, however, no "experimentally observed fundamental particle bosons with the exception of the W^{-}boson". Nor is there evidence for the distortional-particle mimicking a $j = 4$ fermion. However for an "excited $S=1$" distortional electron structure to be created, an additional $S=1/2$ particle (neutrino) would have to be part of the excitation or creation process.

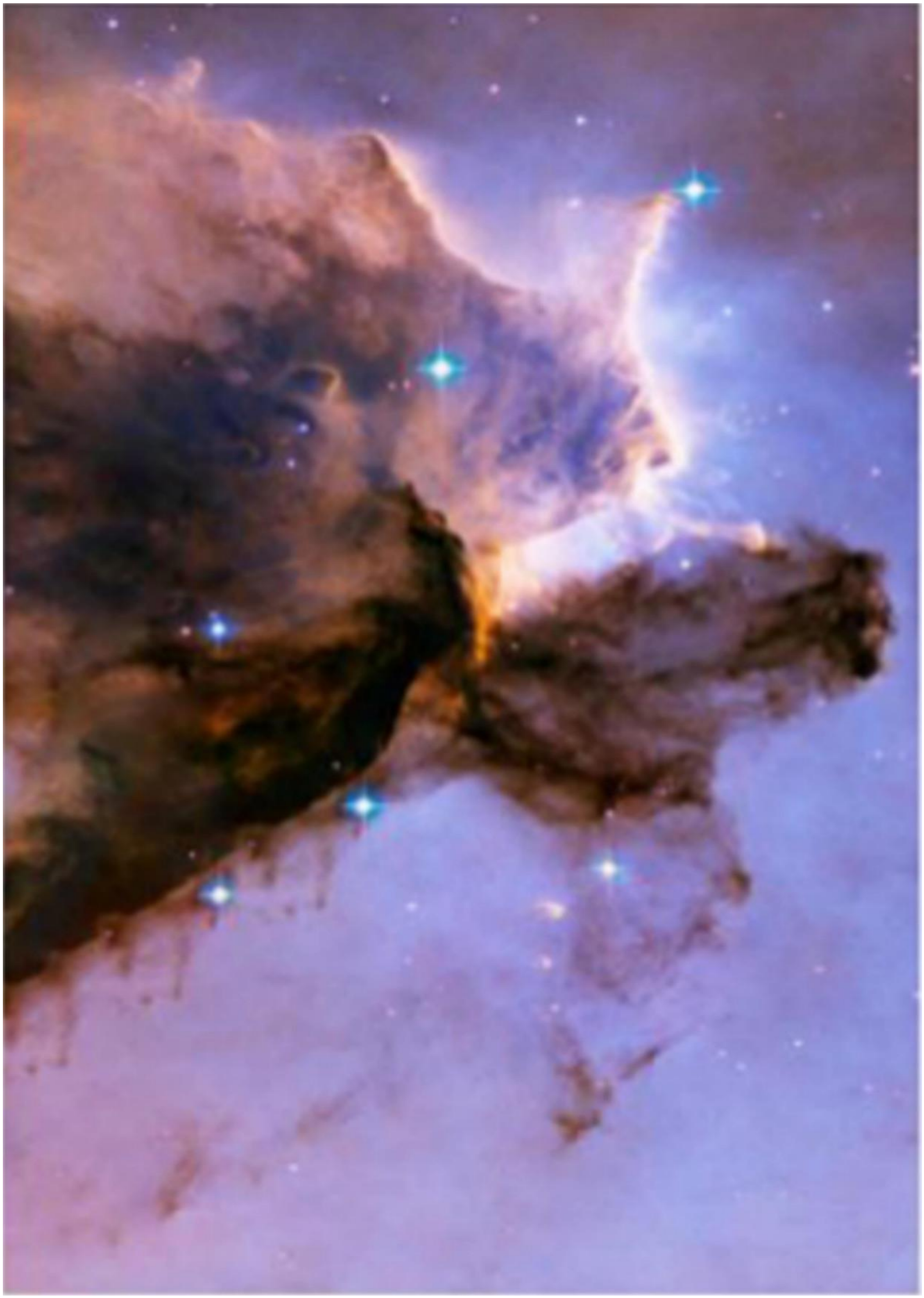

Stellar Spire in the Eagle Nebula.M16@Hubblesite.org

CHAPTER 3

Stability and Decay

+

***Chapter Summary*: The stability of these distorted geometric structures is formulated as a function of the descriptors of the unstable-negative-energy core and a temporal narrative of the decaying distortions is produced with a concomitant geometric descriptive mimic of the neutrino; the geometric-mimic resembles a hole-like structure.**

3.1. INTRODUCTION

The work described in the present chapter extends the modeling effort (Chapter 1 and references 1-12) to describe the stability character of the distortions and characterizes neutrinos as members of this single distortional family [5].

A distortional, or particle, transformation process was previously quantified in terms of a geometrical mediating particle with characteristics mimicking the Fermi β-decay transition [5]. The instability of this distortion is now further described as decay, or morphing of the geometric structure, and quantitatively treated as a radiative energy transfer from the geometric distortion's negative energy core, expressed by the classical Stefan-Boltzmann law.

3.2. STRUCTURAL EQUATIONS AND PHYSICAL MODELING

See Chapter 1 and Chapter_2 for the geometric equations developed to describe the distorted geometry and the particle-mimics.

3.3. STABILITY AND DISTORTIONAL-TRANSITIONS

The question of structural stability is posed as, "under what circumstance is the distortional negative-energy region stable relative to its positive-energy envelope?" We consider the negative-energy core as a region of potential instability; in the previous Chapter 2, the muon and tauon were characterized as the "first two vibrational states of the distortional-electron", the modal energy-structure consisting of a negative-energy core surrounded by an absorptive shell (imaginary-velocity) through which evanescent-wave energy would propagate.

A "stability criterion" and a "stability functionality" are posited as follows; for charged structures ($q \neq 0$, *excluding the neutrino)* "geometric-distortional stability" is manifest when the physical radial extent of the negative-energy-density region, expressed as a geometric-curvature, $(1/\mathrm{ro})$, is not greater than (with $\mathrm{roe} \equiv \mathrm{rM0}(1,1/2,3)$) the electron core radial value,

$$(1)\ \mathrm{roe}^{-1} = \hbar c^{-1} \left(\frac{\mathrm{ge}}{2}\sqrt{\alpha\mathrm{fs}}\right)^{-\frac{2}{3}} \left(\frac{1}{2}\right)^{-\frac{2}{3}} \mathrm{uM0}\left(\frac{1}{2},3\right)\ \mathrm{me}\ c^2\ \mathrm{f}(1,1/2,3) \quad \text{(see Eq.20a for } \beta \text{ correction).}$$

Greater distortional curvature values (within the fermion and boson families) result in an “instability”, a radiating “negative-mass-energy” core (gray-body), with subsequent collapse and transitioning (morphing) to a more stable form of the distortional structure. A “gray-body” is manifest in the vibrational states of the distortionally mimicked electron as an absorptive shell surrounding the negative-energy core allowing evanescent wave-energy leakage. The emission characteristics of the body core therefore determine the temporal performance of the evolving body and development of the radiative-decay time-behavior, for such a classical “radiating-gray-body model” of an “unstable distortion”, is constructed.

Successively, an emissive stability factor, ε_s, is defined as

$$(2) \qquad \varepsilon(f)_s = \left(\frac{1}{rM0(j,S,Q)} - \frac{1}{roe}\right)^2 rM0(j,S,Q)^2 \frac{f(4,S,Q)^2}{\left(f(4,S,Q) - 1\right)^2} =$$

$$= \frac{(f(j,S,Q) - 1)^2}{f(j,S,Q)^2} \frac{f(4,S,Q)^2}{(f(4,S,Q) - 1)^2}$$

varying between 1 (W^- boson; no structural life; “instability”) and 0 (electron; infinite life or stable; no radiance). An additional metastability co-factor, defined as a radiation-inhibition or gray-body factor, is incorporated and constructed as a modified (Lorentzian) “Breit-Wigner (BW) [13] ”, geometric-spherical-radial-resonance, or quantized-radial "mass-energy factor ":

$$(3) \qquad \frac{1}{\varepsilon(f)_{BW}} = 1 + \sum_i \frac{B_i Av_i^2}{\left(f - f_i\right)^2 + Av_i^2} \quad \text{and} \quad \varepsilon(f)_{geo} = \varepsilon(f)_s \, \varepsilon(f)_{BW} \, ;$$

$$f = \frac{Mc^2}{me\ c^2}\ , \quad f_i = \frac{M(i,S,Q)}{me\ c^2}, \quad B_i = \frac{8\ me\ c^2}{\pi\ \hbar}\tau_i(f_i)^3 \quad \text{and}$$

$$Av_i = \frac{\hbar}{2\ me\ c^2\tau_i}\ .$$

The geometric resonance half-width at half-maximum has been set equal to the Breit-Wigner resonance half-width at half maximum, $\hbar/(2\tau\ me\ c^2)$. Emissivity is approximately a constant except @ resonances and @ $f = 1$ as shown in Fig. 3.1.

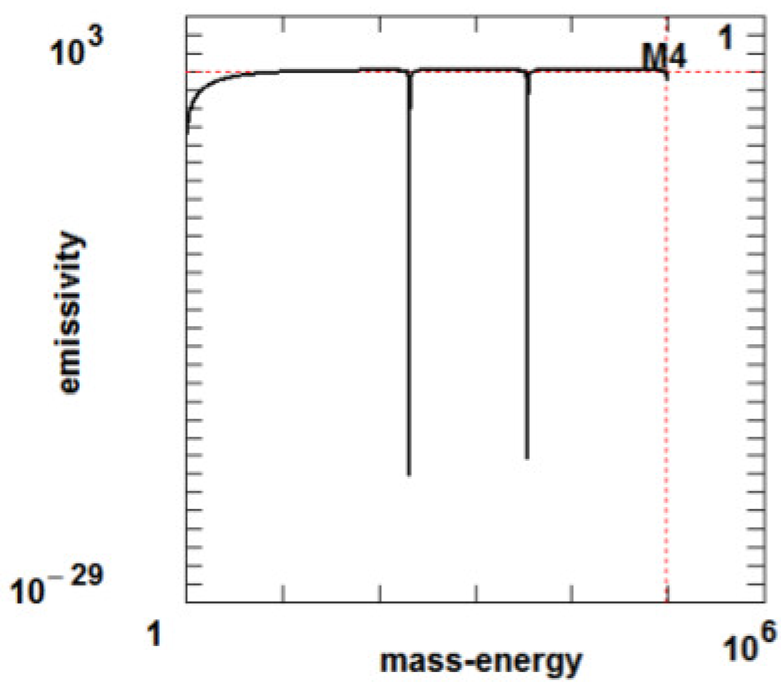

Fig. 3.1 Emissivity function $\varepsilon(j)_{geo}$ as a function of the normalized mass-energy function, $f(j\ ,\ ½,\ 3)$, is represented by *(——)* for the geometric-distortion structure. M4 is the normalized mass-energy value for the W^- fermion.

Mass-energy state-to-state radiation-energies (e.g. $\mathrm{M(muon)c^2 - M(electron)c^2}$) are manifested in “geometric-neutrino” emissions. The creation of a final-state $S = ½$ neutrino structure and the final-state fermion structure however requires an “intermediate” phase or decay stage (for conservation of the *S*-parameter) involving morphing to a facilitating structure and emission of a first neutrino. Subsequent decay ($\Delta t = \frac{\hbar}{\Delta E_j}$) of the distortional-boson ($S = 1$) produces the new final-state fermion (μ, τ, electron) ($S = ½$) and a second final-state “fermion” neutrino ($S = ½$).

When the classical Stefan-Boltzmann equations are applied, the energy-time evolution profile of the unstable structure is created. The mass-energy decay time profile (Stefan-Boltzmann) (see mass Eq. 10 taken from the previous Chapter 2) is,

$$(4) \qquad \mathrm{P} = \frac{\mathrm{df}}{\mathrm{dt}} = -\frac{\sigma}{\mathrm{k}^4}\, \varepsilon(\mathrm{f})_{\mathrm{geo}}\, \mathrm{A(ro)\, f^4} \ \text{ and } \ \mathrm{A(ro)} = 4\pi\, (\mathrm{ro(j,S,Q)})^2 (\mathrm{me\, c^2})^4 \ ,$$

or

$$\mathrm{t} = \int_{\mathrm{fo}}^{\mathrm{fend}} \mathrm{P^{-1} df} = -\tau\varepsilon \int_{\mathrm{fo}}^{\mathrm{fend}} \left(\varepsilon(\mathrm{f})_{\mathrm{geo}}\, \mathrm{f}^2\right)^{-1} \mathrm{df}$$

where

$$\frac{\sigma}{k^4} = c^{-2}\hbar^{-3}\frac{\pi^2}{60} \quad \text{and} \quad \tau\varepsilon = \left(\frac{\pi^3}{15\,\hbar}\frac{\left(\frac{ge}{2}\sqrt{\alpha fs}\right)^{4/3}}{1.877714^2}2^{-7/3}(\text{me } c^2)\right)^{-1} =$$

$$= 2.943107(10)^{-19}\text{sec.}$$

Rapid "change of state" mass-energy-changes at "distortion-lifetimes" are suggestive of "collapse" and are caused by the metastable character of the BW resonances and the associated dM/dt during the radiation morphing at resonance; the energy changes are in turn dependent on the strengths of the emissivity factors $\varepsilon(f)_{BW}$. The mathematical rendition of this structural morphing dynamic is primarily rendered in the $\tan^{-1}$ function of Eq. 10. On time scales $\sim \Delta t$ (Heis), geometric collapse to and expansion from the "virtual facilitating-boson-state" is therefore "allowed" and "energetics" are not violated.

(5) $$\text{timeBW}(f,f_i) = \frac{-\hbar}{2\pi\text{ me } c^2}\frac{f_i^2}{\left[(f_i - 1)^2 + \left(\frac{\hbar}{2\tau_i \text{mec}^2}\right)^2\right]^2}\text{ FT};$$

$$\text{FT} = \left[\frac{(f_i - 1)^2\text{-Av}_i}{\text{Av}_i}\ \tan^{-1}\left(\frac{f - f_i}{\text{Av}_i}\right) + (f_i - 1)\ln\left(\frac{(f - 1)^2}{(f_i - f)^2 + \text{Av}_i^2}\right) - \frac{1}{\left((f_i - 1)^2 + \text{Av}_i^2\right)(f - 1)}\right]$$

and $$\text{TIME}(f) = \frac{\tau\varepsilon}{(f - 1)}\left(\frac{f_4 - 1}{f_4}\right)^2 + \sum_{i=1}^{3}[\text{ timeBW}(f,f_i) - \text{timeBW}(f,f_4)\ ].$$

Fig. 3.2 shows the time development of the radiating, or morphing, W^-boson distortion as it would decay through the tauon-muon-electron branch.

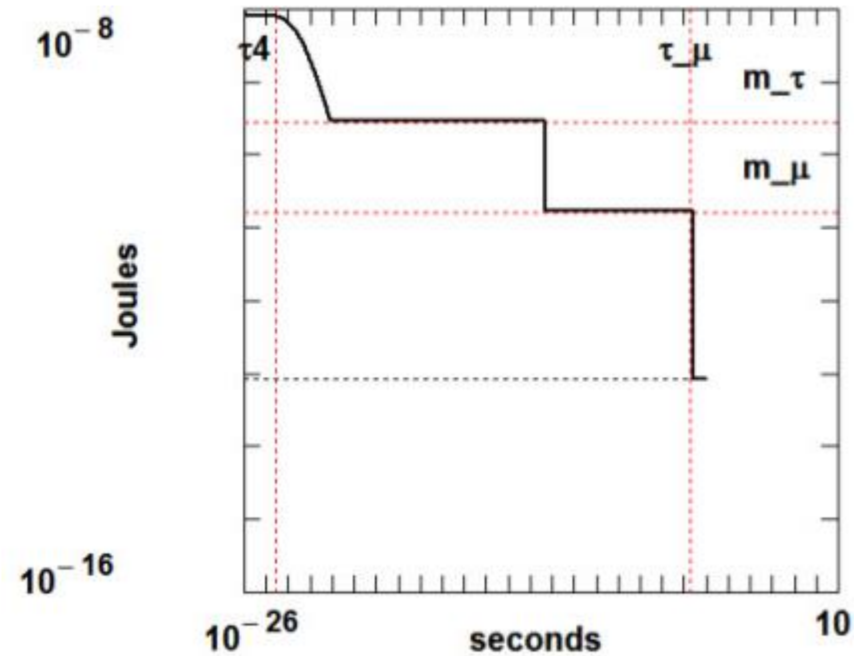

Fig. 3.2 Mass-energy decay profile M(j), represented by *(——)*, for the geometric-distortion structure, as a function of time in seconds; $m_e c^2$ is represented by (…..). The mass-energies m_μ and m_τ are the muon and tauon mass-energies while τ_μ and τ4 are the muon and W^-fermion half-lives.

The structural description for the neutrino-mimic suggested here originates from a consideration of the dynamic details of beta-decay wherein the geometric structure of the "mediating" particle produces the Fermi constant GF [5]. From examination of the "spin equation", with the experimentally measured neutrino characteristics, we see

depicted a structural radial-characteristic approximating that of the mediating beta-decay particle; that is, using $\mu spin_n \equiv \mu spin(\text{neutrino})=$ the experimental neutrino magnetic moment $=< 0.54(10)^{-10}\ \mu B$ [14] , $q_n \equiv q(\text{neutrino})$, $Mn \equiv Mc^2(\text{neutrino}) = < 2$ eV(experimental) and $M_W \equiv Mc^2(W^{-}\text{boson})$, then

(6) $$q_n = < \frac{4M_n\ \mu spin_n}{g_e\ \hbar c^2} < 2.1(10)^{-16}\text{e} \quad \text{and}$$

$$RB0(\text{neutrino}) = \frac{\hbar c\ \beta}{Mn} = 3.28(10)^{-19}\ \text{meter} \ ,$$

$$\text{where } \beta \stackrel{\text{def}}{\equiv} \left(\alpha \frac{2}{3}\ \left(\frac{g_e}{2} S\ q_n\right)^2\right)^{\frac{1}{3}};\ \ S = 1 \ .$$

Compare with

(6a) $$\left[RB0\left(\text{geo\_W}^{-}\text{boson}\right)\right]^{-2} \frac{3}{\pi^3} = \beta W \frac{\hbar c}{GF}\ ,\ \beta W = \left[\alpha\ \frac{2}{3}\ \left(\frac{g_e}{2}\right)^2\right]^{1/3} \quad \text{or}$$

$$RB0(\text{geo\_W}^{-}\text{boson}) = \sqrt{\frac{3\ GF}{\pi^3 \beta W\ \hbar c}}\ =\ 5.09(10)^{-19}\ \text{m}\,.$$

We posit therefore, that, in addition to the mediating boson particle and arising out of the same energy-density structural source, the associated participating geometric neutrino-mimic structure is manifest with the same geometric and physical descriptor (RB0) as the “beta-decay facilitating structure”, the W^{-}boson, and therefore the neutrino-mimic radius is $RB0_{geo}(\text{neutrino}) = RB0_{geo}(W^{-}\text{boson})$ and is a *“maximum-curvature”*

(maximum-energy-density) structure. Then, given the geometric-mimic of the neutrino mass as $\mathrm{Mn(geo)} < 1.796\ \mathrm{eV}$, $\mathrm{\mu spin(geo)} < 0.54\ \mathrm{\mu B}$ and geometrically,

.(7) $$\left(\frac{\mathrm{\mu spin(geo)}}{\mathrm{\mu B}}\right)^2 \ \frac{1}{\mathrm{Mn(geo)}} = \frac{3\ \mathrm{GF}}{\pi^3 \mathrm{M_W}}\ \frac{4\pi}{\mathrm{\mu o}}\frac{1}{\mathrm{\mu B}^2}\ = 0.0126\ \mathrm{Joule}^{-1}\ .$$

According to present experimental evidence [16-18], there are three known types (flavors) of neutrinos consisting of the electron neutrino (mass-energy < 2 eV), the muon neutrino and the tau neutrino and while $\mathrm{q} = 0$ is considered the physical electric-charge descriptor for these neutrinos, the value of the geometrically-mimicked and experimentally-determined electric-charge is of an infinitesimal magnitude-difference from a zero-physical neutrino charge value.

From Eq. 28 Chapter 1 one calculates the radial zero and the physical radius ron of the neutrino-mimic to be 2.95(10)$^{-22}$ m; the geo-Planck length of this same geometric-neutrino is $\sqrt{\hbar \mathrm{c}\ (\,\kappa\mathrm{o} + \mathrm{G}/2\ \mathrm{c}^4)} = 8.86(10)^{-25}\mathrm{m}$, although, as mentioned earlier, the gravitational based fluctuation length may be more appropriate for comparison.

REFERENCES

[1] I Ciufolini and J A Wheeler *Gravitation and Inertia* (USA: Princeton University Press) (1996)

[2] J A Wheeler *Phys. Rev.* 97 511 (1955)

[3] J A Wheeler *Logic, Methodology, and Philosophy of Science, Proc. 1960 International Congress* (USA: Stanford University Press) (ed) E Nagel p 361 (1962)

[4] W K Clifford *Proc. Cambridge philosophical society* 2 157 (1876)

[5] D R Koehler *Indian J. Phys.* 87 1029 (2013) DOI 10.1007/s12648-013-0321-5

[6] B Riemann *Nature* 8 14 (1873)

[7] P R Anderson and D R Brill *Phys. Rev*. *D* 56 4824 (1997)

[8] G P Perry and F I Cooperstock *Class. Quant. Grav*. 16 1889 (1999)

[9] R A Sones arXiv:gr-qc/0506011 (2005)

[10] K A Stevens, K Schleich and D M Witt *Class. Quant. Grav*. 26 075012 (2009)

[11] D N Vollick *Class. Quant. Grav*. 27 169701 (2010)

[12] J Louko *J. Phys.: Conf. Ser.* 222 012038 (2010)

[13] G Breit and E Wigner *Phys. Rev.* 49 519 (1936)

[14] C Amsler *Phys. Lett.* B 667 1 (2010)

Hubble's Sharpest View of the Orion Nebula @ Hubblesite.org

CHAPTER 4

Compound-Structure Modeling

***Chapter Summary*: Utilizing the fundamental curvature equations of Riemannian geometry we have extended the static geometric-distortion modeling to include composite structures. We describe spherically-symmetric combinations of the more fundamental distortions to mimic the neutron and the proton as well as their constitutive components; mass, electric charge and magnetic moments have been simulated.**

4.1 INTRODUCTION

We reference Chapters 1 and 2 for the geometric equations developed to describe the distorted geometry and the particle-mimics.

In Section 4.2 we expand the modeling to mimic bound-quark structures and associated neutron and proton mimics followed by Section 4.3 where we further treat a model of muon-like distortions composing three components of quark-mimics which form the substructure for proton and neutron structures.

4.2 GEOMETROSTATIC DISTORTIONS FOR A 3-COMPONENT NEUTRON AND PROTON

We assume that the neutron and proton magnetic moments derive from a composite of charged mass structures with $Q = -e/3$ and $+2e/3$. We also write a classical mass and binding-energy description of the composite structure as, with masses expressed in electron-mass-energy units and presented in "3-C NEUTRON" .

The quark-like spherically-symmetrical geometrical-distortion structures and the composites constructed therefrom (energy-density-tensor superpositions mimicking the quarks and the neutron and proton) are illustrated in Figures 4.1-4.6.

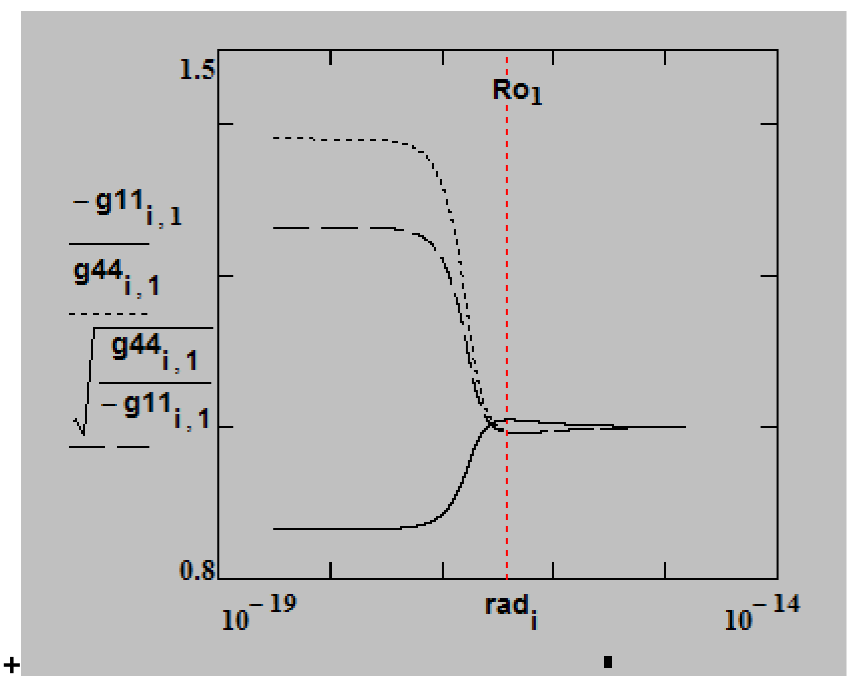

Fig. 4.1 Metrics $(g11 = g_{11}$ and $g44 = g_{44})$ and propagation-velocity factor for distortion-1 (down-quark mimic) structure; abscissa in meters.

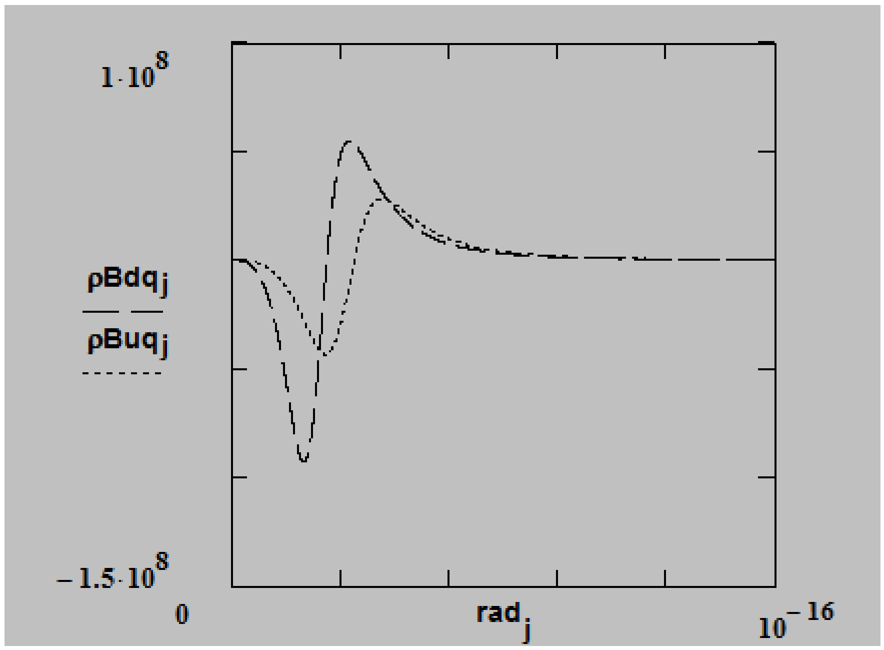

Fig. 4.2 The geometric mass-energy-density mimic for the bound-down-quark distortion is represented as ρ*Bdq* and the geometric mass-energy-density mimic for the bound-up-quark distortion is represented as ρBuq. The linear radial abscissa near the core-origin is shown in meters and the energy-density-ordinate is in units of Joules / meter^3.

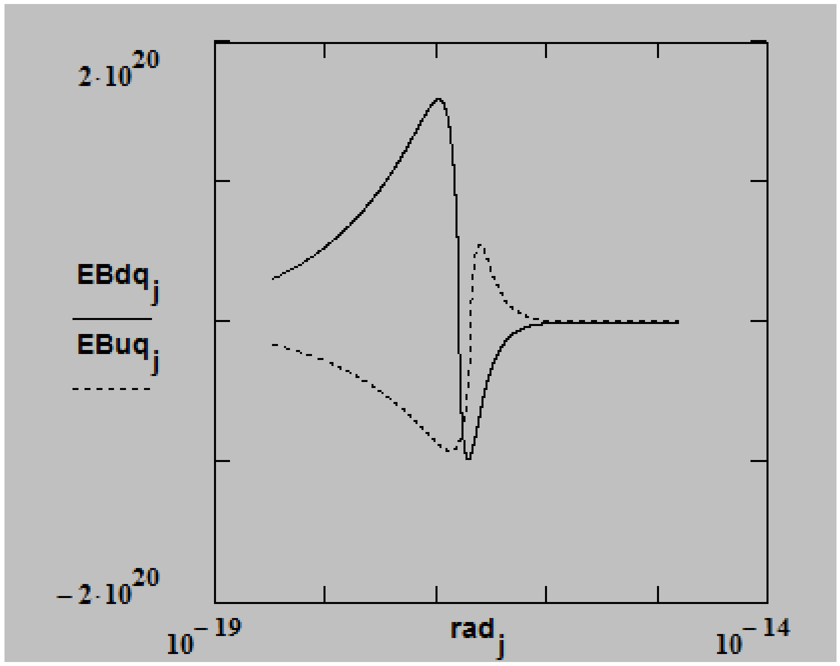

Fig. 4.3 The geometric *E*-field mimic for the bound-down-quark distortion is represented as EBdq and the geometric *E*-field mimic for the bound-up-quark distortion is represented as EBuq. The radial abscissa is shown in meters and the field-ordinate is in units of (Joules / meter^3)$^{1/2}$.

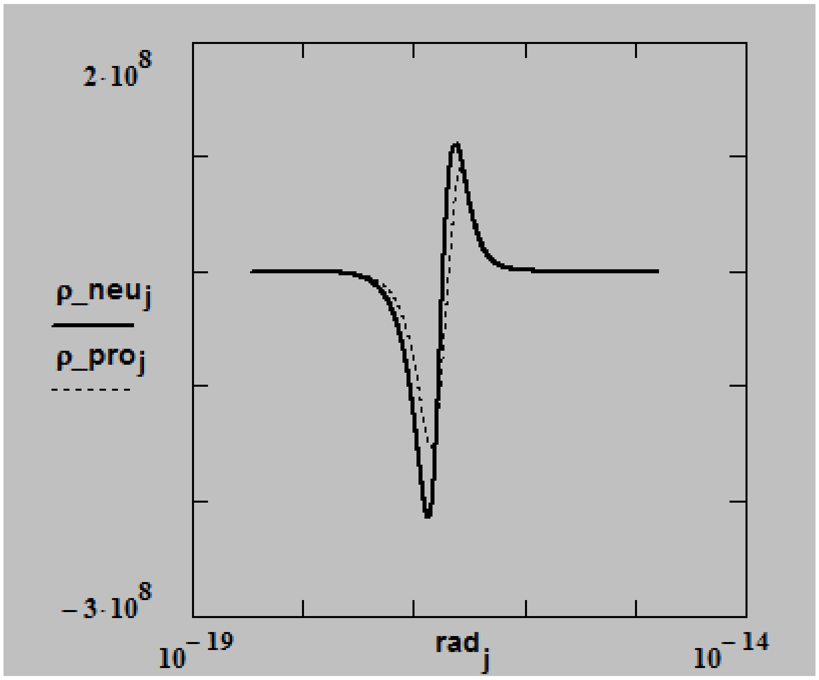

Fig. 4.4 The geometric mass-energy-density mimic for the neutron (constructed from the bound-quark distortions) is represented as ρ_neu and the geometric mass-energy-density mimic for the proton (constructed from the bound-quark distortions) is represented as ρ_pro. The radial abscissa is shown in meters and the energy-density-ordinate is in units of Joules/meter^3.

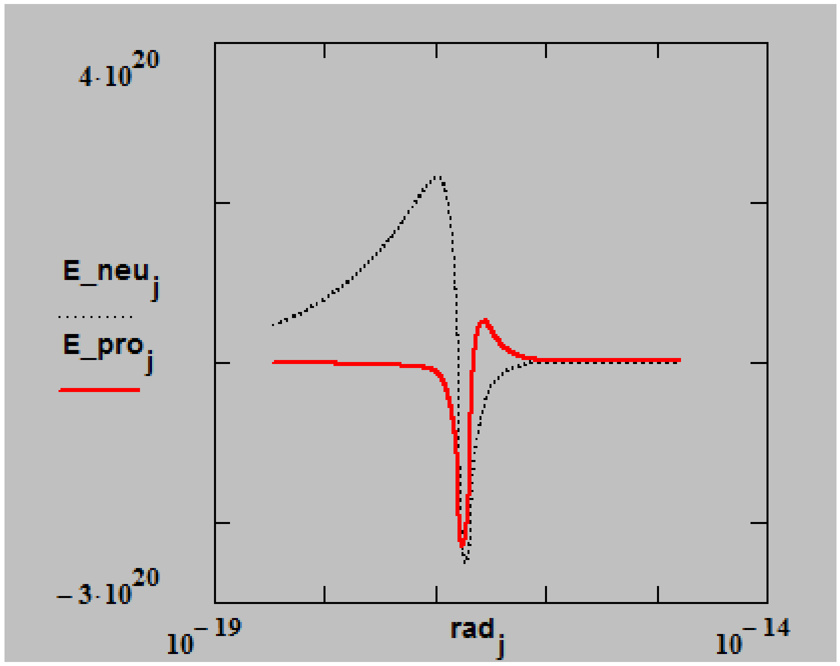

Fig. 4.5 The geometric *E*-field mimic for the neutron (constructed from the bound-quark distortions) is represented as E_neu and the geometric *E*-field mimic for the proton (constructed from the bound-quark distortions) is represented as E_pro. The radial abscissa is shown in meters and the field-ordinate is in units of (Joules/meter^3)$^{1/2}$.

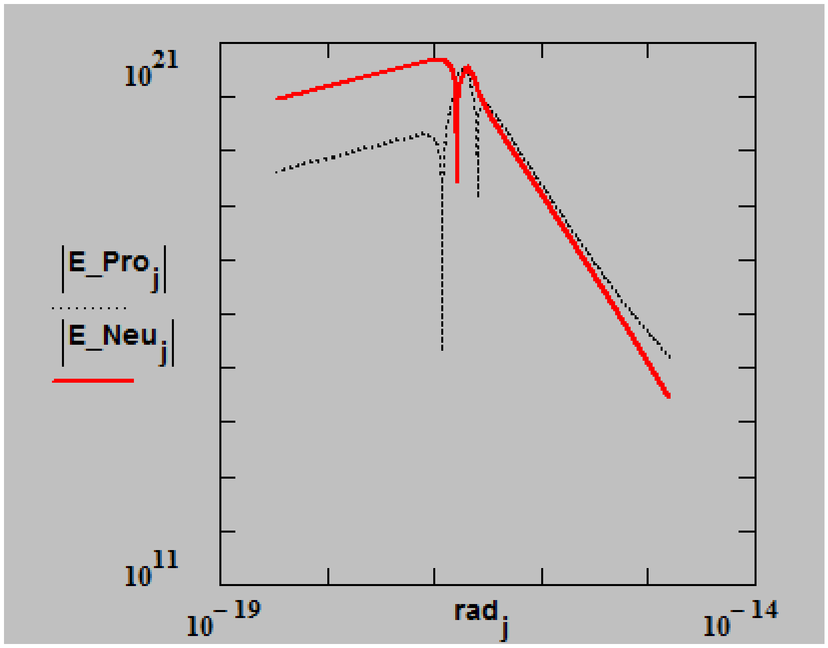

Fig. 4.6 The geometric *E*-field mimic for the neutron (constructed from the bound-quark distortions) is represented as E_Neu and the geometric *E*-field mimic for the proton (constructed from the bound-quark distortions) is represented as E_Pro. The radial abscissa is shown in meters and the field-ordinate is in units of (Joules/meter^3)$^{1/2}$**.**

We consider the geometric-field constructs as vectorially additive and combine the "electric-field mimic" and the "magnetic-field mimic" to produce E_Pro and E_Neu; the "magnetic-field", an r-directed, r^{-3} dependent quantity, has therefore been included in both neutron and proton field representations. The same commentary applies to the field-constructs E_μPro and E_μNeu in Section 4.3. Contrast this field behavior with the commentary in reference [3] where a "negatively charged skin" description is used to

characterize the field behavior at the exterior of the neutron. Furthermore, the “strong interaction” or “nuclear force” is described [4] as “The force is powerfully attractive between nucleons at distances of about 1 fm between their centers, but rapidly decreases to insignificance at distances beyond about 2.5 fm. At very short distances less than 0.7 fm, it becomes repulsive, and is responsible for the physical size of nuclei, since the nucleons can come no closer than the force allows.“ The compound-“distortion-neutron mimic” constructed here does not display the Miller-3-region behavior although the “distortion-proton” exhibits precisely this behavior (Fig. 4.6).

In the absence of free-quark mass information or other characterizing descriptors, we do not calculate the quark binding energies.

4.3 GEOMETROSTATIC DISTORTIONS FOR 3-COMPONENT QUARKS

One can proceed in the classical-structure manner and consider the quark entities as comprised of still smaller (mass) geometric-distortion structures. We assume therefore that the down-quark and up-quark derive from a composite of charged mass structures of the "*geometric muon-family-mimics"* with $\mathrm{Q} = \pm \mathrm{e}/3$, $\pm 2\mathrm{e}/3$ and $\pm 3\mathrm{e}/3$ (the model-3 distortions of Ref 1 Chap 1 and Chap 2); from this material we provide the development in "3-C QUARK" .

The quark substructure description therefore appears geometrically and energetically possible. From the physical perspective, the elements of the "particle anti-particle pair", normally in a physical annihilation condition, coexist when constrained within the distortional field of the third muonic-distortion-substructure. From the geometric perspective, the particle and anti-particle pair maintain their respective negative-mass-energy-density structures but the geometric-fields $\pm(\mathrm{Td}_4{}^4 + \mathrm{Td}_1{}^1)^{1/2}$ cancel (sum to zero) as per their respective charge-mimic structures thus producing a "composite negative-energy-density core"; a fundamental structural feature of the geometric model is that charge is realized (mimicked) through the stress-tensor $\mathrm{Td}_2{}^2$ and the magnetic-field stress-tensor construct $\mathrm{Td}_2{}^2 + \mathrm{Td}_1{}^1$.

The structural change process, omitting the intermediate virtual Fermi-mass phase of beta decay, is conceptualized and diagrammed in Figures 4.9 and 4.10. (quark colorization unimportant [5]).

GEOMETRIC DISTORTION MIMICS for NEUTRON to PROTON TRANSITION

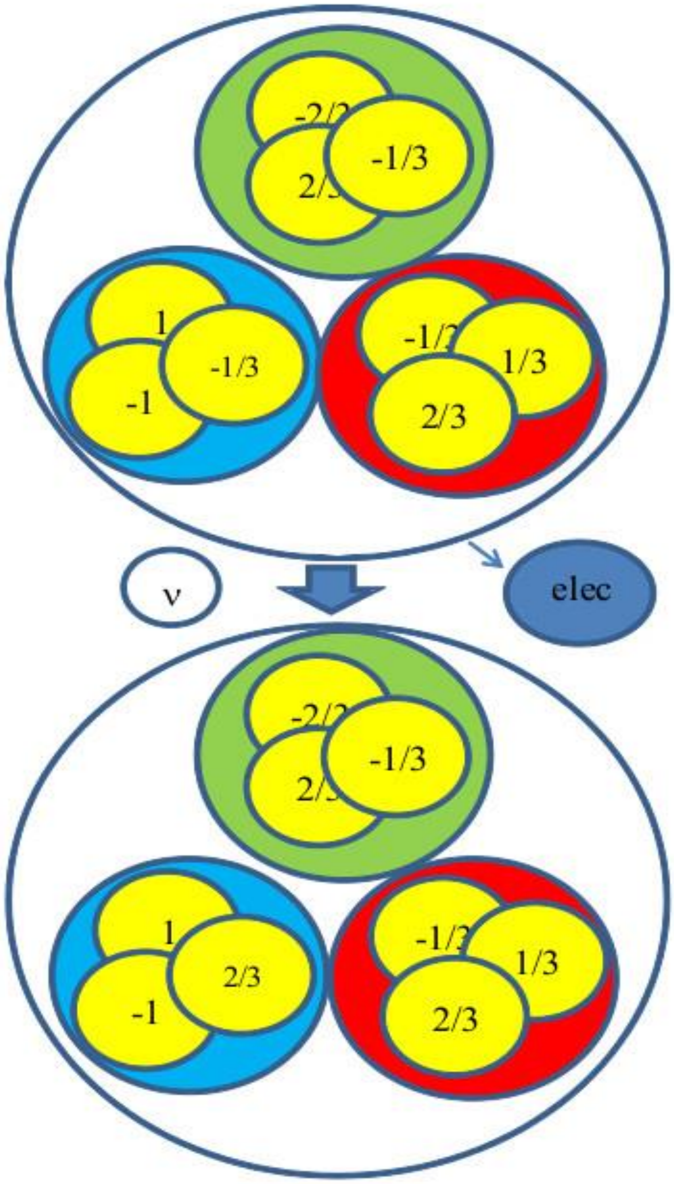

Fig. 4.9 Diagrammatic representation of a neutron-distortional-mimic, with muonic-quark substructures, morphing to a proton-distortional-mimic.

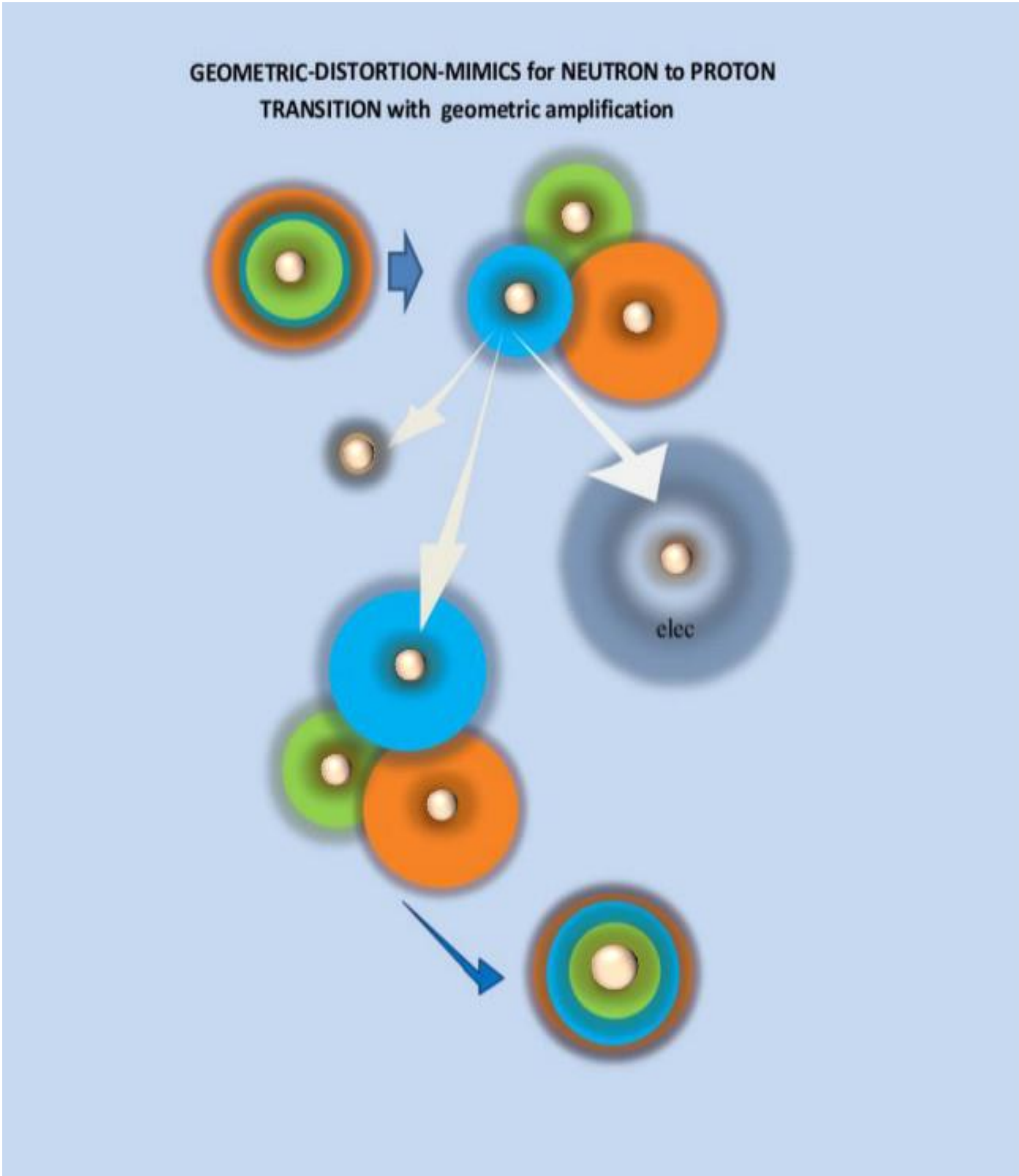

Fig. 4.10 Diagrammatic representation of a neutron-distortional-mimic, with muonic-quark substructures, morphing to a proton-distortional-mimic.

Muonic-like spherically-symmetrical geometrical-distortion structures and the quark, neutron and proton composite-mimics constructed therefrom (calculated as energy-density-tensor superpositions) are illustrated in Figures 4.11- 4.18.

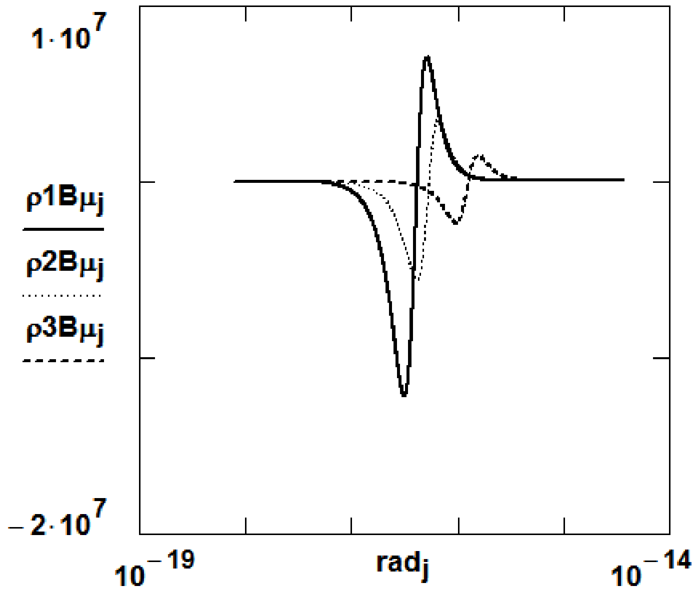

Fig. 4.11 The geometric mass-energy-density mimics for the bound-muon distortions are represented as $\rho 1\mathrm{B}\mu(\mathrm{mass} = 206.26)$, $\rho 2\mathrm{B}\mu(\mathrm{mass} = 203.73\ )$ and $\rho 3\mathrm{B}\mu(\mathrm{mass} = 201.2\ )$. The radial abscissa is shown in meters and the energy-density-ordinate is in units of Joules / meter^3.

Note the effect of distortion-radius $\mathrm{R0}$ on the magnitude of the energy-density functions in Figure 4.11. The distortion-masses are approximately equal but the smaller distortion-radius requires a greater energy-density magnitude to achieve the same

functional integral. Geometric-distortion-fields, of course, (see Figures 4.16 and 4.17) also illustrate the same dependence.

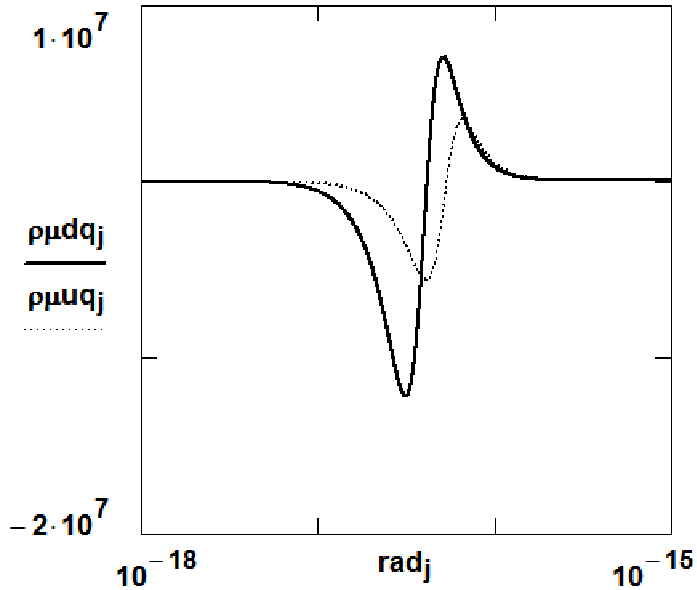

Fig. 4.12 The geometric mass-energy-density mimic for the bound-muon ($q = -1/3$) distortion is represented as $\rho\mu dq$ and the geometric mass-energy-density mimic for the bound-muon ($q = 2/3$) distortion is represented as $\rho\mu uq$. The radial abscissa is shown in meters and the energy-density-ordinate is in units of Joules / meter^3.

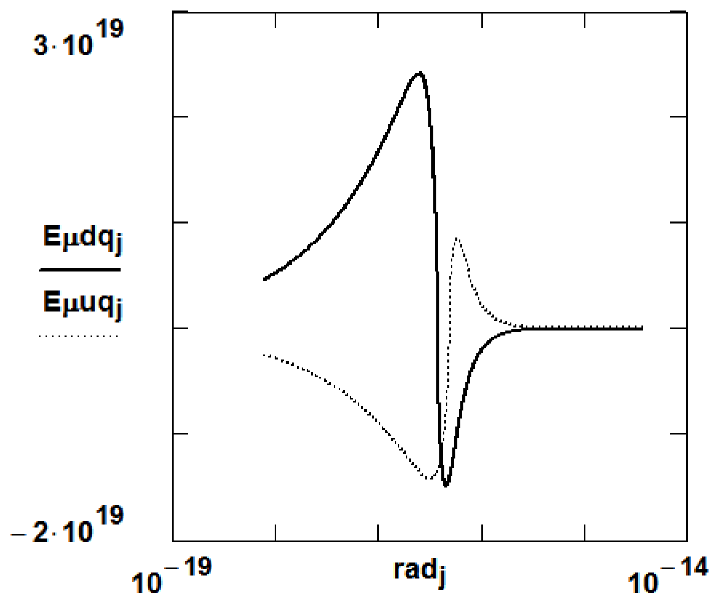

Fig. 4.13 The geometric *E*-field mimic for the bound-muon-down-quark distortion is represented as Eμdq and the geometric *E*-field mimic for the bound-muon-up-quark distortion is represented as Eμuq. The radial abscissa is shown in meters and the field-ordinate is in units of (Joules / meter^3)$^{1/2}$.

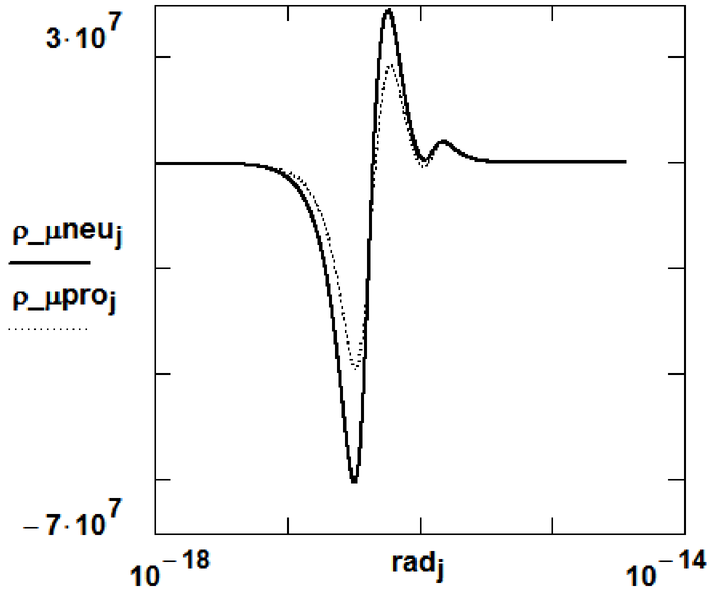

Fig. 4.14 The geometric mass-energy-density mimic for the neutron (constructed from the bound-muon-quark distortions) is represented as ρ_μneu and the geometric mass-energy-density mimic for the proton (constructed from the bound-muon-quark distortions) is represented as ρ_μpro. The radial abscissa is shown in meters and the energy-density-ordinate is in units of Joules / meter^3 .

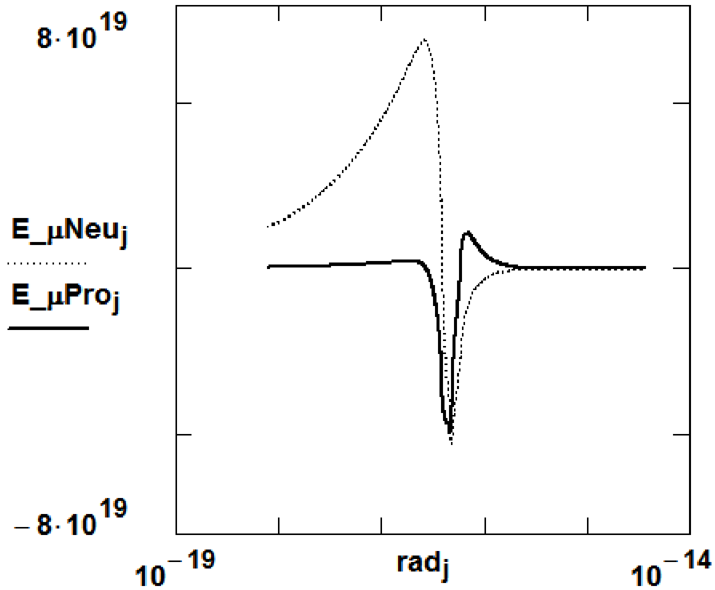

Fig. 4.15 The geometric *E*-field mimic for the neutron (constructed from the bound-muon-quark distortions) is represented as E_μNeu and the geometric *E*-field and B-field mimics for the proton (constructed from the bound-muon-quark distortions) is represented as E_μPro. The radial abscissa is shown in meters and the field-ordinate is in units of (Joules / meter^3)$^{1/2}$.

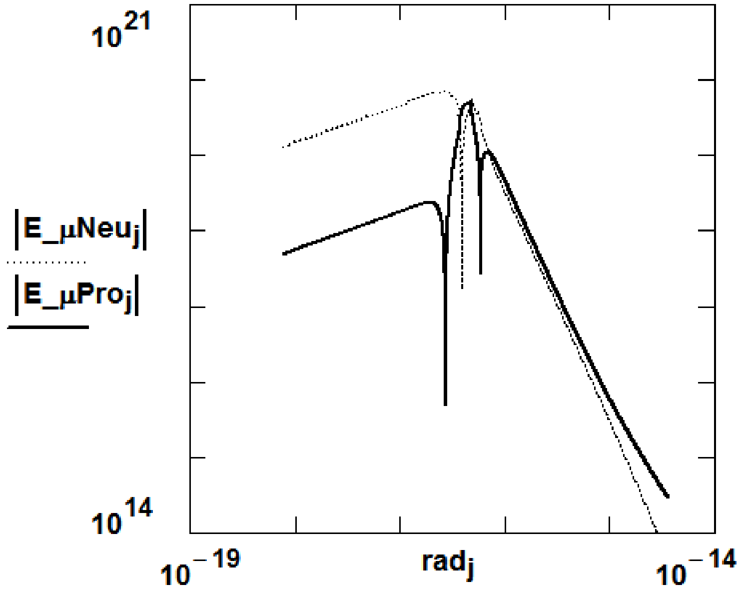

Fig. 4.16 The geometric *E*-field mimic for the neutron (constructed from the bound-muon-quark distortions) is represented as E_μNeu and the geometric *E*-field mimic for the proton (constructed from the bound-muon-quark distortions) is represented as E_μPro. The radial abscissa is shown in meters and the field-ordinate is in units of (Joules / meter^3)$^{1/2}$ on a logarithmic scale to better illustrate the field magnitudes.

As was suggested relative to the earlier neutron field description, *E_Neu*, we also contrast the present E_μNeu field behavior (see Figures 4.15 - 4.18) with the commentary in reference [3] where a "negatively charged skin" description is used to characterize the field behavior at the exterior of the neutron. In the present geometric 2-

region neutron-distortion field, the “skin” is an attractive “negatively” directed radial field. However, in comparison with the description of the “strong interaction” force, we see that the three basic structural-ingredients of the “strong interaction” are manifest in the structure of this geometrical-distortion, notwithstanding the smaller radial-measures in the neutron and proton-mimics. The core-region of the distortion-field is repulsive wherein both the neutron-mimic and the proton-mimic exhibit “positive-field” behavior. Immediately exterior to the “repulsive” core-region is an “attractive” negative-field region in the proton-mimic but absent in the neutron-mimic as a “second (of three) regions”. A distortional envelope encloses these interior regions which finally transitions to the classical Maxwellian-field region where $1/r^2$ and $1/r^3$ field behavior arises. In this field construct, the geometric spatial dependencies, $1/r^4$ and $1/r^6$ of the parent energy-density function, can be considered fundamental attributes of the distorted-geometric vector-field and not sources of independently defined fields although we illustrate the effect of independently-defined Maxwellian-like field constructions in Figure 4.16 for the neutron-mimic and the proton-mimic. The actual radial extensions of the “bound-quark” and the “bound-muon-quark” neutron- and proton-geometric-fields exhibit good agreement with experimental values.

Further recognition, it should be noted, of another constructional detail in the geometric-model is that the sub-structural distortional-components of the “composites” are retained with their respective coupling-constants, thereby preserving the coherent integrity of the sub-structural elements within the composites.

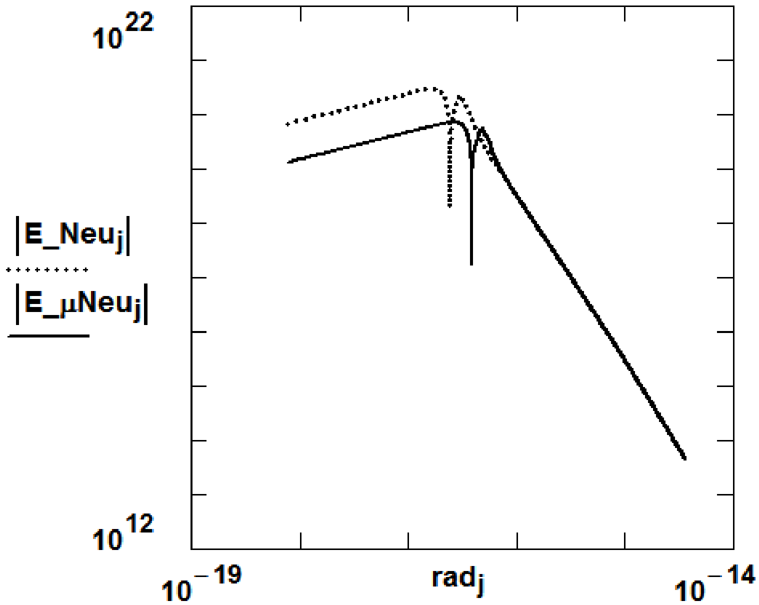

Fig. 4.17 The geometric *E*-field mimic for the neutron (constructed from the bound-muon-quark distortions) is represented as $E\_\mu Neu$ and the geometric *E*-field mimic for the neutron, E_Neu (constructed from the bound-quark distortions), is represented for contrast. The radial abscissa is shown in meters and the field-ordinate is in units of (Joules / meter^3)$^{1/2}$.

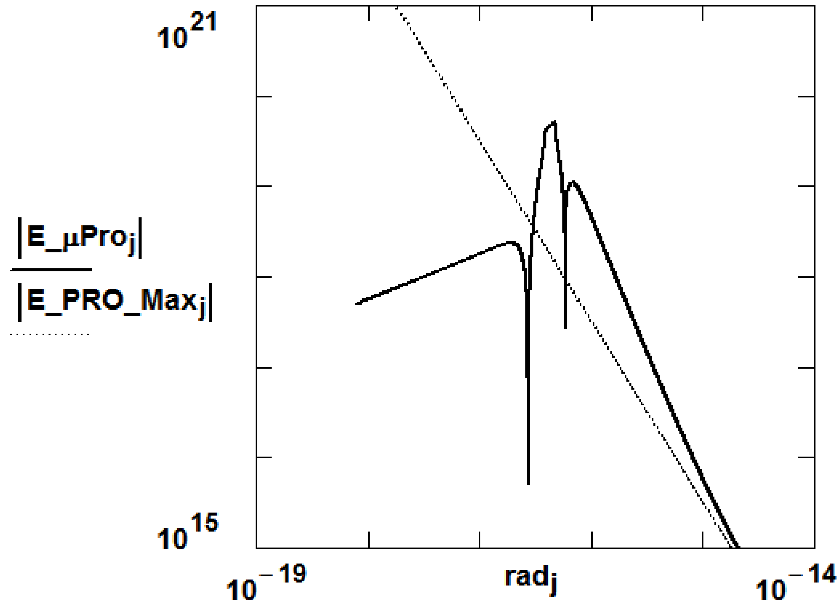

Fig. 4.18 The geometric *E*-field mimic (including the B-field mimic) for the proton (constructed from the bound-muon-quark distortions) is represented as E_μPro and compared with the classical Maxwellian *E*-field for the proton, E_PRO_Max; the radial abscissa is shown in meters and the field-ordinate is in units of (Joules / meter^3)$^{1/2}$.

REFERENCES

[1] Griffiths, D. (2008). *Introduction to Elementary Particles*. p. 135, WILEY-VCH.

[2] D R Koehler *Indian J. Phys.* 87 1029 (2013) DOI 10.1007/s12648-013-0321-5

[3] Miller, G.A. Physical Review Letters 2007, 99: 112001

[4] Fritzsch, H. (1983). *Quarks: The Stuff of Matter*. Basic Books. pp. 167–168. ISBN 978-0465067817

[5] Feynman, R. (1985), *QED: The Strange Theory of Light and Matter*, Princeton University Press. p. 136, ISBN 0-691-08388-6

GEOMETROSTATIC DISTORTIONS FOR A 3-COMPONENT NEUTRON AND PROTON

We assume that the neutron and proton magnetic moments derive from a composite of charged mass structures with $\mathrm{Q} = -\mathrm{e}/3$ and $+2\mathrm{e}/3$. We also write a classical mass and binding-energy description of the composite structure as (with masses expressed in electron-mass-energy units)

(1) $$\text{Mass Defect} \stackrel{\text{def}}{=} \text{Binding Energy(neutron or proton)} =$$

$$= \sum_{\mathrm{i}} \text{mass free quark}_{\mathrm{i}} - \text{Mass neutron(proton)} \quad \text{or}$$

$$\text{Mass neutron(proton)} =$$

$$= \sum_{\mathrm{i}} \text{mass free quark}_{\mathrm{i}} - \text{Binding Energy(neutron or proton)} =$$

$$= \sum_{\mathrm{i}} \text{mass bound quark}_{\mathrm{i}} \stackrel{\text{def}}{=} \sum_{\mathrm{i}} \text{mass uq}_{\mathrm{i}} + \sum_{\mathrm{i}} \text{mass dq}_{\mathrm{i}} \ .$$

The beta-decay transition is understood to be a change (structure-morphing) of the $-\mathrm{e}/3$ structure (*neutron down quark (*$\mathrm{dq2}$*))* to the $+2\mathrm{e}/3$ structure (*proton up quark (*$\mathrm{uq2}$*)*); we write the structural energy equation for this process, with explicit component binding energies, and with the assumption of a maintained integrity of the quark structures within both the neutron and proton to produce the quark-mass results,

$$(2)\qquad \text{(mass bound uq1)} + \text{(mass bound dq1} + \text{mass bound dq2)} = \text{ neutron mass} \stackrel{\text{def}}{=} \text{N},$$

$$\text{(mass bound dq1)} + \text{(mass bound uq1} + \text{mass bound uq2)} = \text{ proton mass} \stackrel{\text{def}}{=} \text{P},$$

$$\text{(mass bound dq2 - mass bound uq2)} \stackrel{\text{def}}{=} \text{Mbdq2 - Mbuq2} = (\text{N - P}) \stackrel{\text{def}}{=} \Delta\ .$$

Experimentally,

$$\Delta = \frac{939.565378\text{-}938.272046}{0.510998928} = 1838.684 - 1836.153 = 2.531 \text{ electron masses}\,.$$

The "geometric-structural model" does not utilize a QCD "constituent quark mass" [1] as an approximation to the quantities Mbdq and Mbuq.

If one further assumes $\text{Mbdq1} = \text{Mbdq2} = 613.7$ *and* $\text{Mbuq1} = \text{Mbuq2} = 611.2$, then the magnetic moments are further related to the component *bound-mass* entities through equations (3), where g_{dq} and g_{uq} are the quark g-factors;

$$(3)\qquad \text{neutron magnetic moment} = -1.913\ \mu_B/1838.7 = \left[2\frac{1/3}{\text{Mbdq}}g_{dq} + \frac{2/3}{\text{Mbuq}}g_{uq}\right]\frac{\mu_B}{2} \quad \text{and}$$

$$\text{proton magnetic moment} = 2.793\ \mu_B/1836.15 = \left[\frac{1/3}{\text{Mbdq}}g_{dq} + 2\frac{2/3}{\text{Mbuq}}g_{uq}\right]\frac{\mu_B}{2} \quad \text{where}$$

$$\mu_B = \text{Bohr magneton} = \hbar\frac{e}{2\ m_{elec}}\ ;\ \text{then}\ \ g_{dq} = -4.42 \ \text{ and } \ g_{uq} = 2.50\,.$$

The g-factors are interpreted in the geometric domain as distortion-produced mass-reduction factors and are quantitatively constrained to achieve agreement with the experimental baryon magnetic-moment values. The quark physical characteristics calculated here differ significantly from the values used in reference [2].

GEOMETROSTATIC DISTORTIONS FOR 3-COMPONENT QUARKS

One can proceed in the classical-structure manner and consider the quark entities as comprised of still smaller (mass) geometric-distortion structures. We assume therefore that the down-quark and up-quark derive from a composite of charged mass structures of the "*geometric muon-family-mimics"* with $\mathrm{Q} = \pm \mathrm{e}/3$, $\pm 2\mathrm{e}/3$ and $\pm 3e/3$ (the model-3 distortions of Ref. 1 Chap. 1 and Chap. 2); from this material we have (with the calculational constraint cited for Fig. 1 of Chapter 2)

(4) $\text{free-muon-mass-3} = \mathrm{mp}_3 = 206.768$ [theo. & experimental], $\mathrm{Q} = \pm 3\mathrm{e}/3$,

$\text{free-muon-mass-2} = \mathrm{mp}_2 = 206.768$, $\mathrm{Q} = \pm 2\mathrm{e}/3$ and

$\text{free-muon-mass-1} = \mathrm{mp}_1 = 206.768$, $\mathrm{Q} = \pm \mathrm{e}/3$.

The *MUON-DOWN-QUARK-1(*$\mathrm{dq1}$*)* is defined as the bound-muon combination $(\mathrm{m}_{-3} + \mathrm{m}_3 + \mathrm{m}_{-1})$ and the *ANTI-MUON-DOWN-QUARK-1* $\equiv (m_3 + m_{-3} + m_1)$ or the *MUON-DOWN-QUARK-2(*$\mathrm{dq2}$*)* $\equiv (m_{-2} + m_2 + m_{-1})$ and the *ANTI-MUON-DOWN-QUARK-2* $\equiv (m_2 + m_{-2} + m_1)$. Additionally, the *MUON-UP-QUARK-1(*$\mathrm{uq1}$*)* $\equiv (m_{-3} + m_3 + m_2)$ and the *ANTI-MUON-UP-QUARK-1* $\equiv (m_3 + m_{-3} + m_{-2})$ or the

MUON-UP-QUARK-2($\mathrm{uq2}$) $\equiv (m_{-1} + m_1 + m_2)$ and the *ANTI-MUON-UP-QUARK-2* $\equiv (m_1 + m_{-1} + m_{-2})$; the bound-muon masses representing the effects of the particle-binding energies or mass-reduction factors.

Considering equal-probability three-particle combinations of the six distortional charge-state building blocks (*muon-mimics*), we create the density-of-states function represented in Figure 7. Such a “density-of-states” formalism is considered the determining structural skeleton for combining the substructure components to form the composite distortional structure.

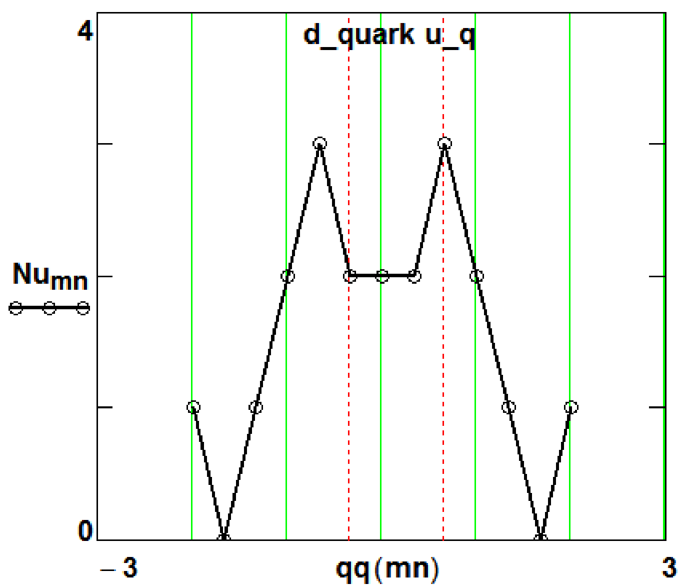

Fig. 4.7 Density-of-states function, Nu, for charged-muonic 3-distortion (particle) constructions; number of combinations on the ordinate versus the total-charge-state, qq, in units of (e), on the abscissa.

We have used the following combinatorial-mathematical formula as descriptive of the technique for creating structure: “For a number of distinguishable unordered distortional-element combinations of N = 6 distinct types (muonic-distortions of charge states $\pm\ e/3$, $\pm\ 2e/3$, and $\pm\ 3e/3$), taken 3 at a time where each distortional-element may occur at most once in any combination (<u>combinations without repetitions</u>), the number of combinations is”

(5) $$\text{Number} = \begin{Bmatrix} \mathrm{N} \\ \mathrm{n} \end{Bmatrix} \overset{\text{def}}{\equiv} \text{binomial coefficient} \overset{\text{def}}{\equiv} \frac{\mathrm{N}!}{\mathrm{n}!(\mathrm{N} - \mathrm{n})!} = \frac{6!}{3!3!} .$$

The up-quark charge-state and its antiparticle-twin appear with $numerical\ maxima = 3$ and the configurations and their anti-states are involved in both beta-decay and positron-emission. The beta-transition process, a $\Delta\mathrm{q}$ change of +1, is satisfied by a down-quark $(-\mathrm{e}/3)$ to up-quark $(+2\mathrm{e}/3)$ muon-distortional-structure-combination (structure-morphing).

Similarly, we could have written for the bound-quark structures of Section 4.2, “For a number of distinguishable unordered distortional-element combinations of $\mathrm{N} = 4$ distinct types (bound-quark-distortions of charge states $\pm\ \mathrm{e}/3$ and $\pm\ 2\ e/3$) taken 3 at a time (the neutron and proton constructions) where each distortional-element may occur at most once in any combination (combinations without repetitions), the number of combinations is” 4!/3!1! = 4; therefore the *down-quark-1* ≡ $(-2\mathrm{e}/3, +2\mathrm{e}/3, -\mathrm{e}/3)$ and the *anti-down-quark-1* ≡ $(2\mathrm{e}/3, -2\mathrm{e}/3, +\mathrm{e}/3)$ or the *down-quark-2* ≡ $(-3\mathrm{e}/3, +3\mathrm{e}/3, -\mathrm{e}/3)$

and the *anti-down-quark-2* ≡ $(3e/3, -3e/3, e/3)$. Additionally the *up-quark-1* ≡ $(e/3, -e/3, 2e/3)$ and the *anti-up-quark-1* ≡ $(-e/3, e/3, -2e/3)$ or the *up-quark-2* ≡ $(3e/3, -3e/3, 2e/3)$ and the *anti-up-quark-2* ≡ $(-3e/3, 3e/3, -2e/3)$.

For a "number of distinguishable unordered distortional-element combinations of $N = 6$ distinct types (muonic-distortions of charge states $\pm\, e/3$, $\pm\, 2e/3$ and $\pm\, 3\, e/3$) taken three ($n = 3$) at a time where each distortional-element may occur 0, 1, 2…or 3 times in any combination (<u>combinations with repetitions</u>)", the number of combinations is"

$$(6) \qquad \text{Number} = \left\{\begin{matrix} N + n - 1 \\ n \end{matrix}\right\} \stackrel{\text{def}}{=} \text{binomial coefficient} \stackrel{\text{def}}{=} \frac{(N + n - 1)!}{n!(N - 1)!} = \frac{8!}{3!5!}.$$

This number-function, or density-of-states, function is plotted in Figure 4.8.

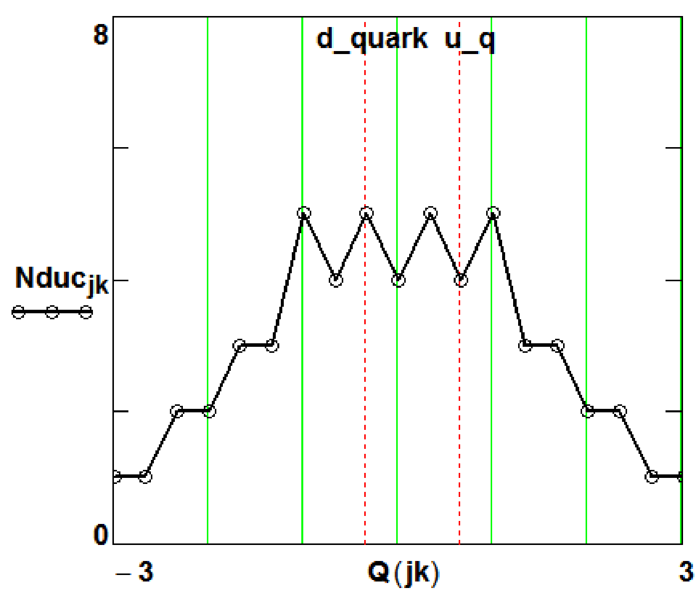

Fig. 4.8 Density-of-states function (Nduc ≡ number of distinguishable unordered combinations) for charged-muonic 3-distortion (particle) constructions; "number of combinations" on the ordinate versus "total-charge-state, Q, in units of (e)", on the abscissa.

Consideration of the form of the "density-of-states" function, Nu, rather than Nduc (more up-quarks than down-quarks, or a "proton", rather than more down-quarks than up-quarks, or a "neutron") suggests a superior rendition of structural formation probability and also produces a "mimic" for "color" [5] (see Fig. 4.9).

We also write a classical mass and binding-energy description of the composite quark-mimic structures and the neutron and proton, in terms of the "bound-muon ground-state mimics", as

$$(\mathrm{m}_{-1} + \mathrm{m}_1) + \mathrm{m}_2 = \mathrm{Mbuq1} \qquad \text{(for uq1 in neu/pro)},$$

$$(\mathrm{m}_{-3} + \mathrm{m}_3) + \mathrm{m}_{-1} = \mathrm{Mbdq2} \qquad \text{(for dq2 in neutron)},$$

$$(\mathrm{m}_{-2} + \mathrm{m}_2) + \mathrm{m}_{-1} = \mathrm{Mbdq1} \qquad \text{(for dq1 in neu/pro)},$$

$$(\mathrm{m}_{-3} + \mathrm{m}_3) + \mathrm{m}_2 = \mathrm{Mbuq2} \qquad \text{(for uq2 in proton)}$$

leading to, with the bound "paired matter-antimatter constituents" manifested at unpaired bound-values,

$$m_1 - m_2 = \Delta \text{, and } (\text{ if } m_2 = m_3 + \Delta), \text{ then } Mbuq1 = 3m_3 + 5\Delta,$$

$$Mbuq2 = 3m_3 + \Delta, \; Mbdq2 = 3m_3 + 2\Delta \quad \text{and} \quad Mbdq1 = 3m_3 + 4\Delta .$$

Also $$N = Mbdq2 + Mbdq1 + Mbuq1 = 9m_3 + 11\Delta \quad \text{and}$$

$$P = Mbuq2 + Mbdq1 + Mbuq1 = 9m_3 + 10\Delta, \quad \text{therefore}$$

$$m_3 = (N - 11\Delta)/9 = 201.2, \quad m_2 = 203.73 \text{ and } m_1 = 206.26;$$

compare with Eq. 4.

The bound-quark mass values are

$$Mbuq1 = 616.25, \; Mbuq2 = 606.13,$$

$$Mbdq1 = 613.72 \quad \text{and} \quad Mbdq2 = 608.66;$$

compare with Eq. 3.

Then, with the same structural assumptions used for Eq. 2, and using the referenced free-muon mass mp_3,

$$\text{Binding Energy (for } m_3 \text{ in dq2 and uq2}) = mp_3 - m_3 \stackrel{\text{def}}{=} bd3 = 5.57 .$$

Such a description makes the more massive entity, the $-e/3$ muon-distortion entity, the more-likely candidate for distortion-morphing or β-decay transformation, and therefore a

transition or morphing of the bound muon (-1/3) structure (m_1), in the neutron, to the less massive bound muon (+2/3) structure (m_2), in the proton.

The muonic-quark g-factor calculations assume that the charge and mass responsible for the quarks' magnetic-moments reside totally in the un-paired muon structures. And in structural similarity to, and using the g-factors of, Eq. 3, we write

(7) $$\text{down quark magnetic moment}_1 = \frac{1/3}{\text{Mbdq1}} g_{dq} \frac{\mu_B}{2} =$$

$$= \text{muon}(q = \text{-}\, e/3, m_1) \text{ magnetic moment} = \left[\frac{1/3}{206.26} g_{md1}\right] \frac{\mu_B}{2} \quad \text{or}$$

$$g_{md1} = \frac{206.26}{\text{Mbdq1}} g_{dq} \quad \text{and} \quad g_{md2} = \frac{206.26}{\text{Mbdq2}} g_{dq} \,.$$

$$\text{up quark magnetic moment}_1 = \frac{2/3}{\text{Mbuq1}} g_{uq} \frac{\mu_B}{2} =$$

$$= \text{muon}(q = 2e/3, m_2) \text{ magnetic moment} = \left[\frac{2/3}{203.73} g_{m2}\right] \frac{\mu_B}{2} \quad \text{or}$$

$$g_{mu1} = \frac{203.73}{\text{Mbuq1}} g_{uq} \quad \text{and} \quad g_{mu2} = \frac{203.73}{\text{Mbuq2}} g_{uq} \,.$$

The $$\text{muon}(q = 3\, e/3, m_3) \text{ magnetic moment} = \left[\frac{3/3}{201.2} \left(\text{-}2.002\right)\right] \frac{\mu_B}{2} \;;$$

$$\mu_B = \text{Bohr magneton} = \hbar \frac{e}{2\, m_{elec}} \,.$$

Then g_{md1}=-1.49 , g_{md2}=-1.50 , $g_{mu1} = 0.826$ and $g_{mu2} = 0.840$.

An alternative to the quark-based structural modeling for the Proton and the Neutron is presented here (manuscript submitted to the journal "SCIENTIFIC REPORTS" on 9/29/2021); a muonic-based model.

The Proton and Neutron as Distortional Structures in the Geometric Manifold

Dale. R. Koehler*

Sandia National Laboratories (retired)

82 Kiva Place, Sandia Park, NM 87047

Email address: drkoehler.koehler@gmail.com

Telephone No. (505) 273-3570

***Abstract*— It is shown in the present work that the distorted-space model of matter as extended to mimics of the proton and neutron can be described as muonic-based structures. These distorted-geometry structures exhibit non-Newtonian features wherein the hole or core-region fields of the structure (negative pressure core for a positive-charge positive-pressure large-r structure) do not behave functionally in a r^{-4} manner and terminate at zero at the radial origin (no singularity). Of particular interest is that of r^{-6} energy-density behavior at structural radial distances near the core of the distortion, a region also displaying potential-well behavior.**

***Ketwords*—Classical field theory; Classical mechanics; General relativity; Geometry; Nuclear Physics; Structural stability**

1. INTRODUCTION

For this distorted-geometry (DG) modeling, we maintain and expand the geometrical perspectives inherent in the "Curved empty space as the building material of the physical world" supposition of Clifford [1];

"RIEMANN has shewn that as there are different kinds of lines and surfaces, so there are different kinds of space of three dimensions; and that we can only find out by experience to which of these kinds the space in which we live belongs. In particular, the axioms of plane geometry are true within the limits of experiment on the surface of a sheet of paper, and yet we know that the sheet is really covered with a number of small ridges and furrows, upon which (the total curvature not being zero) these axioms are not true. Similarly, he says, although the axioms of solid geometry are true within the limits of experiment for finite portions of our space, yet we have no reason to conclude that they are true for very small portions; and if any help can be got thereby for the explanation of physical phenomena, we may have reason to conclude that they are not true for very small portions of space.

I wish here to indicate a manner in which these speculations may be applied to the investigation of physical phenomena. I hold in fact

(1) That small portions of space are in fact of a nature analogous to little hills on a surface which is on the average flat; namely, that the ordinary laws of geometry are not valid in them.

(2) That this property of being curved or distorted is continually being passed on from one portion of space to another after the manner of a wave.

(3) That this variation of the curvature of space is what really happens in that phenomenon which we call the motion of matter, whether ponderable or etherial.

(4) That in the physical world nothing else takes place but this variation, subject (possibly) to the law of continuity.

A quote from Wheeler's work [2] published in 1955 reads; *"In the 1950's, one of us [3] found an interesting way to treat the concept of body in general relativity. An object can in principle be constructed out of gravitational radiation or electromagnetic radiation, or a mixture of the two, and may hold itself together by its own gravitational attraction…A collection of radiation held together in this way is called a geon (a gravitational electromagnetic entity) and is a purely classical object….In brief, a geon is a collection of gravitational or electromagnetic energy, or a mixture of the two, held together by its own gravitational attraction, that describes mass without mass."*

Subsequently at *The International Congress for Logic, Methodology, and Philosophy of Science* in 1960, he [4] began by quoting William Kingdon Clifford's [1] "Space-Theory of Matter" of 1870 and stated *"The vision of Clifford and Einstein can be summarized in a single phrase, 'a geometrodynamical universe': a world whose properties are described by geometry, and a geometry whose curvature changes with time – a dynamical geometry."*

A comprehensive and general treatment of the historical, geometric and physical foundations of modern geometrodynamics is found in the already cited publications of Wheeler [2-4]. Additional work in this field continues, some of which is cited in references [5-10]. The present distorted-geometry treatment departs from these cited "geon constructional methods" in that we do not constrain the distortional descriptions to only gravitational coupling-constant produced structures.

The classical Riemannian four-dimensional curvature equations have been applied to describe the "localized geometrical distortions and associated energy distributions" at both quantum- and galactic-level magnitudes and radial-extensions. By requiring that the geometric distortions mimic the physical characteristics of the elementary particles, a coupling constant between energy and geometry is produced. The theoretical modeling and calculational procedure is limited to those geometric-distortional families satisfying an <u>equation-of-state</u>, which also expresses <u>static, spherically-symmetric Maxwellian tensor behavior</u>.

Functional solutions to Riemann's geometric, non-linear, coupled, partial-differential equations have classically not been forthcoming. A solution however has been found for the Riemannian equation-set by describing the "distorted" space as satisfying the "equation of state", Eq.(1). The Riemannian field equations, produced by the present "metric-solution", Eq.(2), are of such a character that, over portions of the radial extensions of the distortion, the geometrical tensor elements exhibit negative, as well as positive, curvature-magnitudes and energy-densities. The field-observable in the negative energy-density (negative pressure) spatial region (the core region) is non-Coulombic and non-infinite at the radial origin. Mass, electric charge and magnetic moments have been simulated for the down-quark, up-quark, electron, tauon, muon and neutrino as well as for a hypothetical beta-decay transition-mediating distortion-particle; this process also generates a geometric expression for the Fermi constant [11] and conversely predicts a mass-value for the W-boson calculated to the precision of the electron g-factor (gyromagnetic ratio).

Figure 1 displays the field energy-density quantities for three of these particle structures.

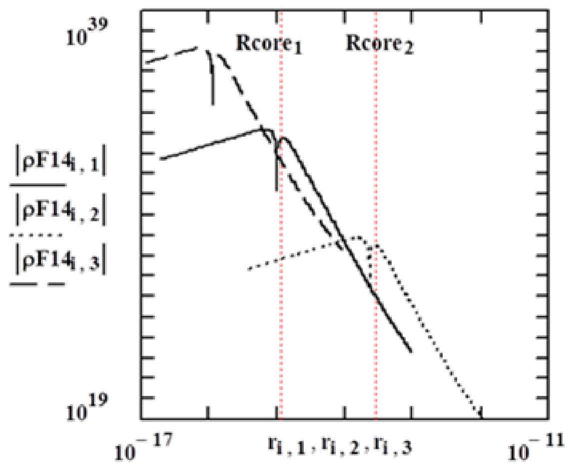

Fig. 1 Electric-Field energy-density distribution function for distortion-1 ≡ down_quark (mass-energy = 9.269 me*c^2), distortion-2 ≡ electron and distortion_3 ≡ muon (mass-energy = 206.768 me*c^2) where $\boldsymbol{\rho F14} \equiv \boldsymbol{Fd_{14}^{2}}$ (see Eqs 12-15**)**; logarithmic ordinate in J/m^3 units and logarithmic abscissa in meters.

The dependence of the field quantities on mass-energy and electric-charge is apparent in the Figure. The field energy-density magnitudes should be compared with the experimental data in reference [17].

By incorporating gravitational-field structures into the geometric modeling and simulation process, a refined coupling-constant is engendered. This process recovers the gravitational coupling-constant of general relativity and leads to a structural description of gravitational-like geometric-distortions.

We showed in [11] that the propagation velocity in the core region (negative pressure core for a positive-charge, positive-pressure (at large-r) structure) of these distorted-geometry (DG) structures was approximately 1.5 times that external to the core; see Fig.2. This feature, which is a fundamental attribute of such structures, is equivalent to a “partial light trapping” phenomenon and for gravitational structures would be classically associated with “black holes”.

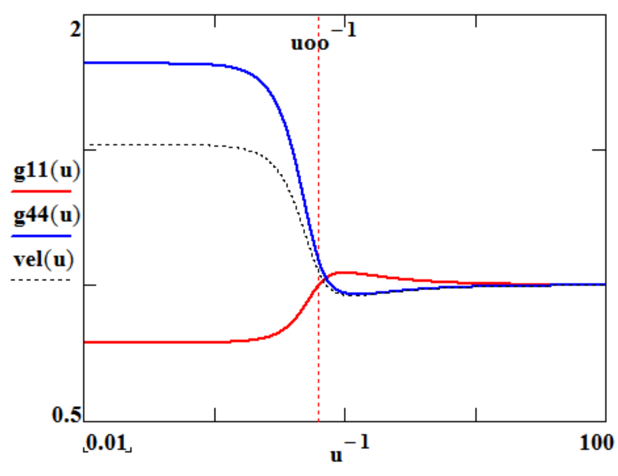

Fig.2 Metrics and propagation-velocity factor for an electron structure; .uoo = 1.27394.

A "geometric maximum-energy-density" feature was successfully exploited to geometrically explain and quantify the Fermi constant [11]; in addition a "*stability-based minimum-energy-density*" condition was fundamental to describing the structure of the "stable DG electron" feature. Energy-densities are equivalent to pressures and the core and shell regions of the structure hold the system in stable equilibrium. Fig.3 graphically displays such structures.

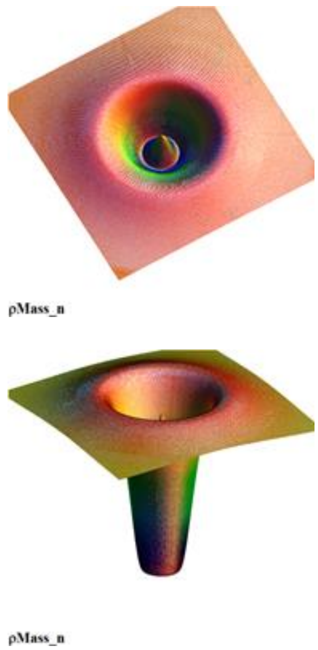

Fig.3 Mass-Energy-Density distribution-function surface-plots (two views) (linear radii and logarithmic amplitudes) for the geometric electron distortion.

In the perspective of [11], the DG model is a departure from the classical geometry model where the Einstein Curvature-tensor is the stress-energy-tensor describing the "material contents" of the energy distribution. The DG model is rather viewed with the energy-content residing in the warping or distorting of the manifold and therefore in its geometric-tensors, and the "curved empty space" [11] referred to above is a "localized curved or distorted space" devoid of an "external or foreign" causative matter-entity.

2. THEORETICAL FOUNDATION

A "constitutive relation" or "equation-of-state" was used as descriptive of the distorted-space volume (the physical spatial volume encompassing the distortion-produced energy), that is,

$$\boldsymbol{Td^4_4} = -\boldsymbol{Td^1_1} - \boldsymbol{Td^2_2} - \boldsymbol{Td^3_3} \quad \textit{and} \quad \boldsymbol{Td^3_3} = \boldsymbol{Td^2_2}\,. \tag{1}$$

This description, Eq.(1), of the *distorted-space volume*, has led to the *universal structural solution*, equation (2), (see equations (5)-(9) for variable definitions) for the fundamental Riemann geometric-equation-set, equations (4).

$$\mu' = \frac{2(1-u^3)u^2}{(\mathrm{I}u-\gamma)R0} \tag{2}$$

where the metric quantities $g_{11} \equiv -e^{\mu}$ and $g_{44} \equiv e^{\nu}$; $\nu' = \left[-2+\frac{1}{1-u^3}\right]\mu'$

and the transformed radial variable $u \equiv \frac{R0}{r}$;

$$\mathrm{Iu} \;=\; -\mathrm{u}\left[\tfrac{3}{7}\mathrm{u}^6 - \tfrac{3}{4}\mathrm{u}^3 + 1\right]. \tag{3}$$

Riemann's geometric equations (Tolman [13]), presented here as equations (4), are expressed in the metric-variables μ' and ν' and the manifestation of the composite coupling-constant appears in the geometric quantities γ and the geometric "transformation radius" *R0,* both determined from the "distorted spatial volume" with electromagnetic and/or gravitational energy-density components.

$$8\pi\kappa\mathbf{T_1^1} = -e^{-\mu}\left[\frac{\mu'^2}{4} + \frac{\mu'\nu'}{2} + \frac{\mu' + \nu'}{r}\right] + e^{-\nu}\left[\ddot{\mu} + \frac{3}{4}\dot{\mu}^2 - \frac{\dot{\mu}\dot{\nu}}{2}\right],$$

$$8\pi\kappa\mathbf{T_2^2} = -e^{-\mu}\left[\frac{\mu''}{2} + \frac{\nu''}{2} + \frac{\nu'^2}{4} + \frac{\mu' + \nu'}{2r}\right] + e^{-\nu}\left[\ddot{\mu} + \frac{3}{4}\dot{\mu}^2 - \frac{\dot{\mu}\dot{\nu}}{2}\right] =$$

$$= 8\pi\kappa T_3^3,$$

$$8\pi\kappa\mathbf{T_4^4} = -e^{-\mu}\left[\mu'' + \frac{\mu'^2}{4} + \frac{2\mu'}{r}\right] + e^{-\nu}\left[\frac{3}{4}\dot{\mu}^2\right],$$

$$8\pi\kappa\mathbf{T_4^1} = +e^{-\mu}\left[\dot{\mu}' - \frac{\dot{\mu}\nu'}{2}\right],$$

$$8\pi\kappa\mathbf{T_1^4} = -e^{-\nu}\left[\dot{\mu}' - \frac{\dot{\mu}\nu'}{2}\right]. \tag{4}$$

While the "energy-density Equation-of-state", equation (1), is equivalent to Maxwell's "energy-density" form for static, spherically-symmetric Maxwellian tensor behavior [11,13], the field equations, in both the EM realm and the gravitational realm (Q = 0), exhibit r^{-6} geometric, static, spherically-symmetric Maxwellian tensor behavior which we have interpreted as constituting a "magnetic monopole" mimic (what is a "magnetic monopole"?).

Building on the earlier work, [11, 12], we apply the geometric concepts to produce a proton- and neutron-conglomerate of distortional-geometric muon-mimics.

This section is a brief summary of the development in [11] and is included here as a less cumbersome introduction or reference to the theoretical modeling concepts.

Symbols [11] are

$$\mathrm{uB0(S = 1, Q = 3)} \equiv \frac{\mathrm{R0}}{\mathrm{ro}} = 1.6,$$

$$\mathrm{uB0(S = 1/2, Q = 3)} \equiv \frac{\mathrm{R0}}{\mathrm{ro}} = 1.239\,. \tag{5}$$

R0 is the geometric transformation radius ($R0_{electron}$ is calculated from the fundamental-particle magnetic-field component) and *ro* is the radial value at which the energy-density distribution-function transitions from the core-value to its negative in the shell ($r \to \infty$) region; $ro \equiv \frac{R0}{uo}$ follows from solution for the *uo* roots of the field equations (6)

$$(1 - 3\mathrm{u}^3)(1 - \mathrm{u}^3)^2 - 4\mathrm{u}^2(\mathrm{Iu} - \gamma) = 0 \ \text{ for } \ \boldsymbol{Td_2^2},$$

$$(1 - 3\mathrm{u}^3)(1 - \mathrm{u}^3)(1 - 2\mathrm{u}^3) - 6\mathrm{u}^2(\mathrm{Iu} - \gamma) == 0 \ \text{ for } \ \boldsymbol{Td_4^4} \ \text{ and}$$

$$(1 - 3\mathrm{u}^3)(1 - \mathrm{u}^3)\mathrm{u}^3 + 2\mathrm{u}^2(\mathrm{Iu} - \gamma) =$$

$$= 0 \ \text{ for } \ \boldsymbol{Td_1^1} + \boldsymbol{Td_2^2}. \tag{6}$$

We also define

$$\gamma \equiv \frac{2\,\mathrm{R0}}{\mathrm{Rs}} \quad \textit{and} \quad \mathrm{Rs} \equiv \text{Schwarzschild radius} = 2\,\kappa\,\mathrm{Mc}^2 \tag{7}$$

$$where\ \ \kappa \equiv \kappa G + \kappa o = Gc^{-4} + \frac{\alpha\, \hbar c \left(\frac{Q}{3}\right)^2}{2(Mc^2)^2}.$$

For the electron we write (me ≡ mass electron, $Q_{elec} = 3$),

$$ro(\text{electron}) = \frac{\beta(1/2,3)}{uB0(1/2,3)} \frac{\hbar c}{me\ c^2}, \qquad (8)$$

$$\text{with}\ \ \beta(S,Q) = \left[\frac{2}{3}\alpha \left(\frac{g_e}{2} S \frac{Q}{3}\right)^2\right]^{\frac{1}{3}},$$

α = fine structure constant, S is the spin quantity and

g_e is the gyromagnetic ratio factor. Then,

$$ro_{geo\_max} = ro(\text{electron}) = 3.3297(10)^{-14}\ \text{meters}. \qquad (9)$$

The core-radii for the EM structures are inversely proportional to the mass-energy of the distorted-geometry-structures and therefore it follows that the ro radius for the muon, or anti-muon, is

$$ro(\text{muon}) = \frac{me\ c^2}{m_{muon}\ c^2} ro(\text{electron}) = 1.61(10)^{-16}\ \text{meters}. \qquad (10)$$

In the earlier development [11] for the geometric Fermi-constant, *GF* is $GF_{geo} \stackrel{\text{def}}{=} \left[fe\ \frac{4\pi}{3} R0^3\right] MW$ and MW = mass-energy of the W^-boson. The quantity, $fe = \frac{3}{2}\left(\frac{\pi}{2}\right)^2$, was originally introduced as a volume-adjustment-factor in this derivation.

The *uo* root values ($uo \equiv \frac{R0}{ro}$), for determining *ro* values, from equations (6), are plotted in Fig.4

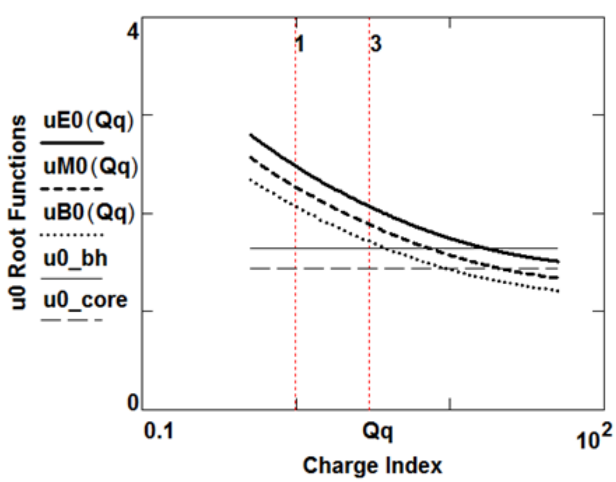

Fig. 4 Radial-zero functions u_0 (from equations (6)) relative to electric-charge values; *uE0* for the electrical $\boldsymbol{Td_2^2}$ function, *uM0* for the mass-energy-density $\boldsymbol{Td_4^4}$ function and *uB0* for the magnetic-energy-density $\boldsymbol{Td_1^1 + Td_2^2}$ function. Abscissa charge-values are displayed as a function of the index *Qq*. *uo(Qq)* is graphically used for the zero-radial-function *uo*. Also indicated is the E_field quantity, *u0_core* = *uE0*(*Qq* = 0), and a gravitational "black-hole *u0_bh*" value.

The radial zero of the gravitational field quantities expressed in equations (6) is $u(ro)$ = 3.27512/2 if $ro = Rs_{geo}$. $Rs_{geo} = R0_{geo}/u(ro)$ is the geometric manifestation of the Schwarzschild "metric-radial-zero", the radial singularity classically interpreted as a "black-hole" radius.

The Riemannian geometric field equations follow from equation (4) and are taken from [13] according to Tolman; *"For the presently described spherically symmetric Maxwellian case, ϕ, the electrostatic potential, is a function of r alone, and the Maxwellian electromagnetic tensor and the associated field tensor $\boldsymbol{F_{1\mu}}$ can be constructed according to my equation (5), where the only surviving field tensor components are"*

$$\mathbf{F_{21} = -\,F_{12}\,,\ F_{13} = -\,F_{31}} \quad \text{and} \quad \mathbf{F_{14} = -\,F_{41}}\,, \qquad \text{i.e.}$$

$$\mathbf{T^{\mu\nu} = -\,g^{\nu\beta}F^{\mu\alpha}F_{\beta\alpha} + \frac{1}{4}g^{\mu\nu}F^{\alpha\beta}F_{\alpha\beta}} \qquad \text{or}$$

$$\mathbf{T^{\mu\mu} = -\,g^{\mu\mu}F^{\mu\alpha}F_{\mu\alpha} + \frac{1}{4}g^{\mu\mu}F^{\alpha\beta}F_{\alpha\beta}}\,, \quad \text{then}$$

$$\mathbf{T^4_4} = \frac{(\mathbf{F_{12}F^{12} + F_{13}F^{13} - F_{14}F^{14}})}{2}, \qquad \mathbf{T^1_1} = \frac{(\mathbf{-\,F_{12}F^{12} - F_{13}F^{13} - F_{14}F^{14}})}{2},$$

$$\mathbf{T^2_2} = \frac{(\mathbf{-\,F_{12}F^{12} + F_{13}F^{13} + F_{14}F^{14}})}{2} \qquad \text{and} \qquad \mathbf{T^3_3} = \frac{(\mathbf{F_{12}F^{12} - F_{13}F^{13} + F_{14}F^{14}})}{2}\,. \tag{11}$$

The resultant field quantities are

$$\mathbf{(F_{14})^2 = -\left(T^4_4 + T^1_1\right)g_{11}\,g_{44} = \left(T^2_2 + T^3_3\right)g_{11}\,g_{44}}\,,$$

$$\mathbf{(F_{12})^2 = -\left(T^2_2 + T^1_1\right)g_{11}\,g_{11}} \quad \textbf{and} \quad \mathbf{(F_{13})^2 = -\left(T^3_3 + T^1_1\right)g_{11}\,g_{11}}\,. \tag{12}$$

Therefore, we see that the static-spherically-symmetric Maxwellian tensors exhibit the same stress and energy relationship as the geometric tensors.

Finally, it is of interest to examine the ratio of the $1/r^6$ tensor-component to the $1/r^4$ tensor-component in the construction of the geometric fields. The geometric-energy-density or field equations [13] are (the "***d***" symbolism denotes the "***distorted space***" modeling)

$$8\pi\kappa\, \boldsymbol{Td^1_1} = -e^{-\mu}\frac{1}{(\mathrm{Iu} - \gamma)}\left(\frac{\mathrm{u}^2}{\mathrm{R0}}\right)^2\left[2\,u^2 + (3\,u^3 - 1\,)\,\frac{1 - \mathrm{u}^3}{(\mathrm{Iu} - \gamma)}\,\right],$$

$$8\pi\kappa\, \boldsymbol{Td^2_2} = e^{-\mu}\frac{1}{(\mathrm{Iu} - \gamma)}\left(\frac{\mathrm{u}^2}{\mathrm{R0}}\right)^2\left[4\,u^2 + (3u^3\ - 1\,)\frac{(1-u^3)^2}{(\mathrm{Iu} - \gamma)}\right],$$

$$\text{and} \quad 8\pi\kappa\,(\,\boldsymbol{Td^2_2} + \boldsymbol{Td^1_1}\,) =$$

$$= e^{-\mu}\frac{1}{(\mathrm{Iu} - \gamma)}\left(\frac{\mathrm{u}^2}{\mathrm{R0}}\right)^2\left[2\,u^2 - (3u^3\ - 1\,)\frac{(1 - \mathrm{u}^3)u^3}{(\mathrm{Iu} - \gamma)}\right] \tag{13}$$

leading to

$$(\boldsymbol{Fd_{14}})^2 = -g_{11}g_{44}\left(\boldsymbol{Td^4_4} + \boldsymbol{Td^1_1}\right) = g_{11}g_{44}\left(\,2\,\boldsymbol{Td^2_2}\,\right) \quad \text{and}$$

$$(\boldsymbol{Fd_{14}})^2(\mathrm{r}\rightarrow\infty) \stackrel{\mathrm{def}}{=} \left(\frac{\mathrm{Rs}}{2}\right)^2\frac{2}{8\pi\kappa}\,\frac{1}{\mathrm{r}^4} = \frac{\mathrm{Rs}^2}{2}\,\frac{1}{8\pi\kappa}\,\frac{1}{\mathrm{r}^4} \stackrel{\mathrm{def}}{=} \left(\frac{\mathrm{q}}{4\pi\varepsilon o\,\mathrm{r}^2}\right)^2\frac{\varepsilon o}{2}. \tag{14}$$

$$(\boldsymbol{Fd_{12}})^2 + (\boldsymbol{Fd_{13}})^2 = 2\,g_{11}g_{11}\left(\frac{\boldsymbol{Td^4_4} - \boldsymbol{Td^1_1}}{2}\right) \stackrel{def}{=} \boldsymbol{Fd_{mag}}^2 =$$

$$= -2\,g_{11}g_{11}\left(\boldsymbol{Td^1_1} + \boldsymbol{Td^2_2}\right) \quad \text{and}$$

$$(\boldsymbol{Fd_{12}})^2 + (\boldsymbol{Fd_{13}})^2(r\rightarrow\infty) = 2\ \mathrm{Rs}\ \mathrm{R0}^3\,\frac{1}{8\pi\kappa}\,\frac{1}{\mathrm{r}^6} \stackrel{\mathrm{def}}{=}$$

$$\stackrel{\text{def}}{\equiv} \ \frac{\mu o}{2}\left(\frac{\mu_{spin}}{2\pi}\right)^2 \frac{1}{r^6} \qquad (15)$$

where

$$\mu\_spin \ \stackrel{\text{def}}{\equiv} \ \left(\frac{g_e}{2}\frac{Qe}{3M}\right) S\, \hbar \quad \text{and} \quad g_e = 2.0023193043\,6\ .$$

In discussions of the negative energy-density (pressure) core-regions of this universal (EM as well as gravitational) distorted-geometry structure, it should be emphasized that a negative energy-density gravitational feature (a repulsive gravitational force or negative pressure) is non-Newtonian. The hole or core region-fields of the structure are repulsive thereby stabilizing the structure, do not behave functionally in an r^{-4} manner and terminate at zero at the radial origin (no singularity). This field behavior is a fundamental feature of these "distorted-space" structures; the field exhibits r^{-4} , r^{-6} and r^{-n} dependences in both the core and shell regions and is thereby able to account for "Newtonian"-, "weak"- and "strong-fields"(see equations (14,15)).

To further illustrate the structural character of the "distortional-geometry mimics", we compare at "near-core radial regions" the geometrostatic field quantities $\boldsymbol{Fd_{14}}^2$ and $\boldsymbol{Fd_{mag}}^2$ which are also the geometric mimics of the Maxwellian tensors. For both gravitational and electromagnetic distortions, the magnetic field component, $\boldsymbol{Fd_{mag}}^2$**,** is non-zero at the "radial field zero", $\boldsymbol{Fd_{14}}^2 = \mathbf{0},$ or "core radius (*ro*)" (in the gravitational realm, this field feature would seem responsible for accretion-disk and galaxy-matter rotational-distribution behavior). Figures 5 and 6 are constructed for the "distorted-space electron-mimic" although the energy-density distribution functions are qualitatively similar in the normalized radial variable $u = \frac{R0}{r}$. The Figures are meant to more dramatically illustrate the magnitude of the structure's magnetic energy-density component vs the $\boldsymbol{Fd_{14}}^2$ energy-density component**.**

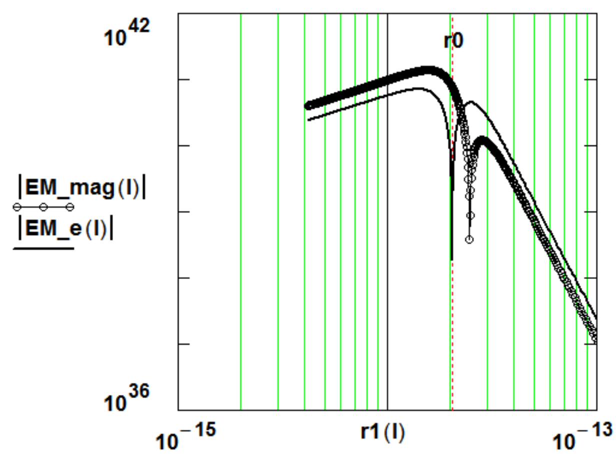

Fig.5 Field-Energy-Density distribution-functions; radii (logarithmic in meters) and amplitudes (logarithmic in joules/m^3) for the DG_geometric electron-distortions. EM_mag ≡ $\boldsymbol{Fd_{mag}}^2(\boldsymbol{electron})$ and EM_e ≡ $\boldsymbol{Fd_{14}}^2(\boldsymbol{electron})$ **.**

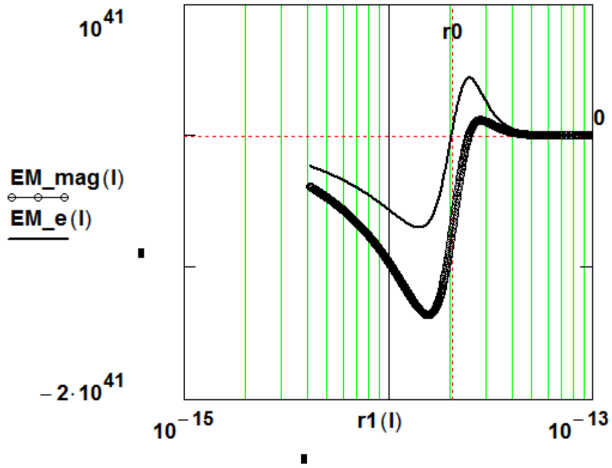

Fig.6 Field-Energy-Density distribution-functions; radii (logarithmic in meters) and amplitudes (linear in joules/m^3) for the DG_geometric electron-distortions. EM_mag ≡ $\boldsymbol{Fd_{mag}}^2(\boldsymbol{electron})$ and EM_e ≡ $\boldsymbol{Fd_{14}}^2(\boldsymbol{electron})$ **.**

Actually, the $\boldsymbol{Fd_{14}}^2$ fields contain r^{-6} elements of a magnitude comparable to the magnetic-field strengths $\boldsymbol{Fd_{mag}}^2$, resulting in a significant departure from the classical Newtonian r^{-4} (or r^{-6}) behavior. The fields also exhibit potential-well behavior as they radially (shell values) transition to repulsion (if attractive in the shell) at the hole-core radius *ro*.

3. PROTON AND NEUTRON MODELING

We use the following experimental data [14-16] to generate and illustrate the model parameters:
mass energy of proton (*Mp*) = 938.2716 MeV, electric charge of proton (*Qp*) = +e and gyromagnetic ratio (*g*-factor) of **proton (*gp*) = 5.585694**;

mass energy of neutron (*Mn*) = 939.564 MeV, electric charge of neutron (*Qn*) = 0, gyromagnetic ratio (*g*-factor) of **neutron (gn) = -3.826085**;

mass energy of muon (*Mμ*) = 105.658 MeV, electric charge of muon (*Qμ*) = -e, gyromagnetic ratio (*g*-factor) of **muon (*gμ*) = -2.002331**, and

mass-energy of anti-muon (*Maμ*) = 105.658 MeV = *Mμ*, , electric charge of anti-muon (*Qaμ*) = +e and gyromagnetic ratio (*g*-factor) of **anti-muon (*gaμ*) = 2.002331**.

The electron characteristics are;
mass energy of electron ($me*c^2$) = 0.510998 MeV, electric charge of electron (*Qe*) = -*e*, gyromagnetic ratio (*g*-factor) of **electron (*ge*) = -2.002319**.

Calculating the binding energy of the **proton**, modeled as a structure of **4 muons and 5 anti-muons**, we get BEp (binding energy of proton) ≡ 9 *Mμ* – *Mp* = 12.6504 MeV. Similarly, the binding energy of the **neutron** ≡ Ben = 9 *Mμ* + *Me* – *Mn* = 11.358 MeV. The muons and anti-muons are posited to coexist within the immediate field environment of the composite structure as, for example, neutrons existing within elemental structures, or, in other field-induced [15,16] modifications. For comparison to other nuclear structures, a binding energy per nucleon, where a "nucleon" definition here incorporates the muon, is BEp_μ = 1.40555 MeV/nucleon and Ben_μ = 1.318666 MeV/nucleon.

For the DG_mimicked-proton, the electric-field is that of an anti-muon (the other 4 muon/anti-muon pairs exhibiting zero-charge or self-neutralization [16] and zero *g*-factors). The g-factor value of the 4th muon is field "flipped" and a resultant sub-structure of two anti-muons and the "flipped" muon-produces a "field induced"

composite g-factor, reduced from the free-field value of (2.002331) per anti-muon to (1.861898) per anti-muon, to create a **proton g-factor** of **(5.585694)**. The proton (stacked-muon) radius, assuming a 3-layer, 3 muon/layer, @ 4 *ro*-muon separation (center to center) between muons, in a stacked-geometry-configuration, would be approximately 10 *ro*_muon or $1.0625(10)^{-15}$ meters.

For the DG-mimicked-neutron, which is here posited as a DG-mimicked proton surrounded by a DG-mimicked electron (*ge* = -2.002319), the simplest formation structure would be that of field "flipping" the g-factor of one DG-proton-anti-muon from (+2.002331) to (-2.002331) with a field induced reduction to (-1.823766). The resultant **neutron g-factor** would then be **(-1.823766) + (-2.002319) = (-3.826085)**.

For this DG_mimicked-neutron, the electric-field is that of the DG_mimicked core-proton plus the field of the shroud DG_mimicked electron registered on the same center as the protonic-core (see Fig.7). In other words, a zero-charge field (at large radii) but a "DG-field" near and within the *ro*(electron) radius. The neutron *ro* radius is that of the shroud-electron-mimic or *ro*(neutron) = *ro*(shroud-electron) = $2.197(10)^{-14}$ meters.

The energy-density features of these structures are illustrated in Fig. 7. The field-energy-density distribution functions are recast as, for example,

$$U\_pro(r) \equiv (Fd_{14})^2 = -g_{11}g_{44}\left(Td_4^4 + Td_1^1\right) = g_{11}g_{44}\left(2\,Td_2^2\right)$$

and the neutron distribution is defined as

$$U\_neu(r) \equiv U\_pro_n(r) - U\_elec_n(r)$$

where the "*n*" subscript denotes the impact of the gyromagnetic factor *ge*. The DG_proton g-factor produces ***U_pro(r)* + *U_elec(r)*** and the DG_neutron g-factor produces $U\_pro_n(r)$ + $U\_elec_n(r)$. Absolute values are displayed because of the energy-density-value transition at the core radii.

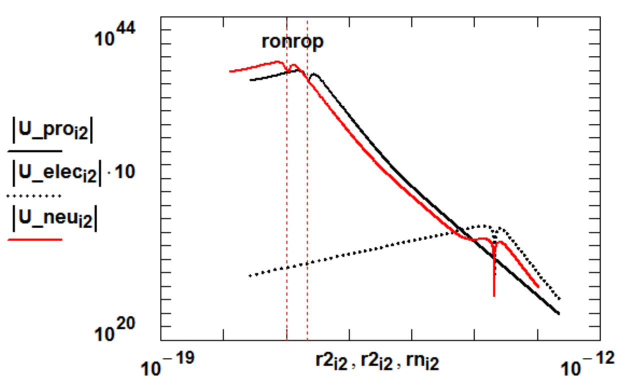

Fig.7 Field-Energy-Density distribution-functions; radii (logarithmic in meters) and amplitudes (logarithmic in joules/m^3) for the DG_geometric distortions ***U_pro(r), U_elec(r)*** and ***U_neu(r).***

The symbols *ron* and *rop* are the DG_neutron and DG_proton core radii.

Some experimental data have been measured for the proton and is detailed in reference [17] as;

"The proton, one of the components of atomic nuclei, is composed of fundamental particles called quarks and gluons. Gluons are the carriers of the force that binds quarks together, and free quarks are never found in isolation—that is, they are confined within the composite particles in which they reside. The origin of quark confinement is one of the most important questions in modern particle and nuclear physics because confinement is at the core of what makes the proton a stable particle and thus provides stability to the Universe. The internal quark

*structure of the proton is revealed by deeply virtual Compton scattering, a process in which electrons are scattered off quarks inside the protons, which subsequently emit high-energy photons, which are detected in coincidence with the scattered electrons and recoil protons. Here we report a measurement of the pressure distribution experienced by the quarks in the proton. We find a strong repulsive pressure near the centre of the proton (**up to 0.6 femtometres**) and a binding pressure at greater distances. The average **peak pressure near the centre is about 10^{35} Pascals** (**Joule/m^3**), which exceeds the pressure estimated for the most densely packed known objects in the Universe, neutron stars. This work opens up a new area of research on the fundamental gravitational properties of protons, neutrons and nuclei, which can provide access to their physical radii, the internal shear forces acting on the quarks and their pressure distributions."*

In the DG_neutron, the core values of the DG energy density distribution for the co-centered electron are of the same sign as the energy-density shell values of the protonic-muon structures but of an almost infinitesimal value compared to the muonic values. At the electron-core radius the two energy density distributions are of opposite magnitudes and produce a composite neutral charge character (*Qneu* = 0)(for radii greater than *ro*(electron)) and the modified *g*-factors discussed above.

4. CONCLUSIONS

It has been shown in the present work that the distorted-space, or distorted geometry (DG), model of matter, as applied to fundamental-particle (muon/anti-muon) constructs, can mimic the composite neutron and proton structures. The distorted-geometry structures exhibit non-Newtonian features wherein the core-region and shell-region fields of the structures do not behave functionally in an r^{-4} manner and terminate at zero at the radial origin (no singularity). This field behavior is a fundamental feature of these "distorted-space" structures; the field behavior exhibits r^{-4} , r^{-6} and other r^{-n} dependence in both the core and shell regions and is thereby able to account for, explain and mathematically elucidate "Newtonian"-, "weak"- and "strong"-fields."

Data Availability:
No separate or additional datasets were produced as part of this manuscript creation..

REFERENCES

1. Clifford, W.K., "On the space theory of matter" in *Proc. Of the Cambridge Philosophical Society,* **2**, pp. 157-58, (1876).
2. Ciufolini, I. and Wheeler, J. A., "*Gravitation and Inertia*", USA, Princeton University Press, (1996).
3. Wheeler J. A., *Phys. Rev*., **97**, p.511, (1955).
4. Wheeler J. A., "Logic, Methodology, and Philosophy of Science", *Proc. 1960 International Congress, USA*, Stanford University Press, p.361, (1962).
5. Anderson, P.R.and Brill, D.R., *Phys.Rev*. , **D56** 4824-33, (1997)
6. Perry, G.P.; Cooperstock, F.I. *Class.Quant.Grav*., **16** (1999)
7. Sones, R.A., *Quantum Geons*, (2018) arXiv:gr-qc/0506011
8. Stevens, K.A.; Schleich, K.; Witt, D.M., *Class.Quant.Grav*., **26**:075012, (2009)
9. Vollick, D.N., *Class.Quant.Grav*., **27**:169701, (2010)
10. Louko, J. J., *Phys.: Conf. Ser.*, 222:012038, (2010)
11. Koehler, D. R., "Geometric distortions and physical structure modeling" in *Indian J. Phys*., **87**, p.1029 (2013). DOI 10.1007/s12648-013-0321-5 .
12. Koehler, D. R., "The distorted universe: from neutrinos to the cosmos, the theory of nothingness", in Universe-neutrinos-cosmos-Nothingness-ebook, Kindle, ASIN B00TG26Q7Y, 2015.
13. Tolman, R., "Relativistic electrodynamics" in *Relativity, Thermodynamics and Cosmology*, Mineola, NY, Dover, p.258, (1987)
14. "2018 CODATA Value: electron mass in u". *The NIST Reference on Constants, Units, and Uncertainty*. NIST., (20 May 2019).
15. Gell, Y. and Lichtenberger, D. B., "Quark model and the magnetic moments of proton and neutron" in *Il Nuovo Cimento A.*, **61**(1), series 10, pp 27-40, (1969) doi: 10.1007/BF02760010. S2CID123822660

16. Alvarez, L.W. and Bloch, F., “Determination of the neutron moment in absolute nuclear magnetons” in *Physical Review*. **57** (2), pp. 111-122, (1940).
17. Burkert, V.D., Elouadrhirim L.and Girod, F.X. , “The pressure distribution inside the proton “ in *Nature* **557**, pp.396-399, (2018). https://www.nature.com/articles/s41586-018-0060-z#auth-L_-Elouadrhiri

---

Supplementary Information is available for this paper.

Additional Information: Author Contribution Statement The work and representation was provided by the sole author

Competing Interests There are no competing interests for this paper

The Cat's Eye Nebula—NGC 6543 HubbleSite.org

CHAPTER 5

THE FOLLOWING MANUSCRIPT IS A CORRECTED VERSION (CORRECTIONS HIGHLIGHTED IN RED) OF THE JOURNAL PUBLICATION "IEEE TRANSACTIONS ON PLASMA SCIENCE, DECEMBER 2017".

Koehler, D. Radiation-Absorption and Geometric-Distortion and Physical-Structure Modeling. *IEEE Transactions on Plasma Science*. **45**, 3306 (2017).

An Absorptive Geometric Manifold

Chapter Summary: *The following chapter material is a corrected version ("corrected version" also available at https://archive.org/details/radobs-5_202110) of the manuscript published in the journal "IEEE Transactions on Plasma Science, Vol. 45, Issue 12, December 2017 pages 3306-3315". After having associated or attributed elastic and deformable characteristics to the geometric manifold in the earlier chapters, we have now considered and examined the possibility and manifestation of the additional material-characteristic of absorption. In addition to interpreting astronomical redshift data as absorptive in origin, as opposed to a non-absorptive universe-expansion interpretation, a simple explosive universe-creating geometric-distortion, with-absorption, model is here posited.*

MATTER AS DISTORTED SPACE

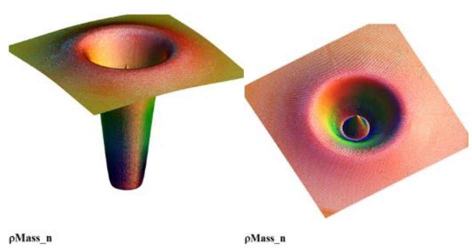

Radiation Absorption, Geometric-Distortions and Physical Structure Modeling (March 2017)

***Abstract*—As latter-day experimental interstellar and intergalactic astronomical data are being related to unknown forms of cosmological energies (hypothesized**

2

as dark-energy and dark-matter), we, in the present development, attribute radiation-absorption properties to the universe's electromagnetic energy content (plasma-energies, etc.) or to the universe's geometric manifold itself. Therefore, for either an electromagnetic energy content or a manifold-energy content (manifold-curvature with radiation absorption), we advance a classical optical attenuation-coefficient model to describe energy propagation throughout the universe thereby providing an alternative analysis and cosmological explanation for the experimental radiative-astronomical data. This modeling is applicable whether one attributes radiation-attenuation to the presence of additional universe-bearing electromagnetic energy sources or as an interpretation of the geometric manifold as a substantive and locally distortable entity. For the geometric-manifold absorption description, the spacetime-absorption-property concept is further utilized to model a radiatively decaying blackbody as the genesis of a propagating decaying shock-wave, which in turn is posited as the energy source to mimic a spatially-distorted universe. The earlier derived composite coupling-constant (gravitational and electromagnetic) is inherently incorporated to classify the elements of the seeded universe. Energy densities derived from a distorted-spacetime model are further assimilated in a fundamental manner to describe the ensuing features of the explosive blackbody event.

Index Terms— Astronomy, Cosmology, General Relativity, Geometry, Plasmas, Structural stability

INTRODUCTION

WE consider electromagnetic-energy components, e.g. plasma energy sources, as fundamental components in inter-stellar and inter-galactic "space" ; this consideration results in modeling with an absorption-dependent (μ) radiation propagation velocity, $c(\mu)$. The presence of electrically- and/or magnetically-active species (plasmas) throughout any propagating medium would produce an observable and acknowledged impact on the propagating radiation energy [1-21] and alternatively explain propagated radiation energy (frequency) shifts throughout the universe thereby impacting distance, size and age characterizations.

Similarly, a substantive or absorptive transmission-medium model for the space-time manifold geometry itself would also generate a different explanation and analysis of experimental astronomical data; these models are developed in the "**Radiation propagation in the manifold**" section to follow.

In the "**Distortional energy decay**" section, the spacetime-absorption-property concept is further utilized to model a radiatively decaying blackbody as the genesis of a propagating decaying shock-wave, which in turn is posited as the energy source to mimic a locally spatially-distorted universe. For this distorted geometry modeling, we maintain and expand the geometrical perspectives inherent in a "Curved empty space

as the building material of the physical world" supposition [22-27]. Building on the earlier work [26,27], we apply the geometric concepts to a distortional-geometric entity, a local-universe mimic, modeled as an unstable radiating blackbody, producing to extinction a spherically propagating and decaying "shock-wave" (the present terminology to describe the approximate "rectangular(time) emission function", see Fig.7) in the geometric-manifold. The shock-wave decays by virtue of the posited absorption-characteristic for the spacetime manifold. In the earlier work the classical Riemannian four-dimensional geometrical curvature equations were applied to describe localized distortional-energy-distributions, with a modified-gravitational model-derived coupling-constant between geometry and physical energy, and making no distinction between "ordinary matter and dark matter" [26,27].

The "negative energy-density" spatial regions manifested in the earlier "distortional fundamental-particle mimics" are not suggested in the large-magnitude energy-density model here employed, however the "geometric maximum-energy-density" feature (successfully exploited to geometrically explain and quantify the Fermi constant [26]) is included, as well as the distortional electron feature.

In the case of the distorted-geometry model, although no localized distortional metric is here constructed, the infinitesimal nature of the absorption coefficient μ does not materially change the calculational procedure or results. However see the work of [28-32] where cosmological "optical" metrics have been proposed, in particular Gordon's optical metric, with modified indices of refraction for manifolds containing "fluids, etc.". These earlier works show that an optical metric on a curved spacetime can be generalized to include absorption by allowing the metric to become complex, or equivalently $c = c(\mu)$.

In the perspective of [26], the distorted-geometry model is a departure from the classical geometry model where the Einstein Curvature tensor is the stress-energy-tensor describing the "material contents" of the energy distribution. The distorted-geometry model is rather viewed with the energy-content residing in the warping of the manifold and therefore in its geometric-tensors, with the associated energy content resulting from the creation process which produced the distorted feature in the manifold; the energy is fundamentally manifested in the distorted manifold itself and the "curved empty space" [25] referred to above is a "curved space" devoid of an "external or foreign" causative matter-entity.

RADIATION PROPAGATION IN THE MANIFOLD

Relating to the classical astronomical "redshift" frequency form, it was historically assumed that astronomically observed frequency shifts, Δv, originated from a moving source (the Doppler effect), however the latter-day interpretation is one of an expanding transmission medium (the spacetime manifold) where

$$z \stackrel{\text{def}}{=} redshift\,, \qquad \frac{\nu_{observed}}{\nu_{emitted}} \stackrel{\text{def}}{=} \frac{1}{1+z} \qquad and \quad \frac{1}{1+z} = \sqrt{\frac{1-\frac{vel}{c}}{1+\frac{vel}{c}}}\,. \tag{1}$$

The "Hubble-velocity (*vel*)" factor [33], thus interpreted and presently accepted as a "space-expansion-velocity" factor, has been experimentally measured at

$$H0 \stackrel{\text{def}}{=} 7.1(10)^4 \frac{m}{\sec * megaparsec}.$$

See the website at Hubble's law for an encyclopedic discussion and illustration of the experimental measurements (scatter plot) and their aberrations or peculiarities.

But consideration of the presence of electromagnetic energy sources in the interstellar and intergalactic media (gas in ionic, atomic, and molecular form, as well as charged dust, cosmic rays and plasma-energy sources), that is energy constituents other than conventional gravitational ingredients, as contributors to universe-energy, would lead to potential sources of radiation absorption and inelastic energy loss, however randomly and anisotropically distributed (a reason for the encyclopedic scatter plot just cited ?). Radiation propagation in and through terrestrial plasma environments have shown the very absorption phenomena we are here advancing [1-21] and being scalable [34], the phenomena could be incorporated into calculations at extra-galactic, or cosmological, dimensions, at least insofar as they create a localized(?) substantive transmission-medium. In this work we evaluate the physical plausibility of such an "inelastic-energy-loss", or substantive-manifold, model.

In addition, having previously [26] ascribed the attribute of "curvature" (interpreted as a distortional-concept or elastic-characteristic) to the geometric manifold, we will also advance an explosive creation-process for a distortional-universe by incorporating this additional theorized manifold feature.

Subsequently we construct a phenomenological mathematical representation of the photon inelastic-energy-loss-process as a mimic of the established exponential-loss characterization-function for particle interactions in nuclear reactions or in an absorbing medium. This function is expressed for a particle (mimicked as a single photon in this case), through a single simple composite inelastic-energy-loss attenuation-coefficient, μ, and over a path distance d; $E(d,v)= hv$ is defined as the energy-magnitude of the "radiation-energy-component-v" at path-distance d and $E(0,v_0)= hv_0$ is defined as the energy-magnitude of the "radiation-energy-component-v" at path-distance $d=0$. Furthermore, the exponential energy-loss function is established experimentally and therefore we write

$$E(d,\nu) \stackrel{\text{def}}{=} E(0,\nu_0)\ \exp(-\mu\, d), \tag{1a}$$

or, explicitly for electromagnetic radiation and for astronomical frequency-spectroscopy, with transmission velocity *c*,

$$h\nu = h\nu_0 \exp(-\mu\, d)\ ; \quad d = c\ t\ . \tag{1b}$$

This is therefore an operational characterization of the radiation (optical) energy exchange process via a mathematical representation other than a modified index of refraction (complex dielectric constant). Such a representation leads to an inelastic/absorption based frequency shift;

$$\frac{\nu}{\nu_0} = \exp(-\mu\, d) = \exp(-\mu s\ c\ t). \tag{2}$$

Given this possibility that the universe is populated with electromagnetic energy sources or that the manifold itself is substantive (absorptive), the cosmological energy- or frequency-shifts be understood as energy-losses to an absorptive medium or to a non-expanding absorptive manifold. Such an absorption/attenuation coefficient allows calculation of the astronomical velocity-factor, although not a velocity in this model. The Hubble-form, *H0*, for the frequency variation as a function of source-to-observer distance and velocity, has been expressed relativistically for a flat-space manifold in equations (3) and (4) where *d* is defined as the “source to observer distance”;

$$\exp(-\,\mu s\ d) = \frac{1}{1+z}\,, \tag{3}$$

and

$$H0\ d = velocity \quad where \quad \frac{velocity}{c} = \frac{1-\left(\frac{1}{1+z}\right)^2}{1+\left(\frac{1}{1+z}\right)^2} \quad =$$

$$= \frac{\exp(\mu s\ d) - \exp(-\mu s\ d)}{\exp(\mu s\ d) + \exp(-\mu s\ d)} = tanh(\mu s\ d). \tag{4}$$

For the simplest of present modeling, absorptive energy-density sources are assumed uniformly distributed throughout the medium.

We use the Hubble relationship to quantify the absorption coefficient as

$$\mu s \stackrel{\text{def}}{=} \mu C = \frac{1}{d}\ ln[1+z\,] \ = 5.36\ (10)^{-26}\ m^{-1}\,,$$

normalized at

$$d = c\ Age \stackrel{\text{def}}{=} d\_\mu C(z),$$

where z ~ 1089 (defined from the cosmic microwave background shift).

The "absorption" distance-redshift (z) functions and the "Hubble" distance-redshift functions are displayed in Fig.1 where the distance-z functions are expressed in (4) for the "Hubble" distance and (3) for the "absorption" distances, with

$$\mu s \stackrel{\text{def}}{=} \mu c = 0.770\ (10)^{-26}\ m^{-1}\ , \quad \text{normalized at} \quad z = 0.1\ (d \stackrel{\text{def}}{=} d\_\mu c(z))$$

and $$\mu s \stackrel{\text{def}}{=} \mu s = 2.33\ (10)^{-26}\ m^{-1}\ , \text{normalized at} \quad z = 19.5\ (d \stackrel{\text{def}}{=} d\_\mu s(z)\ ). \qquad (5)$$

A distance (universe radius) prediction for the *d_μc(z)* profile is approximately 7 times the prediction for the Hubble function value *d_H(1089)*.

A "physical universe under expansion" interpretation of increasing z-data is here fundamentally associated with larger frequency (z) shifts arising from longer radiation-absorption paths, and calculable with (6);

$$Source\ observation\ radius = c\ t = \ d = -\frac{1}{\mu s}\ln\left(\frac{1}{1+z}\right). \qquad (6)$$

Besides fundamental differences with distance and time interpretations, we suggest here that experimental astronomical data at the extremes can be understood within, or as part of, the presently-constructed absorptive (electromagnetic-component)-universe, or an absorptive spacetime-manifold-model, and therefore the need for incorporation of an hypothesized additional dark-energy component to describe a "universe under expansion" behavior would be unwarranted (see (2) through (6)).

If a second absorptive species is present in the medium, resulting in a departure from the simpler uniformly-distributed energy-density characterization, then mathematical fitting of the z-behavior at both distance extremes is possible. We have incorporated such energy-density representations according to the absorption-coefficient *μ(d)* constructions in (7)-(9):

$$\mu s \stackrel{\text{def}}{=} \mu d2 = d20\left(1 + d21\left(\frac{d}{d0}\right)^2\right),$$

$$d20 = \ 0.73\ (10)^{-26}\ m^{-1},\ d21 = 6.4\ and\ \ d0 = \frac{c}{H0}. \qquad (7)$$

$$\mu s \stackrel{\text{def}}{=} \mu d6 = d60\left(1 + d61\left(\frac{d}{do}\right)^6\right),$$

$$d60 = \ 0.77\ (10)^{-26}\ m^{-1}\ \ and\ \ d61 = 7.0\ . \qquad (8)$$

$$\mu s \stackrel{\text{def}}{=} \mu e = E0\left(1 + e^{d(z)E1}\right),$$
$$E0 = 0.34\,(10)^{-26}\,m^{-1} \;\; and \;\; E1 = 2.1(10)^{-26}\,m^{-1}. \tag{9}$$

These “absorption” distance-redshift (*z*) functions, the “Hubble” distance-redshift function and the absorptive energy-density functions are displayed in Figures 2 and 3. We display, on logarithmic scales in Fig. 4, these second order absorption coefficients as a function of distance; this illustration supports the hypothesized condition of an earlier denser universe, that is, radiation propagation through a denser medium (from an earlier time and a longer path) produces a greater frequency-shift (energy-loss). All (a non-exhaustive set) of the functional constructs (*μe(z), μd2(z)* and *μd6(z)*), presently utilized to produce numerical Hubble-distance agreement at the larger-distance z-value (z = 1089), exhibit an early-time larger absorption coefficient.

In the absence however of an independent distance- or absorption-coefficient- “known state-variable”, the radiation-absorption universe model only produces the product-variable “*μ d*”. Therefore either the distance-result quoted from (5) with $\mu s = \mu c = (c\ Age)^{-1}$, and assuming *d_H*(z = 0.1) is physically acceptable, or the absorption-coefficient result quoted from (7-9), would be allowable.

Although many experiments [35-38] have been performed in an attempt to detect the relative motion of radiative-energy through a stationary “luminiferous aether (aether wind)” and to test the tenets of special relativity, the experiments have shown uncertainties (best @ $\leq 10^{-8}$) [38] many orders of magnitude greater than that needed to relate to the magnitude of the attenuation coefficient *μs.* The small magnitude of the astronomical light-source frequency-change effect (now depicted as due to spatial expansion but here modeled as an inelastic electromagnetic-radiation energy-loss) is illustrated by the following ; at earth to moon distances ($4*10^{8}\ m$) the absorptive loss ($1 - exp(-\mu s\ d)$) would be ~ $(10)^{-17}$ and difficult to detect experimentally, however this experimental-measurement challenge exists for all cosmological data acquisition including the spatial-expansion frequency-change model, where the Hubble shift is $\Delta v/v$ = $3(10)^{-18}$ at earth to moon distances (<u>actually the “spatial-expansion Hubble-shift” model (phenomenon) is considered not applicable at “local” distances</u>). We have of course intentionally mimicked or modeled the same astronomical data as for the spatial expansion model. If plasma phenomenology and radiation-absorption characteristics determined in the laboratory could be scaled to cosmological distances, a potential successful outcome could ensue. Other potentially meaningful experimental undertakings are not known at this time.

The vanishingly small character of an absorption coefficient necessary to describe the intergalactic spatial electromagnetic energy sources which will produce the astronomically-measured light-source frequency-shifts would seem however to support the model concept.

DISTORTIONAL ENERGY DECAY

For a distorted-geometry spherical universe model, the observational isotropic perspective would be represented by an observer at *r = 0*, the original center-location of the immense spatial distortion and the spherical center of the subsequent explosively propagating shock-wave. The observer would actually be looking toward the younger (later) created elements from the wave with radiation from said emitting elements having propagated through the longer absorbing path of the manifold; the observer would be sitting at the oldest part of the shock-wave created universe. Whether the energy-seeded and therefore transmission-modified local manifold's absorption properties would further impact the manifold attenuation-coefficient is not addressed at this point although matter-energy absorption in the manifold is treated with a separate and different attenuation-coefficient from radiation-energy absorption.

With this perspective of the absorption-induced energy-density components of the manifold, we display in Fig. 5 the results of such calculations wherein matter-energy sources are assumed detectable via radiation emission for the observer at time *t; t = Age* would apply for a present-day observer. The energy-density equations are taken from the development in the section, (18a) for *ρU_M*.

The deposited energy-density functions inherently contain an equilibrating element through incorporation of the spherical volume-expansion representation in (18a).

In Fig. 6 we show the calculational results responsible for the deposited-energy temperature functions of (21); the post-Age time evolution of the radiation component is also shown.

We depart from the current Big Bang/singularity model and utilize the classical Stefan-Boltzmann equations to describe the time-evolution of a presently engendered massive, unstable (radiating as a blackbody) geometric-distortion; we thereby create an energy-time development profile (an explosive event) for the unstable structure. The mass-energy decay time profile (Stefan-Boltzmann) is,

$$P = \frac{dU}{dt} = -(\sigma T^4)\, A(r) \;\; \text{and} \;\; A(r) = 4\pi\, r^2\,, \tag{10}$$

where the total radiating energy is represented in *U*, or

$$\frac{dU}{dt} = -c(4\pi\rho)^{\frac{1}{3}}(3U)^{\frac{2}{3}} \tag{11}$$

with

$$U = the\ distortional\ energy\ @\ constant\ density = \rho\,,$$

leading to

$$U(t) = -\frac{4}{3}\,\pi\rho(c\,t)^3 + U0\,. \qquad (12)$$

For a geometric (gravitationally-formulated) maximum *ρ,* that is, using the Schwarzschild gravitational radius ≡ r_G as a measure of the geometric-curvature ($1/\,r_G$) and equating it to the "maximum-curvature" [26], which is a Fermi-constant derived curvature for geometrically-distorted structures, a maximum mass-energy-density is calculated;

$$r_G = 2\,\kappa_G M_G = \frac{G}{c^4}\,M_G \qquad \text{and}$$

$$\rho = M_G\left[\frac{4\pi}{3}\left(\frac{G}{c^4}\,M_G\right)^3\right]^{-1} = \left[\frac{4\pi}{3}\frac{G}{c^4}\right]^{-1}\frac{1}{(r_G)^2} =$$

$$= \left[\frac{4\pi}{3}\frac{G}{c^4}\right]^{-1}\frac{1}{r\_min^2} = 4.1678(10)^{80}\,\frac{J}{m^3}$$

where

$$\frac{1}{r\_min^2} = (u0B\,\pi)^2\left(\frac{3\,GF}{MW}\right)^{-2/3}. \qquad (12a)$$

For comparison, as calculated from the geometric (EM(electromagnetic)-formulated) maximum *ρ* for the W⁻boson [26],

$$\rho_{geo\_boson} \stackrel{\text{def}}{=} \rho GF = \frac{u0B^3}{GF}\left(MW\,\frac{\pi}{2}\right)^2 = 1.687(10)^{47}\,\frac{J}{m^3}$$

and

$$Temp_{geo\_boson} = \left(\rho GF\,\frac{c}{\sigma}\right)^{1/4} = 5.46\,(10)^{15}\,K\,. \qquad (12b)$$

We have posited for this radiating geometrically-distorted structure, the maximum geometric distortional density $\underline{\rho}$ expressed in (9a), where *GF* is the Fermi constant, *MW* is the W⁻boson mass-energy and *u0B* = 1.807 [26].

A final extinction time, wherein all of the structural energy has been depleted and converted to wave-energy, is reached at

$$tf = \frac{1}{c}\left(\frac{3\,U0}{4\pi\rho}\right)^{1/3} = \frac{R}{c}\,, \qquad (13)$$

thereby producing a propagating spherical shock-wave with a time-width of *tf* and inherited blackbody features; we assume a shock-wave velocity = *c* and apply such a descriptive-development to characterize the exploding distortion with a mass-energy-

magnitude equal to the total-universe-energy *U0*. Construction of the "*total-universe-energy"* is accomplished by ascribing to the blackbody sphere the energy content presently and experimentally observed as "*ordinary* + *dark*" matter-energy; that is, we use a *radius* = *c*⁎*Age* and an energy-density equal to the *"observational(ord) + dark" matter-energy-density = 5.78* $(10)^{-9}$ J/m^3 to define the "*total-universe-energy"*; *"ord"* = 0.049 *U0* and *"dark"* = 0.268 *U0*. In that case with *U_univ ≡ U0 = 5.38*$(10)^{70}$ *Joules*, *tf =* $1.05(10)^{-12}$ *seconds.*

Displayed in Fig. 7 is the time profile of the emerging shock-wave the instant after extinction of the originating spacetime-distortional. The profile is constructed to illustrate the immediate effects of the expanding geometry on the energy profile.

The emergent spherical shock-wave expands radially through the spacetime manifold at velocity c, seeding the manifold and culminating (an exponentially decreasing culmination) at the ultimate physical boundary characterized by the attenuation coefficient. Such a universe, a propagating energy-shell creating an energy-seeded internal sphere, complicates geometric characterization but the spherical matter-energy-density, radially defined by the shell boundary, would represent a "time-changing geometric descriptor" from *closed (contracting)* ($\Omega = \rho\_U_{matter}/\rho_{critical}$ = *4.21*$(10)^{59}$ *@ tf*) to *open (expanding)* (Ω = *1 @ 1.0064 Age*); $\rho_{critical} = 3H0^2/8\pi G$. The "geometric characterization" of the manifold is therefore not explicitly represented.

The radius of this radiating blackbody and its associated temperature are

$$Radius = \left(\frac{3}{4\pi}\frac{U0}{\rho}\right)^{\frac{1}{3}} = 3.14(10)^{-4}\, meters$$

$$and\ \ Temp = \left(\frac{c}{\sigma}\rho\right)^{1/4} = 1.22(10)^{24}\, K\,, \qquad (14)$$

where σ is the Stefan-Boltzmann constant and ρ is the geometric-maximum-density specified in (12a).

Because the radiation component associated with the wave is small ($\sim 10^{-6}$) compared to the matter component, it has been omitted from the *U0* calculation. Experimental values [39-40] for these energy-density components are incorporated as ρU_{matter} = $5.79(10)^{-9}\ J/m^3$ (reported at Age) representing "ordinary (baryonic) + dark" matter and

$$\rho U_{radiation} = (2.725)^4\ \frac{\sigma}{c}\ = 1.04(10)^{-14}\frac{J}{m^3}\ \ (reported\ @\ Age). \qquad (15)$$

We now advance and investigate the effects of the additional manifold feature developed in the previous section, an energy-absorbent or attenuating characteristic. Energy production in the manifold comprises both the wave's characteristic as energy source and the absorbent medium's characteristic ability to receive (absorb) the energy. Energy and energy-density equations for the resultant wave are expressed as,

$$\rho Wave_{ord-matter}(t) = U0\, f_{ord}\ \ (vol\_wave(t))^{-1} \exp(-\mu a\, c\, t)\ \ ,$$

$$\rho Wave_{dark-matter}(t) = U0\ \ f_{dark}\ (vol\_wave(t))^{-1}\ \exp(-\mu a\, c\, t)$$

and

$$\rho Wave_{radiation}(t) = U0\ \ f_{radiation}\ (vol\_wave(t))^{-1} \exp(-\mu s\, c\, t)$$

where

$$vol\_wave(t) = \frac{4\pi}{3} c^3\ (3\, tf\ t^2 + 3\, tf^2 t + tf^3). \tag{16}$$

After integrating over the volume extent of the wave-shell,

$$U0\, f_{matter}\ \left[\frac{1}{tf^3}\int_t^{t+tf} \frac{1}{\frac{1}{3}+\frac{\tau}{tf}+\left(\frac{\tau}{tf}\right)^2}\tau^2\, d\tau\ \right]^{-1} \exp(-\mu a\, c\, t) = UWave_{matter}(t). \tag{17}$$

The matter and radiation energy components become

$$UWave_{ord\_matter}(t) = U0\, f_{ord}\ \ \exp\big(-\mu a\ c\ (t)\big)\,,$$
$$UWave_{dark\_matter}(t) = U0\, f_{dark}\ \ \exp\big(-\mu a\ c\ (t)\big)$$

and

$$UWave_{radiation}(t) = U0\ \ f_{radiation}\ \ \exp\big(-\mu s\ c\ (t)\big). \tag{17a}$$

With respect to the radiation component of the wave and its deposited/absorbed energy in the manifold, or left in the wake of the propagating wave (specified experimentally through discovery of the cosmic-wave-background-radiation), $f_{radiation}$ = *7.28(10)*$^{-6}$. The deposited manifold energy densities are then

$$\rho U_{ord-matter}(t) = U0\, f_{ord}\left(\frac{4\pi}{3}(c\ t)^3\right)^{-1}\ (1 - \exp(-\mu a\ c\ t)\ )$$
$$\rho U_{dark-matter}(t) =\ U0\, f_{dark}\left(\frac{4\pi}{3}(c\ t)^3\right)^{-1}\ (1 - \exp(-\mu a\ c\ t)\ )$$

and

$$\rho U_{radiation}(t) =\ U0\, f_{radiation}\left(\frac{4\pi}{3}(c\ t)^3\right)^{-1} (1 - \exp(-\mu s\ c\ t)\ ). \tag{18}$$

Deposited-energy-equations are, similarly,

$$U_{ord\_matter}(t) = U0\, f_{ord}\,(1 - \exp(-\mu a\, c\, t))\,,$$
$$U_{dark\_matter}(t) = U0\, f_{dark}\,(1 - \exp(-\mu a\, c\, t))$$

and

$$U_{radiation}(t) = U0\ f_{radiation}\ (1 - \exp(-\mu s\, c\, t)). \tag{18a}$$

In the distorted-space narrative [26], the matter-like distortions include both electromagnetic and gravitational structures, via a composite coupling constant, which we have detailed as "*observational* or *ordinary*" plus "*dark*" matter. Radiation attenuation has been treated with the absorption coefficient *μs,* however, matter, or mass-energy, is here treated with an independent attenuation factor *μa.* This factor is constrained or determined from the time "*tel*" that the wave energy-density reaches the extreme energy-density expressed as the minimum energy-density for distortional-electron formation [26];

$$\rho U_{electron} = U0 * vol\_wave(tel)^{-1} \exp(-\mu a\, c\, tel) \quad \text{or}$$

$$\mu a = -\frac{1}{c\, tel} ln\left(\frac{\rho U_{electron}\ vol_{wave(tel)}}{U0}\right)$$

where

$$\rho U_{electron}\left(\frac{J}{m^3}\right) = (me\, c^2)^4 \frac{3}{\pi\, \alpha fs}\left(\frac{UM0}{\hbar\, c}\right)^3 = 5.09(10)^{26}\ \frac{J}{m^3},$$
$$UM0 = 1.40\ \ and\ \alpha fs = fine\ structure\ constant\,. \tag{19}$$

The propagating wave's matter-temperature at this electron mass energy density is

$$Wave\_Temp_{electron} = \left(\rho U_{electron} \frac{c}{\sigma}\right)^{1/4} = 2.86\ (10)^{10}\ K.$$

We set the time "*tel*" ="*recombination time*"= *1.19(10)*^{13} *s* (from the prevailing cosmological model, the Big Bang theory) as an approximation to the "electron-distortional-structure formation-end-time", which leads to $\mu a = 1.69(10)^{-21}\ m^{-1}$ and a radiation-sphere temperature

$$Sphere\_Temp_{radiation}(tel) = \left(\rho U_{radiation}(tel)\frac{c}{\sigma}\right)^{\frac{1}{4}} = 3962\,K.$$

The radial radiation-expansion volume-factor (18) is $\underline{f_{volume}} = 0.067$. Using the mixing function value (radial radiation-expansion volume-factor) ascribed to the radiation temperature at *time=Age*, the calculated <u>*Sphere_Temp*</u> *750 K*.

The fixing of *μa* allows determination of the starting time for distortional-matter production, that is for production of a structural-energy-density to mimic the W^-boson [26], which represents the maximum distortional-curvature for distortional-matter production in the wave;

$$\rho U_{Wboson} = \rho GF = U0 * vol(tWB)^{-1}\exp(-\mu a\; c\; tWB). \qquad (20)$$

This calculation leads to $tWB = 1.34(10)^4\ s$, although the exponential factor contributes insignificantly; the wave has propagated radially to $r = 4.02(10)^9\ km$.

Radiation deposition, or absorption, is assumed to initiate immediately at *t* = *tf* during the creation process, accompanied by, a "radiation-expansion" from the wave (a shell at radial thickness = *c∗tf*) into the spherical spatial manifold; this "equilibration-expansion" is expressed as the "*volume-change ratio* = $\left[{}^{4\pi}/_{3}\,(c\;t)^3\right]/vol\_wave(t)$" with an accompanying "mixing process function" expressed as a "pseudo volume-radius reduction". The temperature function, $TU_{radiation}$, (18), evaluated at *t* = *Age,* with the observational-absorption function *exp(-μs c t)*, expresses this result;

$$TU_{radiation}(Age) = \left[\frac{c}{\sigma}\,\rho U_{radiation}(Age)\right]^{0.25} = 2.725\,K,$$

$$\rho U_{radiation}(Age) = \begin{bmatrix} U0\; f_{radiation}\left(\frac{4\pi}{3}(c\; Age\; f_{volume})^3\right)^{-1} \times \\ \times\,(1-\exp(-\mu s\; c\; Age)\,)\exp(-\mu s\; c\; Age) \end{bmatrix}^{0.25},$$

$$and\ f_{volume} = 0.616\,. \qquad (21)$$

The radial radiation-expansion volume-factor (*radius* = *c t*) is apparently overstated and a correction factor $\underline{f_{volume}}$ has been added (a radial-reduction to 0.616 c t) to produce temperature agreement.

In summation, creation of matter is understood to take place after the wave has diluted to the "maximum for particle formation" at *ρWB*, the energy-density associated with the maximum distortional-geometric-curvature and at a time $tWB = 1.34(10)^4\ s$. Particle creation continues to a wave energy-density limit for electron formation, *tel* =

1.19(10)^{13} *s*. Radiation creation is considered possible at all energy-density levels. Attributes of the decaying wave-energy-densities are shown in Fig. 8 and Fig. 9.

It is apparent from the initial spatial deposition and distribution of the wave-energy that energy equilibration/mixing processes (via volume-expansion already discussed in the section "**RADIATION PROPAGATION IN THE MANIFOLD**") ensue to achieve a final spatially-independent energy distribution in such a universe.

Decaying wave energies are illustrated in Fig. 10. Accumulating manifold energies are shown in Fig. 11 and Fig. 12. The matter-energy and radiation-energy depositions displayed in Figs. 11 and 12 have reached saturation at times ~ 10^{18} seconds.

CONCLUSION

It has been posited in the present work that the classical astronomically observed electromagnetic frequency shifts can be interpreted as produced by absorption and inelastic energy-loss in a substantive spacetime manifold or as produced by inelastic energy-loss absorption from universe-sited electromagnetic energy sources. The presence of a gravitational dark-energy component throughout the universe may be illusory if extreme radiation-shifted astronomical phenomena are interpreted as originating from such absorptive energy sources or an absorptive geometric manifold. Finally, we have incorporated such absorption concepts to describe an explosively-driven energy-production-model of a distortional-universe to characterize the time-development, distances, energy-densities and matter and radiation production within the manifold.

ACKNOWLEDGMENT

Since this work is a continuation of the fundamental endeavor expressed in [26], we again acknowledge the creative critique offered by, Dr. J T Grissom for his valuable suggestions for technical clarification and material emphasis and, the helpful corrective conceptual commentary of Dr. J D Weiss, relative to that work.

REFERENCES

[1] LiXin Guo and JiangTing Li, Physics of Plasmas, vol. 24, 022108, 2017. [Online]. Available: doi: http://dx.doi.org/10.1063/1.4973654

[2] R. J. Vidmar, " On the use of atmospheric pressure plasma as electromagnetic reflectors and absorbers," IEEE Trans. Plasma Sci., vol. 18, pp 733-741, 1990. [Online], Available: https://doi.org/10.1109/27.57528

[3] M. Laroussi, " Interaction of microwave with atmospheric pressure plasmas," Int. J. Infrared Millimeter Waves, vol. 16, pp. 2069–2083, 1995. [Online], Available: https://doi.org/10.1007/BF02073410

[4] M. Laroussi, " Scattering of electromagnetic waves by a layer of air plasma surrounding a conducting cylinder," Int. J. Infrared Millimeter Waves, vol. 17, pp. 2215–2232, 1996. [Online], Available: https://doi.og/10.1007/BF02069497
[5] Y. P. Bliokh , J. Felsteiner , and Y. Z. Slutsker , " Total absorption of an electromagnetic wave by an overdense plasma," Phys. Rev. Lett., vol. 95, 165003, 2005. [Online], Available: https://doi.org/10.1103/PhysRevLett.95.165003
[6] O. Sakai and K. Tachibana , " Properties of electromagnetic wave propagation emerging in 2-D periodic plasma structures," IEEE Trans. Plasma Sci., vol. 35, pp.1267–1273, 2007. [Online] Available: https://doi.org/10.1109/TPS.2007.906133
[7] M. Laroussi and J. R. Roth , " Numerical calculation of the reflection, absorption, and transmission of microwaves by a nonuniform plasma slab," IEEE Trans. Plasma Sci., vol. 21(4), pp. 366–372, 1993. [Online] Available: https://doi.org/10.1109/27.234562
[8] V. R. Goteti and D. K. Kalluri , " Wave propagation in a switched-on time-varying plasma medium," IEEE Trans. Plasma Sci., vol. 17(5), pp.828–833, 1989. [Online] Available: https://doi.org/10.1109/27.41212
[9] A. B. Petrin , " Transmission of microwaves through magnetoactive plasma," IEEE Trans. Plasma Sci., vol. 29(3), pp. 471–478, 2001. [Online] Available: https://doi.org/10.1109/27.928945
[10] C. X. Yuan , Z. X. Zhou , J. W. Zhang , X. L. Xiang , Y. Feng , and H. G. Sun , " FDTD analysis of terahertz wave propagation in a high-temperature unmagnetized plasma slab," IEEE Trans. Plasma Sci., vol. 39, 2011, pp.1577–1584. [Online] Available: https://doi.org/10.1109/TPS.2011.2151207
[11] J. P. Rybak and R. J. Churchill , " Progress in reentry conmmunications," IEEE Trans. Aerosp. Electron. Syst., vol. AES-7(5), pp.879–894, 1971. [Online] Available: https://doi.org/10.1109/TAES.1971.310328
[12] A. Rokhlenko , " The reflection of electromagnetic waves by a conducting surface shielded with a plasma layer," IEEE Trans. Plasma Sci., vol. 24, pp.182–186, 1996. [Online] Available: https://doi.org/10.1109/27.491757
[13] D. L. Tang , A. P. Sun , X. A. Qiu , and P. K. Chu , "Interaction of electromagnetic waves with a magnetized nonuniform plasma slab," IEEE Trans. Plasma Sci., vol. 31, pp.405–410, 2003. [Online] Available: https://doi.org/10.1109/TPS.2003.811648
[14] C. S. Gurel and E. Oncu , " Frequency selective characteristics of a plasma layer with sinusoidally varying electron density profile," J. Infrared Millimeter Terahertz Wave, vol. 30, pp.589–897, 2009. [Online] Available: https://doi.org/10.1007/s10762-009-9483-9
[15] Y. B. Xi and Y. Liu , " Effect of electron density profile on power absorption of high frequency electromagnetic waves in plasma," Phys. Plasmas, vol. 19, 073301, 2012. [Online] Available: https://doi.org/10.1063/1.4751256 .
[16] C. X. Yuan , Z. X. Zhou , X. L. Xiang , H. G. Sun , and S. Z. Pu , " Propagation of broadband terahertz pulses through a dense-magnetized-collisional-bounded plasma layer," Phys. Plasmas, vol. 17, 113304, 2010.

[17] C. X. Yuan , Z. X. Zhou , X. L. Xiang , H. G. Sun , and H. Wang , " Propagation properties of broadband terahertz pulses through a bounded magnetized thermal plasma," Nucl. Instrum. Methods Phys. Res., Sect. B, vol. 269, pp.23–29, 2011. [Online] Available: https://doi.org/10.1016/j.nimb.2010.10.003

[18] G. Cerri , F. Moglie , R. Montesi , P. Russo , and E. Vecchioni , " FDTD solution of the Maxwell–Boltzmann system for electromagnetic wave propagation in a plasma," IEEE Trans. Antennas Propag., vol. 56, pp.2584–2588, 2008. [Online] Available: https://doi.org/10.1109/TAP.2008.927505

[19] B. J. Hu , G. Wei , and S. L. Lai , " SMM analysis of reflection, absorption and transmission from nonuniform magnetized plasma slab," IEEE Trans. Plasma Sci, vol. 27, pp.1131–1136, 1999.
https://doi.org/10.1109/27.782293

[20] B. Guo and X. G. Wang , " Power absorption of high-frequency electromagnetic waves in a partially ionized magnetized plasma," Phys. Plasmas, vol. 12, 084506, 2005. [Online] Available: https://doi.org/10.1063/1.2033587

[21] R. L. Stenzel and R. W. Gould , " Upper-hybrid resonance absorbtion, emission, and heating of an afterglow plasma column," J. Appl. Phys., vol. 42, pp.4225–4235, 1971. [Online] Available: https://doi.org/10.1063/1.1659758

[22] Ciufolini, I. and Wheeler, J. A. , Gravitation and Inertia, USA, Princeton University Press, 1996.

[23] Wheeler J. A., Phys. Rev., vol. 97, p.511, 1955.

[24] Wheeler J. A., "Logic, Methodology, and Philosophy of Science", Proc. 1960 International Congress, USA, Stanford University Press, p.361,1962.

[25] Clifford, W. K., Proc. Cambridge philosophical society vol.2, p.157, 1876.

[26] Koehler, D. R., Indian Journal of Physics, vol. 87, p.1029, 2013.

[27] Koehler, D. R., The Distorted Universe: From Neutrinos to the Cosmos, The Theory of Nothingness, Kindle: ASIN B00TG26Q7Y, 2015.

[28] Gordon, W., Annals of Physics, vol. 22, p. 421, 1923.

[29] Chen, B. and Kantowski, R., Phys. Rev.; vol. D 78: 044040, 2008.

[30] Chen, B. and Kantowski, R., Phys. Rev., vol. D 79: 104007, 2009.

[31] Chen, B. and Kantowski, R., Phys. Rev., vol. D 80: 044019, 2009.

[32] Lima, J. A. S., Cunha, J. V. and Zanchin, V. T., Astrophysical Journal Letter, vol. 742 : 26, 2012.

[33] Lemaître, G., Annals of the Scientific Society of Brussels, vol. 47A: 41, 1927.

[34] Alfvén, Hannes, "On hierarchical cosmology", Astrophysics and Space Science, vol. 89 (2), pp.313–324, 1983. doi:10.1007/bf00655984.

[35] Braxmaier, C., Müller, H., Pradl, O., Mlynek, J., Peters, J. A. and Schiller, S., Phys. Rev. Lett., vol. 88: 010401, 2002.

[36] Mansouri, R. and Sexl, R.U., Gen. Rel. Gravit., vol. 8, p. 809, 1977.

[37] Müller, J., Nordtvedt, K., Schneider, M. and Vokrouhlicky, D., Proceedings of the 11th International Workshop on Laser Ranging Instrumentation, vol. 10, p. 216, 1999.

[38] Wolf, P., Tobar, M. E., Bize, S., Clairon, A., Luiten, A. N. and Santarelli, G., General Relativity and Gravitation, vol. 36, p. 2351, 2004.
[39] Davies, P., The Goldilocks Enigma, First Mariner Books, vol. 43, 2006.
[40] http://map.gsfc.nasa.gov/universe/uni_matter.html.

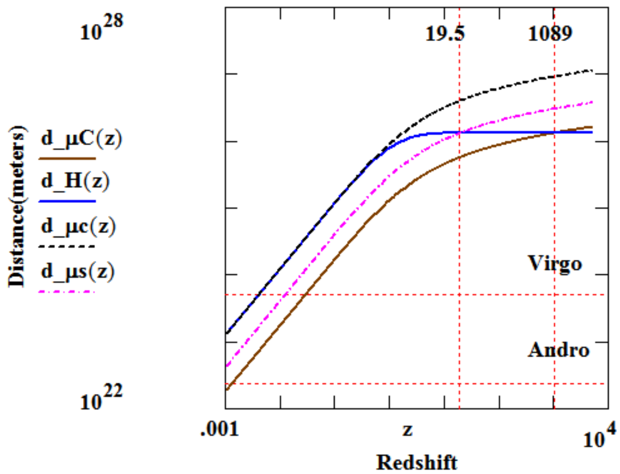

Fig. 1. Distance(source to observer)/frequency-change profiles. Absorption distance *d_μC(z)*-vs-*z* (bold-brown), Hubble distance *d_H(z)*-vs-*z* (bold-blue), Absorption distance *d_μc(z)*-vs-*z* (dash-black) and Absorption distance *d_μs(z)*-vs-*z* (dadot-magenta). Virgo is the defined galaxy-cluster distance at 16.5 megaparsecs and Andro is the defined Andromeda galaxy-distance at 0.78 megaparsecs. The redshift-z at 1089 is the CMB (cosmic microwave background) redshift.

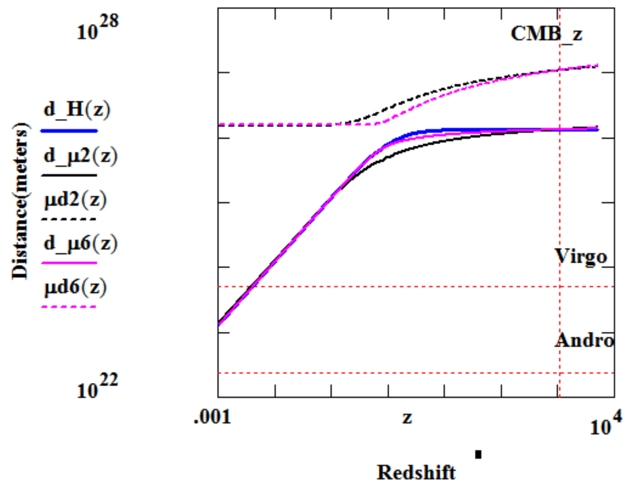

Fig. 2. Distance (source to observer)/frequency-change profiles. Absorption distance *d_μ2(z)*-vs-*z* (bold-black), Hubble distance *d_μH(z)*-vs-*z* (bold-blue) and Absorption distance *d_μ6(z)*-vs-*z* (bold-magenta) are illustrated. The Absorption coefficient *μd2(z)*-vs-*z* (dash-black) and Absorption coefficient *μd6(z)*-vs-*z* (dash-magenta) are displayed in units of m^{-1} and multiplied by a factor of 10^{52} for display purposes. Virgo, Andro and CMB_z are defined in Figure caption 1. .

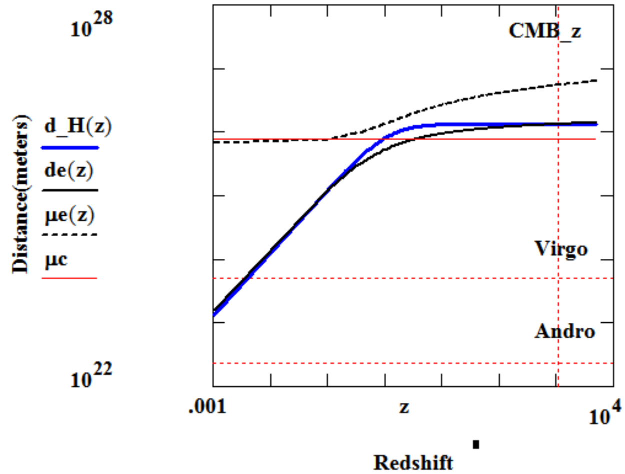

Fig. 3. Distance (source to observer)/frequency-change profiles. Absorption distance *de(z)*-vs-*z* (bold-black) and Hubble distance *d_μH(z)*-vs-*z* (bold-blue) are displayed. The Absorption coefficient *μe(z)*-vs-*z* (dash-black) and the constant-density coefficient *μc* (red) are displayed in units of m^{-1} and multiplied by a factor of 10^{52} for display purposes. Virgo, Andro and CMB_z are defined in Fig. caption 1.

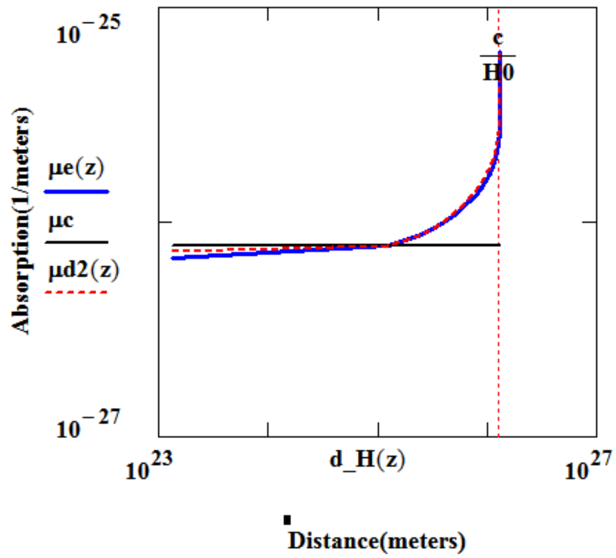

Fig. 4. Absorption-coefficient/Distance profiles. Absorption coefficient *μe(z)*-vs-distance (bold-blue), Absorption coefficient *μd2(z)*-vs-distance (dash-red) and Absorption coefficient *μc(z)*-vs-distance (bold-black) are displayed.

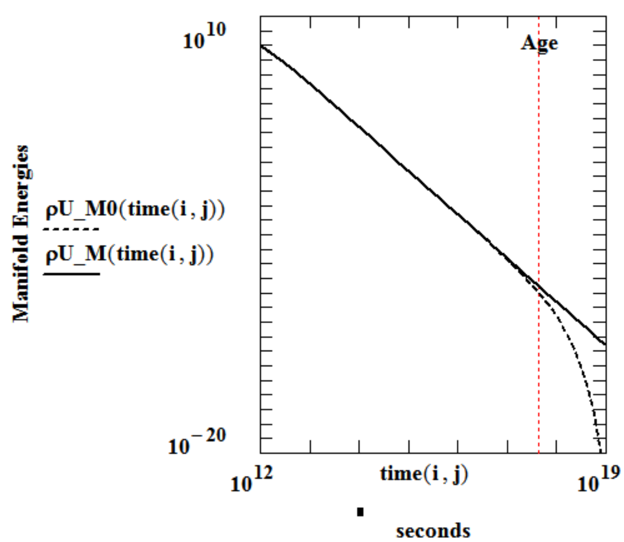

Fig. 5. Ordinary-matter ("as-deposited/absorbed" and "as-observed/altered") energy-density profiles (in *Joules/m*^{3}). *ρU_M* designates the ordinary matter "as-deposited" profile (Eq.15a) while *ρU_M0* designates the path-altered or "as-observed" profile (Eq.15a) $*$ *exp(-μs c t).*

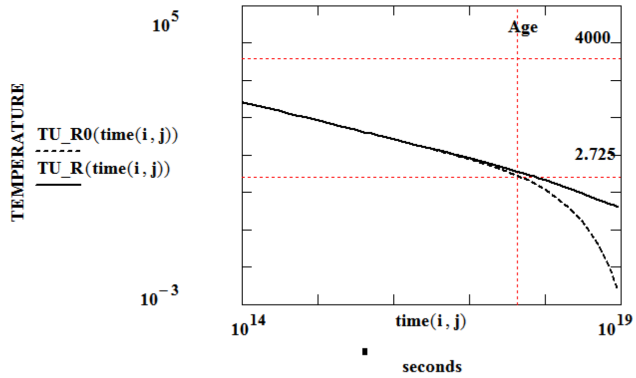

Fig. 6. Radiation-observed temperature-profiles (*TU_R0* for path-altered and *TU_R* non-path-altered) of the wave-deposited radiation component; note the post-age development.

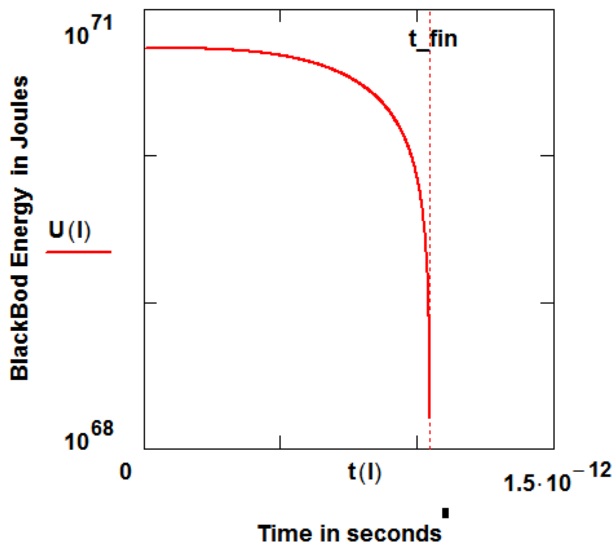

Fig. 7. The Black-Body energy function (*Joules)* versus time on the abscissa. Time *tf* is equal to the extinction time in this graph and therefore the profile is one of the newly emerging wave.

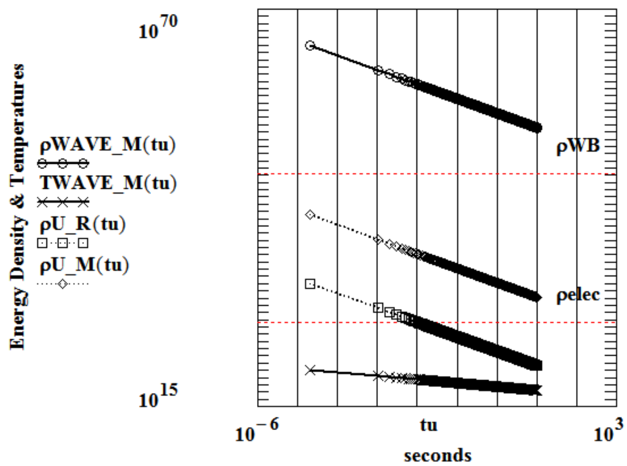

Fig. 8. Matter shock-Wave (⨀) energy-density (*J/m*[3]) and temperature functions (*K*) (⊠; wave) versus time on the abscissa. Deposited energy-densities (*J/m*[3]) functions (⊡, radiation and ◇, matter) versus time on the abscissa. The critical energy-densities, *ρWB* (W-boson) and *ρelec* (electron), already established and cited, are noted.

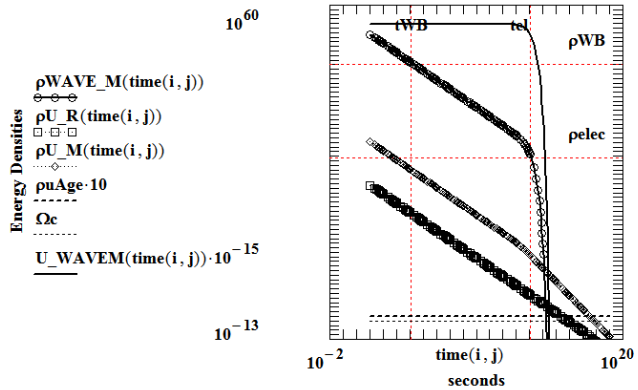

Fig. 9. Matter shock-wave energy-density (J/m^3) functions (⊙; *ρWAVE_matter*) versus time on the abscissa. Deposited energy-density (J/m^3) functions (◇ for matter and ⊡ for radiation) versus time on the abscissa. The critical boson energy-density *ρWB* and the critical electron energy-density *ρelec* in the wave are shown. The equilibrated radiation-energy-density function *ρU_rad* is depicted as (---) and the critical energy-density as (……). Also shown is the total mass-energy in the wave *U_WAVEM* (——).

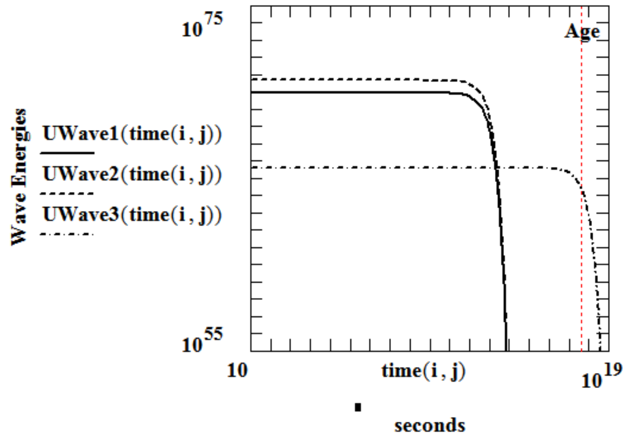

Fig. 10. The depleting matter-wave-energies (*UWave* (Eq.12a) in *Joules*) (solid = 1 = *ord_matter*, dash = 2 = *dark_matter*) and the radiation-wave-energies (dadot = 3 = *rad*) vs later times in the wave's life.

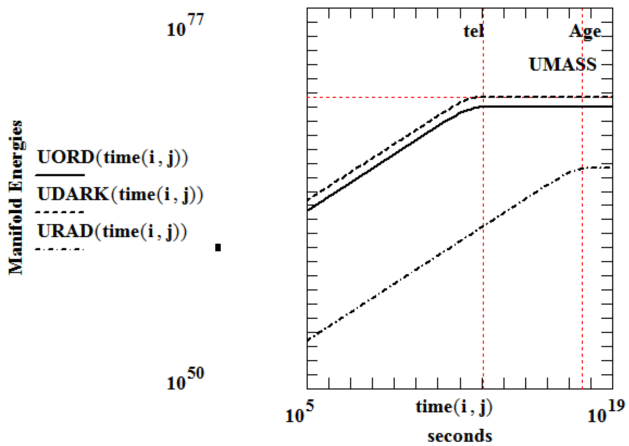

Fig. 11. The accumulating manifold energies (*Joules*) (solid = *ord_matter*, dash = *dark_matter*, dadot = *radiation*) vs time in the wave's life. *time (i,j) = j(10)^{i} . UMASS = U0*.

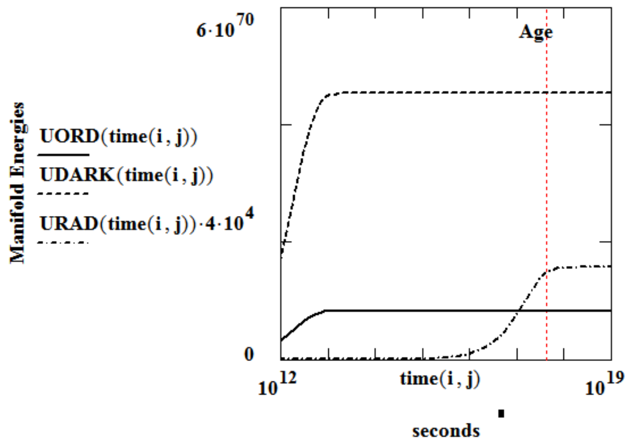

Fig. 12. The accumulating manifold matter energies (*Joules*) (solid = *ord-matter*, dash = *dark-matter*) and the accumulating manifold radiation energy (*Joules*) (dadot) vs time in the wave's life.

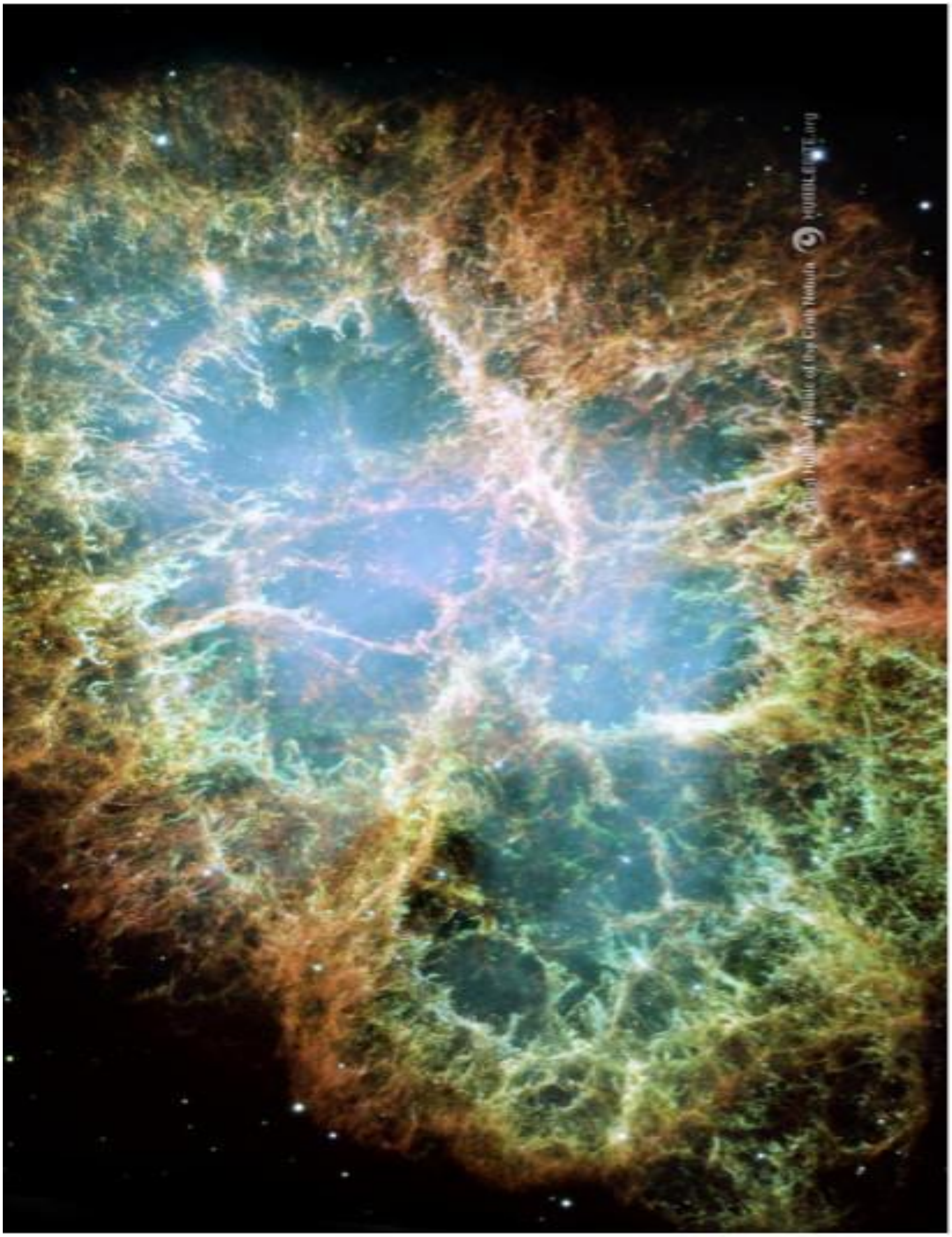
Mosaic of the Crab Nebula
HUBBLESITE.org

Crab Nebula HUBBLESITE .org

CHAPTER 6

Time-Dependent Geometric-Distortions

Chapter Summary: The following chapter material is an investigation of the interpretation of localized geometric distortions as a source of microscopic physical particle-structures. Utilizing the fundamental curvature equations of Riemannian geometry, the static geometric-distortion model for describing such structures has been extended to describe time-dependent oscillatory behavior. The theoretical modeling and calculational procedure is limited to those geometric-distortional families satisfying an equation-of-state based on a simulation of static, spherically-symmetric Maxwellian tensor behavior and incorporating oscillatory time-dependence. Such distortions, with appropriate determination of the included theoretical geometrical descriptors, mimic electromagnetic and gravitational fields and elementary particle characteristics. Inherent to the modeling is the development of a 4-dimensional microscopic-level coupling-constant which supplants the classical gravitational coupling-constant used in general relativity at the more macroscopic level. Over portions of the radial extensions of the distortions, the geometrical tensor elements exhibit negative, as well as positive, curvature-magnitudes and energy-densities (pressures) and beneficially and constructively show no physical singularities. The field-observable in the negative energy-density spatial region (the core region) is non-Coulombic and has fundamentally imparted a geometric character to Fermi's constant. A maximum-geometric-curvature concept is applied to simulate the hypothetical beta-decay transition-mediating particle, the W$^-$boson, and is used here to mimic the structure of an almost invisible photon.

1

INTRODUCTION

Allowing for a space-time manifold itself with absorptive character suggests the possibility of a feature which has been explored earlier [6]. Analysis of such a manifold-attribute results in an alternative explanation to “Hubble-data interpreted as universe expansion”.

In the present time-dependent modeling-endeavors we also describe oscillatory behavior (vibrational or radiation). Subsequently, a particular form of the four-dimensional particle-level metric is yielded. The phenomenological modeling also fundamentally constrains the character of the associated coupling constant and is further used to determine the required values to fit the geometric-distortion descriptors to the physical characteristics of the modeled entities.

In the earlier work [5] we considered a distortional-, or particle-, transformation process wherein the process was described in terms of a .geometrical mediating particle with characteristics mimicking the Fermi beta-decay transition. Gravitationally-configured versions of these distortional-realizations existing throughout our geometric universe would seriously affect cosmological modeling. The present four-dimensional distortional-radiation modeling, with its significant structural emphasis, would additionally affect current “wave-particle duality” interpretations of physical radiation phenomena.

In the Static Distortion section of this chapter, we review the geometrostatic distortion model developed earlier [5] for mathematical introduction to the development of a 4-d time-dependent geometric-distortion elaborated in the Oscillating Distortions section. A

maximum curvature descriptor is posited as the structure for a radiation-like entity. Modification to the geometric coupling constant is necessary and incorporated.

DISTORTION DEVELOPMENT

We write for the relativistic energy for a "distorted-geometry-particle photon";

$$U^2 = (pc)^2 + (mo\ c^2)^2, \ \text{ or } \ U = pc\sqrt{1+\left(\frac{mo\ c^2}{pc}\right)^2} \text{ and}$$

$$U \cong p\,c\left(1+\frac{1}{2}\left(\frac{mo\ c^2}{pc}\right)^2\right);\ pc = h\omega = \frac{hc}{\lambda}. \qquad (1)$$

This distortional photonic total energy then is

$$U \cong p\,c + \frac{1}{2}\frac{(mo\ c^2)^2}{pc} \cong h\omega + \frac{1}{2}\frac{(mo\ c^2)^2}{h\omega} = 2\int_0^\infty Td_4^4\sqrt{(-g_{11})^3 g_{44}}\,4\pi r^2\,dr\,. \qquad (1a)$$

The metric descriptor is

$$ds^2 = g_{11}[dr^2 + r^2 d\Omega +] + g_{44}dt^2 = -e^{\mu}[dr^2 + r^2 d\Omega] + e^{\nu}dt^2. \qquad (2)$$

where $\mu = \mu r + \mu t$ and $v = vr + vt$.

The distortional tensor-densities are specifically denoted with the Td notation and we have introduced the time-dependent metric as

$$e^{\mu t} = e^{\sin(\omega t)} \text{ and we require } vt = \mu t\,, \qquad (3)$$

then $e^{\mu t} = e^{\nu t} = 1$ @ $\omega = 0$, to guarantee transformation to

a 3-dimensional or spatial-model interpretation .

$\dot{\mu}t = \omega \cos(\omega t)$ and $\ddot{\mu}t = -\omega^2 \sin(\omega t)$.

$$e^{\mu t}\left[\ddot{\mu}t + \dot{\mu}t^2/4\right] = e^{\sin(\omega t)}\omega^2\left[-\sin(\omega t) + \frac{1}{4}\cos(\omega t)^2\right] . \tag{4}$$

These metric time-functions are shown in Fig.1. The energy-density functions, considered without the metrics, can be seen to decompose into an explicitly time-dependent component and an explicitly spatial-dependent component. Metrics of the type denoted above couple these components and produce a globally-oscillating spatially-dependent structure. For small masses, the spatial component becomes large and the oscillating elements represented by (3a) are approximately in-phase time-wise (see Fig. 1); this fact is important to the model and bears on physically measurable behavior.

STATIC DISTORTIONS

The spatial solution (eqn 11 in the STRUCTURAL EQUATIONS section)(labelled eqn. (5) here) is used along with the tensor equations in the equation set (6);

$$\mu' = \mu r' = \frac{2}{f(r)(Iu - \gamma)}\frac{R0}{r^2} = \frac{1}{f(r)\left(\frac{Iu}{\gamma} - 1\right)}\frac{Rs}{r^2}$$

and $\quad \mathrm{Iu}(\mathrm{ur}) = \mathrm{ur}\left[-1 + \frac{3}{4}\mathrm{ur}^3 - \frac{3}{7}\mathrm{ur}^6\right].$ (5)

$\gamma \stackrel{\text{def}}{=} 2\frac{\mathrm{R0}}{\mathrm{Rs}}$ where R0 is the model defined radial descriptor and

$\mathrm{Rs} \stackrel{\text{def}}{=} \text{Schwarzschild radius} = 2\,\kappa\,\mathrm{M}c^2.$

Numerical integration produces the metric quantities μ and v. which are displayed in Figs.2, 3 and 4.

The 4-dimensional distortional tensor equations become

$$8\pi\kappa \mathrm{Td}_1^1 = -e^{-\mu t}e^{-\mu r}\left[\frac{\mu r'^2}{4} + \frac{\mu r' \nu r'}{2} + \frac{\mu r' + \nu r'}{r}\right] +$$

$$+\, e^{-\mu t}e^{-\nu r}\left[\ddot{\mu t} + \frac{3}{4}\dot{\mu t}^2 - \frac{\dot{\mu t}\,\dot{\mu t}}{2}\right],$$

$$8\pi\kappa \mathrm{Td}_2^2 = -e^{-\mu t}e^{-\mu r}\left[\frac{\mu r''}{2} + \frac{\nu r''}{2} + \frac{\nu r'^2}{4} + \frac{\mu r' + \nu r'}{2r}\right] +$$

$$+\, e^{-\mu t}e^{-\nu r}\left[\ddot{\mu t} + \frac{3}{4}\dot{\mu t}^2 - \frac{\dot{\mu t}\,\dot{\nu t}}{2}\right] = 8\pi\kappa \mathrm{Td}_3^3\,,$$

$$8\pi\kappa \mathrm{Td}_4^4 = -e^{-\mu t}e^{-\mu r}\left[\mu r'' + \frac{\mu r'^2}{4} + \frac{2\mu r'}{r}\right] + e^{-\mu t}e^{-\nu r}\left[\frac{3}{4}\dot{\mu t}^2\right],$$

$$8\pi\kappa \mathrm{Td}_4^1 = +e^{-\mu t}e^{-\mu r}\left[\dot{\mu t}' - \frac{\dot{\mu t}^2}{2}\right],$$

and $$8\pi\kappa \mathrm{Td}_1^4 = -e^{-\mu t}e^{-\nu r}\left[\dot{\mu t}' - \frac{\dot{\mu t}^2}{2}\right].$$ (6)

The energy-density field-equations (pressures) are

$$(Fd_{14})^2 = -\left(Td_4^4 + Td_1^1\right)g_{11}\, g_{44} = \left(Td_2^2 + Td_3^3\right)g_{11}\, g_{44} =$$

$$= 2\, Td_2^2\, g_{11}\, g_{44}\, ,$$

$$(Fd_{12})^2 = -\left(Td_2^2 + Td_1^1\right)g_{11}\, g_{11}\, ,$$

$$(Fd_{13})^2 = -\left(Td_3^3 + Td_1^1\right)g_{11}\, g_{11} = (Fd_{12})^2\, ,$$

$$(Fd_{12})^2 + (Fd_{13})^2 = \left(Fd_{mag}\right)^2 \tag{7}$$

and $(\nu r = -2\,\mu r + \int f(r)\mu\acute{r}\, dr)$ where $\mu r = \int \mu\acute{r}\, dr$; see Figs. 2-4**.** The energy-density quantity $(Fd_{12})^2$ for an electron-mimic is displayed in Fig. 5 and the quantity Td_4^4 in Fig. 6.

For an electromagnetically predominant distortion,

$$Fd_{14}{}^2 = -g_{11}g_{44}\left(Td_4^4 + Td_1^1\right) \tag{8}$$

with

$$Fd_{14}{}^2(r\to\infty) = \frac{e^{\mu t}}{8\pi\kappa}\left[\frac{Rs^2}{2\, r^4} + 3\,\frac{Rs\; R0^3}{r^6} - \frac{2}{c^2}\left(\ddot{\mu} + \frac{3}{4}\dot{\mu}^2 - \dot{\mu}\frac{\dot{\nu}}{2}\right)\, .\right]$$

In anticipation of the development in the next section, we calculate this particular quantity, $Fd_{14}{}^2$, here to illustrate the strong dependence of these distortions on the energies involved;

$$(Fd_{14})^2(r\to 10^9 ro\,) \sim 3\,\frac{Rs\; R0^3}{(10^9 ro)^6} + \frac{1}{(10^9 ro)^4}\frac{Rs^2}{2} + . \tag{8a}$$

Exclusive of the time-dependent term, the magnetic (r^{-6}) component is approximately 44 orders of magnitude greater than the electric (r^{-4}) component at r = 10^9 ro (ro is the core radius and = $2(10)^{-19}$ m) for an EM distortion with mass-energy $M_{exp} \leq 1.6\ (10)^{-37}$ J and $Q_{exp} \leq (10)^{-35}$ e [**7**], and approximately 60 orders of magnitude greater at r = 10 ro. The distortional gravitational radius (Schwarzschild radius = Rs = $1.8(10)^{-60}$ m) is 41 orders of magnitude smaller than the EM distortional radius (r0E = R0E/u0E ~ $2.2(10)^{-19}$ m) at these electromagnetic-charge magnitudes. Although the magnetic radial (r^{-6}) component is exclusive in the “magnetic term”, the (r^{-6}) behavior is obviously present even in the $(Fd_{14})^2$ tensor energy-density form.

The “magnetic term” is written

$$Fd_{12}{}^2 + Fd_{13}{}^2 = 2\, g_{11} g_{11} \left(\frac{Td_4^4 - Td_1^1}{2}\right) \stackrel{\text{def}}{=} Fd_{mag}{}^2 \ \text{ and}$$

$$Fd_{mag}{}^2(r\rightarrow\infty\ ) = -4\frac{R0^3}{C1}\frac{1}{8\pi\kappa}\frac{1}{r^6} \stackrel{\text{def}}{=} \frac{\mu o}{2}\left(\frac{\mu_{spin}}{2\pi}\right)^2 \frac{1}{r^6}\ ; \quad \text{(original development in [5]).} \quad (9)$$

The factor 4 in (10) should be 3, then

$$Fd_{mag}{}^2(r\rightarrow\infty\ ) = -3\frac{R0^3}{C1}\frac{1}{8\pi\kappa}\frac{1}{r^6} \stackrel{\text{def}}{=} \frac{\mu o}{2}\left(\frac{\mu_{spin}}{2\pi}\right)^2 \frac{1}{r^6} \quad \text{and} \qquad (9a)$$

$$Fd_{mag}{}^2(\ t\ ,\ r\rightarrow\infty\ ) = \frac{e^{-\mu t}}{8\pi\kappa}\left[\frac{3}{2}\left(\frac{Rs\ R0^3}{r^6}\right) - \frac{2}{c^2}\left(\ddot{\mu}t + \frac{1}{4}\dot{\mu}t^2\right)\right]\ .$$

The photonic or oscillating-distortion is primarily magnetic while an electronic-distortion at large radial distances is primarily electric but magnetic near the core. The field determined electromagnetic coupling constant and the geometric-distortion quantifiers are

$$\kappa o \stackrel{\text{def}}{=} \kappa o(EM) = \frac{\alpha\, \hbar c \left(\frac{Q}{3}\right)^2}{2\left(Mc^2\right)^2} = \frac{\mu o}{2\pi}\left(\frac{\mu\_spin}{\hbar c\ S\ ge}\right)^2 , \quad \alpha \text{ is the fine structure constant ,} \tag{10}$$

Q = multiple of e(electronic charge) = 0,1,2,3

and a correction, $R0^3 = (\hbar c\ S\ ge)^2 \frac{\kappa o}{3\ Mc^2}$. (10a)

The 1st mass-moment, R0 Mc^2, characterized as a structural constant in [5], or

$$R0\ Mc^2 = \beta\ \hbar c\ , \quad \text{with a corrected } \beta = \left[\left(S \frac{ge}{2} \frac{Q}{3}\right)^2 \alpha\ \frac{2}{3}\right]^{1/3}, \tag{11}$$

is actually weakly dependent on the structural descriptors S, Q and ge. Although statically, $\kappa = \kappa o(EM) + G/c^4$ [5], the electromagnetic coupling factor κo dominates the characterization as long as Q does not equal zero (no spin). The quantity $\mathrm{Lf} \stackrel{\text{def}}{=} \sqrt{\hbar c\ \kappa}$ in conjunction with a geometrically-defined gravitational coupling constant, (i.e. $\kappa \equiv \kappa_G \equiv G/c^4$) has heretofore been posited as a characteristic Planck-length [2]. In both the earlier work and for the presently conceived 4-dimensional time-dependent construct, we have introduced the concept of a “maximum geometric curvature” of the locally distorted spacetime manifold, with geometric definition to r = 0, and therefore have probably precluded the introduction of an extended Planck-length or vacuum-fluctuation description for geometric-distortions, however, r0W (the W^-boson radius) and $\left(\mathrm{Lf} = [\hbar c\ \kappa o W]^{1/2}\right)$ for the 3-dimensional W^-boson static distortion, differ by only a factor of $\frac{\mathrm{r0W}}{\mathrm{Lf}} = \left[\frac{\hbar c}{\mathrm{u0W\ MW}}\left(\frac{\mathrm{ge}}{2}\right)^{2/3}\left(\alpha\,\frac{2}{3}\right)^{1/3}\right]\left[(\hbar c)^2 \frac{\alpha}{2}\left(\frac{1}{\mathrm{MW}}\right)^2\right]^{-1/2} \cong 1.50$.

OSCILLATING DISTORTIONS

The total distortional time-dependent energy-equation from (1a) is, with

$$\kappa = \kappa o\ \kappa t = (\kappa o(EM) + G\ c^{-4})\kappa t\ ,$$

$$U = 2\int_0^{2\pi} c\ dt\ \int_0^{rmax} Td_4^4(t, r)\sqrt{(-g_{11})^3 g_{44}}\ 4\pi r^2\ dr\ ; \qquad (12)$$

$$rmax = \infty\ \text{ for } Td_4^4(r) \quad \text{and} \quad rmax = Rph = \text{for } Td_4^4(t).$$

Rph is the structural distortional-energy-density radius necessary to satisfy (1) and is calculable via (18) and restated here;

$$Rph^3 = \frac{4\ hc}{3.551}\ \kappa oph\ \kappa t = \frac{8}{3.551}\ 7.955\ \kappa oph\ \frac{(hc)^2}{Mph\ c^2}$$

where Mph c^2 is the distortion's mass-energy and κoph is the distortion's coupling constant.

$$7.9549265 = \int_0^{2\pi} e^{\sin(x)} dx \quad \text{and}$$

$$3.5509993 = \int_0^{2\pi} e^{\sin(x)}(\cos(x))^2\ dx\ .$$

The structural nature of the distorted-geometry concept allows for or requires a g-factor inclusion. Then, with κo = the static distortional coupling constant from (6),

$$Ud \stackrel{\text{def}}{=} 4d\ \text{Distortional MassEnergy}\ .$$

$$\mathrm{Ud} = \frac{\mathrm{M}c^2}{\kappa \mathrm{t}} \int_0^{2\pi} \mathrm{e}^{\mu \mathrm{t}} \mathrm{c}\, \mathrm{dt} \;\; + \frac{3}{4\,\kappa\mathrm{o}\,\kappa\mathrm{t}\,\mathrm{c}^2} \int_0^{2\pi} \left(\frac{\mathrm{d}\mu}{\mathrm{dt}}\right)^2 \mathrm{e}^{\mu \mathrm{t}}\, \mathrm{c}\, \mathrm{dt} \int_0^{\mathrm{Rph}} \mathrm{e}^{\frac{3\mu \mathrm{r} - \nu \mathrm{r}}{2}} \mathrm{r}^2\, \mathrm{dr} \;. \tag{13}$$

Tolman [8] has pointed out that typical volume integrals (like the time-component $\mathrm{Td}_4^4(\mathrm{t},\mathrm{r})$ integral) calculated to r = ∞ are in fact infinite; we also therefore have limited the radial-coordinate integration for the geometric time-extension component to some spatial definition for the distortional energy distribution in question. Also, in the absence of an analytical form for the metrics (although see Appendix in [9]), we use numerical integration to produce the energy-density and metric functions plotted in Figs. 7 to 9.

For the static-distortion mass-energy calculation, the development produced the integral equations

$$\text{MassEnergy} = \int_0^{\infty} \mathrm{Int(r)}\; 4\pi \mathrm{r}^2\, \mathrm{dr} \tag{14}$$

where

$$\mathrm{Int(r)} = \frac{2}{8\pi\kappa} e^{\frac{3\mu r + \nu r}{2}} \left[\mathrm{e}^{-(\mu \mathrm{r})}\, \mu \mathrm{r}' \left[\frac{1}{\mathrm{f}} \mathrm{f}' + \frac{\mu \mathrm{r}'}{4\mathrm{f}} (2\,\mathrm{f} - 3)(\mathrm{f} - 2) \right] \right]. \tag{14a}$$

In the present extension to include the time-dimension, without approximation and after time-integration, the MassEnergy(t_term) is

$$\mathrm{MassEnergy}(\mathrm{t_{term}}) =$$

$$= \frac{3}{4\,\kappa\mathrm{o}\,\kappa\mathrm{t}\,\mathrm{c}^2} \int_0^{2\pi} \left(\frac{\mathrm{d}\mu}{\mathrm{dt}}\right)^2 \mathrm{e}^{\mu \mathrm{t}}\, \mathrm{c}\, \mathrm{dt} \int_0^{\mathrm{Rph}} \mathrm{e}^{\frac{3\mu \mathrm{r} - \nu \mathrm{r}}{2}} \mathrm{r}^2\, \mathrm{dr}. \tag{15}$$

The metric terms, $e^{\frac{3\mu r-\nu r}{2}}$ and $e^{\frac{\nu r+\mu r}{2}}$ are ~ 1 ; see Figs. 7-9. Small mass distortions lead to large core-radii and a "flat-like geometric-metric" with very little distortional impact (parts per 10^{20} for the distortional mimic of the photon) on the spacetime manifold. Radiation seems physically to be one of the likely cosmological-energy-endpoints before further absorption by the manifold [6]. The geometrically modeled electromagnetic, and gravitational distortional-radiation, and the modeled particle-like distortions are a manifestation of geometric compound-metrics, distorted-geometry coupling-constants, non-linear physical functioning and fundamental geometric-coupling [5].

For a distortional EM-photonic mimic with Total energy = Ud and radial extent = Rph, after integration of the mass-energy, (14) becomes,

$$\mathrm{Ud} = \frac{3.551}{4\,\kappa\mathrm{o}\,\kappa\mathrm{t}}\,\mathrm{Rph}^3\;\frac{\omega}{\mathrm{c}} + \frac{\mathrm{M}c^2}{\kappa\mathrm{t}}7.955\;\frac{\mathrm{c}}{\omega}\;, \tag{16}$$

compared to (1) for U,

$$\mathrm{U} = \mathrm{p\,c} + \frac{1}{2}\frac{\left(\mathrm{mo\,c^2}\right)^2}{\mathrm{pc}} = \mathrm{h}\omega + \frac{1}{2}\frac{\left(\mathrm{mo\,c^2}\right)^2}{\mathrm{h}\omega}.$$

Therefore, equating (17) to (1), $\kappa\mathrm{t} = 7.955\;\frac{2\,\mathrm{hc}}{\mathrm{Mph\,c^2}}$

and $\kappa\mathrm{t} = \frac{3.551}{4\,\mathrm{hc}}\;\frac{\mathrm{Rph}^3}{\kappa\mathrm{oph\_EM}}$

where $\kappa\mathrm{oph} = \kappa\mathrm{oph}_{\mathrm{EM}} = \alpha\;\frac{\hbar\mathrm{c}}{2}\left(\frac{\mathrm{Qph}}{\mathrm{Mph\,c^2}}\right)^2$

for an EM distortion and $\kappa\mathrm{oph} = \kappa\mathrm{oph_G} = \mathrm{G}\, c^{-4}$ for a gravitational entity.

The κt equations are satisfied if

$$\mathrm{Rph}^3 = \frac{4\,\hbar c}{3.551}\,\kappa\mathrm{oph}\,\kappa\mathrm{t} = \frac{8}{3.551}\,7.955\,\kappa\mathrm{oph}\,\frac{(\hbar c)^2}{\mathrm{Mph\,c^2}}\,. \tag{17}$$

Using $\gamma(\mathrm{Q}) \stackrel{\mathrm{def}}{=} 2\,\frac{\mathrm{R0ph\_EM+R0ph\_G}}{\mathrm{Rs\_EM+Rs\_G}} = 2\,\frac{\mathrm{R0ph\_EM}}{\mathrm{Rs\_EM}} = \left[\left(\frac{2\,\mathrm{geph}}{\alpha}\,\mathrm{S}\right)^2 \mathrm{Q}^{-4}\,\frac{1}{3}\right]^{\frac{1}{3}}$, (18)

then $\mathrm{u0(Q)} = \left(\frac{7}{4}\,\gamma(\mathrm{Q})\right)^{1/7}$ (applicable @ small Q). (18a)

With geph = the distortional-photon g-factor, $\mathrm{Q = Qph = Q_{exp}} \le 10^{-35}\,\mathrm{e}$, $\mathrm{Mph}\,c^2 = \mathrm{M_{exp}c^2} \le 1.6\,10^{-37}\,\mathrm{J}$, $S = \mathrm{Sph} = 1$, for the distortional-photon, and since the characteristic normalized-radius R0ph is

$$\mathrm{R0ph\_EM} = \frac{\hbar\mathrm{c}}{\mathrm{M_{exp}c^2}}\left(\frac{2}{3}\,\alpha\left(\mathrm{Sph\;Qph}\;\frac{\mathrm{geph}}{2}\right)^2\right)^{\frac{1}{3}}\,, \tag{19}$$

the distortion's negative-energy-density radius is

roph = $\frac{\mathrm{R0ph\_EM}}{\mathrm{u0(Q)}} = 0.201\;10^{-19}\;\mathrm{m}$, having used approx.

geph ~ ge(electron) and $\mathrm{Q = Q_{photon} = Qph}$. (19a)

This result suggests that the "distortional-photon" may exhibit the "maximum-curvature radius" which was calculated for the $\mathrm{W^-}$boson mediator-particle in beta-decay and

incorporated into the Fermi-constant [5, 10]. Although the calculation is based on experimental data-extremes, we posit and model that the "photon creation" process follows a transition path similar to that of beta-decay through creation of, and morphing to (not through), the "distortional W^{-}boson mediator's" radial structure, a "geometric maximum-curvature" condition. The distortional geometric Fermi constant is (GF = $\pi^3/2$ $(r0W\ u0W)^3$ MW) (a correction from [5]). MW is the mass-energy of the W^{-}boson [23] and r0W is the "distortional boson" radius calculated with the distortional electromagnetic coupling constant and is the condition of "distortionally-produced maximum-curvature in the geometric-manifold". In other words, the charge-mass ratio of this oscillating photon-mimic should equal the charge-mass ratio of the W^{-}boson,

$$(\mathrm{Qph\ geph})^{\frac{2}{3}}\ (\mathrm{u0(Q)\ Mph\ c^2})^{-1} =$$

$$= (1\ \mathrm{geW})^{2/3}(1.8777\ \mathrm{MW}\ )^{-1}\ \text{, since QW = 1.} \tag{19b}$$

After determining geW from the Fermi constant equation,

$$\mathrm{geW} = 2\ \mathrm{MW}\ \left((\pi\ \hbar c)^3\ \frac{\alpha}{3\ \mathrm{GF}}\right)^{-1/2}. \tag{19c}$$

Then from (15b),

$$\mathrm{geph} = \left(\frac{\mathrm{geW}}{\mathrm{Qph}}\right)(\mathrm{u0(Qph)\ Mph\ c^2})^{3/2}(1.8777\ \mathrm{MW}\ )^{-3/2}. \tag{19d}$$

If we indeed set roph = r0W, then $\mathrm{roph} = \mathrm{r0W} = \sqrt[3]{\frac{2\ \mathrm{GF}}{\mathrm{MW}}}(\pi\ \mathrm{u0W})^{-1}$ and

$$\text{R0ph\_EM} = \text{u0(Qph) r0W} = \frac{\text{u0(Qph)}}{\text{u0W}} \left(\text{GF} \frac{2}{\text{MW}}\right)^{1/3} \frac{1}{\pi} \tag{20}$$

where u0W = distortional mass-energy root, or root of $\text{Td}(\text{r})_4^4 = 0$, or u0W = 1.877714, and the boson mass-energy = MW [5].

Associated with the "maximum-curvature radius (defined as r0W)" is a "minimum-Q dependent" mass for small-Q EM-distortions;

$$\text{M\_EM}_{\text{min}} c^2 = \frac{\hbar c}{\text{r0W}} \left[\frac{2}{3} \alpha \left(\text{S} \frac{\text{ge}}{2}\right)^2\right]^{\frac{1}{3}} \frac{\text{Q}^{2/3}}{\text{u0(Q)}} = 1.29\ 10^{-38}\ \text{J} \tag{21}$$

employing Q_{exp}. In the earlier "stable-particle" development [5], electric-charge was considered quantizable at Q = 0,1,2,3 electron charge units (e/3), thereby including in the model, a gravitational condition of the distortion-energy at Q = 0. But in the present near-zero (Q ~ 10^{-35} e) charge regime, we are allowing a non-gravitational Q ~ 0 description. The descriptive transition from EM charge-energy to gravitational-energy is explicitly described in the γ function which determines the radius of the negative-energy density core;

$$\gamma = 2\frac{\text{R0E} + \text{R0G}}{\text{RsE} + \text{RsG}} = 2\frac{\alpha 1(\kappa\text{o} + \kappa\text{G})\kappa\text{t}}{2(\kappa\text{o} + \kappa\text{G})\kappa\text{t Mc}^2};$$

$$\alpha 1 = \left(\frac{(\text{S ge})^2}{6}\frac{(\hbar c)^4}{\text{Mc}^2}\right)^{1/3}.$$

$$\gamma_{\text{EM}} = \frac{\alpha 1}{\text{Mc}^2} \quad \text{and} \quad \gamma_{\text{G}} = \frac{\alpha 1}{\text{Mc}^2}. \tag{21a}$$

Therefore with geW = 1.9993485, a photon charge = Q_{exp} and a photon mass-energy Mph c^2 = 0.0808283 M_{exp} (from (22)), then geph = 2.0063152   and

$$\kappa\text{t\_EM} = 7.955\ \frac{2\ \text{hc}}{\text{Mph\_EM}_{\text{min}}\ \text{c}^2} = 2.444\ 10^{14}\ \text{m} \quad \text{where} \quad \gamma_{\text{EM}} = 2.877\ 10^{16}\ . \tag{21b}$$

A "minimum Q ~ 0" criterion leads to a gravitational distortion at $\kappa\text{oph} = \kappa\text{oph\_G}$ producing

$$\text{Mph\_G}_{\text{min}} c^2 = \frac{\text{r0W}}{2\ \text{G}\ \text{c}^{-4}} = 1.343\ 10^{25}\ \text{J.} \tag{22}$$

Such a Q ~ 0, non-spin type deformation-energy is only weakly spatially distorting and

$$\kappa\text{t\_G} = 7.955\ \frac{2\ \text{hc}}{\text{Mph\_G}_{\text{min}} \text{c}^2} = 2.353\ 10^{-49}\ \text{m.} \tag{22a}$$

Also,

$$\kappa\text{oph\_EM} = \alpha \frac{\hbar c}{2} \left(\frac{\text{Qph}}{\text{Mph c}^2} \right)^2 = 8.919\ 10^{-26}\ \text{m/J}, \quad \text{while}$$

$$\kappa\text{oph\_G} \stackrel{\text{def}}{=} \text{G}\ c^{-4} = 8.26\ 10^{-45}\ \text{m/J}, \tag{23}$$

and

$$\kappa_{\text{EM}} \stackrel{\text{def}}{=} \kappa\text{oph\_EM}\ \kappa\text{t\_EM} = 2.180\ 10^{-11}\ \text{m}^2/\text{J}, \quad \text{while}$$

$$\kappa_{\text{G}} \stackrel{\text{def}}{=} \kappa\text{oph\_G}\ \kappa\text{t\_G} = 1.935\ 10^{-93}\ \text{m}^2/\text{J.} \tag{23a}$$

In other words, gravitational energies cause minimal geometric distortions. For comparison with κt, a "solar radius" is quoted as $6.957(10)^8$ m [11]. For comparison with κoph, the static "electron" coupling constant is calculated as 0.0172 m/J [5].

Additionally, if the Fermi-constant concept (a "distortional-geometry spin" concept) can be applied to the distortional photon-mimic transition, then we can write according to [5],

$$\mathrm{R0W}^3\ \mathrm{MW}\ \frac{\pi^3}{2} = \mathrm{GF}$$

or $$(\hbar c)^3 \left[\frac{2}{3}\ \alpha \left(\mathrm{S_W}\ \frac{\mathrm{geW}}{2}\right)^2\right] \left(\frac{Q_W}{\mathrm{MW}}\right)^2 \frac{\pi^3}{2} = \mathrm{GF}\,.$$

$$\left(\frac{\mathrm{Q_W}}{\mathrm{MW}}\frac{\mathrm{geW}}{2}\right)^2 = \mathrm{GF}\ \frac{3}{(\pi\ \hbar c)^3}\ (\ \alpha\ (\mathrm{S_W})^2)^{-1} \quad (\text{Joule})^{-2}; \qquad (24)$$

Q_W and S_W being the boson charge and spin quantities.

We have displayed in Fig. 10 the photonic energy-density quantities $(Fd_{12})^2$, $(Fd_{14})^2$ and Td_4^4, which illustrate the presence of the multiple distortional radial force-functions **(electric (r^{-2}), magnetic (r^{-3})**, **weak**, **strong** etc.) while exhibiting **no physical singularities from $r = 0$ to $r = \infty$.** Gravitational forces can only be seen in the absence of the much stronger magnetic and electric forces or greater energy-densities but gravitational effects are physically represented and mathematically integrated through the geometric coupling constants; see the earlier Fig. 5 for a comparison with the equivalent electronic $(Fd_{12})^2$ functional dependence. The distortional energy-density functions constitute an admixture or sum of the classically-defined radially-expressed force-functions. In this distorted-geometry model however,

structurally-stable mass-energy is constituted by a negative-pressure (energy-density) core surrounded by a positive-pressure (energy-density) envelope holding the core stably in place.

The presence of this core region as part of the functional energy-density solution to the differential equations can be viewed in terms of a geometrically stable (non-fluctuating) adaptation of the uncertainty principle or vacuum fluctuation principle, wherein

$$\Delta\mathrm{E}\,\Delta\mathrm{t} = \frac{\hbar}{2} \text{ is simply rendered as } \Delta\mathrm{E}\,\mathrm{c}\,\Delta\mathrm{t} = \frac{\hbar c}{2}\ (\mathrm{J\ m})\ ,$$

since an equivalent energy-spatial relationship for these geometric EM distortions is already manifest in equation (6b) (a distorted-geometry weak-structural-constant) and reads

$$\mathrm{M}c^2\ \frac{\mathrm{r0W}}{\mathrm{u0W}} = \frac{\hbar \mathrm{c}}{2}\ \beta 1 = \frac{\hbar \mathrm{c}}{2}\ \left[\left(\mathrm{S\ Q}\ \frac{\mathrm{ge}}{2}\right)^2 \alpha\,\frac{16}{3}\right]^{\frac{1}{3}}.$$

The “geometric equivalent” to the “vacuum-fluctuation energy product” is defined in terms of the “maximum-curvature W$^-$boson-radius” as

$$+\Delta\mathrm{E}\ \mathrm{c}\ \Delta\mathrm{t} \stackrel{\mathrm{def}}{=} \mathrm{MW\ c}\ \left(\frac{\mathrm{r0W\ fW}}{\mathrm{c}}\right) =$$

$$= \frac{\hbar \mathrm{c}}{2}\,\mathrm{u0W}^{-1}\ \left[\left(\mathrm{S_W\ Q_W}\ \frac{\mathrm{geW}}{2}\right)^2 \alpha\,\frac{16}{3}\right]^{\frac{1}{3}} \mathrm{fW}$$

$$= \frac{\hbar c}{2} \quad \text{if} \quad \mathrm{fW} = \mathrm{u0W} \quad \left[\left(\mathrm{S_W\,Q_W}\,\frac{\mathrm{geW}}{2} \right)^2 \alpha \frac{16}{3} \right]^{-\frac{1}{3}} , \tag{25}$$

the fluctuation time-equivalent (fW r0W) representing 2.77 time-transits of a boson core-diameter or a "fluctuation-radius" definition at 5.54 r0W.

Fig. 11 displays the Td_4^4 energy-density function for the distortional photon-mimic and Fig. 12 shows a composite of a distortional-electron Td_4^4 energy-density function and the photon-mimic Td_4^4 energy-density function. To further illustrate the spatial-extension and energy-density magnitude of the photonic-distortion, we illustrate in Fig.13 the photonic energy-density radial profile displaced to a point (r = 2 roe) near to the electron mimic's energy-density radial profile.

IV. **CONCLUSIONS**

A 4-dimensional, that is, a time dependent, oscillating geometric distortion has been developed. An earlier distortional solution for Riemann's 3-dimensional geometric equations, which had been utilized to mimic the characteristics of the fundamental particles and the fundamental forces, simultaneously provided a geometric character to Fermi's constant. By extending the spatial solution, which shows no physical singularities, we have mimicked the relativistic behavior of oscillating structures. For a photon mimic, invisible to the manifold, the maximum curvature concept, which is fundamental to these distortional characterizations, leads to a boson-mediator-like

geometrically-structured entity. Metrics and coupling constants display the physical attributes responsible for radiation propagation in the spacetime manifold.

REFERENCES

[1] Ciufolini, I. and Wheeler, J. A. Gravitation and Inertia; Princeton University Press: Princeton, NJ, 1996.

[2] Wheeler, J. A., Phys. Rev. 1955, 97 511-36.

[3] Wheeler, J. A., In Logic, Methodology, and Philosophy of Science. Proc. of the 1960 International Congress; Nagel, E.; Stanford University Press, 1962.

[4] Clifford, W. K. Proc. of the Cambridge philosophical society 1876, 2 157-58.

[5] Koehler, D. R., Indian Journal of Physics, vol. 87, p.1029, 2013.

[6] Koehler, D. R., IEEE Transactions on Plasma Science, vol.12, No. 45, p.3306, 2017.

[7] C. Amsler et al. (Particle Data Group), PL B667, 1 (2008) and 2009 partial update for the 2010 edition (URL: http://pdg.lbl.gov)].

[8] Tolman, R. Phys. Rev., 35 875, 1930.

[9] Koehler, D. R., The Distorted Universe: From Neutrinos to the Cosmos, The Theory of Nothingness, Kindle: ASIN B00TG26Q7Y, 2015.

[10] Chitwood, D. B., MuLan Collaboration, *et al*. (2007) “Improved Measurement of the Positive-Muon Lifetime and Determination of the Fermi Constant”. Physical Review Letters, 99: 032001, arXiv:0704.1981.

[11] Mamajek, E. E., Prsa, A., Torres, G., et al., “IAU 2015 Resolution B3 on Recommended Nominal Conversion Constants for Selected Solar and Planetary Properties”, arXiv:1510.07674.

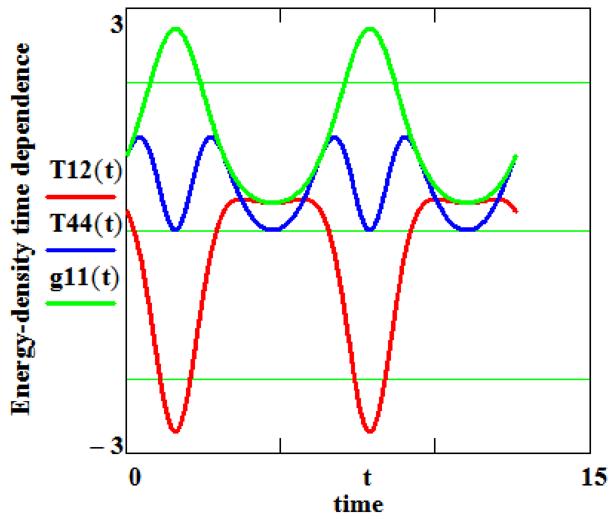

Fig. 1. Time-dependent photonic metric functions where $g_{11}(t) = e^{\mu t} = e^{\sin(\omega t)}$, $T44(t) = e^{\mu t}(\dot{\mu} t)^2$, the time-depenent behavior of $Td(t)^4_4$ and $T12(t) = e^{\mu t}\left(\ddot{\mu} t + \frac{1}{4}(\dot{\mu} t)^2\right)$ the time-dependent behavior of $Td(t)^1_1$ and $Td(t)^2_2$; time is in units of ω.

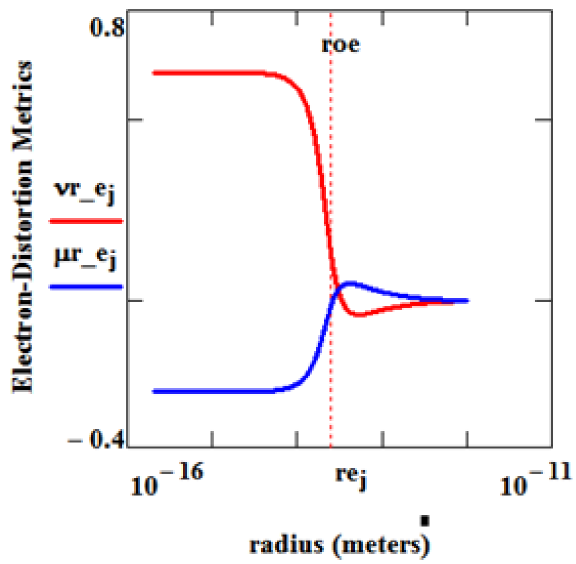

Fig. 2. Metric argument-functions for a distortional electron-mimic as a function of the radius re_j; roe is the radial value for the Td44_e(r) = 0 function.

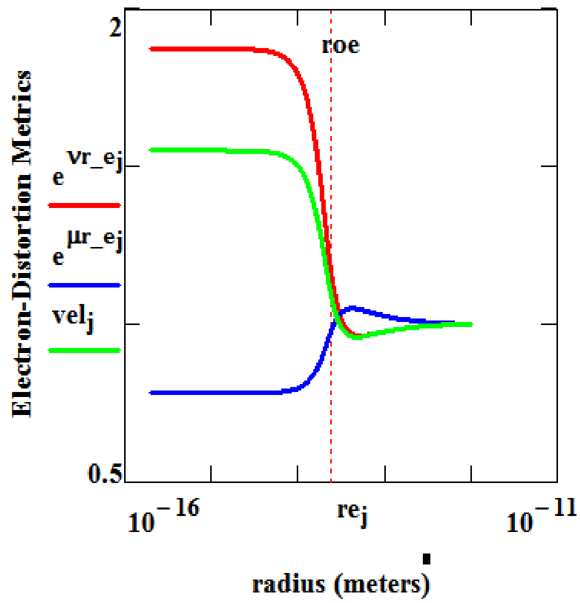

Fig. 3. Metric and velocity functions for a distortional electron-mimic as a function of the radius re_j; roe is the radial value for the Td44_e(r) = 0 function. roe is the radial value for the Td44_e(r) = 0 function.

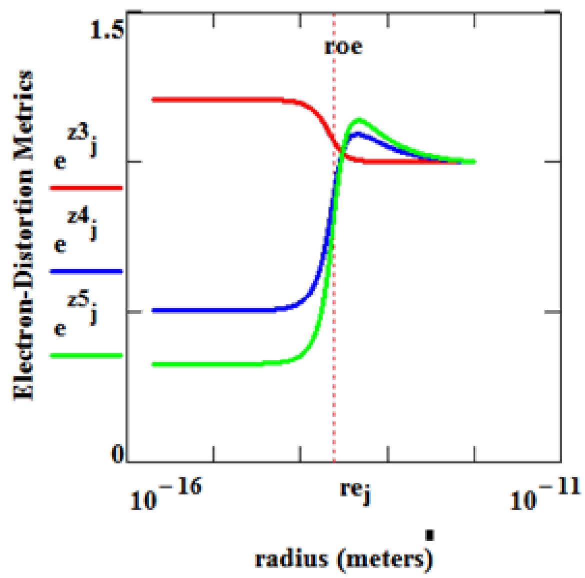

Fig. 4. Metric functions for a distortional electron-mimic as a function of the radius re_j; roe is the radial value for the Td44_e(r) = 0 function. $z3_j$ is the metric function $z3_j = \frac{3\,\mu r\_e_j + \nu r\_e_j}{2}$, $z4_j = \frac{3\,\mu r\_e_j - \nu r\_e_j}{2}$ and $z5_j = 2\,\mu r\_e_j - \nu r\_e_j$. roe is the radial value for the Td44_e(r) = 0 function.

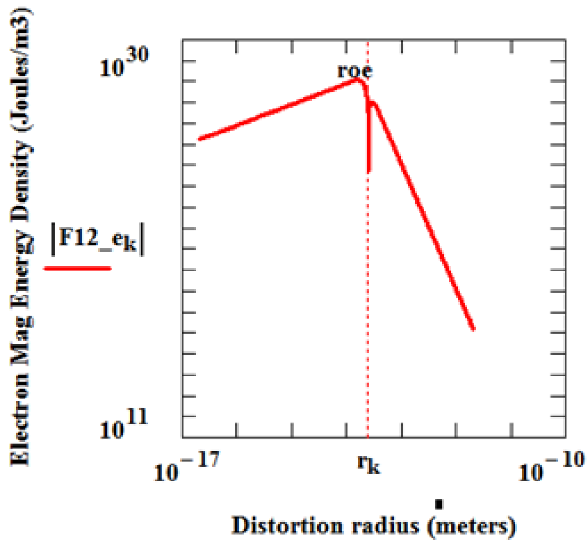

Fig. 5. Magnetic-energy functions for a distortional electron-mimic as a function of the radius r_k. roe is the radial value for the Td44_e(r) = 0 function. $F12\_e_k \stackrel{\text{def}}{=} \left(Fd_{mag}\right)^2$.

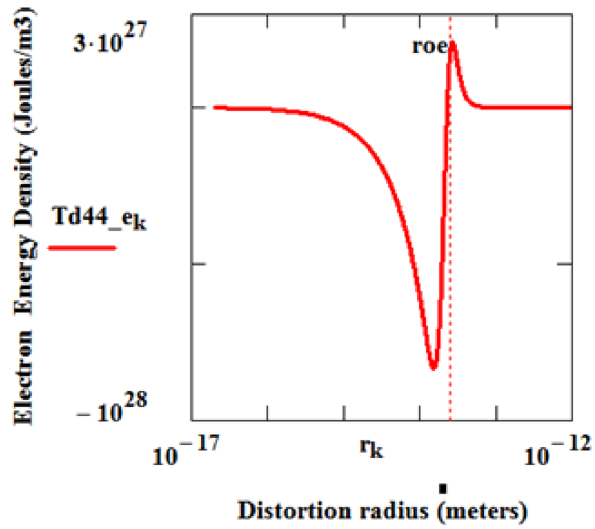

Fig. 6. Total-energy function for a distortional electron-mimic as a function of the radius r_k. roe is the radial value for the Td44_e(r) = 0 function.

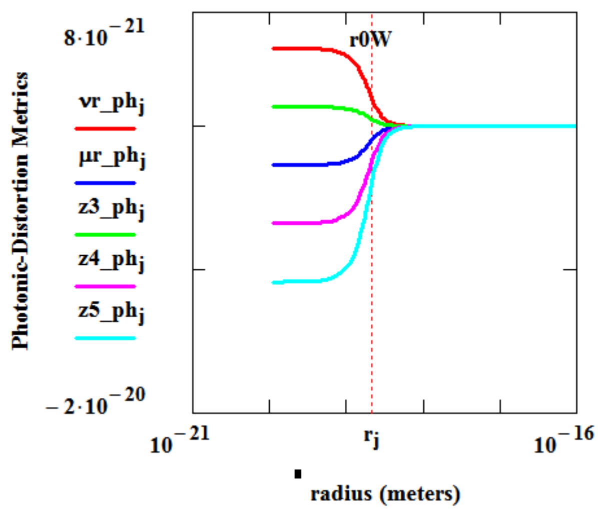

Fig. 7. Metric argument functions for a distortional photon-mimic as a function of the radius r_j; roW is the radial value for the Td44(r) = 0 function. $z3\_ph_j$ is the metric function $z3\_ph_j = \frac{3\ \mu r\_ph_j + \nu r\_ph_j}{2}$, $z4\_ph_j = \frac{3\ \mu r\_ph_j - \nu r\_ph_j}{2}$ and $z5\_ph_j = 2\ \mu r\_ph_j - \nu r\_ph_j$. r0W is the radial value for the Td44(r) = 0 function.

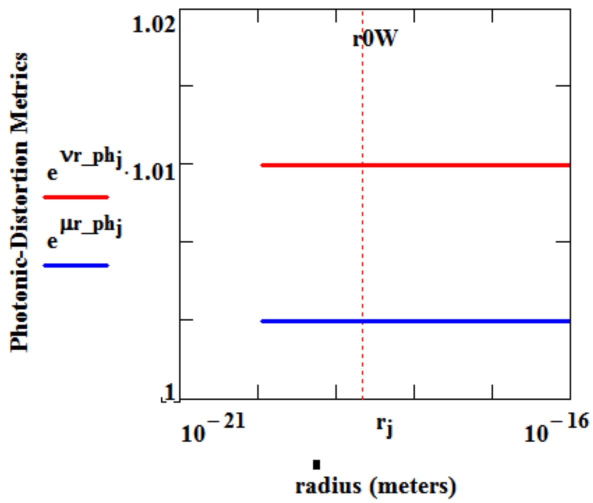

Fig. 8. Metric functions for a distortional photon-mimic as a function of the radius r_j; r0W is the radial value for the Td44(r) = 0 function.

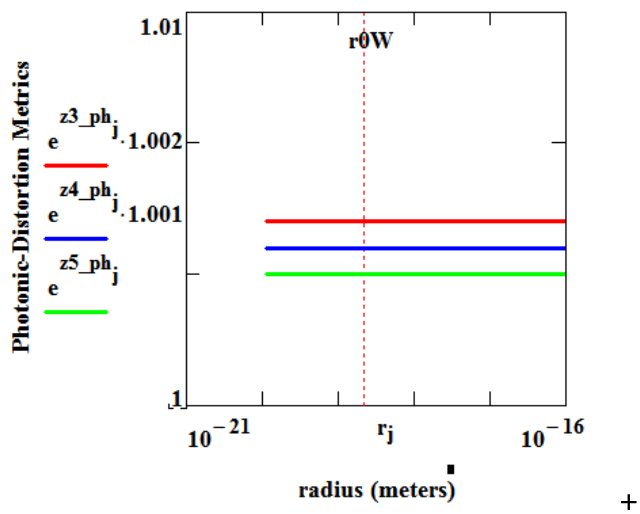

Fig. 9. Metric functions for a distortional photon-mimic as a function of the radius r_j; r0W is the radial value for the Td44(r) = 0 function. $z3\_ph_j$ is the metric function $z3\_ph_j = \frac{3\,\mu r\_ph_j + \nu r\_ph_j}{2}$, $z4\_ph_j = \frac{3\,\mu r\_ph_j - \nu r\_ph_j}{2}$ and $z5\_ph_j = 2\,\mu r\_ph_j - \nu r\_ph_j$.

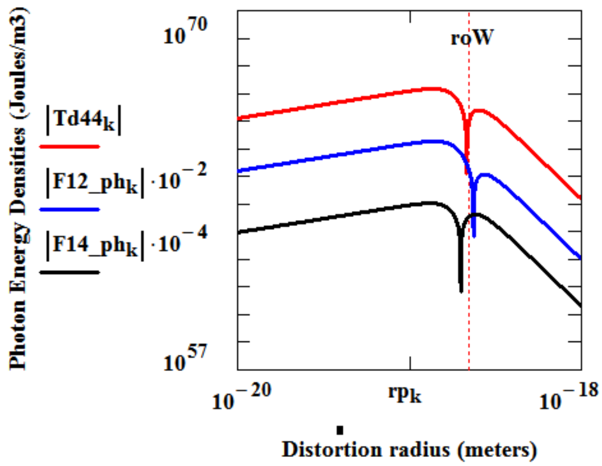

Fig. 10. Total-energy function $Td44_k$, magnetic-energy function $F12\_ph_k \stackrel{\text{def}}{=} \left(Fd\_ph_{mag}\right)^2$ and electric-energy function $F14\_ph_k \stackrel{\text{def}}{=} (Fd_{14})^2$ for a distortional photon-mimic as a function of the radius rp_k . roW is the radial value for the Td44(r) = 0 function.

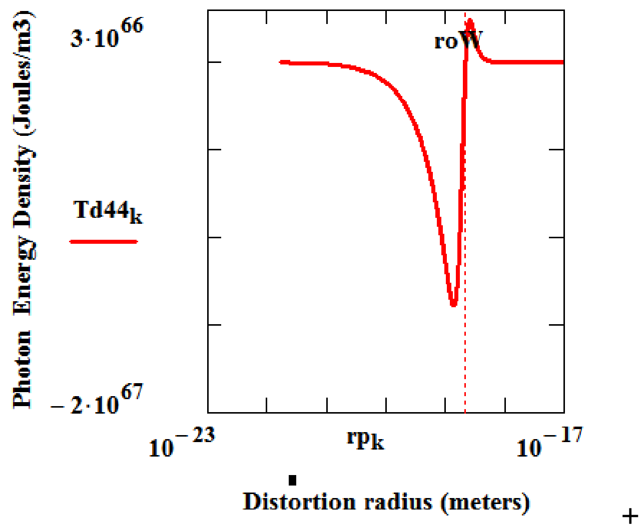

Fig. 11. Total-energy function for a distortional photon-mimic as a function of the radius rp_k r0W is the radial value for the Td44(r) = 0 function. The linear functional graphing shows the negative energy-density (negative pressure) core characteristic of these geometric distortions.

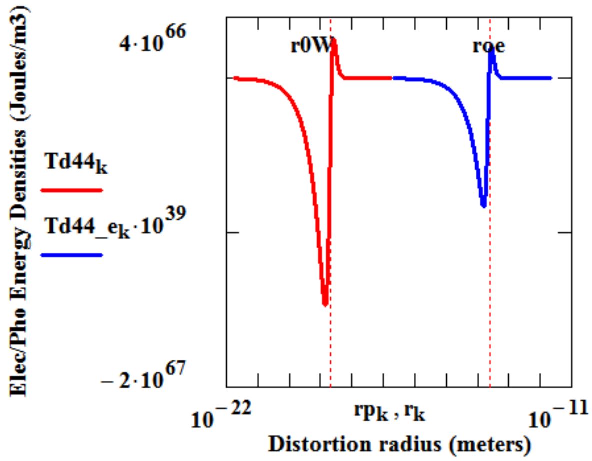

Fig. 12. Composite of Total energy functions for the distortional photon- and electron-mimics; linear ordinates and logarithmic abscissas. Although the total energy function for the electron-mimic is significantly greater than for the photon-mimic, the energy-density function for the photon-mimic is greater than for the distortional electron-mimic.

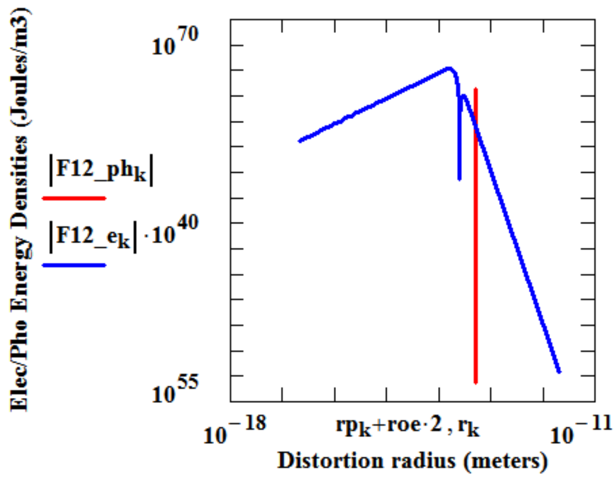

Fig. 13. Composite of magnetic-energy functions for the distortional photon, $F12\_ph_k \overset{\text{def}}{=} (Fd\_ph_{mag})^2$, and electron-mimics $F12\_e_k \overset{\text{def}}{=} (Fd\_e_{mag})^2$; linear ordinates and logarithmic abscissas. The distortional photon's radial profile has been displaced to a radial position at 2 roe, to illustrate more dramatically the spatial interaction overlap or "interaction cross-section". Note also the energy-density magnitudes.

CHAPTER 7

Summary

It has been posited in the present work that the classical Riemannian four-dimensional curvature equations can be applied to describe localized geometrical distortions and associated energy distributions at quantum level magnitudes and distances. By requiring that the geometric distortions mimic the physical characteristics of the elementary particles, a coupling constant between energy and geometry is produced with coupling strengths approximating the electromagnetic coupling constants. The theoretical modeling and calculational procedure is limited to those geometric-distortional families satisfying the equation-of-state, $\mathrm{Td}_4{}^4 = -(\mathrm{Td}_1{}^1+\mathrm{Td}_2{}^2+\mathrm{Td}_3{}^3)$, which also exp+resses static, spherically-symmetric Maxwellian tensor behavior. Functional solutions to the differential equations describing the "distorted" space are of such a character that, over portions of the radial extensions of the distortion, the geometrical tensor elements exhibit negative, as well as positive, curvature-magnitudes and energy-densities. A distortional negative-energy-density (energy-density = pressure) core-

region is the source of mimicked electric-charge. Within the “core regions” of the distortion, the propagation velocity, i.e. “energy propagation in a non-dispersive medium where $v_{group} = v_{phase} = c' =$ null-geodesic propagation velocity $= (c_{44} /(-c_{11})))^{1/2}$ “, exceeds the velocity of light (equivalent to an n < 1 refractive index).

The field-observable in the core region is non-Coulombic and non-infinite at the radial origin; this nonlinearly quantized negative-energy-density region is exclusively a function of geometrically-mimicked electric-charge and geometrically-mimicked gravitational-mass. Mass, electric charge and magnetic moments have been simulated for the electron, tauon, muon and neutrino as well as for a hypothetical beta-decay transition-mediating distortion-particle; this process also generates a geometric expression for the Fermi constant and predicts a mass-value for the W-boson calculated to the precision of the electron magnetic moment.

Eigen-modes, or the unstable vibrational states of the distortion-mimic of the electron, are posited as geometric-mimics of the fundamental fermions while a distortionally mimicked boson family is generated to include the W^-boson. The concept of geometrically-quantized radii manifested in excited vibrational states, as a feature fundamental to the distortional structures, inherently also affects consideration of the “lifetimes” spectra of such structures; $\tau_j = \beta\, ro_j/vp$, vp being the manifold-propagation-velocity within the spherical core.

By comprehensively incorporating gravitational-field energies into the geometric modeling, a refined coupling-constant is engendered, thereby recovering the

gravitational coupling-constant of general relativity and in turn leading to a structural description of gravitational-like geometric-distortions.

The "existence" of gravitational-based "geometrically distorted structures", or regions of space, could seriously influence cosmological calculations in at least two respects: 1) dependent on the density of free electrons in the geometric manifold (galactic and intergalactic space), the existence of electromagnetic propagation core-velocities faster than "*c* " would influence universe-dating calculations and 2), the presence of the massive "geometric" gravitational structures (Eq. 30a in Chapter 1) would be a source of "cosmological energy" heretofore unaccounted for.

Fundamentally, the distinguishing attribute of the distortions is their physical structure, which does not generate the associated infinities of pure r^{-4} field descriptions; the modeling results thereby avoid the need for mathematical renormalization techniques.

We have formulated the stability of these geometric structures as a function of the characteristics of their unstable-negative-energy cores, framed a temporal description of the decaying distortions and produced a concomitant geometric mimic of the neutrino. In a gravitational version of the distortion, the structure is massive and hole-like. In the electromagnetic version of the distortion, the geometric descriptors are used to successfully interpret and simply and precisely calculate the Fermi constant.

Geometrically-detailed composite-quark structures, formed with muonic substructures, have been incorporated to mimic mass, electric charge and magnetic moments for the proton and neutron as well as for a geometric down-quark and up-quark.

After having associated or attributed elastic and deformable characteristics to the geometric manifold in the earlier chapters, we have also examined the possibility of the additional material-characteristic of absorption. In addition to interpreting astronomical redshift data as absorptive in origin, as opposed to a non-absorptive universe-expansion interpretation, a simple explosive universe-creating geometric-distortion, absorption-model has here posited.

Spiral Galaxy M74 HUBBLESITE .org

ACKNOWLEDGEMENTS

Throughout the ongoing substance of this work, specific mention has been made recognizing the author's indebtedness to Dr. J.T. Grissom for his valuable suggestions for technical clarification and material emphasis and for his editorial contributions. The helpful corrective conceptual commentary of Dr. J.D. Weiss has also been acknowledged and should prove beneficial to the readers of this manuscript as well.

The publishing encouragement and treasured journalistic assistance throughout the book creation process of writing peer Ms. T.K. Koehler is respectfully recognized.

Finally we acknowledge the Hubble and NASA creation of the illustrations incorporated as examples of visible ingredients of the universe.